

OPTIMUM DESIGN OF RIGID AND SEMI-RIGID STEEL SWAY  
FRAMES INCLUDING SOIL- STRUCTURE INTERACTION

A THESIS SUBMITTED TO  
THE GRADUATE SCHOOL OF NATURAL AND APPLIED SCIENCES  
OF  
MIDDLE EAST TECHNICAL UNIVERSITY

BY

ERKAN DOĞAN

IN PARTIAL FULFILLMENT OF THE REQUIREMENTS  
FOR  
THE DEGREE OF DOCTOR OF PHILOSOPHY  
IN  
ENGINEERING SCIENCES

AUGUST 2010

Approval of the thesis

**OPTIMUM DESIGN OF RIGID AND SEMI-RIGID STEEL SWAY  
FRAMES INCLUDING SOIL - STRUCTURE INTERACTION**

submitted by **ERKAN DOĞAN** in partial fulfillment of the requirements for the degree of **Doctor of Philosophy in Engineering Sciences Department, Middle East Technical University** by,

Prof. Dr. Canan ÖZGEN  
Dean, Graduate School of **Natural and Applied Sciences**

Prof. Dr. Turgut TOKDEMİR  
Head of Department, **Engineering Sciences**

Prof. Dr. Mehmet Polat SAKA  
Supervisor, **Engineering Sciences Dept., METU**

Prof. Dr. Turgut TOKDEMİR  
Co- Supervisor, **Engineering Sciences Dept., METU**

**Examining Committee Members :**

Prof. Dr. Ayşe DALOĞLU  
Civil Engineering Dept., KTU

Prof. Dr. Mehmet Polat SAKA  
Engineering Sciences Dept., METU

Prof. Dr. Ayşe Gülin BİRLİK  
Engineering Sciences Dept., METU

Assoc. Prof. Dr. Oğuzhan HASANÇEBİ  
Civil Engineering Dept., METU

Assoc. Prof. Dr. Zafer EVİS  
Engineering Sciences Dept., METU

**Date :**

**I hereby declare that all information in this document has been obtained and presented in accordance with academic rules and ethical conduct. I also declare that, as required by these rules and conduct, I have fully cited and referenced all material and results that are not original to this work.**

Name, Surname : Erkan DOĞAN

Signature :

## **ABSTRACT**

### **OPTIMUM DESIGN OF RIGID AND SEMI-RIGID STEEL SWAY FRAMES INCLUDING SOIL- STRUCTURE INTERACTION**

Doğan, Erkan

Ph.D., Engineering Sciences Department

Supervisor: Prof. Dr. M. Polat Saka

Co-Supervisor: Prof. Dr. Turgut Tokdemir

August 2010, 240 Pages

In this study, weight optimization of two dimensional steel frames is carried out in which the flexibility of beam-to-column connections and the soil-structure interaction are considered. In the analysis and design of steel frames, beam-to-column connections are assumed to be either fully rigid or perfectly pinned. However, the real behavior of beam-to-column connections is actually between these extremes. Namely, even the simple connections used in practice possess some stiffness falling between these two cases mentioned above. Moreover, it is found that there exists a nonlinear relationship between the moment and beam-to-column rotation when a moment is applied to a flexible connection. These partially restrained connections influence the drift ( $P-\Delta$  effect) of whole structure as well as the moment distribution in beams and columns. Use of a direct nonlinear inelastic analysis is one way to account for all these effects in frame design. To be able to implement such analysis, beam-to-column connections should be assumed and

modeled as semi-rigid connections. In the present study, beam-to-column connections are modeled as “end plate without column stiffeners” and “top and seat angle with web angles”. Soil-structure interaction is also included in the analysis. Frames are assumed to be resting on nonlinear soil, which is represented by a set of axial elements. Particle swarm optimization method is used to develop the optimum design algorithm. The Particle Swarm method is a numerical optimization technique that simulates the social behavior of birds, fishes and bugs. In nature fish school, birds flock and bugs swarm not only for reproduction but for other reasons such as finding food and escaping predators. Similar to birds seek to find food, the optimum design process seeks to find the optimum solution. In the particle swarm optimization each particle in the swarm represents a candidate solution of the optimum design problem. The design algorithm presented selects sections for the members of steel frame from the complete list of sections given in LRFD- AISC (Load and Resistance Factor Design, American Institute of Steel Construction). Besides, the design constraints are implemented from the specifications of the same code which covers serviceability and strength limitations. The optimum design algorithm developed is used to design number of rigid and semi-rigid steel frames.

**Keywords:** Optimum structural design, soil-structure interaction, particle swarm algorithm, minimum weight, semi-rigid connections, combinatorial optimization, steel frames.

## ÖZ

### RİJİT VE YARI-RİJİT ÇELİK ÇERÇEVELERİN ZEMİN-YAPI ETKİLEŞİMİNİ DE İÇEREN OPTİMUM BOYUTLANDIRILMASI

Doğan, Erkan

Doktora, Mühendislik Bilimleri Bölümü

Tez Danışmanı: Prof. Dr. M. Polat Saka

Ortak tez Danışmanı: Prof. Dr. Turgut Tokdemir

Ağustos 2010, 240 Sayfa

Bu çalışmada, iki boyutlu çelik çerçevelerin kiriş-kolon bağlantısının esnekliğini ve zemin-yapı etkileşimini gözönüne alarak ağırlık optimizasyonu yapılmıştır. Çelik çerçevelerin analiz ve tasarımında kiriş-kolon bağlantılarının ya tam rijit ya da tam mafsallı olduğu kabul edilmektedir. Fakat, kiriş-kolon bağlantılarının gerçek davranışı bu iki durumun arasındadır. Pratikte kullanılan basit bağlantılar bile yukarıda belirtilen iki durumun arasında kalan bir rijitliğe sahiptirler. Öte yandan esnek bağlantıya moment uygulandığında, kiriş-kolon dönme açısı ile uygulanan moment arasında lineer olmayan bir bağlantının varlığı bulunmuştur. Bu tür kısmi tutulmuş bağlantılar tüm yapının yanal deplasmanını ( $P-\Delta$  etkisi) ve kiriş ve kolonlardaki moment dağılımını etkilemektedir. Doğrudan lineer ve elastik olmayan analiz yöntemi kullanmak, bu etkilerin çerçeve tasarımındaki etkisini hesaba katmak için var olan yöntemlerden birisidir. Bu tür bir analiz yapmak için kiriş-kolon bağlantısı yarı-rijit olarak kabul edilmeli ve ona göre modellenmelidir. Bu çalışmada kiriş-kolon bağlantıları “kolon berkitmeleri olmayan uç levhali” ve “üst,

alt ve gövdelerinde korniyer” kullanılan türde bağlantılar olarak modellenmiştir. Analizde zemin-yapı etkileşimi de göz önüne alınmıştır. Çerçevelerin bir grup aksenal elemanlarla temsil edilen lineer olmayan bir zemine oturduğu varsayılmıştır. Optimum boyutlandırma algoritmasının geliştirilmesinde parçacık kümesi optimizasyonu metodu kullanılmıştır. Parçacık kümesi yöntemi kuşların, balıkların ve böceklerin sosyal davranışını simule eden bir sayısal optimizasyon tekniğidir. Doğada balıklar, kuşlar ve böcekler sadece üreme için değil, yemek bulma ve düşmanlarından kaçma gibi diğer sebeplerden dolayı da sürü halinde olurlar. Kuşların yemek aramasına benzer olarak, optimum boyutlandırma işlemi de, optimum çözümü arar. Parçacık küme optimizasyonunda kümedeki her parçacık optimum boyutlandırma probleminin aday çözümünü temsil eder. Sunulan boyutlandırma algoritması, LRFD-AISC (Yük ve Direnç Faktörü Tasarımı- Amerikan Çelik Konstrüksiyon Enstitüsü) de verilen w-profillerinin tümünün bulunduğu listeden çelik çerçevenin elemanları için w-profilini seçer. Ayrıca dayanım ve deplasman sınırlarını kapsayan aynı şartnamede belirlenmiş kısıtlar, optimum boyutlandırma probleminin sınırlayıcıları olarak uygulanmıştır. Geliştirilen optimum boyutlandırma algoritması ile rijit ve yarı-rijit çelik çerçevelerin tasarımı yapılmıştır.

**Anahtar Kelimeler:** Optimum boyutlandırma, parçacık sürü optimizasyonu yöntemi, minimum ağırlık, zemin-yapı etkileşimi, yarı-rijit bağlantı noktaları, çelik çerçeveler.

*To my family*

## **ACKNOWLEDGEMENTS**

I would like to express my deepest gratitude to my thesis supervisor Prof. Dr. M. Polat SAKA for his guidance, understanding, kind support, encouraging advices, criticism, and valuable discussions throughout my thesis.

I am greatly indebted to Prof. Dr. M. Ruşen GEÇİT and Prof. Dr. Turgut TOKDEMİR for their guidance and providing me every opportunity to use in Engineering Sciences Department.

I would sincerely thank to Hakan BAYRAK, Ferhat ERDAL, Fuat KORKUT, and Semih ERHAN for their endless friendship, making my stay in METU happy and memorable and being always right beside me.

I would also like to thank to my friends Özge ERDEMLİ, Serdar ÇARBAŞ, Refik Burak TAYMUŞ, İbrahim AYDOĞDU, Memduh KARALAR, Alper AKIN, Mehmet DOĞAN, Kaveh HASSANZEHTAB, Ali GÖK, Engin KURŞUN, Fatih GÖKÇE, Ali Sinan DİKE and E. Emre ÇALIK, for cooperation and friendship, and helping me in all the possible ways.

My greatest thanks go to my parents, Perihan DOĞAN and Adnan DOĞAN for their support, guidance and inspiration all through my life, my sisters Nurhan DOĞAN and Tuğçe DOĞAN who are always there for me.

I dedicate this dissertation to my aunt İhame DOĞAN, my uncle Özkan KIRKPINAR, his wife Arzu KIRKPINAR and every other members of my family who always offered their advice, love, care and support. My family's absolute unquestionable belief in me, have been a constant source of encouragement and have helped me achieve my goals.

## TABLE OF CONTENTS

ABSTRACT .....	iv
ÖZ.....	vi
ACKNOWLEDGEMENTS.....	ix
TABLE OF CONTENTS .....	x
LIST OF TABLES .....	xvi
LIST OF FIGURES .....	xviii
LIST OF ABBREVIATIONS.....	xxii
CHAPTERS	
1 INTRODUCTION.....	1
1.1 Modeling of steel frames.....	1
1.2 Semi-Rigid Steel Frames .....	2
1.3 Soil-Structure Interaction.....	3
1.4 Optimization .....	4
1.4.1 Optimization models .....	7
1.4.1.1 Continuous-variable models .....	7
1.4.1.2 Discrete-variable models .....	8
1.4.2 Structural optimization.....	8
1.4.2.1 Structural Optimization Problems .....	11
1.4.2.1.1 Sizing Optimization Problems .....	13
1.4.2.1.2 Shape Optimization Problems .....	14
1.4.2.1.3 Topology Optimization Problems.....	15
1.4.2.2 Structural Optimization Methods .....	16
1.4.2.2.1 Analytical Methods.....	16

1.4.2.2.2	Numerical Methods.....	17
1.4.2.2.2.1	Mathematical Programming.....	20
1.4.2.2.2.2	Optimality Criteria.....	22
1.4.3	Stochastic search methods.....	23
1.4.3.1	Genetic algorithms.....	24
1.4.3.2	Tabu Search.....	25
1.4.3.3	Evaluation Strategies.....	26
1.4.3.4	Simulated Annealing.....	27
1.4.3.5	Ant Colony Optimization.....	28
1.4.3.6	Harmony Search Algorithm.....	31
1.4.3.7	Big bang- big crunch Optimization.....	32
1.4.3.8	Particle Swarm Optimization.....	33
1.4.4	Constraint Handling Methods.....	34
1.4.4.1	Penalty Functions Method.....	35
1.4.4.2	Fly-back Mechanism.....	38
1.5	Literature Survey.....	38
1.6	Scope of Work.....	40
<b>2</b>	<b>PARTICLE SWARM ALGORITHM.....</b>	<b>42</b>
2.1	Introduction.....	42
2.1.1	Swarm Intelligence.....	42
2.1.2	Evolutionary Computation.....	44
2.2	Particle Swarm Algorithm.....	45
2.2.1	Inertia Weight.....	49
2.2.2	Control Parameters.....	49
2.2.3	Vmax.....	49
2.2.4	Neighborhood Topology.....	50
2.3	Particle Swarm Optimization in Continuous Design Space.....	52
2.3.1	Numerical Examples in Continuous Design Space.....	52
2.3.1.1	Example 1.....	52

2.3.1.2	Example 2 .....	56
2.3.1.3	Example 3 .....	61
2.3.1.4	Example 4.....	63
2.4	Particle Swarm Optimization in Discrete Design Space.....	67
2.4.1	Numerical Examples in Discrete Design Space.....	70
2.4.1.1	Example 1 .....	70
2.4.1.2	Example 2 .....	72
<b>3</b>	<b>OPTIMUM DESIGN OF RIGIDLY CONNECTED STEEL SWAY</b>	
	<b>FRAMES TO LRFD .....</b>	<b>74</b>
3.1	Steel Frames.....	74
3.2	Analysis of Frames.....	76
3.2.1	Matrix Stiffness Method.....	76
3.2.1.1	Analytical Model .....	77
3.2.1.1.1	Global and Local Coordinate System .....	78
3.2.1.1.2	Relationship between Local and global Coordinates.....	80
3.2.1.1.3	Degrees of Freedom.....	81
3.2.1.1.4	Relationship between Member End Forces and Member End Deformations... ..	83
3.2.1.1.5	Relationship between the Joint Displacements and Member End Deformations.....	89
3.2.1.1.6	Relationship between External Loads and Member Forces.....	91
3.3	Load and Resistance Factor Design for Rolled Beam-columns.....	93
3.3.1	Compact sections.....	96
3.3.2	Non-compact sections.....	97
3.3.3	Partially Compact Sections ... ..	98
3.3.4	Slender Sections .....	98
3.3.5	Load and Resistance Factor Design for Combined Strength in Rolled Beam- columns ... ..	100

3.3.5.1	Load and Resistance Factor Design for Beam-columns subject to Bending and Axial tension.....	100
3.3.5.2	Load and Resistance Factor Design for Beam-columns subject to Bending and Axial compression.....	102
3.3.5.2.1	Effective Length of a Beam-column Member.....	103
3.3.6	Load and Resistance Factor Design for Shear in Rolled Beam-columns.....	105
3.3.7	Load and Resistance Factor Design for Serviceability of Beam-columns.....	107
3.3.7.1	Deflection.....	108
3.3.7.2	Drift.....	109
3.3.7.3	Geometric Compatibility.....	110
3.4	Optimum Design of Steel Frames.....	111
3.4.1	Mathematical Model of Optimum Design Problem of Unbraced Steel Frames.....	112
3.4.2	Optimum Design of Steel Frames in Continuous Design Space....	115
3.4.3	Optimum Design of Steel Frames in Discrete Design Space.....	118
3.4.4	Particle Swarm Optimization Design of Unbraced Steel Frames ..	119
3.4.5	Design Examples.....	120
3.4.5.1	Three Storey, Two Bay Steel Frame.....	121
3.4.5.2	Four Storey, Four Bay Steel Frame.....	123
3.4.5.3	Five Storey, Three Bay Steel Frame.....	125
3.4.5.4	Six Storey, Two Bay Steel Frame.....	128
3.4.5.5	Ten Storey, One Bay Steel Frame.....	131
3.4.5.6	Ten Storey, Three Bay Steel Frame.....	134
3.4.5.7	Fifteen Storey, Three Bay Steel Frame.....	137
<b>4</b>	<b>OPTIMUM DESIGN OF SEMI-RIGID STEEL SWAY FRAMES TO LRFD.....</b>	<b>141</b>
4.1	Semi-Rigid Connections.....	141
4.2	Types of Semi-Rigid Connections.....	148

4.2.1	Single Web-angle Connections and Single Plate Connections .....	148
4.2.2	Double Web-angle Connections.....	149
4.2.3	Top and Seat Angle Connections .....	150
4.2.4	Top and Seat Angle Connections with Double Web Angle.....	151
4.2.5	Extended End – Plate Connections and Flush End-Plate Connections. ....	151
4.2.6	Header Plate Connections .....	154
4.3	Modeling of Semi-Rigid Connections .....	155
4.3.1	Polynomial Model .....	156
4.4	Analysis of Unbraced Steel Frames with Semi-Rigid Connections .....	158
4.4.1	End-plate without Column Stiffeners Model .....	163
4.4.2	Top and Seat Angle with Web Cleats Model.....	166
4.5	Particle Swarm Optimization Design of Unbraced Steel Frames with Semi-Rigid Connections .....	174
4.6	Design Examples.....	175
4.6.1	Three Storey, Two Bay Steel Frame .....	176
4.6.2	Four storey, four bay steel frame .....	179
4.6.3	Five storey, three bay steel frame.....	181
4.6.4	Six Storey, Two Bay Steel Frame .....	184
4.6.5	Ten Storey, Three Bay Steel Frame .....	188
4.6.6	Fifteen Storey, Three Bay Steel Frame .....	191
<b>5</b>	<b>OPTIMUM DESIGN OF RIGID AND SEMI-RIGID STEEL SWAY FRAMES INCLUDING SOIL-STRUCTURE INTERACTION .....</b>	<b>195</b>
5.1	Characteristics of Soils.....	195
5.2	Nonlinear Behavior of Soils.....	195
5.3	Soil-structure interaction.....	198
5.3.1	Modeling the Soil-Structure Interaction.....	200
5.3.1.1	Idealized Soil Behavior Models .....	201
5.3.1.1.1	Elastic Models.....	201
5.3.1.1.1.1	Winklerian Spring Model.....	202

5.3.1.1.1.2	Elastic Continuum Models .....	205
5.3.1.1.1.3	Two Parameter Elastic Models .....	206
5.3.1.1.1.4	Finite Element Models .....	207
5.3.1.1.2	Elastic-Plastic, Perfectly Plastic Models .....	208
5.3.1.2	Winklerian Modeling of Planar Steel Frame-Soil Interaction System .....	209
5.4	Particle Swarm Optimization Design of Rigid and Semi-Rigid Steel Frames Including Soil-Structure Interaction.....	217
5.4.1	Design Examples .....	219
5.4.1.1	Three Storey-Two Bay Steel Frame .....	219
5.4.1.2	Four storey-Four Bay Steel Frame .....	223
<b>6</b>	<b>SUMMARY AND CONCLUSIONS .....</b>	<b>226</b>
6.1	Overview and Summary of the Thesis .....	226
6.2	Conclusions .....	228
	<b>REFERENCES.....</b>	<b>230</b>
	<b>CV .....</b>	<b>239</b>

## LIST OF TABLES

### TABLES

<b>Table 2.1</b>	Sensitivity analysis of PSO parameters.....	54
<b>Table 2.2</b>	PSO algorithm parameters used for Himmelblau's Function .....	55
<b>Table 2.3</b>	Optimum solutions for Himmelblau's function .....	55
<b>Table 2.4</b>	PSO algorithm parameters used for welded beam design.....	57
<b>Table 2.5</b>	Optimum solutions for welded beam design.....	60
<b>Table 2.6</b>	Optimum solutions for pressure vessel design.....	63
<b>Table 2.7</b>	Optimum solutions for spring design .....	66
<b>Table 2.8</b>	PSO algorithm parameters used for discrete design example 1 .....	71
<b>Table 3.1</b>	Optimum designs for three-storey, two-bay rigid steel frame.....	122
<b>Table 3.2</b>	Optimum designs for four-storey, four-bay rigid steel frame .....	125
<b>Table 3.3</b>	Optimum designs for five-storey, three-bay rigid steel frame .....	127
<b>Table 3.4</b>	Optimum designs for six-storey, two-bay rigid steel frame.....	130
<b>Table 3.5</b>	Optimum designs for ten-storey, one-bay rigid steel frame.....	133
<b>Table 3.6</b>	Optimum designs for ten-storey, three-bay rigid steel frame.....	136
<b>Table 3.7</b>	Optimum designs for fifteen-storey, three-bay rigid steel frame .....	140
<b>Table 4.1</b>	Standardized Connection Constants.....	157
<b>Table 4.2</b>	Optimum designs for three-storey, two-bay rigid steel frame.....	178
<b>Table 4.3</b>	Optimum designs for four-storey, four-bay steel frame.....	180
<b>Table 4.4</b>	Optimum designs for five-storey, three-bay steel frame.....	183
<b>Table 4.5</b>	Optimum designs for six-storey, two-bay steel frame .....	186
<b>Table 4.6</b>	Optimum designs for ten-storey, three-bay steel frame .....	190
<b>Table 4.7</b>	Optimum designs for fifteen-storey, three-bay steel frame.....	194
<b>Table 5.1</b>	Stress-strain and corresponding modulus of elasticity values of each linear segment obtained from nonlinear	

stress-stress curve.....	213
<b>Table 5.2</b> Optimum designs for three-storey, two-bay steel frame .....	222
<b>Table 5.3</b> Optimum designs for four-storey, four-bay steel frame.....	224

## LIST OF FIGURES

### FIGURES

<b>Figure 1.1</b>	Geometry of a steel frame with semi-rigid connections .....	3
<b>Figure 1.2</b>	Two-variable optimum design problem.....	6
<b>Figure 1.3</b>	A sizing structural optimization problem .....	14
<b>Figure 1.4</b>	A shape optimization problem.....	14
<b>Figure 1.5</b>	Topology optimization of a simple truss .....	15
<b>Figure 1.6</b>	Diagram for iterative steps of a numerical optimization method .....	19
<b>Figure 1.7</b>	Path which is designed by ants to reach the destination .....	29
<b>Figure 1.8</b>	Global minimum in the feasible space.....	35
<b>Figure 2.1</b>	Examples of swarm intelligence found in the nature.....	43
<b>Figure 2.2</b>	Demonstration of an update in the velocity vector of a particle.....	47
<b>Figure 2.3</b>	Flowchart of the basic particle swarm algorithm.....	48
<b>Figure 2.4</b>	Different neighborhood topologies.....	51
<b>Figure 2.5</b>	Design-history graph for Himmelblau's function.....	56
<b>Figure 2.6</b>	Welded beam design.....	57
<b>Figure 2.7</b>	Design-history graph for the welded beam design .....	60
<b>Figure 2.8</b>	Pressure vessel design.....	62
<b>Figure 2.9</b>	Design-history graph for the pressure vessel design .....	63
<b>Figure 2.10</b>	Spring design .....	64
<b>Figure 2.11</b>	Design-history graph for the spring design.....	67
<b>Figure 2.12</b>	Particle swarm optimization in discrete design space .....	69
<b>Figure 2.13</b>	Contour plot of the function $f(x) = 5x_1^2 - 9x_1x_2 + 5x_2^2$ .....	71
<b>Figure 2.14</b>	Three Dimensional plot of the function $f(x) = 5x_1^2 - 9x_1x_2 + 5x_2^2$ .....	72
<b>Figure 3.1</b>	Column, beam and beam-column members of a frame .....	75
<b>Figure 3.2</b>	Analytical model of a simple frame.....	78

<b>Figure 3.3</b>	Global and local coordinates.....	79
<b>Figure 3.4</b>	Relationship between Global and Local axes.....	81
<b>Figure 3.5</b>	Degrees of Freedom of a simple frame.....	82
<b>Figure 3.6</b>	End deformations and end forces of a rigid frame member .....	83
<b>Figure 3.7</b>	A small piece of a rigid frame member .....	86
<b>Figure 3.8</b>	Derivation of the second column of the stiffness matrix [ $k$ ] for rigid frame member r. ....	88
<b>Figure 3.9</b>	Member end forces and end displacements in local coordinates.....	89
<b>Figure 3.10</b>	Member end forces and end displacements in global coordinates.....	90
<b>Figure 3.11</b>	Most common rolled steel sections used in practice.....	94
<b>Figure 3.12</b>	W (wide-flange) shape steel beam.....	95
<b>Figure 3.13</b>	Classification of cross sections for local plate buckling.....	96
<b>Figure 3.14</b>	End connections of a rigid beam-column member .....	103
<b>Figure 3.15</b>	Nominal shear strength of a W section.....	106
<b>Figure 3.16</b>	Geometry of beam to column connection.....	111
<b>Figure 3.17</b>	Graphical representations of cross-sectional properties of 272 W- sections. ....	117
<b>Figure 3.18</b>	Three storey-two bay steel frame.....	121
<b>Figure 3.19</b>	Design history graph for three-storey, two-bay steel frame .....	123
<b>Figure 3.20</b>	Four storey- four bay steel frame.....	124
<b>Figure 3.21</b>	Design history graph for four-storey, four-bay steel frame.....	125
<b>Figure 3.22</b>	Five storey- three bay frame .....	126
<b>Figure 3.23</b>	Design history graph for five-storey, three-bay steel frame .....	128
<b>Figure 3.24</b>	Six storey- two bay frame.....	129
<b>Figure 3.25</b>	Design history graph for six-storey, two-bay steel frame.....	131
<b>Figure 3.26</b>	Ten storey-one bay steel frame.....	132
<b>Figure 3.27</b>	Design history graph for ten-storey, one-bay steel frame.....	134
<b>Figure 3.28</b>	Ten storey- three bay steel frame.....	135
<b>Figure 3.29</b>	Design history graph for ten-storey, three-bay steel frame .....	137
<b>Figure 3.30</b>	Fifteen-storey, three-bay steel frame .....	138

<b>Figure 3.31</b>	Design history graph for fifteen-storey, three-bay steel frame.....	140
<b>Figure 4.1</b>	Moment- rotation behavior of connections.....	142
<b>Figure 4.2</b>	Comparison of semi-rigid connections vs. pinned and fixed connections with respect to moment distribution.....	143
<b>Figure 4.3</b>	Rotational deformation of a connection.....	144
<b>Figure 4.4</b>	P- $\Delta$ effect of unbraced frame .....	144
<b>Figure 4.5</b>	Connection moment-rotation curves.....	146
<b>Figure 4.6</b>	Single web-angle connections .....	149
<b>Figure 4.7</b>	Single plate connections .....	149
<b>Figure 4.8</b>	Double web-angle connection .....	150
<b>Figure 4.9</b>	Top and seat angle connection.....	150
<b>Figure 4.10</b>	Top and seat angle with double web angle connection .....	151
<b>Figure 4.11</b>	Extended End – Plate Connections (Tension Side Only).....	152
<b>Figure 4.12</b>	Extended End-Plate Connections (Tension and Compression Sides). .....	153
<b>Figure 4.13</b>	Flush End-Plate Connections.....	154
<b>Figure 4.14</b>	Typical Header Plate Connections.....	155
<b>Figure 4.15</b>	Semi-rigid plane beam member with rotational springs.....	158
<b>Figure 4.16</b>	Moment rotation behavior of semi-rigid connection .....	162
<b>Figure 4.17</b>	End-plate without column stiffeners.....	164
<b>Figure 4.18</b>	Top and seat angle with web cleats connection model.....	167
<b>Figure 4.19</b>	Bearing stress assumptions for seated connections .....	169
<b>Figure 4.20</b>	Top and seat angle with web cleats connection detail .....	170
<b>Figure 4.21</b>	Three storey-two bay steel frame.....	177
<b>Figure 4.22</b>	Design history graph for three-storey, two-bay steel frame .....	178
<b>Figure 4.23</b>	Four storey- four bay steel frame.....	179
<b>Figure 4.24</b>	Design history graph for four-storey, four-bay steel frame .....	181
<b>Figure 4.25</b>	Five storey- three bay steel frame.....	182
<b>Figure 4.26</b>	Design history graph for five-storey, three-bay steel frame .....	184
<b>Figure 4.27</b>	Six storey- two bay steel frame.....	185

<b>Figure 4.28</b>	Design history graph for six-storey, two-bay steel frame.....	187
<b>Figure 4.29</b>	Ten storey- three bay steel frame.....	189
<b>Figure 4.30</b>	Design history graph for ten-storey, three-bay steel frame .....	191
<b>Figure 4.31</b>	Fifteen-storey, three-bay steel frame .....	192
<b>Figure 4.32</b>	Design history graph for fifteen-storey, three-bay steel frame.....	194
<b>Figure 5.1</b>	Diagrammatic representation of soil as a three-phase system .....	196
<b>Figure 5.2</b>	Interaction between structure, foundation plate and soil .....	198
<b>Figure 5.3</b>	Redistribution of loads in a frame due to soil–structure interaction...	199
<b>Figure 5.4</b>	Surface displacements of the Winkler approach.....	202
<b>Figure 5.5</b>	Typical surface displacement profiles of an elastic continuum.....	205
<b>Figure 5.6</b>	Representation of soil-structure interaction with finite element approach. ....	208
<b>Figure 5.7</b>	A simple beam element with one rigid and one semi-rigid supports. ....	210
<b>Figure 5.8</b>	Representation of a simple planar frame-soil interaction .....	210
<b>Figure 5.9</b>	Soil-foundation-structure interaction systems .....	211
<b>Figure 5.10</b>	Stress-strain curves and Linearized load-deformation diagram .....	212
<b>Figure 5.11</b>	A simple strip foundation-soil interaction problem.....	216
<b>Figure 5.12</b>	Settlements of strip foundation resting on dense silica sand .....	217
<b>Figure 5.13</b>	Three storey-two bay steel frame.....	220
<b>Figure 5.14</b>	Design history graph for three-storey, two-bay steel frame .....	222
<b>Figure 5.15</b>	Four storey-four bay steel frame.....	223
<b>Figure 5.16</b>	Design history graph for four-storey, four-bay steel frame .....	225

## **LIST OF ABBREVIATIONS**

AISC-ASD	American Institute of Steel Construction-Allowable Stress Design
CBR	California Bearing Ratio
CPU	Central Processing Unit
EA	Evolutionary Algorithm
FR	Fully Restrained
GA	Genetic Algorithm
GRG	Generalized Reduced Gradient
LRFD-AISC	Load and Resistance Factor Design-American Institute of Steel Construction
NPT	Number of Particles
PR	Partially Restrained
PSO	Particle Swarm Optimization
SA	Simulated Annealing
TSWC	Top and Seat Angle with Web Cleats

# **CHAPTER 1**

## **INTRODUCTION**

### **1.1 Modeling of steel frames**

Structural design is one of the prime tasks of a structural engineer. In the design process, the first step is to select the topology of the structural systems. In the case of steel skeletal frame, designer has to adopt steel profiles from the steel sections table available in practice for the beams and columns of the frame such that the response of the frame under the external loads is within the limitations imposed by steel codes. In order to determine the behavior of the frame, designer has to carry out structural analysis of the frame with the selected steel sections. This necessitates structural modeling of the frame under consideration. Designers make some assumptions particularly about beam-to-column and column-to-support connections to simplify the analysis problem. It is apparent that to determine the realistic behavior of a steel frame, one has to use a realistic modeling of these connections. Determination of the realistic behavior yields realistic design of the frame. Hence, it is important that designer models the steel frame under consideration such that its response to external loads is close to response of the constructed frame.

In the analysis and design of steel frames, the realistic modeling of beam-to-column connections provides an accurate response of the frame under the external loads. In practice, these connections are assumed to be either fully

rigid or perfectly pinned. In the former assumption, it is implied that there is no relative rotation of connection and the column takes the whole end moment of the beam. On the other hand, the pinned connection assumes that the moment of connection is always zero and there is no existing restraint for rotation of the connection. However, experiments have revealed that the real behavior of beam-to-column connections is between these extremes. Namely, all these practically used connections possess some stiffness falling between two cases mentioned above. Moreover, it is found that there exists a nonlinear relation of relative beam-to-column rotation when a moment is applied to a flexible connection [1]. These partially restrained connections influence the drift ( $P-\Delta$  effect) of the whole structure as well as the moment distribution in beams and columns. Use of a direct nonlinear inelastic analysis is one way to account for all these effects in frame design [2]. To be able to implement such analysis, beam-to-column connections should be assumed and modeled as semi-rigid connections.

## **1.2 Semi-Rigid Steel Frames**

The semi-rigid connection flexibility depends on the geometric parameters of the elements used in beam-to-column connection such as dimensions of end plates and bolt size. A typical steel frame with semi-rigid connections, which is modeled by attaching rotational springs, is illustrated in Figure 1.1.

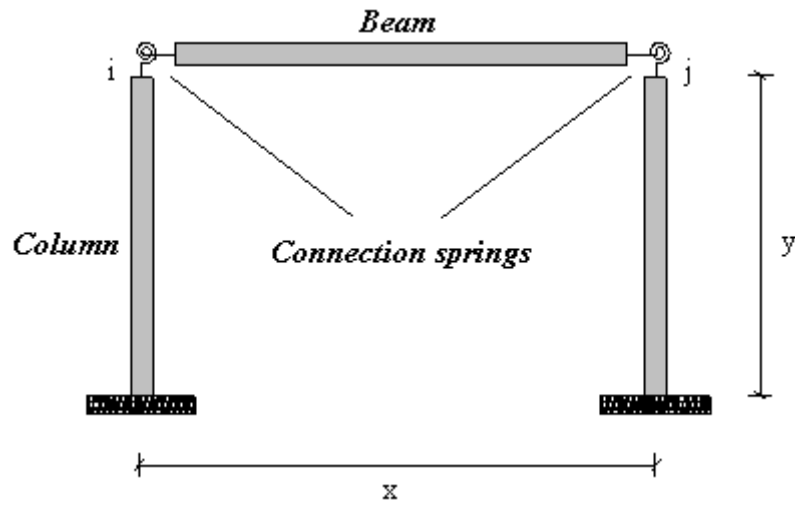


**Figure 1.1** Geometry of a steel frame with semi-rigid connections.

### **1.3 Soil-Structure Interaction**

Soil, as an elastic material, behaves nonlinearly after the initial loading. This behavior is also time-dependent. This nonlinearity is the main factor of the uncertainties of static behavior of soil-foundation-superstructure system after construction.

Due to these uncertain behaviors of soil, the realistic structural modeling of three dimensional buildings necessitates to consider the superstructure, its foundation and the soil on which it rests as a complete system. This requirement comes from the fact that any differential settlement within the foundation system of the building effects the internal force distribution in its members. The importance of this effect depends upon the load settlement characteristics of the soil and the rigidity of the superstructure. In contrast to this fact, in the analysis and design of a structure, supports are considered to

be either fixed or pinned without paying any attention to the characteristics of the soil on which structure rests. The usual practice to account for the soil under the foundation is to assume the soil as an elastic media which implies that the reaction forces of the foundation at every point are proportional to the deflection of the foundation at that point. This assumption leads to the representation of the underlying soil by closely spaced, independent springs. In some other studies, a stretched elastic membrane subjected to a constant-tension field at the top ends of the spring was additionally introduced, in order to achieve mathematically simple, but more realistic representation.

Furthermore, in some other works, a vertically incompressible beam was placed on the springs which only deformed by transverse shear. There are also finite element formulations in the literature.

## **1.4 Optimization**

Since the earlier history, due to the limited sources in the nature, human beings have tried to maximize the profit, economize the energy and keep the outgoings, discomforts and pain at minimum. This phenomenon can be possible only if the best one amongst all choices, which are the ways of accomplishing the tasks in the course of day-to-day events, is made. Therefore, it is required to decide upon the optimal way. The process, optimization, as a mathematical application of this aim, is concerned with achieving the best outcome of a given operation while satisfying certain restrictions.

As a more general definition, the term ‘optimization’ can be defined as the science of determining the best solution to a mathematically defined problem,

which is generally a model of a physical reality. Every activity in which numerical information is processed is in the bound of applicability of optimization.

In order to consider attaining certain goals in an optimal manner, one should first define the objective. Objective functions defined in an optimization problem represent some quantity, such as profit or cost that is willing to be optimized. Afterwards, the design variables and constraints should be properly identified on problem formulation state. Types of design variables may also vary depending on the class of problems and needs. Constraints usually consist of either system limitations or physical and economic laws that the variables must satisfy. A general structural optimization problem can be expressed as selecting optimal values of the design variables such that the specified objective function is the minimum and constraints that are generally non-linear functions of these variables, are satisfied. Mathematical model of a typical optimization problem is expressed as in the following.

$$\text{Minimize } z = f(\mathbf{x}) \quad (1.1)$$

Subject to:

$$h_j(\mathbf{x}) = 0, \quad j = 1, 2, \dots, p \quad (1.2)$$

$$g_k(\mathbf{x}) \leq 0, \quad k = p+1, \dots, m \quad (1.3)$$

$$\mathbf{x}_i \in \mathbf{X}, \quad \mathbf{X} = \{x_1, x_2, \dots, x_q\} \quad (1.4)$$

where,  $f(\mathbf{x})$  is the objective function and  $\mathbf{x}$  is design variable vector. In most of the optimization problems, the constraint functions are grouped as equality constraints  $h_j$  and inequality constraints  $g_k$ . In addition, some structural

optimization problems require the use of geometric constraints, which vary dependent upon the type of the problem.  $X$  represents the set of design variables and  $q$  is the total number of these variables. Number of constraints which restrict the objective function is represented by  $m$  [3].

The selection of the objective and constraint functions defined in terms of the quantities does condition the structural optimization design. In practice, weight of the structure is the most commonly used objective function due to the fact that it is readily quantified. Typical inequality constraints considered in most structural optimization problems are displacement or/and stress limitations.

Geometric representation of the optimum design problem which consists of two design variables is shown in Figure 1.2. Upper and lower limits may be specified for each designated stress and displacement amplitude for each alternative load condition; so that a large number of constraint surfaces are present.

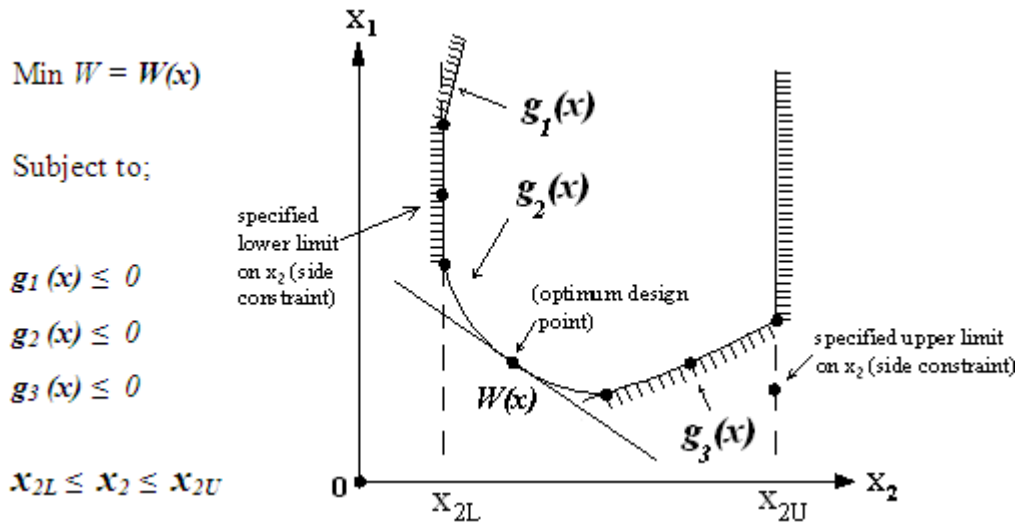


**Figure 1.2** Two-variable optimum design problem.

Side constraints appear as planes parallel to the coordinate directions when they refer to minimum or maximum values of the design variables. If a design point located in the space above the composite constraint surface, it is in free space and known as a feasible-design or exterior point. Conversely, a design point that represents the violation of constraints is infeasible or interior. In geometric terms, Figure 1.2 discloses that the optimum-design problem consists in finding the optimum design point of the weight and constraint surfaces [4]. Sometimes optimization problems appear to be unconstrained problems. At this time, since there are no constraints, all points are feasible and hence one needs to be concerned only with the value of  $f(\mathbf{x})$  at neighboring points.

### **1.4.1 Optimization Models**

Representation of an optimization problem in a mathematical formulation is a critical step in the optimization process. Acceptability of a solution for an optimization problem is dependent upon the correct formulation of three basic ingredients, namely design variables, objective functions and constraints. Depending on the problem, models of optimization problems can be divided into two categories as continuous optimization problems and discrete optimization problems.

#### **1.4.1.1 Continuous-Variable Models**

This model can be stated as an optimization problem which involves variables for which it is possible to take an intermediate value from an interval of real

numbers. For instance, cross-sectional area of a beam and length of an aircraft wing can be assumed to be variables of two continuous optimization problems. Continuous optimization can detect branch mis-predictions earlier and thus reduce the mis-prediction penalty.

#### **1.4.1.2 Discrete-variable Models**

Discrete-variable models involve discrete set of variables. These variables describe a finite set of conditions and take values from a finite, usually small, set of states. In most of the practical applications of optimization, discrete variables occur naturally in the formulation of the problem. For instance, material properties must correspond to the available materials or number of bolts must be integer.

The distinction between discrete and continuous quantities is rather vague, while the distinction between discrete and continuous variables is crisp. Many quantities can be represented as both discrete and continuous. In general, discrete variables are convenient approximations of real world quantities, sufficient for the goal of reasoning.

#### **1.4.2 Structural Optimization**

In the last three decades a prominent progress has been achieved in the field of structural analysis. With the help of computer almost all structural problems can be solved within the limits of human beings' knowledge of materials. While these achievements are of the greatest importance in allowing the

behavior of a particular design to be assessed, their full benefits for the society will not be materialized until they are reflected in the improved design of structures.

The purpose of inventing better design solutions which, while satisfying safety and performance constraints, do it at least cost, is clearly not a new one. From the time of earlier history engineers have investigated several alternatives and chosen the best one of these. Unfortunately, many factors limit severely the number of alternatives that can be investigated. After the implementation of computerization to the structural analysis process, it is natural that a development of more effective and rapid techniques for the search of the optimum structural design is required.

The optimal design of structures, theoretically, aiming at designing economical and reliable structures and systems at various conditions and technological constraints, is an important branch of general science of optimization.

Much work has been done in the field of structural optimization in recent years and obviously many techniques exist in the literature. Still, rapid changes in methods and focus are being witnessed in this relatively new field. However, there is lack of applications to practical design problems in spite of the huge amount of literature on the subject. This imbalance is redressed gradually. These hopeful applications result in the increase in the use of structural optimization methods to real-life problems.

However, these real-life problems, sometimes, may be so complex that due to the high computational cost the designers cannot afford to analyze them several times. Besides, in the analysis of structures most of the designers use general-purpose software packages such as finite element based commercial

software. Generally, the source program of the algorithms cannot be accessed and the engineers have only scant knowledge of the details of the analysis programs used in these software packages.

Designers have shown great interest to structural design optimization when it was first emerged. With the aid of this tool a systematic solution to age-old structural design problems, handled by utilizing trial-error methods or engineering intuition or both, is provided.

Traditional algorithms for structural design optimization are usually driven with deterministic mathematical re-sizing procedures and essentially one design is replaced through the iteration until a convergence criterion is reached. These gradient-based and direct algorithms are founded upon a uniquely human field depicting physical and natural phenomena. Direct and gradient-based algorithms are powerful search and optimization tools which can be effectively used in structural optimization problems. Direct mathematical methods can be described as point-to-point search algorithms employing objective function and constraints to guide the search through the feasible design space while gradient-based methods are the algorithms which utilize derivatives of objective functions and/or constraint equations to guide the search. Convergence of both methods depends upon the selection of an initial solution for subsequent modification through iteration and design variable changes.

Mathematical algorithms are generally problem-specific and the efficiency and ability of the algorithm in finding the optimum varies. Practical engineering problems often use discrete design variables such as structural steel cross-section sizes in building design.

The structural optimization problems usually need more than one objective function, such as, minimum weight which is related to cost, maximum stiffness, minimum displacement at specific structural points and minimum structural strain energy provided that the design satisfies all the constraints. These problems are called as multi-objective optimization problems. For instance, it is often required that a structure be stiff enough so that the maximum deflection is within the prescribed limit. The design constraints provide bonds on member stress, deflection, local buckling, system buckling, frequency and dynamic response. Since mathematical programming methods tackle with continuous design variables, the algorithms developed has provided to designer cross-sectional dimensions that were neither practical nor standard.

Consequently, from practical point of view the structural design optimization methods without discrete set of variables cannot be effectively used in real-life problems. As a result, efforts have been concentrated on the use of discrete variables in structural optimization algorithms.

#### **1.4.2.1 Structural Optimization Problems**

Discrete structural optimization problems can be expressed as finding optimum values for discrete member design vector  $\mathbf{x}$  that minimizes the objective function  $f(\mathbf{x})$ , which is restricted by the constraints related to the design and the behavior of the structure. Structural optimization algorithms are generally formulated to tackle optimization problems whose statements take the following general form [5];

Find a design vector  $\mathbf{x}$ ,  $\mathbf{x}_i \in X$  ,  $X = \{x_1, x_2, \dots, x_q\}$

For weight optimization;

$$f(\mathbf{x}) = \sum_{i=1}^q \gamma_i L_i x_i \quad (1.5)$$

Subject to;

$$\mathbf{g}'_j(\mathbf{x}) = \sigma_j^i - \sigma_j^a \leq 0 \quad \begin{array}{l} j = 1, \dots, q \\ l = 1, \dots, n \end{array} \quad (1.6)$$

$$\mathbf{f}'_k(\mathbf{x}) = u_k^i - u_k^a \leq 0 \quad \begin{array}{l} k = 1, \dots, m \\ l = 1, \dots, n \end{array} \quad (1.7)$$

$$\mathbf{X}_{lb} \leq \mathbf{x} \leq \mathbf{X}_{ub} \quad (1.8)$$

Where;

$f(x)$  : the objective function (usually the weight of the structure)

$\mathbf{X}$  : table of available discrete size

$q$  : total number of design variables or elements

$n$  : total number of load condition

$m$  : total number of displacement constraints

$\gamma_i$  : the specific weight of the  $i$ -th element

$L_i, x_i$  : the length and the cross sectional area of the  $i$ -th element respectively

$\sigma'_i, \sigma_i^a$  : the absolute value of stress under the  $l$ -th load condition and allowable stress in the  $i$ -th element respectively.

$u_k^l, u_k^a$  : the absolute value of displacement under the  $l$ -th load condition at the degree of freedom corresponding to the  $k$ -th displacement constraint and corresponding allowable value respectively.

$X_{lb}$  : the vector of lower bounds on design variables

$X_{ub}$  : the vector of upper bounds on designs variables

The complexity of optimum design problem can vary dramatically depending on the number of these objective functions, number of constraints and size of the decision space. In addition, the mapping of decision space to objective space can lead to increased problem complexity [5].

Structural optimization problems, depending on the geometrical feature, are divided to three main categories as; sizing optimization, shape optimization, topology optimization.

#### **1.4.2.1.1 Sizing Optimization Problems**

In a simple sizing optimization problem generally cross-sectional areas of each element are selected as design variables. Structure is optimized by obtaining the areas of individual elements that minimize the weight or maximize the stiffness. Sizing optimization is the simplest way of doing structural optimization. A simple sizing optimization problem for a truss structure is illustrated in Figure 1.3. [6].

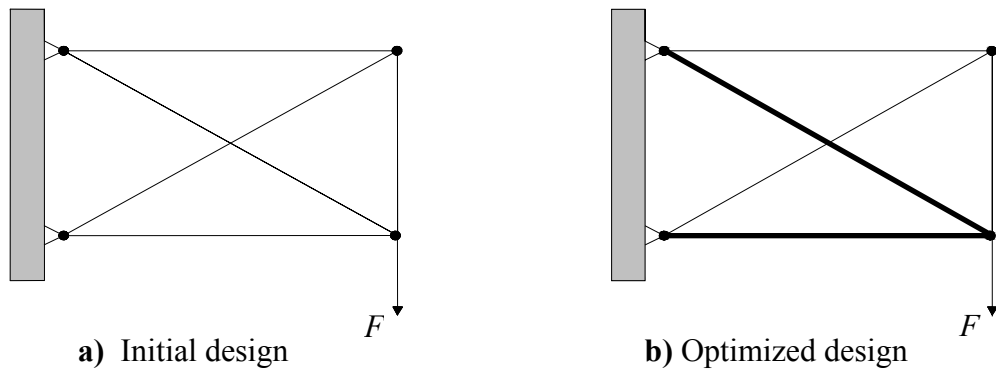


**Figure 1.3** A sizing structural optimization problem.

### 1.4.2.1.2 Shape Optimization Problems

In the case of shape optimization problem structural design variables represent the form or contour of some part of the boundary on the structural domain. Minimization of mass can be led by changing or determining boundary shape while satisfying all design requirements. For over three decades, the subject of shape optimization has been a topic of in-depth research. It has been implemented into several commercial finite element programs [5]. Geometric representation of a two-dimensional shape optimization problem is illustrated in Figure 1.4 [6] where  $\eta(x)$  denotes the shape of the beam-like structure.

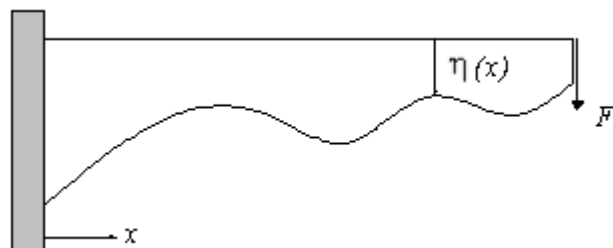


**Figure 1.4** A shape optimization problem.

### 1.4.2.1.3 Topology Optimization Problems

The topology or “landscape” of the structure must be an outcome of the procedure. In principle the result of a topology optimization procedure is also optimal with respect to shape and size, however it should be noted that fundamental differences in the design parameterization means that direct comparisons are difficult in practice [5].

Topological optimization of a simple structure can be achieved by considering cross-sectional areas of members to be design variables, and then allowing these variables to take the value zero. In other words, bars are removed from the truss. In this way, the connectivity of nodes becomes variable and the topology of the structure changes (Figure 1.5.).

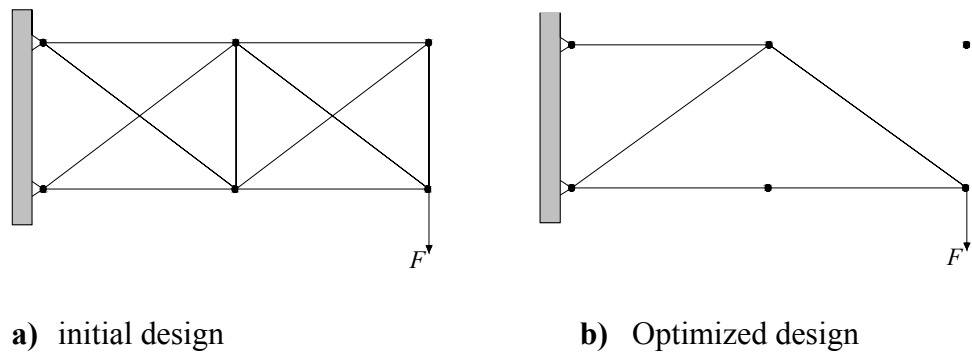


**Figure 1.5** Topology optimization of a simple truss.

### **1.4.2.2 Structural Optimization Methods**

Optimization theory and methods tackle with selecting the best alternative in the sense of a given objective function. These methods are perceived to be at the heart of computer methods for designing engineering systems. With the help of these methods, the designer can evaluate more alternatives, thus leading to a better and more cost-effective design. Structural optimization methods can be categorized as numerical methods and analytical methods. Numerical methods emphasize the algorithmic aspect, while analytical methods are concerned with the conceptual aspect.

#### **1.4.2.2.1 Analytical Methods**

In the determination of optimum solutions for layouts or geometrical form of simple structural elements such as beams, columns and plates, analytical methods usually apply mathematical theory of calculus, variation methods, etc. They do determine the parameter values of the theoretical model on the basis of known experimental results. One can easily state that these analytical methods are most convenient for such fundamental studies of single structural components. The design of structural systems is represented by a number of unknown functions and the purpose is to find out the form of these functions. Theoretical determination of the optimal design is made through the solution of a system of equations expressing the optimality conditions.

Analytical methods have great importance on the design optimization of structures. Although they sometimes have insufficiency of the practical aspects of realistic structures, when they can be found, they provide valuable insight

and theoretical lower bound optimum against which more practical designs may be judged. Structural design optimization problems employing the analytical methods are known as continuous problems or distributed parameter optimization problems.

#### **1.4.2.2.2 Numerical Methods**

The solution of practical optimization problems, when the number of design variables is more than two or the constraint functions are complex, is challenging to obtain with use of closed form analytical solution methods. Thus, numerical method based algorithms are preferred to solve most structural optimization problems. These methods employ a branch in the field of numerical mathematics called mathematical programming. Recent developments of the numerical methods seem to be result of rapid growths in computer capacities.

Numerical methods for the structural design optimization problems conceptually differ from analytical methods described above. In analytical methods one does write the optimality conditions and solve them for candidate local optimum designs. However, when numerical methods are used, a candidate design is selected as an initial estimate for the optimum point and improved until to further improvements are possible without violating any of the constraints. The process may require several cycles and number of these cycles is problem dependent. This iterative formula is acceptable for both constrained and unconstrained optimization problems.

In summary, the main concept of numerical methods is to start with a reasonable estimate for the optimal design. Objective and constraint functions

are calculated at that point. Based on these evaluations, the design is moved to a newly generated point. The process is repeated until a stopping criterion is satisfied. The general algorithm of this iterative scheme can be illustrated as in the following, which is also demonstrated graphically in Figure 1.6;

**Step 1.** Estimate an appropriate candidate design  $x^{(0)}$ . Set the iteration counter  $t = 0$ .

**Step 2.** Calculate a search direction  $d^{(t)}$  in the design space. This computation usually requires objective function value and its constraints.

**Step 3.** Check for convergence of the algorithm. If it has converged, terminate the process. Otherwise, continue.

**Step 4.** Compute a positive step size  $\alpha_t$ .

**Step 5.** Compute the new design as;

$$x^{(t+1)} = x^{(t)} + \alpha_t d^{(t)} \tag{1.9}$$

Set  $t = t + 1$  and go to Step 2.

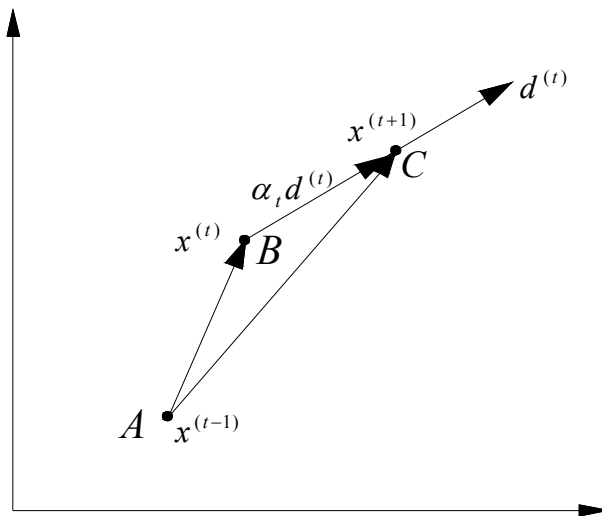


**Figure 1.6** Diagram for iterative steps of a numerical optimization method.

It can be clearly seen that such an iterative process represents an organized search through the design space for points which represents local minima. That is why the procedures are sometimes called the direct methods or search techniques of optimization.

Mathematical programming methods are basis of early numerical optimization algorithms. It is common for all of these optimization techniques that the design variables are considered to be continuous and the objective function values as well as constraints are expressed as functions of these variables. Many optimization techniques employ the gradient methods which require the first derivatives of objective and constraint functions with respect to the design variables.

Among the all mathematical programming methods, linear, quadratic, dynamic, and geometric programming algorithms are the ones which have been developed to deal with specific classes of optimization problems. In spite of its

relatively short history, there have been a large number of optimization algorithms which employ the mathematical programming.

Another approach for numerical optimization of structures is to derive, from mathematical considerations, conditions termed optimality criteria which must be fulfilled by an optimal solution. Although these conditions can be essential and sufficient for optimality, in most practical design problems, they are only necessary ones. The most important advantages of this method are that it can be easily programmed for the computer, it is independent of problem size and it requires relatively less number of structural analyses.

#### **1.4.2.2.1 Mathematical Programming**

Mathematical programming approach was first applied to structural optimization in the late 1950's. This approach was developed to solve large problems which have thousands of constraints and variables. Mathematical programming problems can be divided into two categories as linear programming and non-linear programming.

Non-linear programming problems, in which higher degrees of any variables or the reciprocal of the variables may appear, are more general than linear programming problems. It is developed for non-linear unconstrained optimization problems. Non-linear programming algorithms necessitate either gradient or differentiability information of both the objective function and constraints with respect to the design variables.

The simpler one of these is the linear programming problem, in which the variables are of first degree. In order to be able to apply linear programming

techniques to structural optimization problems, one must express the relationship between the objective function and the constraints as linear functions of design variables.

Linear programming problems, in which both objective function and constraints are linear, can be solved with gradient methods. Algorithm of this method starts with a feasible solution and proceeds through the direction of the gradient vector of the objective function until a point on the boundary of the feasible region is reached. At that point the direction of search is changed according to certain rules in an iterative manner until the value of the objective function is the maximum.

The programming methods of calculus of variations, such as the Galerkin method and the Rayleigh-Ritz method are limited to extremizing an integral without additional constraints. These methods make use of the approximation of the free functions by means of finite summations of appropriate known functions, for which the coefficients of the individual terms are determined, with the help of ordinary calculus in such a way that the value of the integral in question becomes a maximum or a minimum.

Kuhn-Tucker conditions and Lagrange equations are necessary conditions for optimum solutions of non-linear problems. These conditions provide very basic method for solving non-linear programming problems, although in practice very few problems can be solved by use of Lagrange equations.

#### **1.4.2.2.2 Optimality Criteria**

The concept of optimality criteria as the basis of selection of a minimum-volume structure emerged in the early 1960s. This approach derives from the extremum principles of structural mechanics, and for the most part has been limited to simple structural forms and loading conditions. Prager and Taylor have been instrumental in the development of much of this work. The procedures of Venkayya and Gellatly and Berke are the foremost procedures of employing this method. A detailed review of these procedures can be found in [4].

The methods of optimality criteria include two components. The first is the stipulation of the optimality criteria, which can be rigorous mathematical statements such as the Kuhn-Tucker conditions, or an intuitive one such as the stipulation that the strain energy density in the structure is uniform. The second ingredient is the algorithm used to resize the structure for the purpose of satisfying the optimality criterion [8].

Methods of optimality criteria assume continuous design variables. In the case where the discrete variables are considered, a two-step optimality criteria procedure is used. First, optimum solution is obtained using continuous variables. Then, using these variables a set of discrete values is estimated. In an optimum solution procedure where the optimality criteria methods are used, the design variables represent a single cross-sectional property of a structural member. A number of functions of the selected design variable express all other cross-sectional properties of this member.

### **1.4.3 Stochastic Search Methods**

Optimization problems in practice depend mostly on several model parameters, noise factors, uncontrollable parameters, etc., which are not given fixed quantities at the planning stage. Typical examples from engineering and economics/operations research are; Material parameters (e.g. modulus of elasticity, yield stresses, allowable stresses, moment capacities, specific gravity), external loadings, friction coefficients, moments of inertia, length of links, manufacturing errors, tolerances, noise terms, demand parameters, technological coefficients in input-output functions, cost factors, etc.. Due to several types of stochastic uncertainties (physical uncertainty, economic uncertainty, statistical uncertainty, and model uncertainty) these parameters must be modeled by random variables having a certain probability distribution. In order to cope with these uncertainties, instead of relying on ordinary deterministic parameter optimization methods, stochastic search methods are applied [9].

Some of the optimization algorithms developed recently employ stochastic optimization methods in which random numbers are generated. Stochastic search methods do not require the evaluation of the gradients of the objective and constraint functions; however, they require more function evaluations. An advantage of these algorithms to nonlinear algorithms is that they can be applied to optimization problems involving discrete variables.

### **1.4.3.1 Genetic Algorithms**

Genetic algorithms are stochastic search techniques on the basis of the mechanism of natural selection as well as natural genetics and rely on the principle of Darwin's theory of survival of the fittest. Algorithms were first introduced by John Holland in the 1960s and developed by Holland, his students and colleagues in the 1960s and the 1970s [10].

Genetic algorithm routine starts with an initial set of random solutions called population. This population includes some individuals called chromosomes, representing a solution to the problem. Each chromosome is a string of symbols, which is usually a binary bit string. A positive value, generally called fitness value, is used to reflect the degree of "goodness" of the chromosome for the problem which would be highly related with its objective value.

The initial population is set by constructing each chromosome where all the variables are in a binary coded form. Each character in this code can take either the symbol of '0' or '1'. After the decoding process, the fitness of each solution string is evaluated. Throughout a genetic evolution, the fitter chromosome tends to yield good quality offspring which means a better solution to any problem. In each cycle of genetic operation, termed as an evolving process, a subsequent generation is created from the chromosomes in the current population. This can only succeed if a group of these chromosomes, generally called "parents" or a collection term "mating pool" is selected via a specific selection routine. The genes of the parents are mixed and recombined for the production of offspring in the next generation. It is expected that from this process of evaluation (manipulation of genes), the "better" chromosome will create a larger number of offspring, and thus has a higher chance of surviving in the subsequent generation, emulating the survival-of-the-fittest

mechanism in nature [10]. The cycle of evolution is repeated until a desired termination criterion is reached. This criterion can also be set by the number of evolution cycles, or the amount of variation of individuals between different generations, or a pre-defined value of fitness.

### **1.4.3.2 Tabu Search**

The philosophy of tabu search is to derive and exploit a collection of principles of intelligent problem solving. In this sense, it can be said that tabu search is based on selected concepts that unite the fields of artificial intelligence and optimization. The basic form of tabu search is founded on the ideas proposed by Fred Glover [11]. The method is based on the procedures designed to cross boundaries of feasibility or local optimality, which were usually treated as barriers. It is an iterative improvement procedure that starts from any initial solution and attempts to determine a better solution.

The algorithm begins by marching to a local minimum. To avoid retracing the steps used, the method records recent moves in one or more tabu lists. The original intent of the list was not to prevent a previous move from being repeated, but rather to insure it was not reversed. The tabu lists are historical in nature and form the tabu search memory. The role of the memory can change as the algorithm proceeds.

Algorithm is initialized with the random construction of initial design which is considered as the current solution. Design variables are then selected and a number of candidate designs are created considering the neighborhood of the current solution. All the candidate solutions are analyzed and objective function values are calculated. The one which has the lowest value is

determined and stored as the best candidate. It is checked if the best candidate is forbidden or not. If it is not forbidden then the candidate design is replaced by current solution, and the design is accepted and recorded in the tabu list. If a prohibited candidate satisfies the aspiration criterion, it replaces the current solution and tabu list is revised. If not the candidate design is not accepted and the search is carried on with the current design. Once all the design variables are selected, a single iteration is completed. This procedure is repeated until the predefined number of generations is completed.

### **1.4.3.3 Evaluation Strategies**

Evolution strategies is an optimization technique developed in 1963 [12]. The strategy performs well in domains where it is impossible, difficult or expensive to define a precise mathematical description of the problem at hand. The method deals with vectors of real numbers for the representation of designs and optimization parameters. It is very similar to genetic algorithms. The main differences between evolutionary strategies and the genetic algorithms are the method of selection and whether the sensible strategy parameters are adjusted or not. Moreover, only the best fit individuals are allowed to reproduce in the evolution strategies method. Steps of the algorithm can be summarized as follows;

Algorithm is initialized generating a number of parent individuals to construct the initial population. Each individual in the initial population is evaluated. Parent population then undergoes recombination and mutation operators to yield the offspring population. With recombination, a trade of design information between the parents is provided to generate new individuals. Mutation, on the other hand, is the main operator of evolution strategies. It is

based on a normal distribution requiring the mean  $\xi$  and the standard deviation  $\sigma$ . In order to determine the survivors out of parent and offspring populations, selection should be implemented. The selected individuals become the parents of the next generations. This procedure is repeated until the predefined number of generations is completed.

#### **1.4.3.4 Simulated Annealing**

The simulated annealing is a random-search technique which utilizes an analogy between the way where a metal cools and freezes into a minimum energy crystalline structure (the annealing process) and the search for a minimum in a more general system; it forms the basis of an optimum design method for combinatorial and other problems.

The algorithm was developed in 1983 [12] to be able to solve highly nonlinear problems. The behavior of the algorithm is similar to solidification of metals or formation of crystals. The achievement of a number of solid states with different internal atomic or crystalline structure that correspond to different energy levels depends on the rate of cooling. If the cooling is too rapid, it is most likely that the resulting solid state would have a solid margin of stability because the atoms will assume relative positions in the lattice structure to reach an energy state which is only locally minimal. In order to obtain a more stable, globally minimum energy state, the annealing process is used where the metal is reheated to a high temperature and cooled slowly; letting the atoms enough time to find positions that minimize a steady state is reached.

The major advantage of the algorithm is an ability to avoid becoming trapped in local minima. Random search employed by simulated annealing accepts not

only changes that decrease the objective function value  $f$  (assuming a minimization problem), but also some changes that increase it. The cooling schedule is the main process of the algorithm. The cooling schedule of a simulated annealing algorithm involves four components as; starting temperature, final temperature, temperature reduction, iterations at each temperature.

Algorithm starts with a certain temperature value. It must be hot enough to allow a move to almost any neighborhood state. If it is not hot enough then the ending solution may be the same (or very close) with the starting solution. However, if the initial temperature is too high then the search can move to any neighbor and thus convert the search (at least in the early stages) into a random search. It is usual to allow the temperature decrease until its final value reaches zero. In practice, however, it is not essential to let the temperature reach zero because as it approaches to zero the possibility of accepting a worse design is almost the same as the temperature being equal to zero. To make the final temperature equal or close to zero a temperature reduction is needed. This is done by using simple linear method or geometric decrement method. Another important factor is the number of iterations at each temperature. A constant number of iteration at each temperature is a common scheme.

#### **1.4.3.5 Ant Colony Optimization**

The ant colony optimization is a meta-heuristic search technique which is used to find optimum solutions for combinatorial optimization problems, which is inspired by the foraging behavior of the social insects. The algorithm belongs to the class of model-based search algorithm. These types of algorithms are characterized by the probabilistic model which is used to generate solutions to

the optimization problem. Ant colony optimization algorithms use a given probabilistic model without changing the model structure during run-time.

Real ants have the capability of finding the shortest path from food to their nests. They can also adapt to changes in the environment, for instance, finding a new shortest path if the old one is no longer available. They can do this with the help of pheromone trails, which ants use to communicate information among individuals regarding the walking path or the decision about where to go. Once an ant finds a food source, it brings some of the food to the nest. It releases a pheromone trail on the ground while it is walking. Other ants find the food source following this pheromone trails deposited on the ground. Each ant would rather follow a direction rich in pheromone. They find the shortest path between their nest and the food sources with the help of this indirect communication [12], which is demonstrated in Figure 1.7.

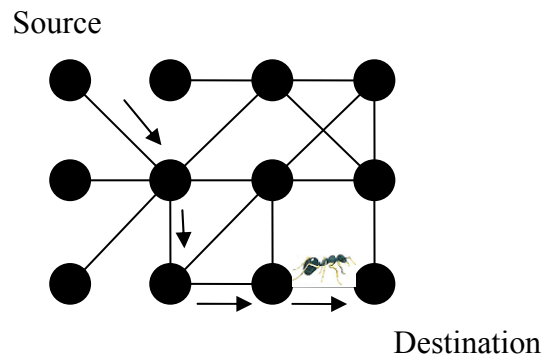


**Figure 1.7** Path which is designed by ants to reach the destination.

Ant colony algorithm can be summarized as follows: A set of agents, a colony of ants, moves through states of the problem corresponding to partial solutions of the optimization problem. They apply a stochastic local decision policy to

move. The trails and attractiveness are two parameters of the algorithm, which are the basis of this policy. By moving, each ant incrementally forms a solution to the problem. When an ant reaches to the destination .i.e. completes a solution, or during the construction phase, the ant evaluates the solution and modifies the trail value on the components used in its solution. This pheromone information will direct the search of the future ants [13]. The skeleton of ant colony optimization algorithm includes three major phases, namely, the initialization phase, the solution construction phase and pheromone updating phase.

In the initialization phase first the pheromone trail strength for all the edges is initialized. Then the number of artificial ants in a colony is set and each ant is put on a randomly chosen vertex. Afterwards, the termination criteria for the iteration looping are set up, which may be that the iteration number exceeds the predefined number of solution construction steps or that the computation time has exceeded a given CPU-time limit. Secondly, the solution construction phase starts. At the beginning of this phase, ants have already been put on randomly chosen vertices on the construction graph, and their paths consist of their initial vertices. In each construction step, all the ants arrange their feasible paths by moving to the next vertex based on the probabilistic decision according to the transition rule. After all the ants have moved once, their current feasible paths may be improved by applying local pheromone updating rule. When all the ants have completed their feasible paths, the solution construction phase is stopped. Then the pheromone trails are updated using global pheromone updating rule.

### **1.4.3.6 Harmony Search Algorithm**

Harmony search optimization is a stochastic optimization technique developed by Geem and Kim [14]. It is relatively simple method which imposes fewer mathematical requirements for the solution of optimization problems. It requires neither initial starting values for the decision variables nor the derivative information of the objective function and constraints. Therefore, it is easy to program harmony search method. As in the nature of stochastic optimization methods, harmony search algorithm starts with randomly selected candidate solutions to the optimization problem from a solution set. Feasible ones amongst all are selected and a harmony search memory in which each candidate solution is stored in descending order is constructed. Then the procedure is followed by filling the harmony memory matrix with new solutions depending on the parameters called the harmony memory considering rate and the pitch adjusting rate.

The idea behind the algorithm is found in the paradigm of natural phenomena. Harmony search algorithm, belonging to the class of meta-heuristic algorithms that seek a stable state, drives its roots in the harmony of a musical performance. In other words, it imitates the musical improvisation process in which the musicians search for the best harmony. Music harmony may be defined as a combination of sounds considered pleasing from an aesthetic point of view. For example, during jazz operation, jazz improvisation tries to obtain musically pleasing harmony as determined by an aesthetic standard. It is similar to an optimization process that seeks to find an optimum solution. The aesthetic quality is determined by the pitch of each musical instrument just as the set of values assigned to each design variable define the objective function value. Musicians can improve the sounds for better quality through practice

after practice, similarly, design values for better objective function evaluation can be improved iteration by iteration [15].

Algorithm starts with the specification of harmony search algorithm parameters (harmony memory size, harmony memory considering rate, pitch adjusting rate, number of objective function evaluations). Harmony memory is filled with as many randomly generated solution vectors as the size of the harmony memory. New harmony vector is then improvised by three rules as random selection, harmony memory consideration and pitch adjustment. If the new harmony vector is better than the worst harmony in the harmony memory, the new harmony and the existing worst harmony are replaced. This procedure is repeated until the predefined number of improvisation is reached.

#### **1.4.3.7 Big bang- big crunch Optimization**

The big bang-big crunch optimization method is a recent addition to meta-heuristic optimization techniques. This new optimization method is developed by Erol and Eksin [16] which has a low computational time and high convergence speed. The basic idea behind the algorithm is the theory of the evolution of the universe. Algorithm is divided into two main steps: The first is the big bang phase and the second step is the big crunch. In the former step, energy dissipation produces disorder and randomness just as in optimization method candidate solutions are randomly generated and distributed over the search space. In the big crunch step, randomly distributed particles are drawn into an order just as the optimization method a center of mass for the population is calculated by a contraction procedure. That is, the contraction operator takes the current positions of each candidate solution in the population and its associated objective function value and computes a center of mass. The

term mass refers to the inverse of the objective function value. After the big crunch phase, new positions of candidate solutions are generated using the center of mass.

These successive explosion and contraction phases are carried out repeatedly until maximum number of iterations has been met. The steps of the big bang-big crunch optimization method can be summarized as follows;

- 1) Big bang phase: Initial candidate solutions are randomly generated in the search space.
- 2) Objective function value of each candidate solution is calculated.
- 3) Center of the mass is determined.
- 4) Using center of the mass calculated in previous step new candidate solutions are obtained.
- 5) Step 2- 4 are repeated until termination criterion is satisfied.

#### **1.4.3.8 Particle Swarm Optimization**

Particle Swarm Optimization technique was firstly developed by Kennedy and Eberhart and has been used for various optimization fields [17]. It is a numerical optimization technique that simulates the social behavior of birds, fishes and bugs. In nature fish school, birds flock and bugs swarm not only for reproduction but for other reasons such as finding food and escaping predators. Similar to birds seek to find food, the optimum design process seeks to find the optimum solution. Each individual is called particle and whole

population is named as swarm. In the particle swarm optimization, each particle in the swarm represents a candidate solution of the optimum design problem.

Experiments show that the particle swarm method is an efficient and robust technique in finding the optimum solution [18-27].

In this study, optimum design of semi-rigid steel frames including soil structure interaction is determined by using particle swarm algorithm. This technique is discussed in detail in Chapter 2.

#### **1.4.4 Constraint Handling Methods**

There exist several ways of incorporating the constraints into the fitness function available in the literature [28]. Amongst all, penalty functions have been the most common way of incorporating constraints into meta-heuristic search techniques. One recent addition to these techniques is fly-back mechanism. The constraint handling methods work in a search space involving feasible and infeasible sub-spaces as illustrated in Figure 1.8.

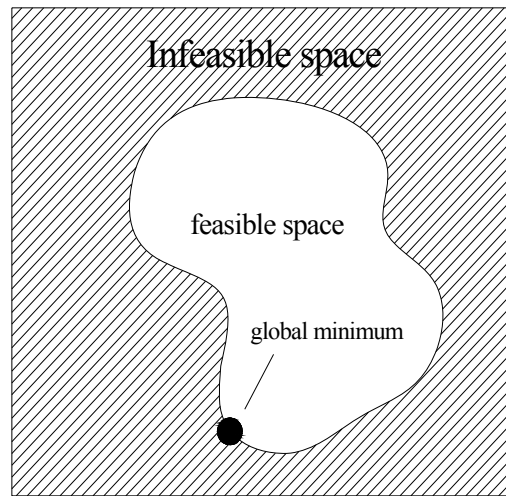


**Figure 1.8** Global minimum in the feasible space.

#### **1.4.4.1 Penalty Functions Method**

In the literature, the penalty functions approach has been employed in conjunction with all meta- heuristic search techniques. This approach was originally proposed in the 1940s [28]. The main concept of this method is transforming a constrained- design optimization problem into an unconstrained one by adding or subtracting a certain value to/from the objective function value based on the amount of constraint violation present in a certain solution. There are two kinds of penalty functions considered in classical optimization called exterior and interior methods. While employing the exterior methods, the process is initialized with an infeasible solution and let move towards the feasible region. In the case of latter methods, the penalty term is determined in such a way that its value will be small at points away from the constraint boundaries and will tend to be infinite as the constraint boundaries are

approached. Then, if starting point is feasible, the points generated subsequently will always lie within the feasible region. In most of the optimization problems, exterior penalty functions method is used due to the fact that this method does not require an initial feasible design. The formulation of exterior penalty functions method is given as follows;

$$\phi(x) = f(x) \pm \left[ \sum_{i=1}^n r_i \cdot G_i + \sum_{j=1}^p c_j \cdot L_j \right] \quad (1.10)$$

In which,  $\phi(x)$  is the expanded objective function to be optimized,  $G_i$  and  $L_j$  are the constraint functions and  $r_i$  and  $c_j$  are the constants called penalty factors.  $G_i$  and  $L_j$  is generally defined as in the following form;

$$\begin{aligned} G_i &= \max [ 0, g_i(x)^\beta ] \\ L_j &= |h_j(x)|^\gamma \end{aligned} \quad (1.11)$$

Where;  $g_i(x)$  and  $h_j(x)$  are the constraints,  $\gamma$  and  $\beta$  are generally 1 or 2.

Ideally, the penalty should be kept as low as possible, just above the limit below which infeasible solutions are optimal. This is due to the fact that if the penalty is too high or too low, then the problem might become very difficult. If the penalty is too high and the optimum lies at the boundary of the feasible region, the process will be pushed inside the feasible region very quickly, and will not be able to move back towards the boundary with the infeasible region. A large penalty discourages the exploration of the infeasible region since the

very beginning of the search process. On the other hand, if the penalty is too low, a lot of the search time will be spent exploring the infeasible region because the penalty will be negligible with respect to the objective function. These issues are very important in optimization algorithms, because many of the problems in which they are used have their optimum lying on the boundary of the feasible region. It is known that the relationship between an infeasible individual and the feasible region of the search space plays a significant role in penalizing such an individual [28].

Several researchers have studied heuristics on the design of penalty functions, one of which has the following guidelines [28]:

- 1) Penalties which are functions of the distance from feasibility are better performers than those which are only functions of the number of violated constraints.
- 2) For a problem having few constraints, and few feasible solutions, penalties which are solely functions of the number of violated constraints are not likely to produce any solutions.
- 3) Good penalty functions can be constructed from two quantities: the maximum completion cost and the expected completion cost. The completion cost refers to the distance to feasibility.
- 4) Penalties should be close to the expected completion cost, but should not frequently fall below it. The more accurate the penalty, the better will be the solution found. When a penalty often underestimates the completion cost, then the search may fail to find a solution.

#### **1.4.4.2 Fly-back Mechanism**

This method was first proposed to handle the constraints of the optimization problems employing particle swarm optimization technique. The intuitive idea to maintain a feasible population is for a design point to fly back to its previous position when it is outside the feasible region. This is the so called ‘fly-back mechanism’. The technique starts from a feasible initial population. A closed set of operators is used to maintain the feasibility of the solutions. If new design violates the constraints then previous design is returned. Therefore, the subsequent solutions generated at each iteration are also feasible. Algorithms based on this technique are much more reliable than those based on a penalty approach [22].

### **1.5 Literature Survey**

The studies and the algorithms developed in recent years for the particle swarm algorithm, optimum design of rigid and semi-rigid steel frames and the analysis of soil-structure interaction can be reviewed in a historical order as follows;

Particle swarm optimization technique [17-27] is originally formulated as a continuous optimization method, which is first introduced by Kennedy and Eberhart [18]. Continuous applications of this algorithm have been reported in He et al. [22]. Tasgetiren et al. [23] and Arumugam et al [25] have been the first researchers using binary numbers in particle swarm optimization to achieve discrete set. Liu et al. [24] used rounding off method in their research. A few studies in the literature, such as Li et al. [26], focused on improving the performance of particle swarm algorithm developed for solution of structural

optimization problems. Kaveh and Talatahari [27] increased the performance of particle swarm optimizer by hybridizing it with ant colony optimization algorithm.

Khan [29] and Saka and Kameshki [33] used optimality criteria for the optimum design of steel frames. Camp et al. [31] and Saka and Kameshki [34] used genetic algorithms to optimize the weight of framed structures. Huang and Arora [32], Park and Sung [35] employed SA in the optimum design of steel plane frames subjected to design constraints of American Institute of Steel Construction-Manual of steel construction: allowable stress design (AISC-ASD) [30]. An ant colony optimization based optimum design algorithm is developed for the design of steel frames by Camp et al. [36]. Degertekin [37] applied SA and GAs to the optimum design of geometrically non-linear steel space frames. Saka has presented an extensive review for the optimum design of steel frames in [38]. Recently, Dogan and Saka [39] carried out the particle swarm method based optimum design of steel frames with rigid end connections.

Chen and Kishi tackled the modeling of semi-rigid connections of steel frames in [40]. Hsieh and Deierlein [41] and Xu [42] dealt with the analysis of steel frames with semi-rigid connections. Hadianfard and Razani [43] considered the effects of semi-rigid behavior of the connections in the finite element analysis and in the reliability analysis of steel frames. Various algorithms developed for the optimum design of steel frames with semi-rigid connections have been presented in [44-47]. Recently, Dogan and Saka [48] developed a particle swarm method based optimum design algorithm for partially restrained steel frames subjected to design constraints of American Institute of Steel Construction-Manual of steel construction: load and resistance factor design (LRFD-AISC) [49].

Literature in the soil-structure interaction area is rather extensive. Finite and boundary element methods and spring models [50-59] are the main approaches used to represent the soil media. Lysmer and Kuhlemeyer [53], Godbole et al. [54], Rizos [55] and Park et al. [56] are the ones dealing with the finite element and boundary element approaches. Vesic [58] and Allam and Subba [59] used this approach in their researches. Soil media can be represented using spring models, as presented in [57]. Dutta and Roy presented an extensive review for the modeling of soil-structure interaction in this study.

## **1.6 Scope of Work**

This thesis is concerned with optimum design of semi-rigid steel frames including soil-structure interaction, in which the optimum design algorithm is based on the particle swarm optimization method. The organization of the thesis is as in the following: In the first chapter, a brief introduction is given to semi-rigid steel frames, soil-structure interaction, optimization, structural optimization, an overview on existing structural optimization methods. In chapter 2, the fundamentals of particle swarm algorithm and the basis of the algorithm what is called swarm intelligence are discussed. In the last part of the chapter, numerical test problems available in the literature are solved by using particle swarm algorithm and the results are compared with those of other optimization techniques. Chapter 3 contains explanation of rigidly connected steel sway (moment resisting) frames, design of steel frames to LRFD, structural optimization of steel frames including the definition and selections of design variables. Several steel frames are optimized using particle swarm optimization and optimum designs are compared with the ones obtained with other stochastic optimization methods. In Chapter 4, semi-rigid

steel frames are carried out, design of such frames to LRFD is formulated, particle swarm optimization based optimum design algorithm is introduced and a number of semi-rigid steel frame examples are optimized with optimum design algorithm developed. Chapter 5 is devoted to the consideration of soil-structure interaction in the analysis and design of rigid and semi-rigid steel frames. In sixth and the last chapter, some brief discussions and conclusions are presented.

## **CHAPTER 2**

### **PARTICLE SWARM ALGORITHM**

#### **2.1 Introduction**

The particle swarm optimization method is one of the stochastic random search methods that is developed by Eberhart and Kennedy in 1995 [18], inspired by social behavior of bird flocking or fish schooling. This behavior is concerned with grouping by social forces that depend on both the memory of each individual as well as the knowledge gained by the swarm. The phenomenon behind this behavior is called swarm intelligence. Besides, the particle swarm optimization is also related to evolutionary computation, and has some common features with genetic algorithm and evolutionary strategies.

##### **2.1.1 Swarm Intelligence**

The basic definition of intelligence can be pointed out as; a word that is usually used to describe the mental abilities of humans, although it can be applied to other organisms and even to inanimate things such as computers. Collection of these agents that interact with one another is called swarm. Researchers have discovered that behavior of swarm is different from that of individual itself. Swarm intelligence, which is first used as an expression by Hackwood and

Wang [60] in the context of cellular robotic systems, is the discipline focuses on the collective behaviors that result from the local interactions of the individuals with each other and with their environment. Examples of systems studied by swarm intelligence are colonies of ants and termites, schools of fish, flocks of birds, herds of land animals. Some of them are illustrated in Figure 2.1.

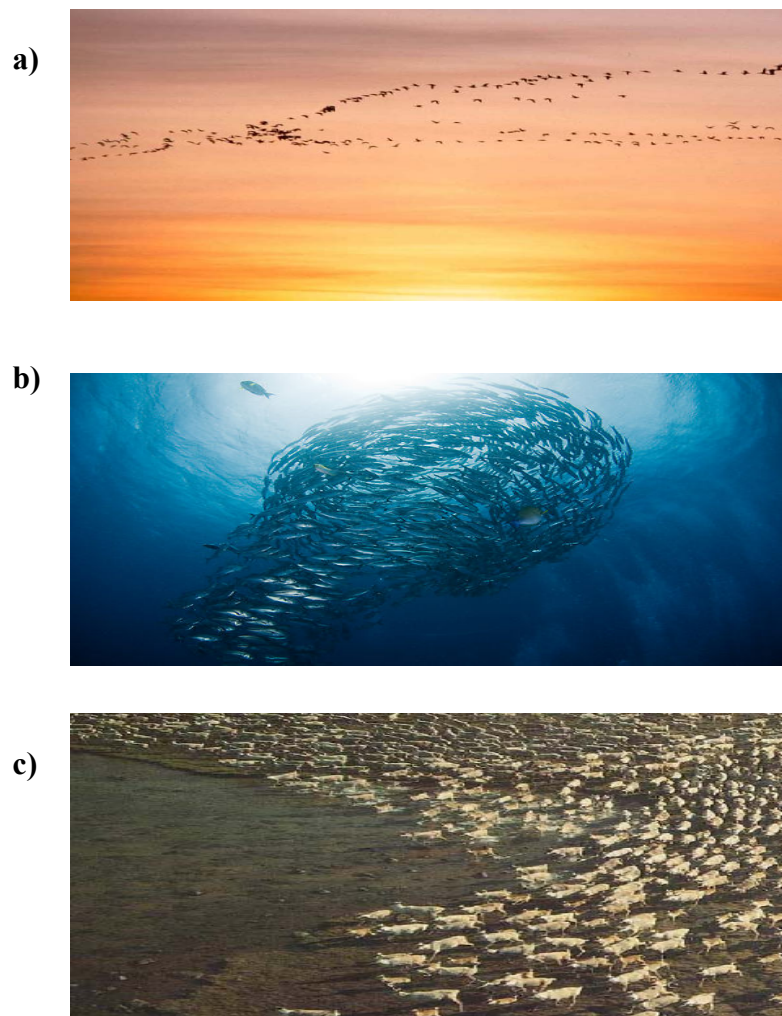


**Figure 2.1** Examples of swarm intelligence found in the nature **a)** Bird flocking, **b)** Fish schooling, **c)** Animal herding (<http://www.cs4fn.org/optimization/swarmintelligence.php>).

Swarm intelligence has some basic principles. The first, the proximity principle, means that swarm should be able to do elementary space and time computations. Because space and time translate into energy expenditure, the swarm should have some ability to compute the utility of a given response to the environment in these terms. Despite the kinds of activity may vary greatly, depending on both the type and complexity of the organisms, some typical activities consist of the search and retrieval of food, the building of nests, defense of the swarm, collective movement, and in the case of higher organisms, the interaction necessary for many social functions. Second is the quality principle: The swarm should be capable of responding not only to time and space considerations but to quality factors such as the quality of foodstuffs or safety of location. Third principle is the principle of diverse response which means that the swarm should not allot all of its resource along consumedly narrow lines. Resources should be distributed along many modes as insurance against the sudden change in any one of them. The last principle is the principle of stability where it is declared that the swarm should not change its behavior from one mode to another upon every fluctuation of the environment, since such changes take energy and may not produce a worthwhile return for the investment [61].

### **2.1.2 Evolutionary Computation**

Mind and evolution are known as the two great stochastic systems in nature. These systems have provided some of the most exciting challenges in the history of computer science. Modeling the information-processing methods of minds was the task of the artificial intelligence movement. Evolutionary computation, subfield of artificial intelligence, uses iterative progress, such as growth or development in a population. This population is then chosen in a

guided random search using parallel processing to obtain the desired end. Such processes are often inspired by biological mechanisms of evolution.

Evolutionary computing paradigms are closely related to the swarm methods. These paradigms provide tools to built intelligent systems that model intelligent behavior. Evolutionary computation is divided into four areas as; genetic algorithms, evolutionary programming, evolution strategies, genetic programming. Particle swarm algorithm has some common features with these areas. For example, particle swarm algorithm is similar to evolutionary programming, in which each population member is mutated to produce a candidate population member for the next generation. In addition, in both evolutionary strategies and particle swarm optimization, one parent can produce only one child. Moreover, particle swarm algorithm and genetic algorithms are similar in that the system is initialized with a population of random solutions.

## **2.2 Particle Swarm Algorithm**

Based on the natural phenomena emphasized above, the particle swarm optimization technique is developed to deal with many optimization problems in engineering. It is pretty simple mathematically, and has been applied to a wide range of problems in several different areas [17-27]. It can be thought of as a process whereby particles move in n-dimensional space, each particle being a solution and the space being the problem. Particle swarm algorithm defines three properties, one of which is velocity which directs movement throughout the problem space, and the rest of which are particle's best and global best which are communicated throughout the swarm. Particle's best represents the fitness of each solution so far and global best represents global

fitness of each solution as it passes through the problem space. Particles follow the neighboring optimum particles by adapting these properties in each iteration or generation.

The steps of the particle swarm algorithm can be outlined as in the following. The flowchart of the basic particle swarm optimization technique is also given in Figure 2.3.

1. Initialize swarm of particles with positions  $x_0^i$  and initial velocities  $v_0^i$  randomly distributed throughout the design space. These are obtained from the following expressions.

$$x_0^i = x_{\min} + r (x_{\max} - x_{\min}) \quad (2.1)$$

$$v_0^i = [(x_{\min} + r (x_{\max} - x_{\min})) / \Delta t]$$

where; the term  $r$  represents a random number between 0 and 1,  $x_{\min}$  and  $x_{\max}$  represent the design variables upper and lower bounds respectively.

2. Evaluate the objective function values  $f(x_k^i)$  using the design space positions  $x_k^i$ .
3. Update the optimum particle position  $p_k^i$  at the current iteration  $k$  and the global optimum particle position  $p_k^g$ .
4. Update the position of each particle from the following expression.

$$x_{k+1}^i = x_k^i + v_{k+1}^i \Delta t \quad (2.2)$$

Where;  $x_{k+1}^i$  is the position of particle  $i$  at iteration  $k+1$ ,  $v_{k+1}^i$  is the corresponding velocity vector and  $\Delta t$  is the time step value.

5. Update the velocity vector of each particle. There are several formulas for this depending on the particular particle swarm optimizer under consideration. The one has the following form.

$$v_{k+1}^i = wv_k^i + c_1r_1 \frac{(p_k^i - x_k^i)}{\Delta t} + c_2r_2 \frac{(p_k^g - x_k^i)}{\Delta t} \quad (2.3)$$

Where;  $r_1$  and  $r_2$  are random numbers between 0 and 1,  $p_k^i$  is the best position found by particle  $i$  so far, and  $p_k^g$  is the best position in the swarm at time  $k$ .  $w$  is the inertia of the particle which controls the exploration properties of the algorithm.  $c_1$  and  $c_2$  are the trust parameters. This expression is also shown schematically in Figure 2.2.

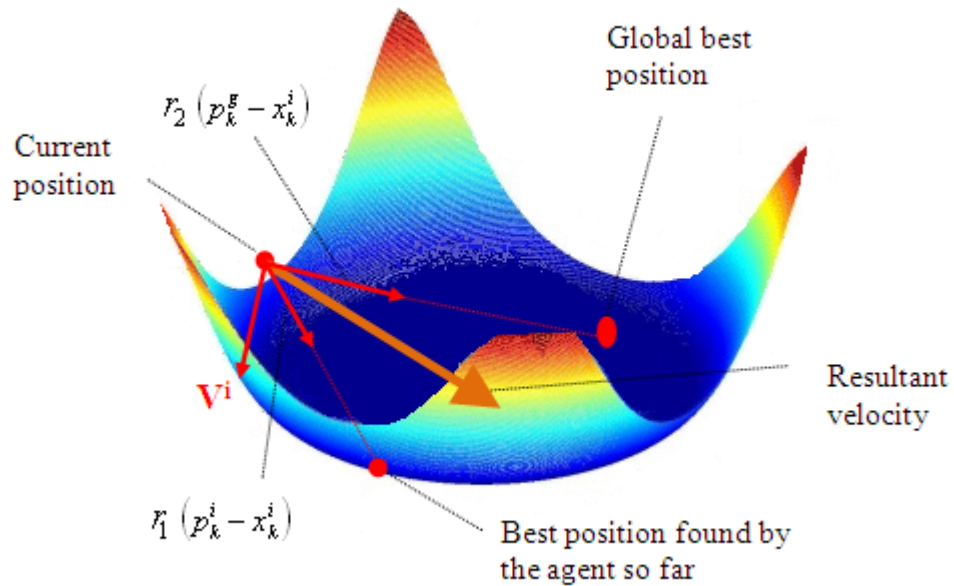


**Figure 2.2** Demonstration of an update in the velocity vector of a particle.

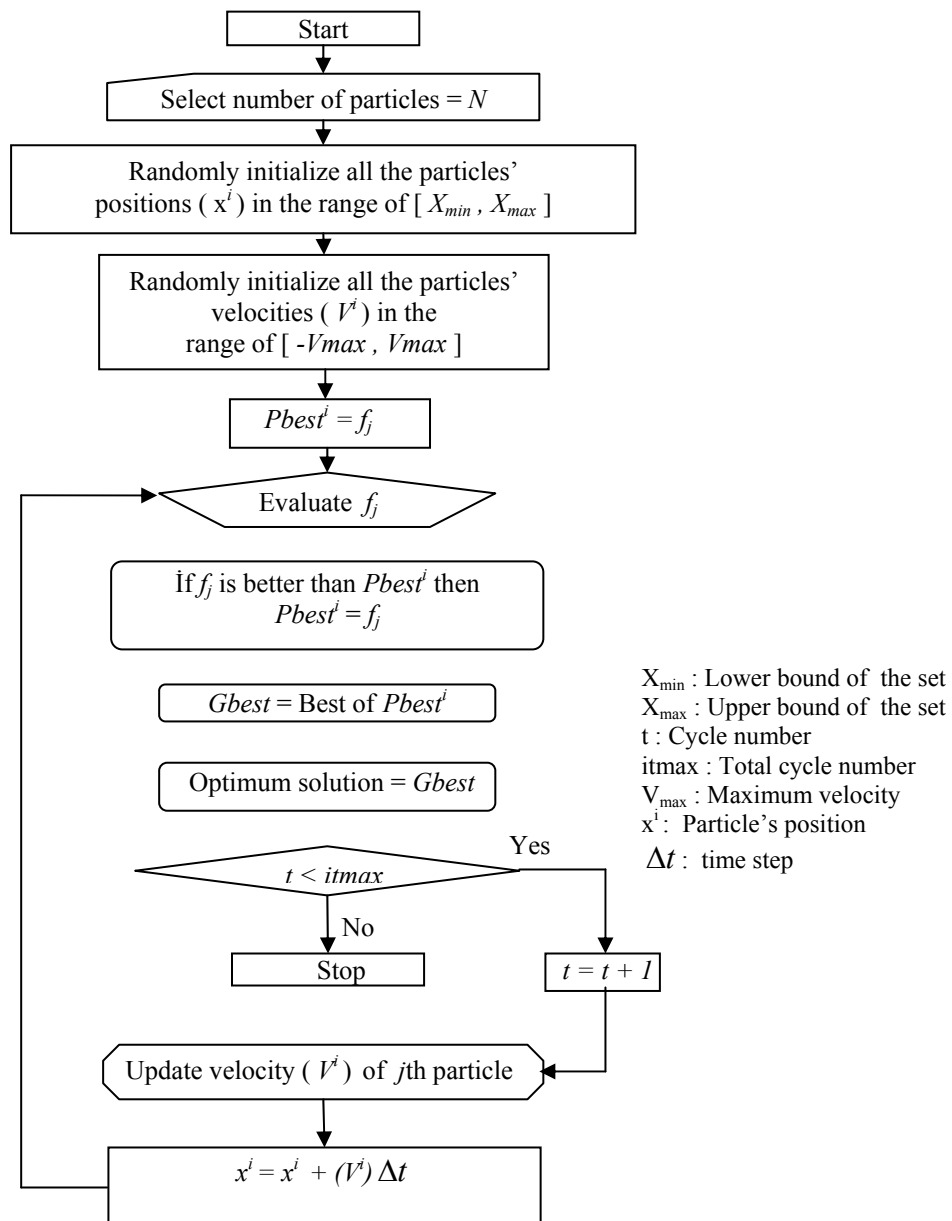


**Figure 2.3** Flowchart of the basic particle swarm algorithm.

### **2.2.1 Inertia Weight**

The inertia weight can be defined as a scaling factor associated with the velocity during the previous time step, resulting in a new velocity update equation. In other words, it is employed to control the impact of the previous history of velocities on the current velocity thereby, influencing the trade-off between global and local exploration abilities of the flying points. If larger inertia weight is selected then global exploration is facilitated, whereas a smaller inertia weight tends to facilitate local exploration. Suitable selection of inertia weight parameter makes it possible to have a balance between global and local exploration abilities and therefore optimization process requires less iteration to find the optimum.

### **2.2.2 Control Parameters**

The control parameter, sometimes called acceleration constant, is very important in determining the type of the path that particle travels. If selected value is very small then the trajectory rises and falls slowly over time. Specifically,  $c_1$  indicates how much confidence the particle has in itself whereas  $c_2$  indicates how much confidence the particle has in the swarm.

### **2.2.3 Vmax**

The particle swarm algorithm involves the modification of the distance that each particle moves on each dimension per iteration. Velocity changes in a

stochastic manner and if the result of this change is undesirable the particle's trajectory can expand into wider cycles through the problem space, eventually approaching infinity. A traditional method to reduce the oscillations is to restrict the velocity of the particle with a constant value called system parameter, a representation of which is illustrated as;

$$v^i > v_{\max} \quad \text{then} \quad v^i = v_{\max} \quad (2.4)$$

$$v^i < -v_{\max} \quad \text{then} \quad v^i = -v_{\max}$$

The system parameter  $V_{\max}$  has an important effect of preventing explosion and adjusts the exploration of the particle's search. It would be better to take smaller values in approaching an optimum.

## 2.2.4 Neighborhood Topology

An important feature of the particle swarm optimization algorithm is that the fitness information is shared with individuals in a particle's neighborhood. The robustness of the algorithm comes from the interactions of particles with their neighbors. As one particle explores a local optimum, it becomes the best in its neighbors' neighborhoods and they too attracted to the optimal region. As the particles move toward the new optimum, their search may uncover new regions which are even better, and they may end up attracting the first particle toward their best positions, and so on. The kind of neighborhood structure used affects the rate at which information is disseminated throughout the population.

There are two types of neighborhoods in which the particles have been studied; *gbest* and *lbest*. In the *gbest* neighborhood each particle is attracted to the best

solution found by any member of the swarm. This structure becomes equivalent to a fully connected network where each member of the swarm is able to compare the performances of every other member of the population, mimicing the very best. In the *lbest* network, on the other hand, each individual is affected by the best of its immediate neighbors. The selection of social structure used has been a matter of artistry with little data to help the researcher decide a strategy. It is determined that *gbest* neighborhood tends to converge more rapidly on optimum than *lbest* population, but are also more convenient to converge on local optimum. In Figure 2.4 three different neighborhood topologies are illustrated. In the star topology, every particle can communicate with every other particle and is attracted to the global best solution. In the ring (circle) topology, individuals which are distant from one another are also independent of one another, however neighbors are closely connected. The wheel topology, on the other hand, isolates individuals from one another, as all information has to be communicated through the focal individual. This focal individual compares all the individuals in the swarm and adjusts its trajectory through the best of them. Present study uses this type of neighborhood topology.

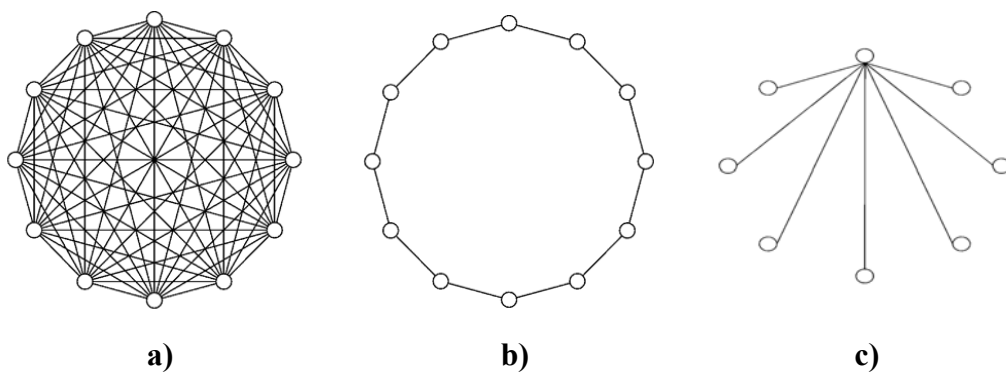


**Figure 2.4** Different neighborhood topologies: **a)** Star topology used in *gbest*; **b)** Ring topology used in *lbest*; **c)** Wheel topology (Focal)

## **2.3 Particle Swarm Optimization in Continuous Design Space**

Continuous optimization can be defined as the study of the problems where it is demanded to optimize a continuous function in which the variables take the values from real numbers. In real number space, the parameters of a function conceived as a point in multidimensional space. From this point of view, change over time is represented as movement of the points or particles.

Particle swarm optimization algorithm is originally developed as a continuous optimization method. It has been implemented to various optimization problems in real-number space and proved that it is simple to use, robust and it converges rapidly.

### **2.3.1 Numerical Examples in Continuous Design Space**

The particle swarm optimization method described in the previous sections is used to determine the optimum solutions of number of continuous optimization problems. Fly-back mechanism, a powerful constraint handling technique described in previous chapter, is used in each example.

#### **2.3.1.1 Example 1**

The first problem, called Himmelblau's function [62], is a commonly used benchmark function for nonlinear constrained optimization problems. This problem is adopted to test the performance of the particle swarm optimization

algorithm. Problem has five design variables and fifteen constraints. Problem definition and optimum design results are as in the following;

Minimize;

$$f(x) = 5.3578547x_3^2 + 0.8356891x_1x_5 + 37.293239x_1 - 40792.141 \quad (2.5)$$

Subject to;

$$0 \leq g_1(x) \leq 92$$

$$90 \leq g_2(x) \leq 110 \quad (2.6)$$

$$20 \leq g_3(x) \leq 25$$

and side constraints;

$$78 \leq x_1 \leq 102, \quad 33 \leq x_2 \leq 45, \quad 27 \leq x_3 \leq 45, \quad 27 \leq x_4 \leq 45, \quad 27 \leq x_5 \leq 45 \quad (2.7)$$

where;

$$g_1(x) = 85.334407 + 0.0056858x_2x_5 + 0.0006262x_1x_4 - 0.0022053x_3x_5$$

$$g_2(x) = 80.51249 + 0.0071317x_2x_5 + 0.0029955x_1x_2 + 0.0021813x_3^2 \quad (2.8)$$

$$g_3(x) = 9.300961 + 0.0047026x_3x_5 + 0.0012547x_1x_3 + 0.0019085x_3x_4$$

Himmelblau [62] first solved this problem by using the generalized reduced gradient (GRG) method. Then it is studied by Gen and Cheng [63] using genetic algorithm (GM). Runarsson and Yao [64] proposed an evolutionary strategies algorithm with stochastic ranking for the solution of this problem.

This problem is first used to test ten different parameter cases with varying set of particle swarm algorithm parameters (i.e. number of particles, control parameters, inertia weight,  $V_{max}$ ) shown in Table 2.1.

Since the original form of the particle swarm optimization technique uses continuous numbers as the design variables, the optimum design algorithm is easily applied to Himmelblau's function without any change in the structure of the procedure.

**Table 2.1** Sensitivity analysis of PSO parameters.

<i>Case</i>	<i>NPT</i>	$C_1$	$C_2$	$w$	$V_{max}$	$f(x)$
1	20	1	1	0.1	2	-29758.90
2	35	1.2	1.2	0.07	2	-30170.03
3	30	1.5	1.5	0.06	2	-30171.95
4	30	1.6	1.6	0.07	2	-30242.82
5	35	1.4	1.4	0.05	2	-30280.06
6	40	1.5	1.5	0.05	2	-30508.97
7	50	1.8	1.8	0.09	2	-30518.17
8	30	1.9	1.9	0.08	2	-30598.60
9	35	1.7	1.7	0.04	2	-30652.80
10	40	2	2	0.08	2	-30665.40

According to the test results listed above, best performance is obtained when the set in the case 10, in which the number of particles, i.e.  $NPT$ , is 40, control parameters ( $C_1$ ,  $C_2$ ) are 2, and the inertia weight and  $V_{max}$  are 0.08, 2 respectively, is implemented. The steps of the algorithm are repeated until maximum number of iterations is taken as 2000 as given in Table 2.2.

The results obtained with the particle swarm optimization technique are compared with the ones obtained with other methods mentioned above in Table 2.3. The PSO parameters used for this comparison are listed in Table 2.2. The convergence rate of the problem is shown in the design-history graph given in Figure 2.5.

**Table 2.2** PSO algorithm parameters used for Himmelblau's Function

<i>NPT</i>	<i>C<sub>1</sub></i>	<i>C<sub>2</sub></i>	<i>w</i>	<i>Vmax</i>	<i>Number of iterations</i>
40	2	2	0.08	2	2000

**Table 2.3** Optimum solutions for Himmelblau's function

<i>Optimum solutions obtained by different methods</i>				
<i>Design variables</i>	<i>PSO</i>	<i>Runarsson and Yao [64]</i>	<i>GRG [62]</i>	<i>Gen and Cheng [63]</i>
$x_1$	78.0000	78.0000	78.6200	81.4900
$x_2$	33.0003	33.0000	33.4400	34.0900
$x_3$	29.9962	29.9953	31.0700	31.2400
$x_4$	44.9999	45.0000	44.1800	42.2000
$x_5$	36.7734	36.7758	35.2200	34.3700
$g_1(x)$	92.0000	92.0000	91.7927	91.7819
$g_2(x)$	98.8402	98.8405	98.8929	99.3188
$g_3(x)$	20.0000	20.0000	20.1316	20.0604
$f(x)$	<b>-30665.40</b>	<b>-30665.54</b>	<b>-30373.95</b>	<b>-30183.58</b>

Results show that the particle swarm based optimum design algorithm has performed well in finding the optimum solution of continuous optimization problems.

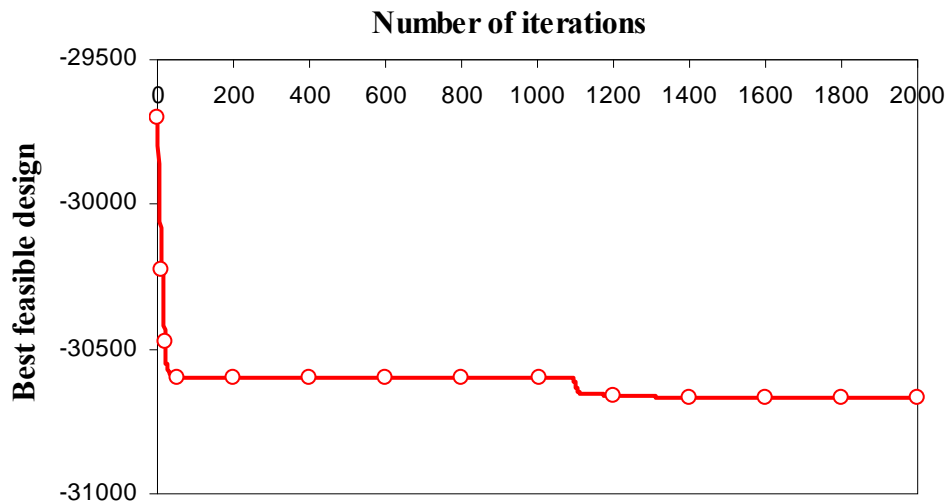


Figure 2.5 Design-history graph for Himmelblau's function.

### 2.3.1.2 Example 2

A rectangular beam, designed as a cantilever beam, is selected as second example. The geometric view and the dimensions of the beam are illustrated in Figure 2.6. The beam is designed to carry a certain load with minimum overall cost of fabrication. The optimization problem has four design variables.

$h = x_1$  : the thickness of the weld

$l = x_2$  : the length of the welded joint

$t = x_3$  : the width of the beam

$b = x_4$  : the thickness of the beam

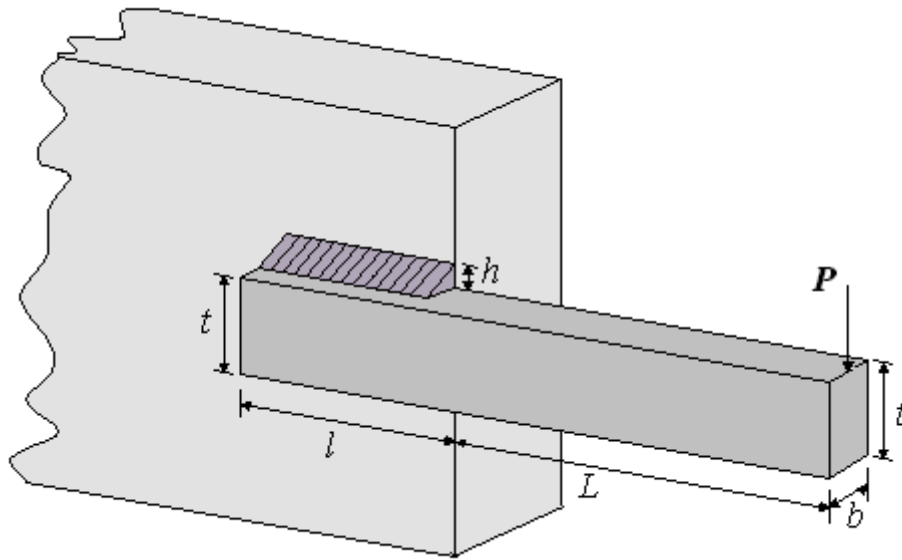


**Figure 2.6** Welded beam design.

The parameter set used for this problem is given in Table 2.4.

**Table 2.4** PSO algorithm parameters used for welded beam design.

<i>NPT</i>	<i>C1</i>	<i>C2</i>	<i>w</i>	<i>Vmax</i>	<i>Number of iterations</i>
40	2	2	0.08	2	1000

The mathematical model of welded beam problem given in [22] is repeated in the following;

Minimize;

$$f(x) = 1.10471x_1^2 x_2 + 0.04811x_3 x_4 (14.0 + x_2) \quad (2.9)$$

Subject to;

$$g_1(x) = \tau(x) - \tau_{\max} \leq 0 \quad : \quad \text{shear stress} \quad (2.10)$$

$$g_2(x) = \sigma(x) - \sigma_{\max} \leq 0 \quad : \quad \text{bending stress in the beam} \quad (2.11)$$

$$g_3(x) = x_1 - x_4 \leq 0 \quad : \quad \text{side constraint} \quad (2.12)$$

$$g_4(x) = 0.10471x_1^2 + 0.04811x_3 x_4 (14.0 + x_2) - 5 \leq 0 \quad : \quad \text{side constraint} \quad (2.13)$$

$$g_5(x) = 0.125 - x_1 \leq 0 \quad : \quad \text{side constraint} \quad (2.14)$$

$$g_6(x) = \delta(x) - \delta_{\max} \leq 0 \quad : \quad \text{end deflection of the beam} \quad (2.15)$$

$$g_7(x) = P - P_c(x) \leq 0 \quad : \quad \text{buckling load on the bar} \quad (2.16)$$

Where

$$\tau(x) = \sqrt{(\tau')^2 + 2\tau'\tau'' \frac{x_2}{2R} + (\tau'')^2} \quad (2.17)$$

$$\tau' = \frac{P}{\sqrt{2}x_1x_2} \quad (2.18)$$

$$\tau'' = \frac{MR}{J} \quad , \quad M = P(L + \frac{x_2}{2}) \quad (2.19)$$

$$R = \sqrt{\frac{x_2^2}{4} + \left(\frac{x_1 + x_3}{2}\right)^2} \quad (2.20)$$

$$J = 2 \left\{ \frac{x_1 x_2}{\sqrt{2}} \left[ \frac{x_2^2}{12} + \left(\frac{x_1 + x_3}{2}\right)^2 \right] \right\} \quad (2.21)$$

$$\delta(x) = \frac{4PL^3}{E x_3^3 x_4}, \quad \sigma(x) = \frac{6PL}{x_4 x_3^2} \quad (2.22)$$

$$P_c(x) = \frac{4.013 \sqrt{\frac{(E G x_3^2 x_4^6)}{36}}}{L^2} \left(1 - \frac{x_3}{2L} \sqrt{\frac{E}{4G}}\right) \quad (2.23)$$

$$P = 6000 \text{ lb}, \quad L = 14 \text{ in.}, \quad E = 30 \times 10^6 \text{ psi}, \quad G = 12 \times 10^6 \text{ psi} \quad (2.24)$$

$$\tau_{\max} = 13,600 \text{ psi}, \quad \sigma_{\max} = 30,000 \text{ psi}, \quad \delta_{\max} = 0.25 \text{ in.}$$

The side constraints for the design variables are given as follows:

$$\begin{aligned} 0.1 \leq x_1 \leq 2.0, \quad 0.1 \leq x_2 \leq 10 \\ 0.1 \leq x_3 \leq 10, \quad 0.1 \leq x_4 \leq 2.0 \end{aligned} \quad (2.25)$$

The same problem was also solved by Ragsdell and Philips [65] using geometric programming. Deb [66] used a simple Genetic Algorithm (GA) with traditional penalty function to solve the same problem. Ray and Liew solved this problem using a society and civilization algorithm [67].

The optimum design obtained by the particle swarm method is given in Table 2.5 where the minimum value of the objective function as well as the optimum values of design variables are shown. Particle swarm algorithm determined the lowest value for the objective function compare to other methods. It is apparent from the table that the optimum solution found by PSO is 25% smaller than the best of the rest. It took 1000 iterations to reach to optimum solution. The convergence rate of the problem is illustrated in Figure 2.7.

**Table 2.5** Optimum solutions for welded beam design.

<i>Optimum solutions obtained by different methods</i>				
<i>Des. var.</i>	<i>PSO</i>	<i>Ray and Liew [67]</i>	<i>Ragsdell and Phillips [65]</i>	<i>Deb [66]</i>
$x_1$	0.23886	0.2444	0.2455	0.2489
$x_2$	2.5296	6.2379	6.1960	6.1730
$x_3$	9.1796	8.2885	8.2730	8.1789
$x_4$	0.2389	0.2445	0.2455	0.2533
$f(x)$	<b>1.90308</b>	<b>2.3854</b>	<b>2.3859</b>	<b>2.4331</b>

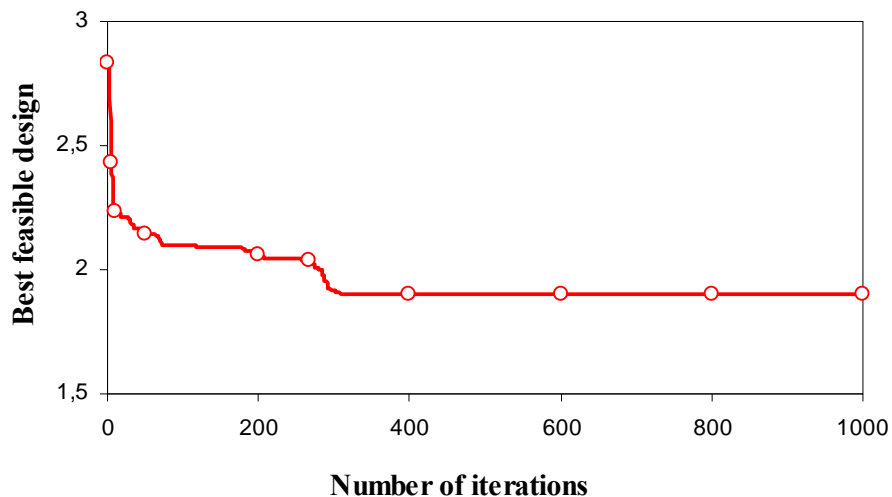


**Figure 2.7** Design-history graph for the welded beam design.

### 2.3.1.3 Example 3

The third example is the pressure vessel design problem which is shown in Figure 2.8 was first introduced by Sandgren [68]. The purpose of this optimization problem is to find the minimum cost of material, forming and welding of the pressure vessel. The design variables included in the problem are as follows;

$T_s = x_1$  : The shell thickness

$T_h = x_2$  : the thickness of the head

$R = x_3$  : The inner radius

$L = x_4$  : The length of the cylindrical section of the vessel

The optimum design problem of pressure vessel can be expressed as in the following;

Minimize;

$$f(x) = 0.6224x_1 x_3 x_4 + 1.7781x_2 x_3^2 + 3.1661x_1^2 x_4 + 19.84x_1^2 x_3 \quad (2.26)$$

Subject to;

$$g_1(x) = 0.0193x_3 - x_1 \leq 0 \quad (2.27)$$

$$g_2(x) = 0.00954x_3 - x_2 \leq 0 \quad (2.28)$$

$$g_3(x) = 1296000 - \pi x_3^2 x_4 - \frac{4}{3}\pi x_3^3 \leq 0 \quad (2.29)$$

$$g_4(x) = x_4 - 240 \leq 0 \quad (2.30)$$

and side constraints;

$$\begin{aligned} 0.0625 \leq x_1 \leq 6.1875, & \quad 0.0625 \leq x_2 \leq 6.1875 \\ 10 \leq x_3 \leq 200, & \quad 10 \leq x_4 \leq 200 \end{aligned} \quad (2.31)$$

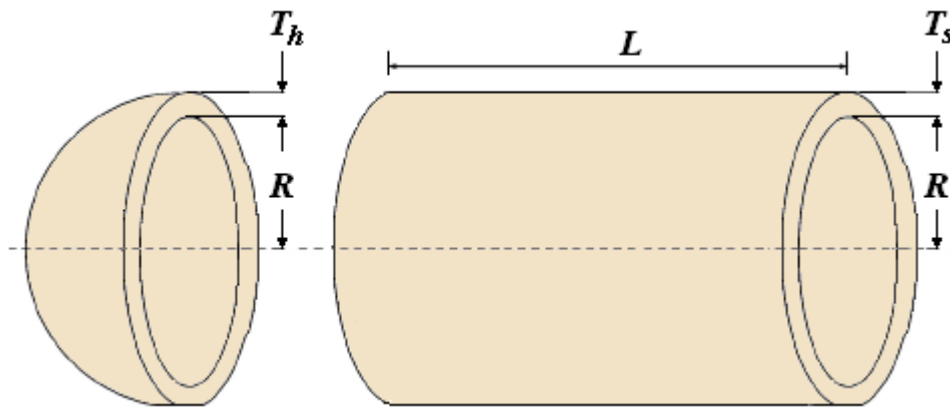


**Figure 2.8** Pressure vessel design.

Deb dealt with this problem in [69]. It has also been investigated by Cao and Wu [70].

The parameter set listed in Table 2.4 is also used for the pressure vessel design problem. For this problem, the maximum number of iterations is limited to 1000, corresponding to 40000 fitness function evaluation. The minimum objective function value is found as  $f(x)=6230.71$  which is obtained after 500 runs. The results are given in Table 2.6 and the time-history graph is shown in Figure 2.9.

**Table 2.6** Optimum solutions for pressure vessel design.

<i>Optimum solutions obtained by different methods</i>			
<i>Design variables</i>	<i>PSO</i>	<i>Deb [69]</i>	<i>Cao and Wu [70]</i>
$x_1$	0.7979	0.9345	1.000
$x_2$	0.3944	0.5000	0.625
$x_3$	41.3450	48.3290	51.1958
$x_4$	199.9843	112.6790	90.7821
$f(x)$	<b>6230.6960</b>	<b>6410.3811</b>	<b>7108.6160</b>

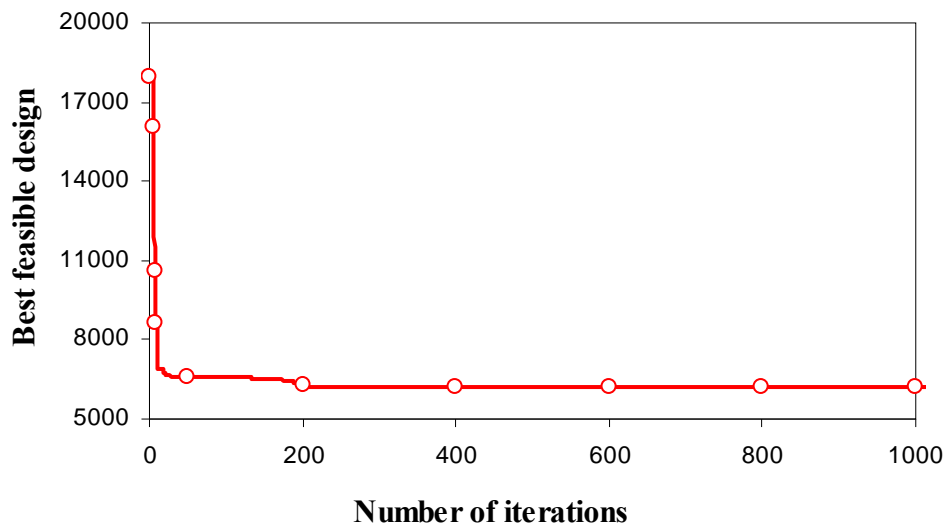


**Figure 2.9** Design-history graph for the pressure vessel design.

### 2.3.1.4 Example 4

Spring design is considered as the fourth example for the continuous particle swarm algorithm. The design problem as shown in Figure 2.10 has three design variables as;

$d = x_1$  : the wire diameter

$D = x_2$  : the mean coil diameter

$N = x_3$  : the number of active coils

This problem is first suggested by Belegundu [71] and Arora [72] and aims to minimize the weight of a tension/compression spring. There are four constraints which relate to minimum deflection, shear stress, surge frequency, and limits on outside diameter and design variables [72].

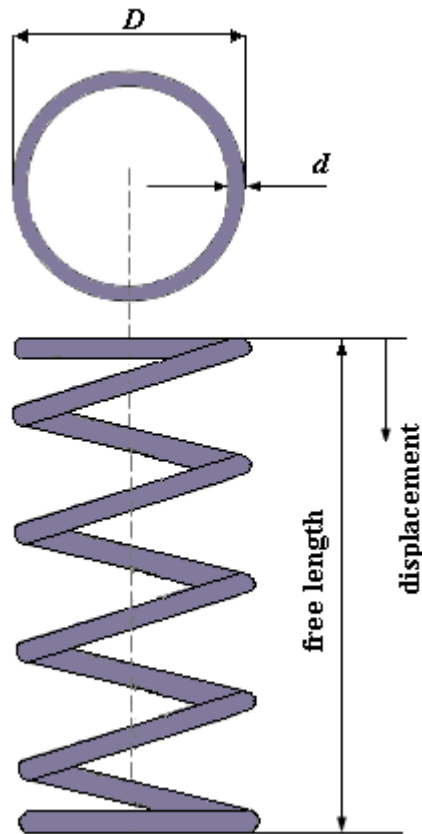


**Figure 2.10** Spring design.

The mathematical model of the problem can be expressed as follows;

Minimize;

$$f(x) = (x_3 + 2)x_2 x_1^2 \quad (2.32)$$

Subjected to;

$$g_1(x) = 1 - \frac{x_2^3 x_3}{71785x_1^4} \leq 0 \quad (2.33)$$

$$g_2(x) = \frac{4x_2^2 - x_1 x_2}{12566(x_2 x_1^3 - x_1^4)} + \frac{1}{5108x_1^2} - 1 \leq 0 \quad (2.34)$$

$$g_3(x) = 1 - \frac{140.45x_1}{x_2^2 x_3} \leq 0 \quad (2.35)$$

$$g_4(x) = \frac{x_1 + x_2}{1.5} - 1 \leq 0 \quad (2.36)$$

And side constraints;

$$0.05 \leq x_1 \leq 2, \quad 0.25 \leq x_2 \leq 1.3, \quad 2 \leq x_3 \leq 15 \quad (2.37)$$

The parameter set, excluding the maximum number of iteration, listed in Table 2.4 is also used for the pressure vessel design problem. The maximum number of iterations is taken as 4000 in this problem.

The same spring was also designed by Arora [72], Coello [73] and Ray and Liew [67]. Arora [72] proposed an optimization technique called constraint

correction at constant cost to solve the same problem. Coello and Carlos [73] solved this problem with a GA with a self-adaptive penalty approach to handle constraints. Ray and Liew [67] investigated this problem using an EA inspired by a formal society and the civilization model.

The optimum design obtained by the particle swarm method is given in Table 2.7 and the design-history graph obtained for the problem is shown in Figure 2.11. The optimum design is obtained after 3500 iterations. The minimum objective function value which is the weight of the spring is determined as  $f(x)=0.012666$ . Once again PSO has obtained the least weight compare to other techniques considered.

**Table 2.7** Optimum solutions for spring design.

<i>Optimum solutions obtained by different methods</i>				
<i>Design variables</i>	<i>PSO</i>	<i>Ray and Liew [67]</i>	<i>Coello [73]</i>	<i>Arora [72]</i>
$x_1$	0.05194	0.05216	0.05148	0.05339
$x_2$	0.36266	0.36816	0.35166	0.39918
$x_3$	10.9483	10.6484	11.6322	9.18540
$f(x)$	<b>0.012666</b>	<b>0.012669</b>	<b>0.012704</b>	<b>0.012730</b>

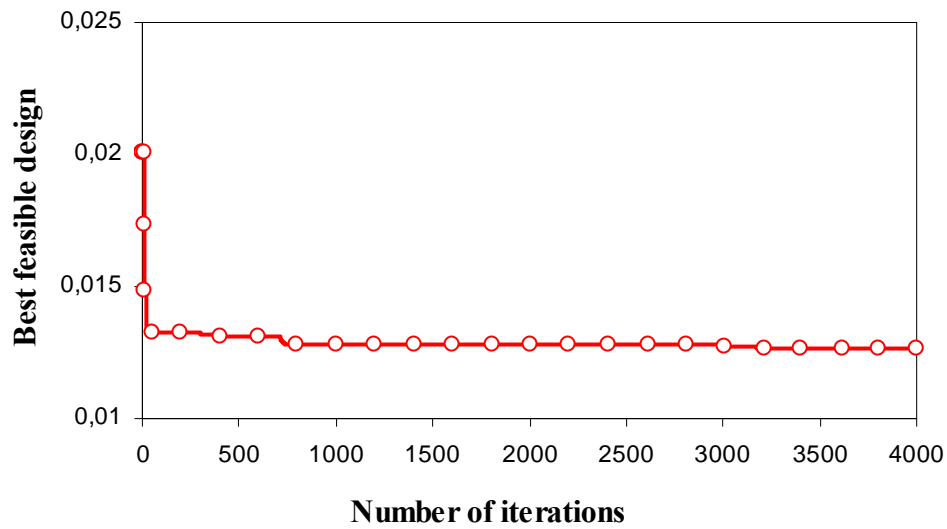


**Figure 2.11** Design-history graph for the spring design.

## 2.4 Particle Swarm Optimization in Discrete Design Space

In contrast to continuous optimization problems in which the variables can take all values within the limits, variables in the discrete optimization problem can only take discrete values. Discrete variables can be defined as the quantitative variables, which can be measured in terms of numbers, with possible values of only specific points on a scale.

The standard particle swarm algorithm, as mentioned in previous section, considers a swarm which contains particles in continuous design space. Researchers have been used this assumption in most of the applications of particle swarm optimization algorithm to the optimization problems in the literature [18-24]. However, such an assumption cannot be made in the optimum design problem where integer numbers are used as design variables.

In the literature two approaches exist to obtain integer numbers from continuous ones. The first was suggested by Kennedy and Eberhart [18] where binary numbers are used in particle swarm optimization to achieve a discrete set. The second method is called rounding off which is suggested by Liu et al. [24]. In this study the rounding off methods is employed in the algorithm.

Rounding-off is a simple approach in which an optimum design is first obtained by assuming all the variables to be continuous. Then by use of heuristics, the variables are rounded off to the nearest available integer values to obtain a discrete solution. The procedure can be applied to a limited class of problems in which the discrete variables can have non-discrete values during the solution process. Continuous numbers are rounded off by using the following expression.

$$x_k^i = INT(x_k^i) \quad (2.38)$$

Where  $x_k^i$  represents the value of continuous position of particle  $i$  at iteration  $k$ .

To be able to use the particle swarm algorithm for discrete design variables some adjustments are required to be carried out. Firstly the discrete values among which the values of design variables  $x_j$  are to be selected in set  $\mathbf{X}$  are arranged in ascending sequence. The sequence number of these values is then treated as design variables instead of  $x_j$  itself. For example in a design set which consists of 272 values, the sequence numbers from 1 to 272 are the main design variables. At any stage of design cycle, once a sequence number is generated by the algorithm, then the real value of the design variable which corresponds to this sequence number is easily taken from the discrete set. The flowchart of the discrete particle swarm algorithm is given in Figure 2.12.

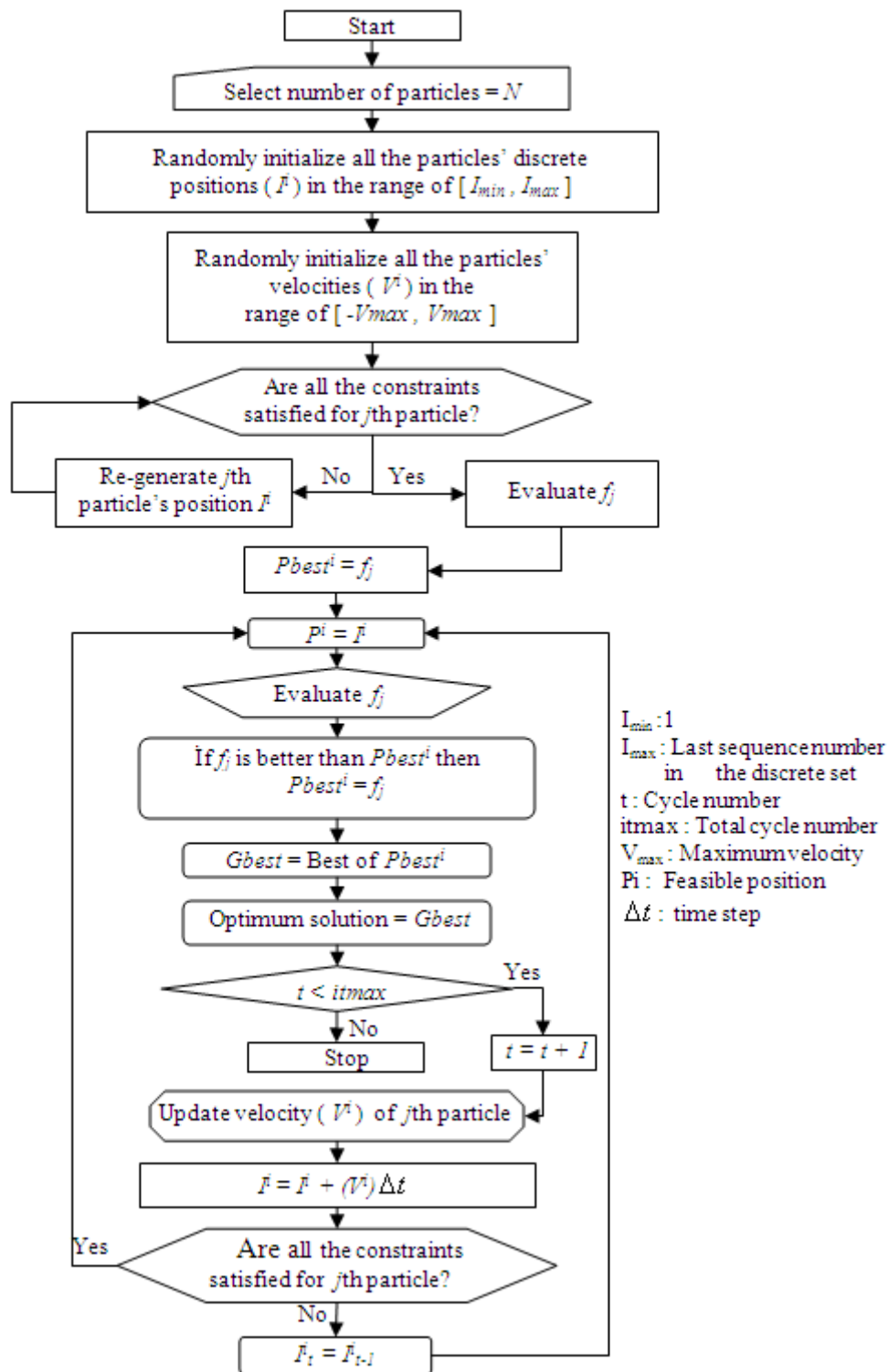


Figure 2.12 Particle swarm optimization in discrete design space.

## 2.4.1 Numerical Examples in Discrete Design Space

Particle swarm algorithm is modified for the solution of optimum design problems in discrete design space and performance of the algorithm is tested with numerical examples.

### 2.4.1.1 Example 1

In this example, aim is to find the optimum solution of a standard test function taken from [74]. Problem involves two discrete variables and one constraint, which can be expressed as;

Minimize;

$$f(x) = 5x_1^2 - 9x_1x_2 + 5x_2^2 \quad (2.39)$$

Subjected to;

$$g(x) = 25 - 16x_1x_2 \leq 0 \quad (2.40)$$

The values of  $x_1$  and  $x_2$  are limited to the set;

$$X = \{ 0.5, 1.0, 1.5, 2.0, 2.5, 3.0, \dots, 10.0 \} \quad (2.41)$$

The parameter set used for this problem is given in Table 2.8. Maximum number of iterations is taken as 500.

**Table 2.8** PSO algorithm parameters used for discrete design example 1.

<i>NPT</i>	<i>C1</i>	<i>C2</i>	<i>w</i>	<i>Vmax</i>	<i>Number of iterations</i>
20	2	2	0.08	2	500

The optimum values of the discrete variables  $x_1, x_2$  are obtained as  $[1.5 \ 1.5]^T$ . The minimum objective function value in the optimum solution is  $f(x) = 2.25$ . These values are verified from the Kuhn-Tucker conditions. It takes only 8 out of 500 iterations for the particle swarm algorithm to reach the optimum. A contour plot and three-dimensional plot drawn with respect to the values obtained from the optimization process are given in Figures 2.13 and 2.14.

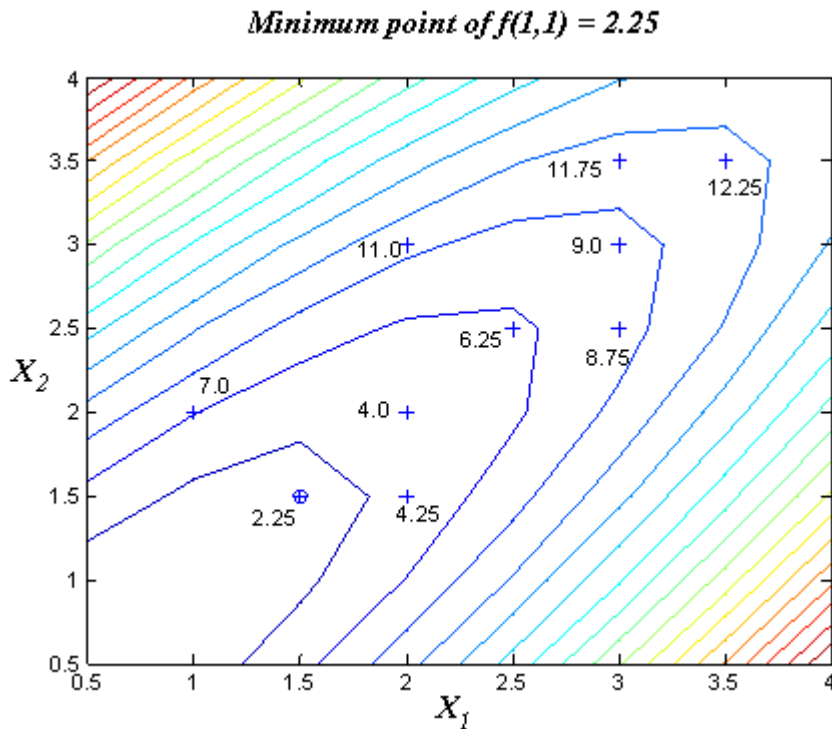


**Figure 2.13** Contour plot of the function  $f(x) = 5x_1^2 - 9x_1x_2 + 5x_2^2$ .

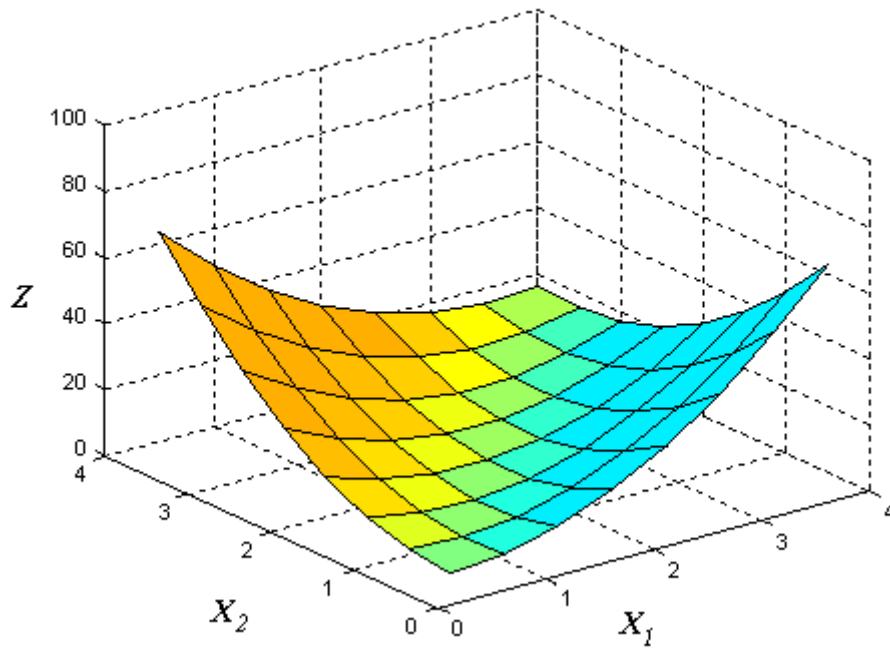


**Figure 2.14** Three Dimensional plot of the function  $f(x) = 5x_1^2 - 9x_1x_2 + 5x_2^2$ .

### 2.4.1.2 Example 2

The second example is another numerical problem used many times in the literature to test the efficiency of the algorithms. Function involves six discrete variables and two inequality constraints. The definition of the optimization problem can be given as in the following;

Minimize;

$$f(x) = x_1 + 2x_2 + 2x_3 + 3x_4 + 4x_5 + 5x_6 \quad (2.42)$$

Subject to;

$$g_1(x) = 4x_1 + 3x_2 + 2x_3 + 3x_4 + 4x_5 + 6x_6 \geq 510 \quad (2.43)$$

$$g_2(x) = 3x_1 + 2x_2 + 3x_3 + 4x_4 + 2x_5 + 3x_6 \geq 400 \quad (2.44)$$

The values of the discrete variables are limited to the sets;

$$x_i \in \mathbf{X} = \{1, 2, 3, 4, 8, 9, 11, 14, 18, 20, 21, 27\}, \quad i = 1, \dots, 5$$

$$x_6 \in \mathbf{X} = \{3, 4, 8, 9, 11, 14, 18, 20, 21, 27, 28, 29\} \quad (2.45)$$

The number of particles, i.e. the *NPT*, is 40, and the *Vmax*, *c1*, *c2* and *w* are 2 and 1, 1, 0.08 respectively. Maximum number of cycles is assumed to be 1000.

The problem is solved with particle swarm algorithm and the minimum objective function value is determined as  $f(x) = 373$  with the design variable set of  $x^* = (27, 27, 27, 27, 3, 29)$ . Shi and Fu [75] also tackled this problem in their study and they found the same results.

## **CHAPTER 3**

### **OPTIMUM DESIGN OF RIGIDLY CONNECTED STEEL SWAY FRAMES TO LRFD**

#### **3.1 Steel Frames**

Frame is a structure which is made up of linear elements called beams and columns, connected to one another at their ends. Most frames are three-dimensional, however, they may often be considered as a series of parallel two-dimensional frames, or as two perpendicular series of two-dimensional frames. In the present study, the structures are assumed that they can be represented as the latter. The arrangement and the loading of frame members and the type of connections used at the ends have important role on the behavior of a frame.

The beams and columns of a moment resisting frame are connected to each other with rigid joints. In this assumption where the end connections are assumed to be fully restrained, it is implied that there is no relative rotation and the whole design bending moment of the beam is transmitted to the column. Figure 3.1 shows the members of such a simple frame.

Beam is a structural element that is capable of withstanding load primarily by resisting bending. They generally carry vertical gravitational forces but can also be used to carry horizontal loads. The loads carried by a beam are

transferred to columns, walls, or girders, which then transfer the force to adjacent structural compression members.

Column is a vertical structural element that transmits, through compression, the weight of the structure above to other structural elements below. They are the most common vertical support elements. Columns are not normally subject to bending that is directly induced by loads acting transverse to their axes [76]. They are frequently used to support beams or arches on which the upper parts of walls or ceilings rest. In earthquake engineering, they may be designed to resist lateral forces. They can be divided into two categories in terms of their length. Short columns have tendency to fail by crushing, which is called strength failure. Long columns, on the other hand, tend to fail by buckling, which is an instability failure rather than a strength failure.

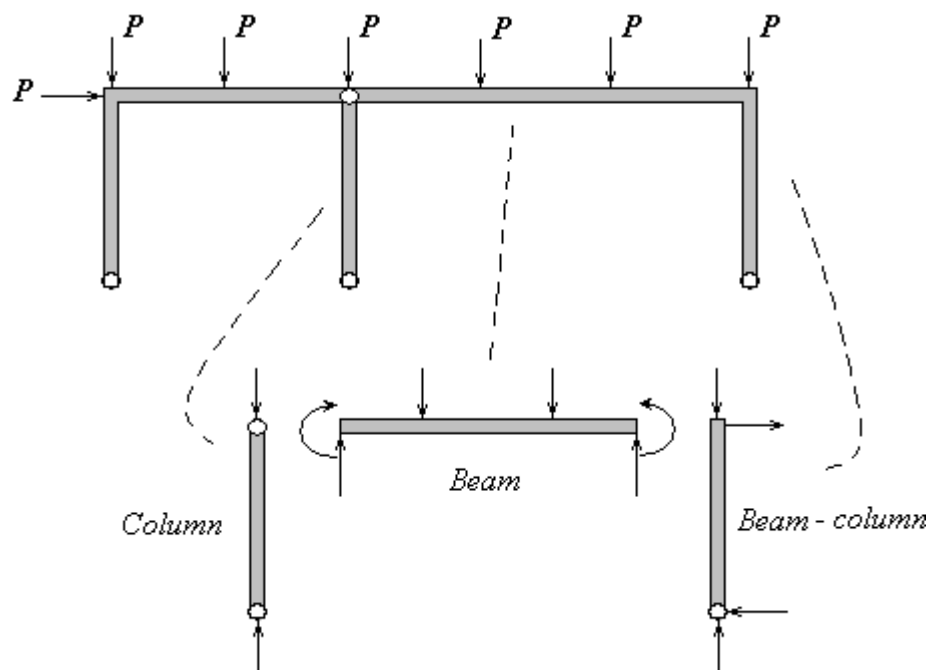


**Figure 3.1** Column, beam and beam-column members of a frame.

Beam-column is a structural member that is subjected to axial compression and transverse bending moment at the same time. A beam-column differs from a column only by the presence of the eccentricity of the load application, end moment, or transverse load. Beam-columns are found in frame-type structures where the columns are subjected to other than pure concentric axial loads and axial deformations, and where the beams are subjected to axial loads in addition to transverse loads and flexural deformations.

## **3.2 Analysis of Frames**

Frame structures, of which the beams are continuous, are statically indeterminate, and their reactions, shears and moments cannot be determined through the application of the basic equations of statics alone. Because there are more unknowns than equations, and reactions, shears and moments are dependent on the characteristics of the structure.

In current practice, computer-based programs can do all the analyses of rigid-frame structures. Users can define the geometry of overall configurations; specify types of members and support conditions, and different types of loading conditions. The matrix displacement techniques frequently form the basis for the computer-based formulations.

### **3.2.1 Matrix Stiffness Method**

During the past three decades, there have been enormous changes in the structural analysis techniques used in engineering practice. The reason behind

these changes is primarily the great developments made with high-speed digital computers and the matrix methods in the use of very complex structures. Matrix structural analysis methods are convenient mathematical representation of a structural system that is easily solved with computers. Most of the commercial computer programs for structural analysis are based on the stiffness method due to its ease in the implementation on computers.

Analysis of structures using matrix methods does not involve new concepts of structural engineering; but the basic relationships of equilibrium, compatibility and force-displacement relations of members are expressed in the form of matrix equations, so that the computer can efficiently perform the numerical computations.

### **3.2.1.1 Analytical Model**

The matrix-stiffness method, which is also known as the matrix-displacement method, uses the stiffness properties of the elements of a structure to form a set of simultaneous equations relating displacements of the structure to loads acting on the structure. The structure is assumed to be an assemblage of members, which can be defined as a part of the structure for which the member force-displacement relations to be used in the analysis are valid, connected at their ends to joints. A joint, which is also called node, is a structural part of infinitesimal size to which the member ends are connected.

Before proceeding with the analysis, an analytical model of the structure should be defined. A line diagram, on which all the joints and members are identified by numbers, represents the structural model. An analytical model of a simple frame is illustrated in Figure 3.2, where the joint numbers are

enclosed within circles to distinguish them from the member numbers, which are enclosed within rectangles.

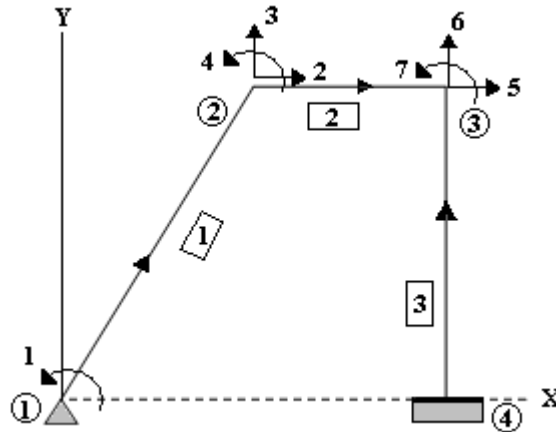


**Figure 3.2** Analytical model of a simple frame.

### 3.2.1.1.1 Global and Local Coordinate System

In the matrix-stiffness method, Cartesian or rectangular global coordinate system is used to describe the overall geometry and behavior of the structure. The global coordinate system (X, Y, Z) shown in Figure 3.3(a) follows the orthogonal right hand rule.

Due to the convenience of deriving the basic force-displacement relations in terms of the forces and displacements in the directions along and perpendicular to members, a local coordinate system shown in Figure 3.3(b) is defined for each member of the structure.

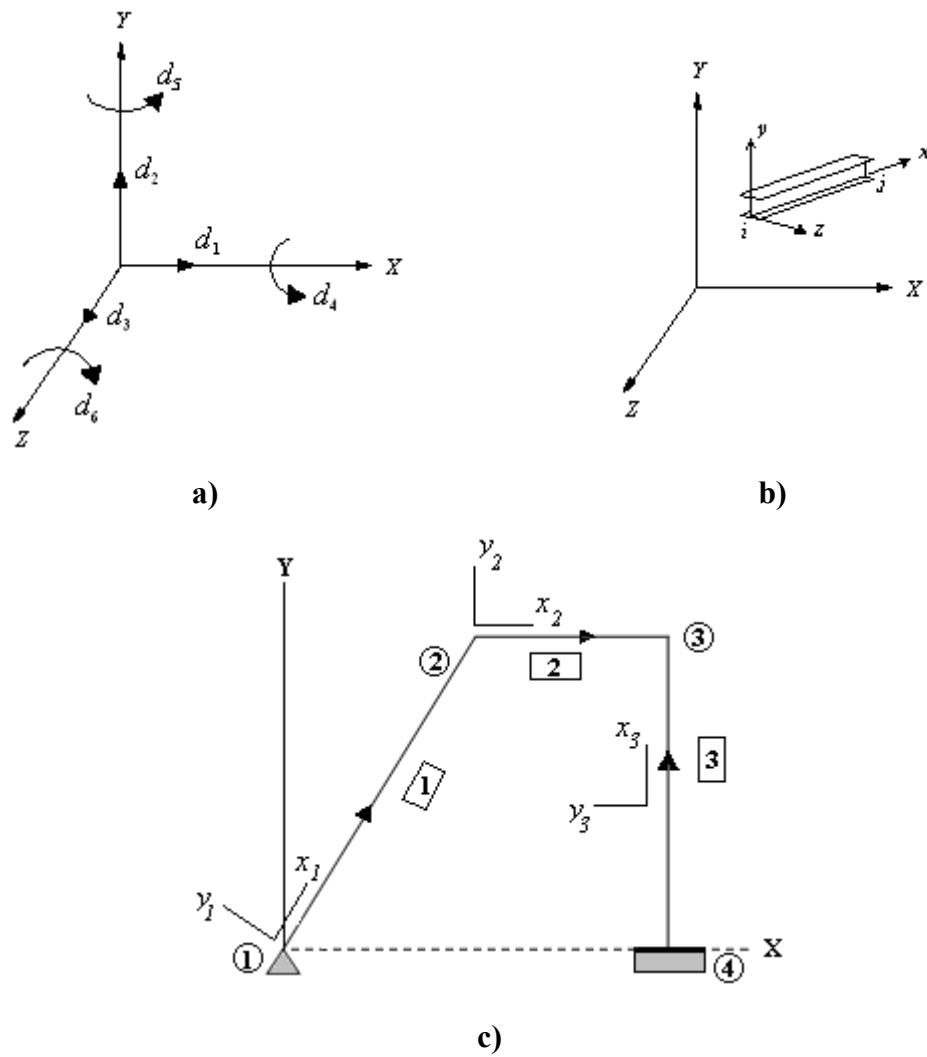


**Figure 3.3** Global and local coordinates **a)** Cartesian (Rectangular) Coordinate System, **b)** Local coordinates of a beam member, **c)** Global and Local coordinates of a simple frame.

The origin of the local xyz coordinate system for a member may be arbitrarily located at one of the ends of the member, with the x axis directed along the centroidal axis of the member. The positive direction of the y axis is selected so that the coordinate system is right-handed, with the local z axis pointing in the positive direction of the global Z axis [77]. The positive direction of the

local x axis for each frame member given in Figure 3.2 is indicated by drawing an arrow along each member on the line diagram. For example, the origin of the local coordinate system for member 1 is located at its end connected to joint 1, with the  $x_1$  axis directed from joint 1 to joint 2. The joint to which the member end with the origin of the local coordinate system is connected is referred to as beginning joint for the member, whereas the joint adjacent to the opposite end of the member is called the end joint. Once the local x axis is determined for a member, the corresponding y axis can be easily obtained by applying right-hand rule. Figure 3.3(c) shows the local and global coordinates of a simple frame.

#### **3.2.1.1.2 Relationship between Local and Global Coordinates**

Since the first step in the formation of the force and displacement vectors is to define the nodal points and their locations with respect to a coordinate system, it is an important fact to know the relationship between the local and global coordinate systems for an accurate analysis. The input for member loads can be provided in the local and global coordinate system, besides, the output for member end forces is printed in the local coordinate system. Thus, it is necessary to transform one coordinate system to the other during the analysis. This transformation is implemented through the use of transformation matrix which is constructed in terms of an angle which is defined as the alpha ( $\alpha$ ) angle.

If the local x-axis of a member is parallel to the global Y-axis, as in the case of a column member in a frame, the alpha angle is the angle through which the local z-axis has been rotated about the local x-axis from a position of being parallel and in the same positive direction of the global Z-axis.

When the local x-axis is not parallel to the global Y-axis, the alpha angle is the angle through which the local coordinate system has been rotated about the local x-axis from a position of having the local z-axis parallel to the global X-Z plane and the local y-axis in the same positive direction as the global Y-axis. Following figure gives details of the positions for alpha equals 0 degrees or 90 degrees. This figure may be helpful for a quick determination of the local axis system when providing member loads in the local member axis.

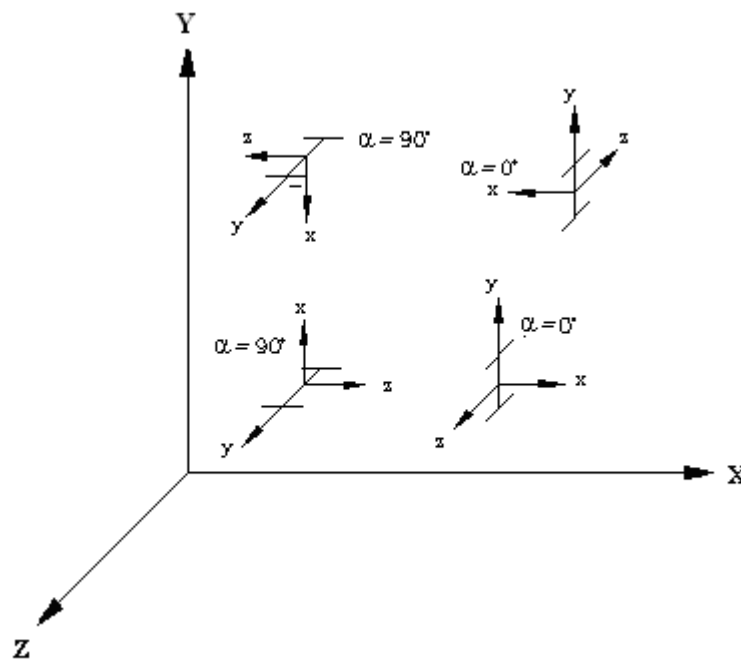


**Figure 3.4** Relationship between Global and Local axes

### 3.2.1.1.3 Degrees of Freedom

The degrees of a freedom of a structure can be defined as the independent joint displacements (translations and rotations) required to specify the deformed

shape of the structure when subjected to loading. The deformed shape of the frame given in Figure 3.2 is depicted in Figure 3.5 considering an arbitrary loading. Unlike the classical methods of analysis, matrix analysis method usually does not require to neglect the member axial deformations. In Figure 3.5 the only degree of freedom, rotation, in joint 1 is represented by  $d_1$ . Other rotational deformations in joint 2 and joint 3 are represented by  $d_4$  and  $d_7$  respectively. While  $d_2$  and  $d_5$  represent the axial deformations,  $d_3$  and  $d_6$  symbolize the vertical translations in the joints 2 and 3, respectively. Finally, joint 4, which is attached to the fixed support, can neither translate nor rotate; therefore it does not have any degrees of freedom. Thus, the entire frame has seven degrees of freedom.

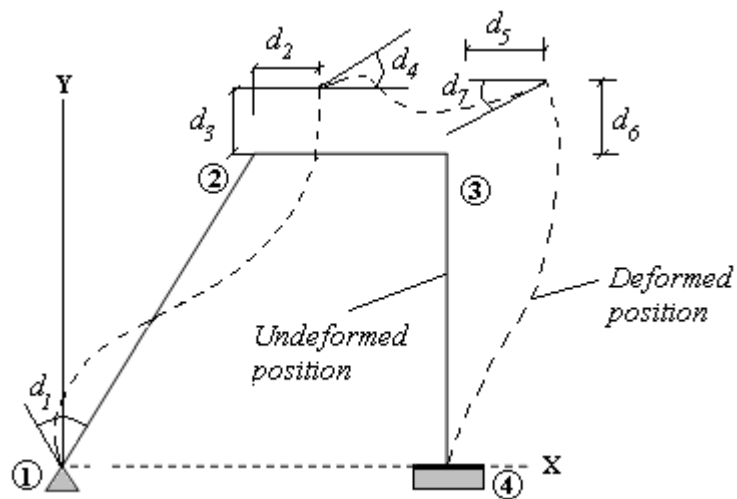


**Figure 3.5** Degrees of freedom of a simple frame.

### 3.2.1.1.4 Relationship between Member End Forces and Member End Deformations

The first step to obtain the overall stiffness matrix of a structure necessitates the construction of the local stiffness matrix belonging to each frame member. Consider a rigid frame member shown in the following figure.

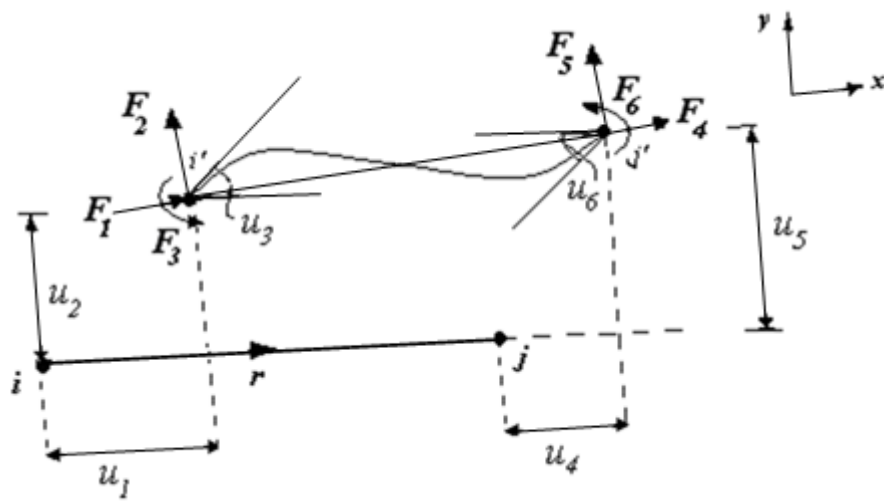


**Figure 3.6** End deformations and end forces of a rigid frame member.

When the frame is subjected to external loading, member  $r$  shown in Figure 3.6 deforms and internal forces are induced at its ends. The deformed and undeformed positions of the member are also illustrated in this figure. As indicated in the figure, the member has six displacements or degrees of freedom. End displacements are denoted by  $u_1$  through  $u_6$  and the corresponding member end forces are denoted by  $F_1$  through  $F_6$ . It should be noted that these end displacements and end forces are defined relative to the local coordinate system of the member. Translations and forces are considered

as positive when in the positive directions of the local x and y axes, and rotations and moments are considered as positive when counterclockwise.

To determine the relationships between the member forces and end displacements in terms of the external loads, equilibrium equations are applied to the member.

$$F_1 = k_{11}u_1 + k_{12}u_2 + k_{13}u_3 + k_{14}u_4 + k_{15}u_5 + k_{16}u_6 \quad (3.1)$$

$$F_2 = k_{21}u_1 + k_{22}u_2 + k_{23}u_3 + k_{24}u_4 + k_{25}u_5 + k_{26}u_6 \quad (3.2)$$

$$F_3 = k_{31}u_1 + k_{32}u_2 + k_{33}u_3 + k_{34}u_4 + k_{35}u_5 + k_{36}u_6 \quad (3.3)$$

$$F_4 = k_{41}u_1 + k_{42}u_2 + k_{43}u_3 + k_{44}u_4 + k_{45}u_5 + k_{46}u_6 \quad (3.4)$$

$$F_5 = k_{51}u_1 + k_{52}u_2 + k_{53}u_3 + k_{54}u_4 + k_{55}u_5 + k_{56}u_6 \quad (3.5)$$

$$F_6 = k_{61}u_1 + k_{62}u_2 + k_{63}u_3 + k_{64}u_4 + k_{65}u_5 + k_{66}u_6 \quad (3.6)$$

Afterwards, the stiffness matrix is constructed using the terms in these equations as in the following;

$$\begin{Bmatrix} F_1 \\ F_2 \\ F_3 \\ F_4 \\ F_5 \\ F_6 \end{Bmatrix} = \begin{bmatrix} k_{11} & k_{12} & k_{13} & k_{14} & k_{15} & k_{16} \\ k_{21} & k_{22} & k_{23} & k_{24} & k_{25} & k_{26} \\ k_{31} & k_{32} & k_{33} & k_{34} & k_{35} & k_{36} \\ k_{41} & k_{42} & k_{43} & k_{44} & k_{45} & k_{46} \\ k_{51} & k_{52} & k_{53} & k_{54} & k_{55} & k_{56} \\ k_{61} & k_{62} & k_{63} & k_{64} & k_{65} & k_{66} \end{bmatrix} \begin{Bmatrix} u_1 \\ u_2 \\ u_3 \\ u_4 \\ u_5 \\ u_6 \end{Bmatrix} \quad \text{or } \{F\}_i = [k]\{U\}_i \quad (3.7)$$

Where;  $\{F\}_i$  and  $\{u\}_i$  represent the vector of end forces and the vector of end deformations respectively, and  $[k]$  is member stiffness matrix in local coordinates.  $k_{ij}$ 's are the elements of the stiffness matrix. These elements which are the forces per unit displacement are referred to as stiffness coefficients. First subscript of the stiffness coefficients identifies the force and the second one identifies the displacement.

Vector of end forces for member  $r$  in local coordinates is;

$$\{F\}_r = \{F_1 \ F_2 \ F_3 \ F_4 \ F_5 \ F_6\}^T \quad (3.8)$$

Vector of end deformations for member  $r$  in local coordinates is;

$$\{U\}_r = \{u_1 \ u_2 \ u_3 \ u_4 \ u_5 \ u_6\}^T \quad (3.9)$$

Vector of joint displacements for member  $r$  in global coordinates is;

$$\{D\}_r = \{d_1 \ d_2 \ d_3 \ d_4 \ d_5 \ d_6\}^T \quad (3.10)$$

One way to evaluate the stiffness matrix  $[k]$  is to implement the elementary beam theory as described in the following;

Consider the rigid frame member  $r$  given in Figure 3.6. Taken a small piece of this member, the curvature is defined as;

$$\frac{d^2y}{dx^2} = \frac{M(x)}{EI} \quad (3.11)$$

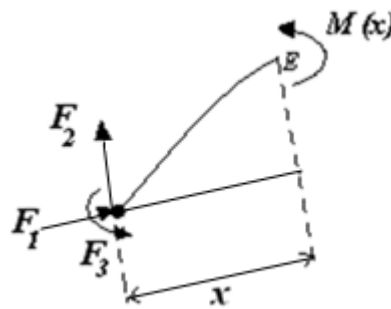


**Figure 3.7** A small piece of a rigid frame member.

From which,

$$M(x) = EI \frac{d^2y}{dx^2} = F_2x - F_3 \quad (3.12)$$

After two integration steps,

$$EI y = F_2 \frac{x^3}{6} - F_3 \frac{x^2}{2} + c_1x + c_2$$

Where  $c_1$  and  $c_2$  are integration constants. Using the boundary conditions and then implementing the necessary substitutions through the use of equations of equilibrium, one can obtain the general slope-deflection equations;

$$F_1 = \frac{EA}{L}u_1 - \frac{EA}{L}u_4 \quad (3.13)$$

$$F_2 = \frac{12EI}{L^3}u_2 + \frac{6EI}{L^2}u_3 - \frac{12EI}{L^3}u_5 + \frac{6EI}{L^2}u_6 \quad (3.14)$$

$$F_3 = \frac{6EI}{L^2}u_2 + \frac{4EI}{L}u_3 - \frac{6EI}{L^2}u_5 + \frac{2EI}{L}u_6 \quad (3.15)$$

$$F_4 = -\frac{EA}{L}u_1 + \frac{EA}{L}u_4 \quad (3.16)$$

$$F_5 = -\frac{12EI}{L^3}u_2 - \frac{6EI}{L^2}u_3 + \frac{12EI}{L^3}u_5 - \frac{6EI}{L^2}u_6 \quad (3.17)$$

$$F_6 = \frac{6EI}{L^2}u_2 + \frac{2EI}{L}u_3 - \frac{6EI}{L^2}u_5 + \frac{4EI}{L}u_6 \quad (3.18)$$

Collecting these equations in a matrix form;

$$k = \begin{bmatrix} \frac{EA}{L} & 0 & 0 & -\frac{EA}{L} & 0 & 0 \\ 0 & \frac{12EI}{L^3} & \frac{6EI}{L^2} & 0 & -\frac{12EI}{L^3} & \frac{6EI}{L^2} \\ 0 & \frac{6EI}{L^2} & \frac{4EI}{L} & 0 & -\frac{6EI}{L^2} & \frac{2EI}{L} \\ -\frac{EA}{L} & 0 & 0 & \frac{EA}{L} & 0 & 0 \\ 0 & -\frac{12EI}{L^3} & -\frac{6EI}{L^2} & 0 & \frac{12EI}{L^3} & -\frac{6EI}{L^2} \\ 0 & \frac{6EI}{L^2} & \frac{2EI}{L} & 0 & -\frac{6EI}{L^2} & \frac{4EI}{L} \end{bmatrix} \quad (3.19)$$

The stiffness coefficients,  $k_{ij}$ , can also be evaluated by subjecting the member, separately, to unit values of each of the six end displacements. The member end forces required to cause the individual unit displacements are then determined by using the principles of mechanics of materials and the slope-deflection equations and by applying the equations of equilibrium.

The  $i$ -th column of the member stiffness matrix involves the end forces required to cause a unit value of the displacement  $u_i$  while all other displacements are zero. For example, as shown in the Figure 3.8, the second column of  $[k]$  consists of the six end forces required to cause the displacement  $u_i = 1$ .

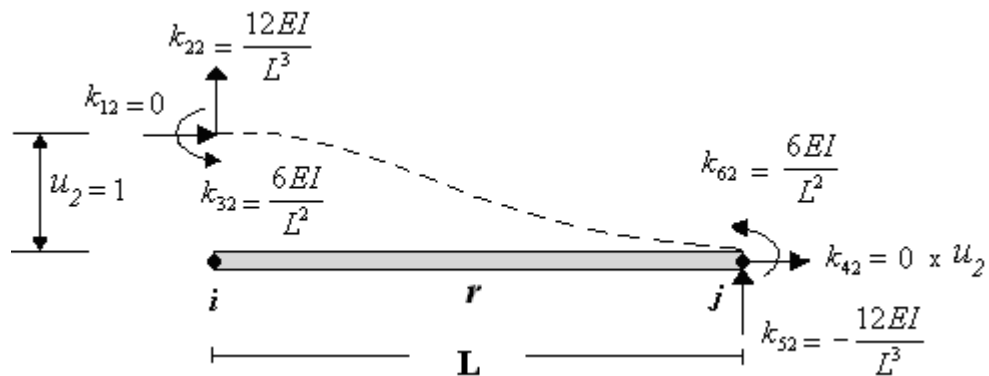


**Figure 3.8** Derivation of the second column of the stiffness matrix  $[k]$  for rigid frame member  $r$ .

As indicated above stiffness matrix  $[k]$ , it can be declared that matrices for linearly elastic structures are always symmetric.

### 3.2.1.1.5 Relationship between the Joint Displacements and Member End Deformations

Consider an arbitrary frame member  $m$  shown in Figure 3.9. The orientation of the member with respect to the global  $XY$  coordinate system is defined by an angle  $\alpha$  measured counterclockwise from the positive direction of the global  $X$  axis to the positive direction of the local  $x$  axis.

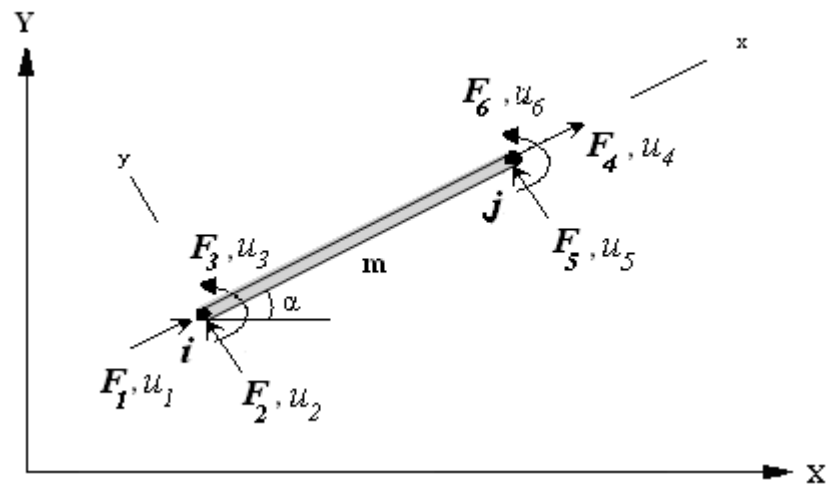


**Figure 3.9** Member end forces and end displacements in local coordinates.

Comparison of Figures 3.9 and 3.10 indicates that at the end  $i$  of the member the local displacement  $u_1$  must be equal to the algebraic sum of the components of the global displacements  $d_1$  and  $d_2$  in the direction of local  $x$  axis. In a similar manner the local displacement  $u_2$  equals to the algebraic sum of the components of  $d_1$  and  $d_2$  in the direction of local  $y$  axis and so on.

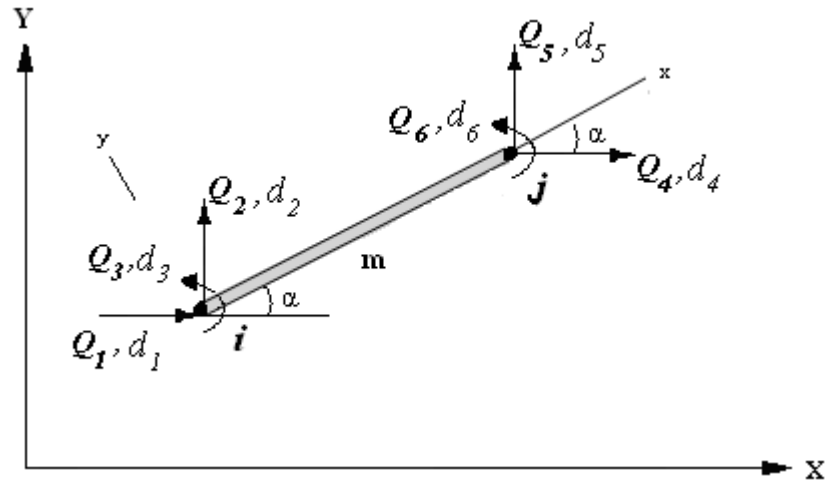


**Figure 3.10** Member end forces and end displacements in global coordinates.

These equalities are given in the following;

At joint  $i$ ;

At joint  $j$ ;

$$\begin{aligned}
 u_1 &= d_1 \cos \alpha + d_2 \sin \alpha & u_4 &= d_4 \cos \alpha + d_5 \sin \alpha \\
 u_2 &= -d_1 \sin \alpha + d_2 \cos \alpha & u_5 &= -d_4 \sin \alpha + d_5 \cos \alpha \\
 u_3 &= d_3 & u_6 &= d_6
 \end{aligned} \tag{3.20}$$

$$\begin{bmatrix} u_1 \\ u_2 \\ u_3 \\ u_4 \\ u_5 \\ u_6 \end{bmatrix} = \begin{bmatrix} \cos \alpha & \sin \alpha & 0 & 0 & 0 & 0 \\ -\sin \alpha & \cos \alpha & 0 & 0 & 0 & 0 \\ 0 & 0 & 1 & 0 & 0 & 0 \\ 0 & 0 & 0 & \cos \alpha & \sin \alpha & 0 \\ 0 & 0 & 0 & -\sin \alpha & \cos \alpha & 0 \\ 0 & 0 & 0 & 0 & 0 & 1 \end{bmatrix} \begin{bmatrix} d_1 \\ d_2 \\ d_3 \\ d_4 \\ d_5 \\ d_6 \end{bmatrix} \tag{3.21}$$

$$\{U\}_m = [B]_m \{D\}_m \tag{3.22}$$

In a similar manner, one can express the relationship between the local and global forces.

### 3.2.1.1.6 Relationship between External Loads and Member Forces

If an elastic structure is subjected to external loads then it deforms and joint displacements and member end displacements occur. In this case, due to the principal of conservation of the energy, the work done by the external loads is equal to the work done by the internal forces. Thus;

$$\frac{1}{2} \{P\}_m^T \{D\}_m = \frac{1}{2} \{F\}_m^T \{U\}_m \quad (3.23)$$

In which;  $\{F\}_m$  is the vector of member forces,  $\{U\}_m$  is the vector of member end deformations,  $\{P\}_m$  is the vector of external loads and  $\{D\}_m$  is the joint displacement vector in the structure.

Remembering that  $\{U\}_m = [B]_m \{D\}_m$

$$\frac{1}{2} \{P\}_m^T \{D\}_m = \frac{1}{2} \{F\}_m^T [B]_m \{D\}_m \quad (3.24)$$

$$\{P\}_m^T = \{F\}_m^T [B]_m \quad (3.25)$$

Taking transpose of both sides

$$\{P\} = [B]_m^T \{F\} \quad (3.26)$$

To obtain the overall stiffness matrix, the equations (3.7), (3.22), and (3.26) are collected together.

$$\{F\}_i = [k] \{U\}_i \quad (3.7)$$

$$\{U\}_m = [B]_m \{D\}_m \quad (3.22)$$

$$\{P\} = [B]_m^T \{F\} \quad (3.26)$$

Substituting (3.22) into (3.7);

$$\{F\}_m = [k] [B]_m \{D\}_m \quad (3.27)$$

Substituting (3.27) into (3.26)

$$\{P\} = \underbrace{[B]_m^T [k] [B]_m}_{[K]} \{D\}_m \quad (3.28)$$

Where;  $[K] = [B]_m^T [k] [B]_m$  is called overall stiffness of the structure.

$$\begin{array}{c}
\begin{array}{cc}
\textit{First end} & \textit{Second end} \\
\left[ \begin{array}{cccccc}
a & b & c & . & -a & -b & c \\
b & d & e & . & -b & -d & e \\
c & e & f & . & -c & -e & g \\
. & . & . & . & . & . & . \\
-a & -b & -c & . & a & b & -c \\
-b & -d & -e & . & b & d & -e \\
c & e & g & . & -c & -e & f
\end{array} \right] & \\
\end{array} \\
\end{array} \quad (3.29)$$

Where;

$$a = \frac{EA}{L} \cos^2 \alpha + \frac{12EI}{L^3} \sin^2 \alpha$$

$$b = \left( \frac{EA}{L} - \frac{12EI}{L^3} \right) \cos \alpha \sin \alpha$$

$$c = -\frac{6EI}{L^2} \sin \alpha$$

$$d = \frac{EA}{L} \sin^2 \alpha + \frac{12EI}{L^3} \cos^2 \alpha$$

$$e = \frac{6EI}{L^2} \cos \alpha$$

$$f = \frac{4EI}{L}$$

$$g = \frac{2EI}{L}$$

### 3.3 Load and Resistance Factor Design for Rolled Beam-columns

The traditional method of producing high-strength steels consists of adding alloying elements to the steel bath and controlling the temperatures during the rolling process, by doing the so-called Thermo Mechanical (TM) rolling. Most common rolled-sections used in practice are shown in Figure 3.11.



**Figure 3.11** Most common rolled steel sections used in practice. (<http://www.marginup.com/products/29878/Steel-Plate-3.html>)

In actual structures, most columns, in addition to axial load, must support lateral loads and/or transmit moments between their ends, and are thus subjected to combined stress due both to axial load and moment. Such members are termed beam-columns. Members of a rigid frame behave as beam-columns.

Figure 3.12 shows the most common rolled steel beam-column cross section, the W (wide-flange) shape, with much of the material in the top and bottom flange, where it is most effective in resisting bending moment.

The concepts of tension members and compression members are combined in the treatment as a beam. The compression element (a flange) that is integrally braced perpendicular to its plane through its attachment to the stable tension flange by means of the web is assumed also to be braced laterally in the direction to the plane of the web.

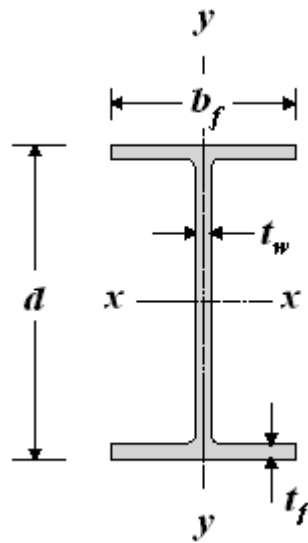


**Figure 3.12** W (wide-flange) shape steel beam.

Where;

$b_f$  = the width of flange

$t_f$  = the thickness of flange

$t_w$  = the thickness of web

$d$  = overall depth of steel section

To be able to compute the nominal moment strength ( $M_n$ ) of a beam-column, it is required to determine whether the beam is compact, non-compact or slender. In Figure 3.13, the cross sections are classified graphically in terms of the relationship between slenderness ratio and nominal flexural strength.

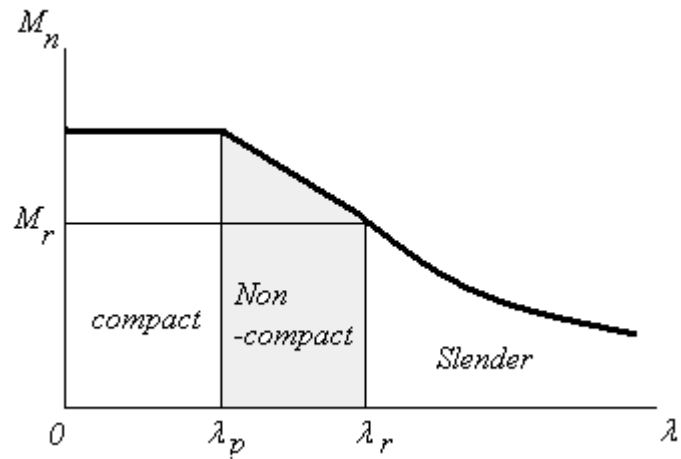


**Figure 3.13** Classification of cross sections for local plate buckling.

### 3.3.1 Compact sections

Compact beam sections can be defined as beam section that the compression plate element is not buckle due to compression force. Since it is subjected to compression, the compression flange of the beam is treated as compression plate element. The classification of compact section is depended to the width-thickness ratio of the plate element.

If  $\lambda \leq \lambda_p$  for both the compression flange and the web, the capacity is equal to  $M_p$  and shape is compact and nominal moment strength  $M_n$  for laterally stable compact sections according to LRFD-F1 may be stated;

$$M_n = M_p \tag{3.30}$$

where;

$$M_p = \text{plastic moment strength} = Z F_y \quad (3.31)$$

$Z$  = plastic modulus

$F_y$  = yield stress

### 3.3.2 Non-compact sections

If compression plate element of a beam section is buckled due to the compression force, this beam section is called non-compact beam section. For the non-compact sections, the yield stress can be reached in some, but not all, of its compression elements before buckling occurs. It is not capable of reaching a fully plastic stress distribution. Slenderness ratio  $\lambda$  of a non-compact section exactly equals the limit  $\lambda_r$ . Because of the residual stress the strength is expressed as

$$M_n = M_r = S(F_y - F_r) \quad (3.32)$$

Where;

$M_r$  is the residual moment that will result in the extreme fiber stress to rise from its residual stress  $F_r$  value when there is no applied load acting to the yield stress  $F_y$ . The elastic section modulus  $S$  equals the moment of inertia  $I$  divided by the distance from the neutral axis to the extreme fiber.

### 3.3.3 Partially Compact Sections

If the slenderness ratio  $\lambda$  of a section is greater than  $\lambda_p$  but not greater than  $\lambda_r$ , this section is called partially compact section. The nominal strength  $M_n$  for such laterally stable non-compact sections must be linearly interpolated between  $M_r$  and  $M_p$ , as in the following;

$$M_n = M_p - (M_p - M_r) \frac{\lambda - \lambda_r}{\lambda_r - \lambda_p} \quad (3.33)$$

### 3.3.4 Slender Sections

If the slenderness ratio of a section exceeds the limit  $\lambda_r$ , this section is referred to as slender. Nominal moment strength of a slender section is expressed as;

$$M_n = M_{cr} = S_x F_{cr} \quad (3.34)$$

where ;

$\lambda = b_f / (2t_f)$  ; for I-shaped member flanges, in which  $b_f$  and  $t_f$  are the width and the thickness of the flange.

$\lambda = h/t_w$  ; for beam web, in which  $h = d - 2k$  plus allowance for undersize inside fillet at compression flange,  $d$  is the depth of the section and  $k$  is the distance from outer face of flange to web toe of fillet.

$$\left. \begin{aligned} \lambda_p &= 0.38 \sqrt{\frac{E}{F_y}} \\ \lambda_r &= 0.83 \sqrt{\frac{E}{F_y - F_r}} \end{aligned} \right\} \text{for compression flange} \quad (3.35)$$

$$\left. \begin{aligned} \lambda_p &= 3.76 \sqrt{\frac{E}{F_y}} \\ \lambda_r &= 5.70 \sqrt{\frac{E}{F_y}} \end{aligned} \right\} \text{for the web} \quad (3.36)$$

Where;

$E$  is the modulus of elasticity and  $F_y$  is the yield stress of steel.  $F_r$  is the compressive residual stress in flange which is given as 69 MPa for rolled shapes in the code.

It is apparent that  $M_n$  is computed for the flange and for the web separately by using corresponding  $\lambda$  values. The smallest amongst all is taken as the nominal moment strength of the  $W$  section under consideration.

### **3.3.5 Load and Resistance Factor Design for Combined Strength in Rolled Beam- columns**

In practice, generally, most columns must carry not only axial loads but also lateral loads and/or transmit moments between their ends. These members, called beam-columns, are therefore subjected to combined stress. The end moments may be caused by frame reaction and/or by the effective eccentricity of the longitudinal loads. For instance, consider a column in a tall building. This column resists live and dead loads of the structure. However, when wind load or lateral inertia forces due to earthquake act on the frame, column must also transmit the resulting bending moments. Failure mode of a beam-column varies depending on the behavior of axial force, whether it is tension or compression.

#### **3.3.5.1 Load and Resistance Factor Design for Beam-columns subject to Bending and Axial tension**

If the case is the combination of bending and axial tension, the chance of instability is reduced and failure usually occurs by yielding.

The combined strength requirement for beam-column under bending and axial tension in load and resistance factor design may be stated as;

$$\left(\frac{P_u}{\phi_c P_n}\right)_{il} + \left(\frac{8}{9}\left(\frac{M_{ux}}{\phi_b M_{nx}}\right)\right)_{il} \leq 1.0 \quad \text{for } \frac{P_u}{\phi_c P_n} \geq 0.2$$

$$i = 1, \dots, nm$$

$$l = 1, \dots, nl \quad (3.37)$$

$$\left(\frac{P_u}{2\phi_c P_n}\right)_{il} + \left(\frac{M_{ux}}{\phi_b M_{nx}}\right)_{il} \leq 1.0 \quad \text{for } \frac{P_u}{\phi_c P_n} \leq 0.2$$

Where;

$nm$  is the number of members,  $nl$  is the number of load cases,  $M_{nx}$  is nominal flexural strength,  $M_{ux}$  is applied moment,  $P_u$  is applied axial load,  $\phi_c$  is resistance factor for columns if the axial force is in compression,  $\phi_b$  is resistance factor in bending.  $P_n$  is nominal axial tension strength, which is calculated from the following expression;

$$P_n = AF_y \quad (3.38)$$

Where;

$A$  is cross-sectional area and  $F_y$  is specified minimum yield stress.

### 3.3.5.2 Load and Resistance Factor Design for Beam-columns subject to Bending and Axial compression

If a beam-column member is subjected to axial compression and bending, the possibility of instability is increased. This is checked by use of interaction formulas which accounts for the stability of columns. In other words, the influence of the slenderness ratio and local buckling is included in the calculation of nominal axial capacity of the member. Similar to tension members, the strength capacity of compression members are checked with the use of Equation (3.38), which is mentioned in previous section. However, the calculation of nominal axial capacity of compression member, included in this equation, differs from that of tension member in that former one requires critical stress as expressed in the following.

$$P_n = AF_{cr} \quad (3.39)$$

where;

$$F_{cr} = 0.658\lambda_c^2 F_y \quad \text{for } \lambda_c < 1.5 \quad (3.40)$$

$$F_{cr} = \frac{0.877}{\lambda_c^2} \quad \text{for } \lambda_c \geq 1.5$$

In which the slenderness ratio  $\lambda_c$  is calculated as follows;

$$\lambda_c = \frac{kl}{r\pi} \sqrt{\frac{F_y}{E}} \quad (3.41)$$

Where;  $A$  is cross-sectional area,  $F_{cr}$  is critical stress,  $F_y$  is yield stress,  $k$  is effective length factor,  $l$  is length of beam member,  $r$  is radius of gyration and  $E$  is modulus of elasticity.

It is apparent from Expression (3.39) that computation of compressive strength  $\phi_c P_n$  of a compression member requires its effective length.

### 3.3.5.2.1 Effective Length of a Beam-column Member

The computation of the effective length of a compression member in a frame, shown in Figure 3.14 can be automated by using Jackson and Moreland monograph [78].

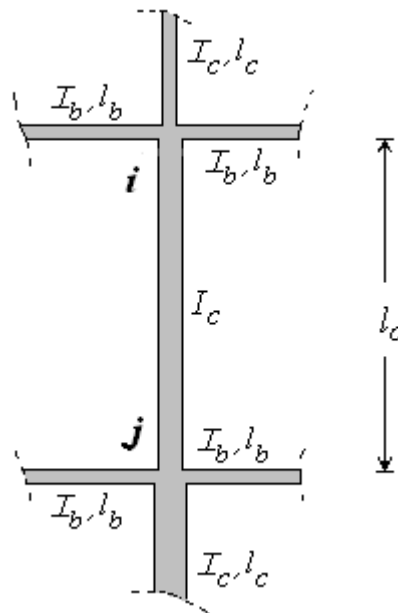


**Figure 3.14** End connections of a rigid beam-column member.

The relationship for the effective length of a column in a swaying frame is given as:

$$\frac{(\gamma_i \gamma_j)(\pi/k)^2 - 36}{6(\gamma_i + \gamma_j)} = \frac{\pi/k}{\tan(\pi/k)} \quad (3.42)$$

where  $k$  is the effective length factor and  $\gamma_i$  and  $\gamma_j$  are the relative stiffness ratio for the compression member which are given as:

$$\gamma_i = \frac{\sum I_{ci} / \ell_{ci}}{\sum I_{bi} / \ell_{bi}} \quad \text{and} \quad \gamma_j = \frac{\sum I_{cj} / \ell_{cj}}{\sum I_{bj} / \ell_{bj}} \quad (3.43)$$

The subscripts c and b refer to the compressed and restraining members respectively and the subscripts  $i$  and  $j$  refer to two ends of the compression member under investigation. The solution of the Nonlinear Equation (3.42) for  $k$  results in the effective length factor for the member under consideration. The Equation (3.42) has the following form for non-swaying frames.

$$\frac{\gamma_i \gamma_j}{4} \left( \frac{\pi}{k} \right)^2 + \left( \frac{\gamma_i + \gamma_j}{2} \right) \left( 1 - \frac{\pi/k}{\tan(\pi/k)} \right) + \frac{2 \tan(\pi/2k)}{\pi/k} = 1 \quad (3.44)$$

### 3.3.6 Load and Resistance Factor Design for Shear in Rolled Beam-columns

While long beams may be governed by deflection and medium length beams are usually controlled by flexural strength, short span beams may be governed by shear.

Beam-columns are usually selected on the basis of their bending capacity and then checked for the shear capacity.

The shear strength requirement in load and resistance factor design according to LRFD may be stated as;

$$\phi_b V_n = V_u \quad (3.45)$$

Where;

$\phi_b$  = Resistance factor for = 0.90

$V_n$  = Nominal strength in shear

$V_u$  = Required shear strength

Nominal shear strength of a rolled compact and non-compact  $W$  section is computed as follows as given in LRFD-AISC [49].

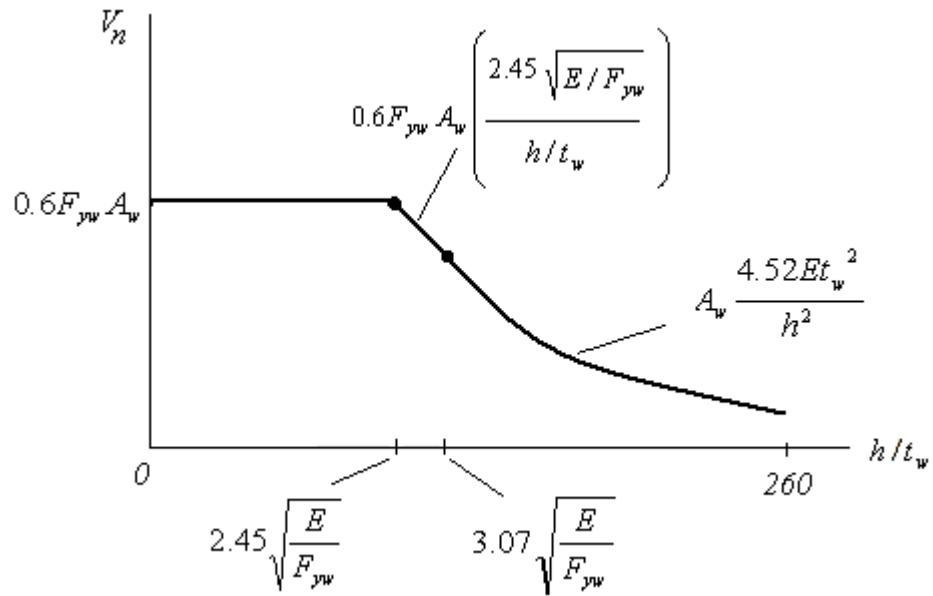


**Figure 3.15** Nominal shear strength of a W section.

- a) When  $\frac{h}{t_w} \leq 2.45 \sqrt{\frac{E}{F_{yw}}}$ , shear yielding of the web is the mode of failure, and the nominal shear strength definition is expressed as;

$$V_n = 0.6F_{yw}A_w \quad (3.46)$$

- b) When  $2.45 \sqrt{\frac{E}{F_{yw}}} < \frac{h}{t_w} \leq 3.07 \sqrt{\frac{E}{F_{yw}}}$ , inelastic shear buckling of the web is the mode of failure, and the nominal shear strength definition is;

$$V_n = 0.6F_{yw}A_w \left( \frac{2.45 \sqrt{\frac{E}{F_{yw}}}}{\frac{h}{t_w}} \right) \quad (3.47)$$

c) When  $3.07 \sqrt{\frac{E}{F_{yw}}} < \frac{h}{t_w} \leq 260$ , elastic shear buckling of the web is the mode of failure, and the nominal shear strength definition is

$$V_n = A_w \frac{4.52Et_w^2}{h^2} \quad (3.48)$$

Where;  $E$  is the modulus of elasticity and  $F_{yw}$  is the yield stress of web steel.

$V_n$  is computed from one of the Expressions (3.46)-(3.48) depending upon the value of  $h/t_w$  of the  $W$  section under consideration.

### 3.3.7 Load and Resistance Factor Design for Serviceability of Beam-columns

Designers formulate the serviceability criteria to prevent disruptions of the functional use and damage to the structure during its normal everyday use. Malfunctions may not cause the collapse of a structure or loss of life or injury; however, they can seriously impair the usefulness of the structure and lead to costly repairs. If this fact is neglected, the structure may become unacceptably flexible.

Types of structural behavior which may impair the serviceability can be listed as follows;

1. Extreme local damage such as local yielding, slip, buckling or cracking that may necessitate excessive maintenance or result in corrosion.
2. Enormous rotation or deflection that may affect the appearance, function or drainage of the structure, or may lead to damage to nonstructural components and their attachments.
3. Excessive vibrations caused by wind or transient live loads which affect the comfort of occupants of the structure or the operation of mechanical equipment.

Serviceability checks in Load and Resistance Factor Design (LRFD-AISC) [49] requires the consideration of the appropriate loads, the response of the structure, and the reaction of the occupants to the structural response.

### 3.3.7.1 Deflection

Extreme transverse deflections or lateral drift may result in permanent damage to building elements or undesirable changes in appearance of portions of the buildings, and discomfort of occupants. Following equation defines the displacement restrictions that may be required to include other than drift constraints such as deflections in beams.

$$\delta_i \leq \delta_{iu} \quad , \quad i = 1, \dots, nd \quad (3.49)$$

Where;

$nd$  is the total number of restricted displacements in the frame.  $\delta_i$  is the deflection of  $i$ th member and  $\delta_{iu}$  is the upper bound on the deflection of beams which is given as  $span / 300$  if they carry plaster or other brittle finish.

Horizontal deflection of columns is also limited due to unfactored imposed load and wind loads to height of column / 300 in each storey of a building with more than one storey.

### 3.3.7.2 Drift

Designers generally believe that inter-storey drift can be used as a measure of expected damage. Damage can be controlled only if the relationship between inter-storey drift and different levels of damage is understood accurately. A large story drift may lead to the occurrence of a weak story that may cause catastrophic building collapse in a seismic event. Thus, uniform story ductility over all stories for a multistory building is usually desired in seismic design.

Following equation represents the inter-storey drift of a multi-storey frame.

$$(\delta_j - \delta_{j-1}) / h_j \leq \delta_{ju} \quad , \quad j = 1, \dots, ns \quad (3.50)$$

Where;  $\delta_j$  and  $\delta_{j-1}$  are lateral deflections of two adjacent storey levels and  $\delta_{ju}$  is the allowable lateral displacement.  $h_j$  is the storey height and  $ns$  is the total number of storeys in the frame.

### 3.3.7.3 Geometric Compatibility

In the design of structural frames, geometry and material properties of structural members (beams and columns) are determined considering the strength requirements given in design specifications available in the literature. However, in some situations, even though the complete design of a frame satisfies the strength and displacement limitations, it may not be practically applicable due to the geometric incompatibilities. In other words, from the practical point of view, geometries of columns and beams connected at one point, as shown in Figure 3.16, must be compatible with each other. These compatibility restrictions are given in the following.

1. The flange width of the beam section at each beam-column connection at one joint should be less than or equal to the flange width of column section, which is formulated as;

$$B_{jb} \leq B_{jc} \quad j = 1, \dots, nj \quad (3.51)$$

Where;  $B_{jb}$  and  $B_{jc}$  are the flange width of beam and column respectively and  $nj$  represents the total number of joints in the frame.

2. The depth and the mass per meter of column section at storey joint  $s+1$  at each beam-column connection should be less than or equal to depth and mass of the column section at the lower storey joints  $s$ , which is expressed as in the following.

$$D_{s+1} \leq D_s \quad s = 1, \dots, nu \quad (3.52)$$

$$m_{s+1} \leq m_s$$

Where;

$D_{s+1}$ ,  $m_{s+1}$  and  $D_s$ ,  $m_s$  are the depth and the mass per meter of column section at storey  $s+1$  and  $s$  respectively.  $nu$  is the total number of these constraints.

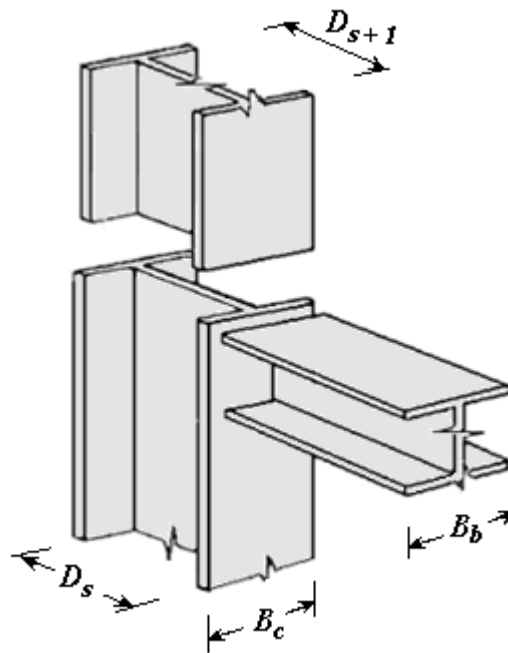


Figure 3.16 Geometry of beam to column connection.

### 3.4 Optimum Design of Steel Frames

Structural design may be defined as grossly abbreviated name of an operation, which for major projects may involve the knowledge of hundreds of experts from a variety of disciplines. Therefore, a code of practice may be regarded as a consensus of what is considered acceptable at the time it was written, containing a balance between accepted practice and recent research presented

in such a way that the information should be of immediate use to the design engineer. As such, rather than a manual or textbook on design, it is regarded more as an aid to design, which includes stress limitations, member capacities, design formulations and recommendations for good practice.

Once it is decided to construct a particular building, a suitable structural system must be selected. Attention is then given to the way where loads are to be resisted. Then, critical loading patterns must be determined to suit the purpose of the building. Therefore, the design operation involves a fundamental two-stage process. Firstly, a structural system analysis is conducted to determine the forces acting on the structural members and joints, secondly, the sizes of various structural members and details of the structural joints are chosen by checking against specification member-capacity formulae.

The design of steel frames is one of the common problems of steel structures that practicing engineer has to deal with. The design should be carried out in such a way that the frame satisfies the serviceability and strength requirements specified by the code of practice while the economy is observed in the overall cost of the frame. Although there are many factors that may affect the construction cost, the first and most obvious one is the amount of material used to build the structure. Therefore, minimizing the weight of the structure is usually the goal of optimum design in steel structures.

### **3.4.1 Mathematical Model of Optimum Design Problem of Unbraced Steel Frames**

Any optimization problem requires proper identification of objective function, design variables and constraints at problem formulation state. When the design

constraints, mentioned in previous sections, are implemented from LRFD-AISC [49] in the formulation of the design problem, the following mathematical programming problem is obtained.

$$\text{Minimize;} \quad W = \sum_{k=1}^{ng} m_k \sum_{i=1}^{nk} L_i \quad (3.53)$$

Subject to;

$$(\delta_j - \delta_{j-1}) / h_j \leq \delta_{ju} \quad , \quad j = 1, \dots, ns \quad (3.54)$$

$$\delta_i \leq \delta_{iu} \quad , \quad i = 1, \dots, nd \quad (3.55)$$

$$\phi_b V_n = V_u \quad (3.56)$$

$$\left( \frac{P_u}{\phi_c P_n} \right)_{il} + \left( \frac{8}{9} \left( \frac{M_{ux}}{\phi_b M_{nx}} \right) \right)_{il} \leq 1.0 \quad \text{for } \frac{P_u}{\phi_c P_n} \geq 0.2$$

$$i = 1, \dots, nm$$

$$l = 1, \dots, nl \quad (3.57)$$

$$\left( \frac{P_u}{2\phi_c P_n} \right)_{il} + \left( \frac{M_{ux}}{\phi_b M_{nx}} \right)_{il} \leq 1.0 \quad \text{for } \frac{P_u}{\phi_c P_n} \leq 0.2$$

$$B_{jb} \leq B_{jc} \quad j = 1, \dots, nj \quad (3.58)$$

$$D_{s+1} \leq D_s \quad s = 1, \dots, nu \quad (3.59)$$

$$m_{s+1} \leq m_s \quad (3.60)$$

Where;

Equation (3.53) defines the weight of the frame,  $n_g$  is total numbers of groups in the structural system,  $m_k$  is the unit weight of the steel section selected for group k,  $L_i$  is the length of member  $i$  that belongs to group k,  $n_k$  is total number of members in group k.

Equation (3.54) represents the inter-storey drift of the multi-storey frame.

Equation (3.55) defines the displacement restrictions.

Equation (3.56) represents the shear capacity check for beam-columns.

The combined strength constraints are given in Equation (3.57).

Equations (3.58), (3.59), (3.60) are the geometric compatibility constraints as presented in previous sections.

The main concept in the optimum design of unbraced steel frames is to select the appropriate steel sections for its columns and beams so that design code provisions are satisfied and the frame has the minimum weight. This selection of steel sections can be made by assuming the design variables to be continuous or to be discrete.

As mentioned in Chapter 2, results of optimum design problems may vary according to the design space used in the optimum design algorithm. This study proposes optimum design algorithms for unbraced steel frames in both continuous and discrete design spaces.

### **3.4.2 Optimum Design of Steel Frames in Continuous Design Space**

Unlike discrete design algorithm developed for unbraced steel frames where the real numbers are converted to integer numbers which represent the line numbers of ready steel section tables, continuous design algorithm uses real numbers directly as design variables.

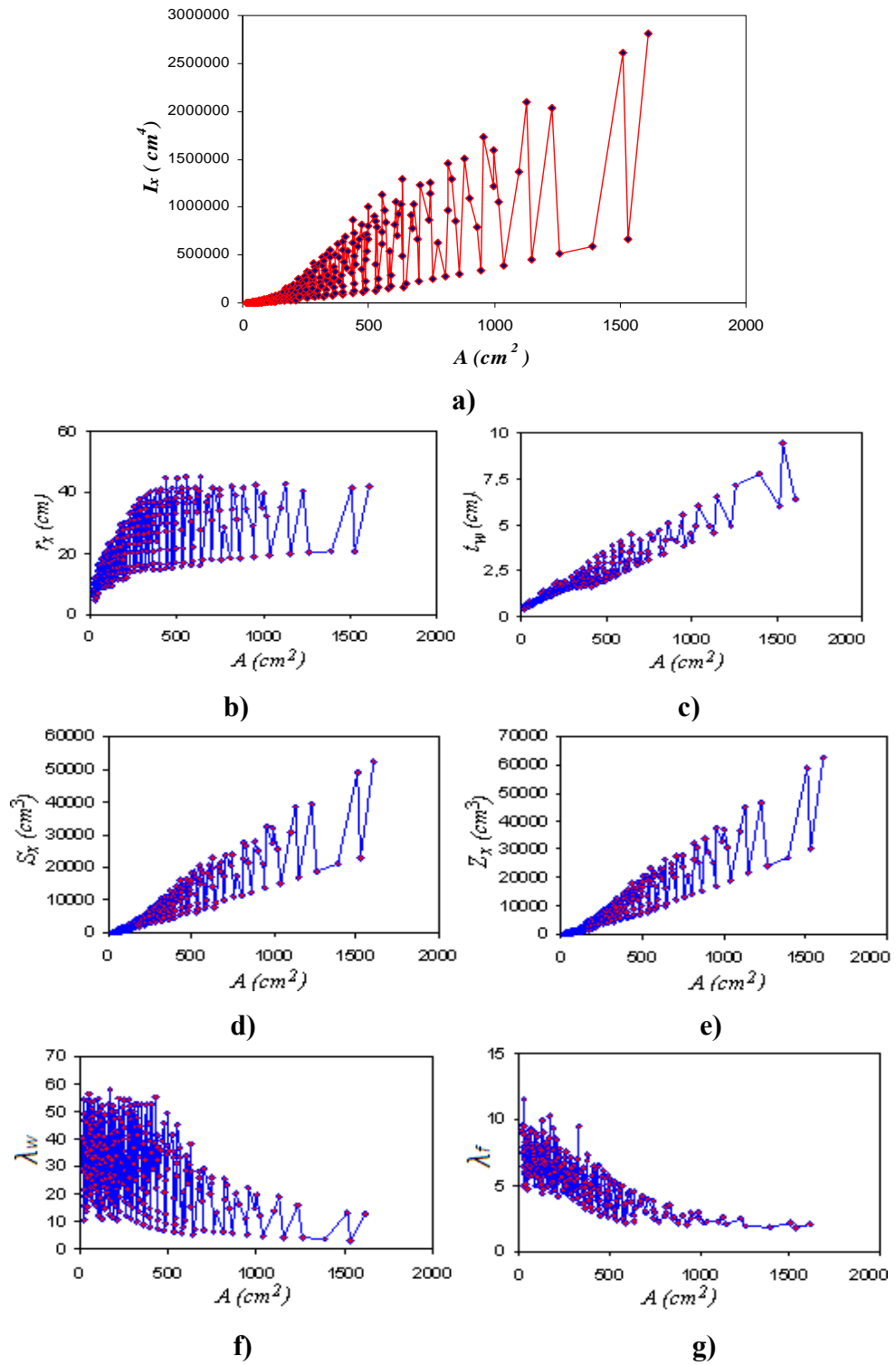
In the continuous optimization procedure developed for unbraced steel frames, the cross-sectional areas of the frame members are treated as design variables. However, it is clear that the computation of displacement and stress distribution of the frame members necessitates the employment of the other sectional properties i.e. moment of inertia, sectional modulus and radius of gyration. Therefore, it becomes necessary to relate these properties to the cross-sectional areas. This can be achieved by applying the linear interpolation approximation to sectional properties of ready steel sections available in practice.

Figure 3.17 illustrates the relationships between areas and other sectional properties. In Figure 3.17a, moment of inertias and corresponding cross-sectional areas of 272 ready steel sections, included in W-section list are plotted. Each point on the graph is connected to the following one by linear lines. Through the use of these lines, one can perform linear interpolation and obtain the approximate value of moment of inertia for each group, i.e. selected continuous value of cross-sectional area. For example, consider a value in the bounds of the areas of first and last sections of W-section list. Let 51.523 be the selected value of cross-sectional area of group 1. This value is between 49.9 and 53.1, which correspond to the areas of the sections of W410X38.8 and W200X41.7 respectively. Besides, the moment of inertias of these sections are

12700cm<sup>4</sup> and 4090cm<sup>4</sup> respectively. Performing a linear interpolation process one can easily calculate the approximate value of moment of inertia as  $I_x : 8333.12 \text{ cm}^4$ . Other cross-sectional properties are determined by applying the same procedure.

Where;  $A$  is the area;  $I_x$  is the moment of inertias about  $x-x$  axis of the member,  $r_x$  is the radius of gyration.  $S_x$  and  $Z_x$  represent the elastic and plastic section modulus respectively. Thickness of web of a W-section is represented by  $t_w$ . Finally,  $\lambda_w$  and  $\lambda_f$  are the slenderness ratios of web and flange of a W-section respectively.

Once the areas of members belonging to each group are selected, the values of above mentioned properties of the corresponding group are determined. Afterwards, the whole structure is analyzed and checked if the design constraints are satisfied. If this design is feasible, it is kept in the memory. Then, the area variables are changed in the next iteration to obtain a better design. This process is repeated until the minimum weight and the optimum values of corresponding areas are achieved.



**Figure 3.17** Graphical representations of cross-sectional properties of 272 W-sections.

### **3.4.3 Optimum Design of Steel Frames in Discrete Design Space**

The realistic design of steel frames involves the selection of steel sections for its columns and beams from ready steel section list available in practice. As such, the design variables of the optimum design problem turn out to be discrete. These values, the design variables in the design problem described, are selected as the sequence numbers of the W-sections in the available set. Since 272 W-sections are considered in the present study, the sequence number which can have a value between 1 to 272 is randomly selected for a design variable. For example if 65 is selected for group 2, the W-section which is W 310 x 342 will be used for the members which belong to group 2. Once the W-section is selected the cross sectional properties of the section becomes available from the w-section list. The stress distributions and the displacements of the frame members are then determined by using an available structural analysis method. These values are checked if they are inside the limits of the corresponding constraints. If this is satisfied, it is considered as a feasible design and the weight of the whole structure is calculated. Later, a new design is created by the algorithm and the same constraint-check procedure is applied to this new one. If this design is lighter than the previous one it is assumed to be current optimum design. This routine is repeated until a predefined number of iteration is reached and the weight obtained at the end of this process is considered as the optimum design.

### **3.4.4 Particle Swarm Optimization Design of Unbraced Steel Frames**

The optimum design procedure is based on the particle swarm optimization algorithm mentioned in the previous chapter and coded using FORTRAN programming language. Steps of this design optimization procedure can be summarized as follows;

1. Firstly, the geometry and loadings of frame are defined. Afterwards, beams and columns of the frame are grouped together.
2. Particle swarm design algorithm is started by generating initial values (positions of particles) for the design variables i.e. cross sectional areas of steel sections for continuous design or sequence numbers of steel sections in the available steel profile table for discrete design. Then, all the cross sectional properties such as moment of inertia, sectional modulus and radius of gyration belonging to each group are determined.
3. Structure is analyzed with the use of analysis subroutine which is based on matrix stiffness method. Member forces and displacements are computed.
4. Fly-back mechanism is used to handle the design constraints. It is checked if the strength and displacement requirements given in design code are satisfied. If one or a number of constraints are not satisfied, this design is discarded and new one is generated.
5. After feasible designs are obtained, particle swarm iteration process is initialized. Objective function values, weights of frames belonging to

each design, are calculated. The particle which has the minimum weight is accepted as current optimum design. The values of design variables are updated using velocity and position update equations of particle swarm algorithm and new designs are generated.

6. Analysis routine is repeated for these new designs and constraints are checked. If all the constraints are satisfied, weights of these designs are computed. If the lightest of them is also lighter than the current optimum design, it is accepted as new optimum.
7. This iteration procedure is repeated until the predefined number of iterations is completed. The design from which the minimum weight obtained at the end of this iteration process is taken as the optimum design.

### **3.4.5 Design Examples**

Seven unbraced steel frames are designed using particle swarm method based optimum design algorithm presented in the previous section. In each example, frame models are designed with both continuous and discrete optimum design algorithms to compare the overall weight of the structure obtained with each approach. The areas, which are the variables of the former approach to be optimized in the iteration process, are bounded with the values of first and last steel sections of the ready W-section list. In the second approach, on the other hand, the discrete set from which the design algorithm selects the sectional designations for frame members is considered to be the complete set of 272 W-sections starting from W100x19.3 to W1100x499mm as given in LRFD-AISC [49].

### 3.4.5.1 Three Storey, Two Bay Steel Frame

The two bay, three storey frame shown in Figure 3.18 is selected as first design example to demonstrate the application of the particle swarm optimization based optimum design algorithm developed. The dimensions, member grouping and the external loading of the system are also shown in the figure. The upper bound imposed on lateral deflections of the top storey joints is limited to  $1/300$  of the frame height, which corresponds to 30.48 mm. The frame members are collected in two different groups. Columns are considered to be group 1 while beams are taken as group 2 as shown in the figure. Hence there are only two design variables in the design problem. A single distributed load of 40 kN/m is applied on each beam of the frame and lateral loading of 20kN is applied to each storey level. The strength capacities of steel members are computed according to LRFD-AISC [49]. Fixed supports are used for the connection of the columns to the foundation.

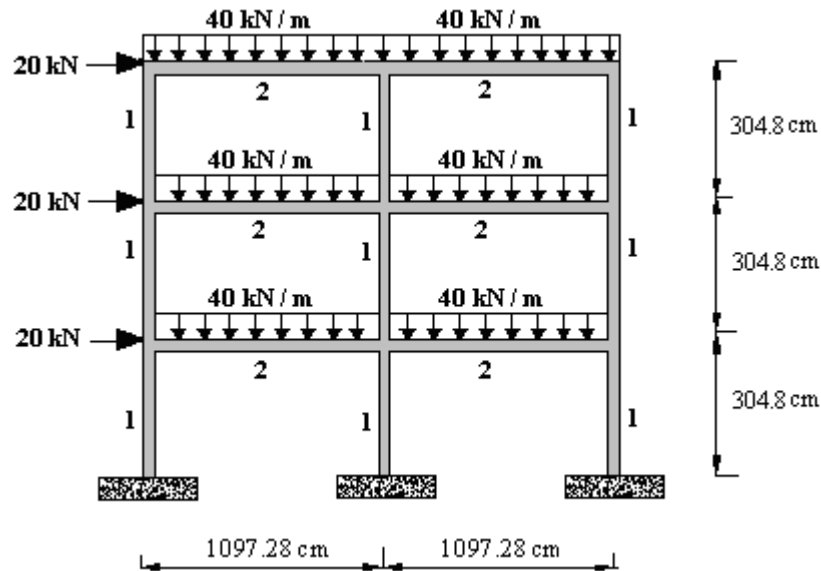
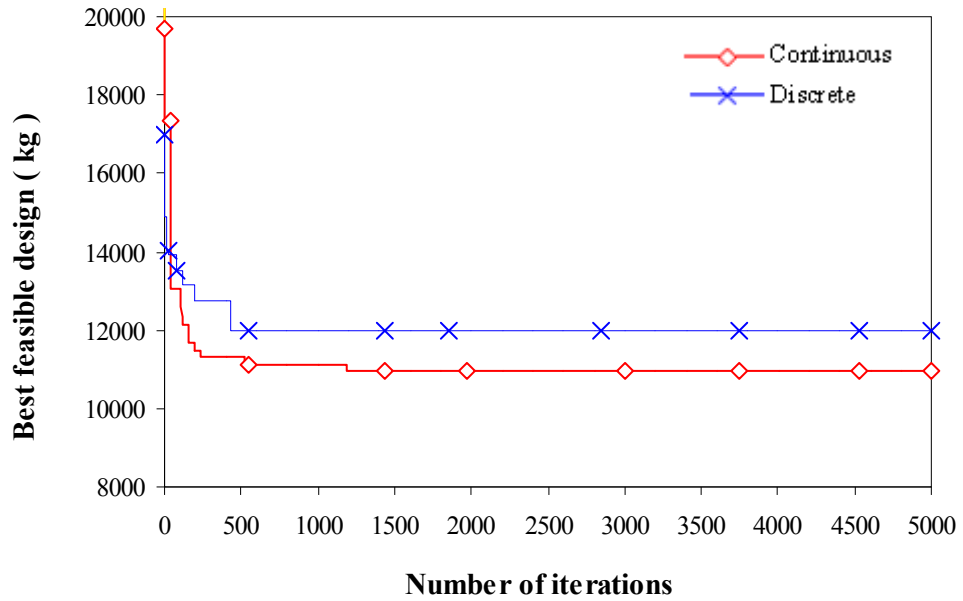


Figure 3.18 Three storey-two bay steel frame.

**Table 3.1** Optimum designs for three-storey, two-bay rigid steel frame.

<b>Group No.</b>	<b>Member Type</b>	<b>Continuous variables Area (cm<sup>2</sup>)</b>	<b>Discrete variables W- sections- Area (cm<sup>2</sup>)</b>
1	Column	63.957	W250X73 (92.8)
2	Beam	186.995	W690X152 (194)
Max. Int. St. Drift Ratio		0.28	0.30
Maximum Strength Ratio		1.00	0.98
Top storey drift (cm)		0.741	0.80
Minimum Weight. kg		10968.25	12005.990
(kN)		(107.556)	(117.738)

The frame is designed twice considering both discrete and continuous algorithms. The design history of these runs is shown in Figure 3.19. The best designs obtained by the discrete and continuous particle swarm optimizer are tabulated in Table 3.1 with section designations or cross sectional areas attained for each member group. Continuous treatment gives lighter design, which is 10968.25kg. The frame weight of discrete design is 12005.99kg. This means that the continuous design algorithm produces 9.5% lighter frame. The strength ratios obtained are 1.00 and 0.98 and top storey drifts are 0.74 and 0.80 for continuous and discrete frames respectively. This indicates that strength constraints dominate the designs.



**Figure 3.19** Design history graph for three-storey, two-bay steel frame.

### 3.4.5.2 Four Storey, Four Bay Steel Frame

The four-bay, four storey steel frame shown in Figure 3.20 is considered as the second design example. The frame consists of thirty-six members that are collected in two groups as shown in the figure. Columns are considered to be group 1 while beams are taken as group 2. The lateral displacement of the top storey is limited to 4cm. The modulus of elasticity is  $200\text{kN/mm}^2$ . Fixed supports are used for the connection of the columns to the foundation.

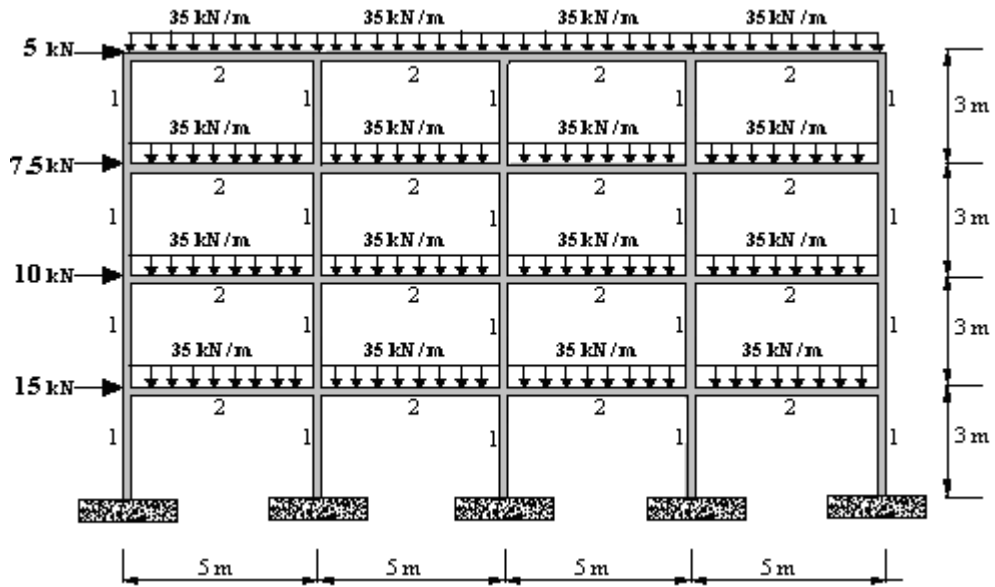


**Figure 3.20** Four storey- four bay steel frame.

The optimum W-sections designation and the cross sectional areas obtained by the discrete and continuous particle swarm method respectively are given in Table 3.2. The discrete optimum design is attained after 340 iterations and the minimum weight of the frame is 5914.37kg while the continuous one is determined after 700 cycles and the minimum weight is obtained as 5399.96kg. This means that the continuous design algorithm produces 9.6% lighter frame. The convergence rate of the problem is shown in the design-history graph given in Figure 3.21. It is noticed that in the optimum frame obtained with discrete set the lateral displacement of top storey was 1.59 cm against its upper bound of 4cm. The highest ratio among the combined strength constraints was 0.99 compare to 1. This clearly indicates that strength constraints dominate this design. Similarly, in the continuous design, the maximum strength ratio dominates the design with the value of 0.99.

**Table 3.2** Optimum designs for four-storey, four-bay rigid steel frame.

Group No.	Member Type	Continuous variables Area (cm <sup>2</sup> )	Discrete variables W- sections- Area (cm <sup>2</sup> )
1	Column	28.818	W150X37.1 (47.3)
2	Beam	65.719	W410X46.1 (58.9)
Max. Int. St. Drift Ratio		0.48	0.47
Maximum Strength Ratio		0.99	0.99
Top storey drift (cm)		1.61	1.59
Minimum Weight. kg (kN)		5399.96 (52.955)	5914.37 (58.00)

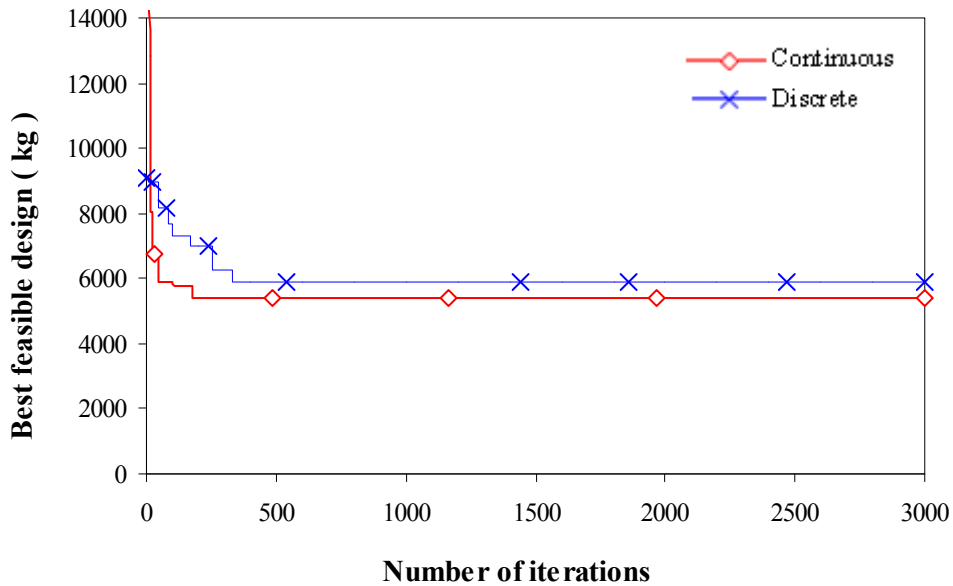


**Figure 3.21** Design history graph for four-storey, four-bay steel frame.

### 3.4.5.3 Five Storey, Three Bay Steel Frame

Third example is the three -bay, five storey steel frame as shown in Figure 3.22. This frame is designed by particle swarm optimizer based continuous and



The optimum W-sections designation and the cross sectional areas are given in Table 3.3. The optimum continuous design is obtained after just 450 iterations with the minimum weight of 1249.526kg while the minimum weight of discrete one is 1375.194kg attained after 870 iterations. It is clear from the results that both the maximum inter storey drift ratio and the maximum strength ratio are dominant in the designs. The maximum lateral displacement is recorded as 5.00cm and 4.19cm in the continuous and discrete design respectively. The design-history graphs are shown in Figure 3.23. It is apparent from the results that the continuous optimum design algorithm produces 10% lighter frame.

**Table 3.3** Optimum designs for five-storey, three-bay rigid steel frame.

<b>Group No.</b>	<b>Member Type</b>	<b>Continuous variables Area (cm<sup>2</sup>)</b>	<b>Discrete variables W- sections- Area (cm<sup>2</sup>)</b>
1	Column	17.877	W310X28.3 (36.1)
2	Column	17.645	W130X23.8 (30.1)
3	Column	26.653	W310X23.8 (30.4)
4	Column	19.871	W250X17.9 (22.7)
5	Beam	26.964	W310X21 (26.9)
6	Beam	49.672	W310X23.8 (30.4)
7	Beam	18.733	W200X15 (19.1)
Max. Int. St. Drift Ratio		0.99	1.00
Maximum Strength Ratio		0.99	0.98
Top storey drift (cm)		5.00	4.19
Minimum Weight. kg (kN)		1249.526 (12.254)	1375.194 (13.486)

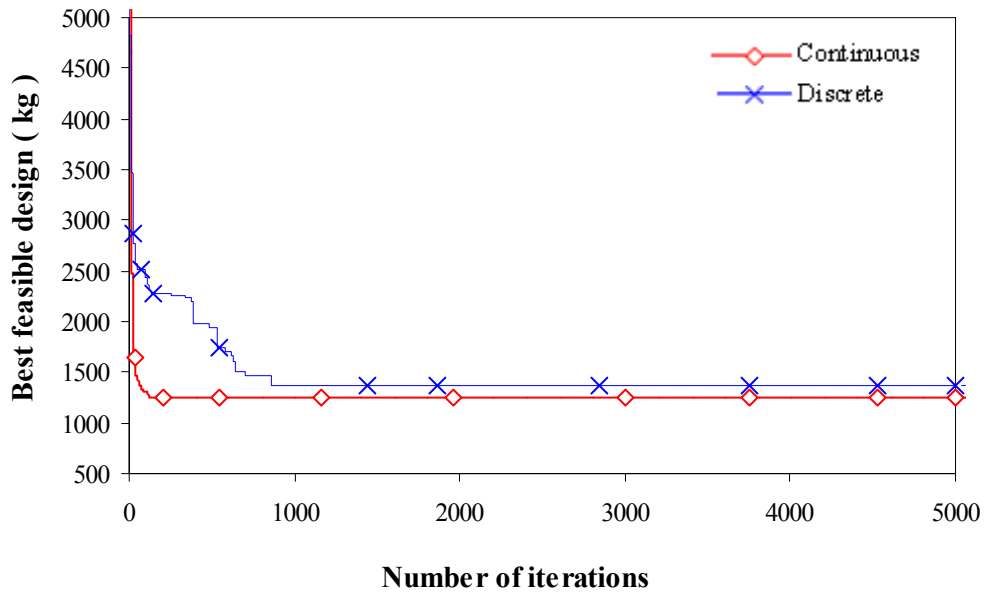


**Figure 3.23** Design history graph for five-storey, three-bay steel frame.

#### 3.4.5.4 Six Storey, Two Bay Steel Frame

The two-bay, six storey steel frame shown in Figure 3.24 is considered as the fourth design example. The frame consists of thirty members that are collected in eight groups as shown in the figure. The lateral displacement of the top storey is limited to 4cm. The modulus of elasticity is  $200\text{kN/mm}^2$ . A distributed load  $50\text{ kN/m}$  and a single lateral load is applied to each horizontal member of the frame. Fixed supports are used for the connection of the columns to the foundation.



1450 cycles and the minimum weight is 6071.036kg. The convergence rate of the problem is illustrated in the design-history graph given in Figure 3.25. This means that continuous design algorithm produces 24% lighter frame. It is noticed that in the optimum frame obtained with discrete set the lateral displacement of top storey was 4.533 cm against its upper bound of 7.17cm. The highest ratio among the combined strength constraints was 0.99 compare to 1 which was attained in member 30. Maximum inter-storey drift ratio is recorded as 0.78 at joint 15. This clearly indicates that strength constraints dominate this design. In the continuous design, similarly, the maximum strength ratio which is attained as 1 is dominant.

**Table 3.4** Optimum designs for six-storey, two-bay rigid steel frame.

<b>Group No.</b>	<b>Member Type</b>	<b>Continuous variables Area (cm<sup>2</sup>)</b>	<b>Discrete variables W- sections- Area (cm<sup>2</sup>)</b>
1	Column	75.932	W530X74 (95.2)
2	Column	58.977	W310X52 (66.7)
3	Column	22.860	W200X41.7 (53.1)
4	Column	64.590	W460X89 (114)
5	Column	41.977	W460X89 (114)
6	Column	64.872	W360X72 (91.1)
7	Beam	82.981	W460X60 (75.9)
8	Beam	65.930	W460X68 (87.3)
Max. Int. St. Drift Ratio		0.97	0.78
Maximum Strength Ratio		1.00	0.99
Top storey drift (cm)		5.98	4.5325
Minimum Weight. kg (kN)		6071.036 (59.536)	7532.11 (73.865)

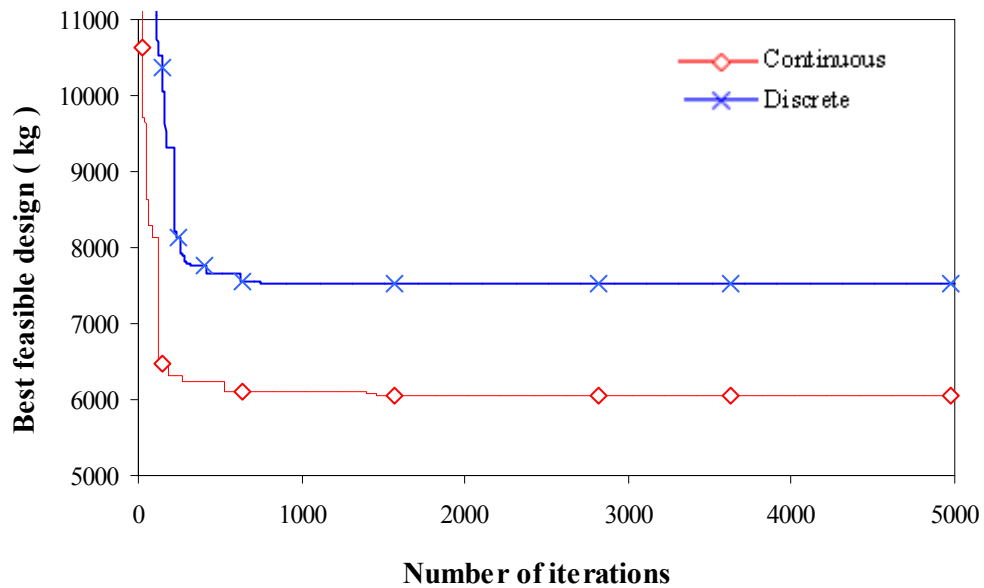


**Figure 3.25** Design history graph for six-storey, two-bay steel frame.

### 3.4.5.5 Ten Storey, One Bay Steel Frame

Fifth example is one -bay, ten storey steel frame as shown in Figure 3.26. This problem is separately designed by continuous and discrete particle swarm algorithms. The frame involves thirty members that are collected in nine groups as shown in the figure. First five of these groups are assigned to the columns and the rest is assigned to the beams. Top storey beam is considered to be one group and beams in every three floor are considered to be different groups as shown in the figure. The allowable inter-storey drift is 12.19mm while the lateral displacement of the top storey is limited to 121.93mm. Beams of the frame are loaded by the distributed load of 80kN/m and lateral loading is applied at each storey level. The modulus of elasticity is 200kN/mm<sup>2</sup>. Maximum number of iterations is selected as 9000. Fixed supports are used for the connection of the columns to the foundation.

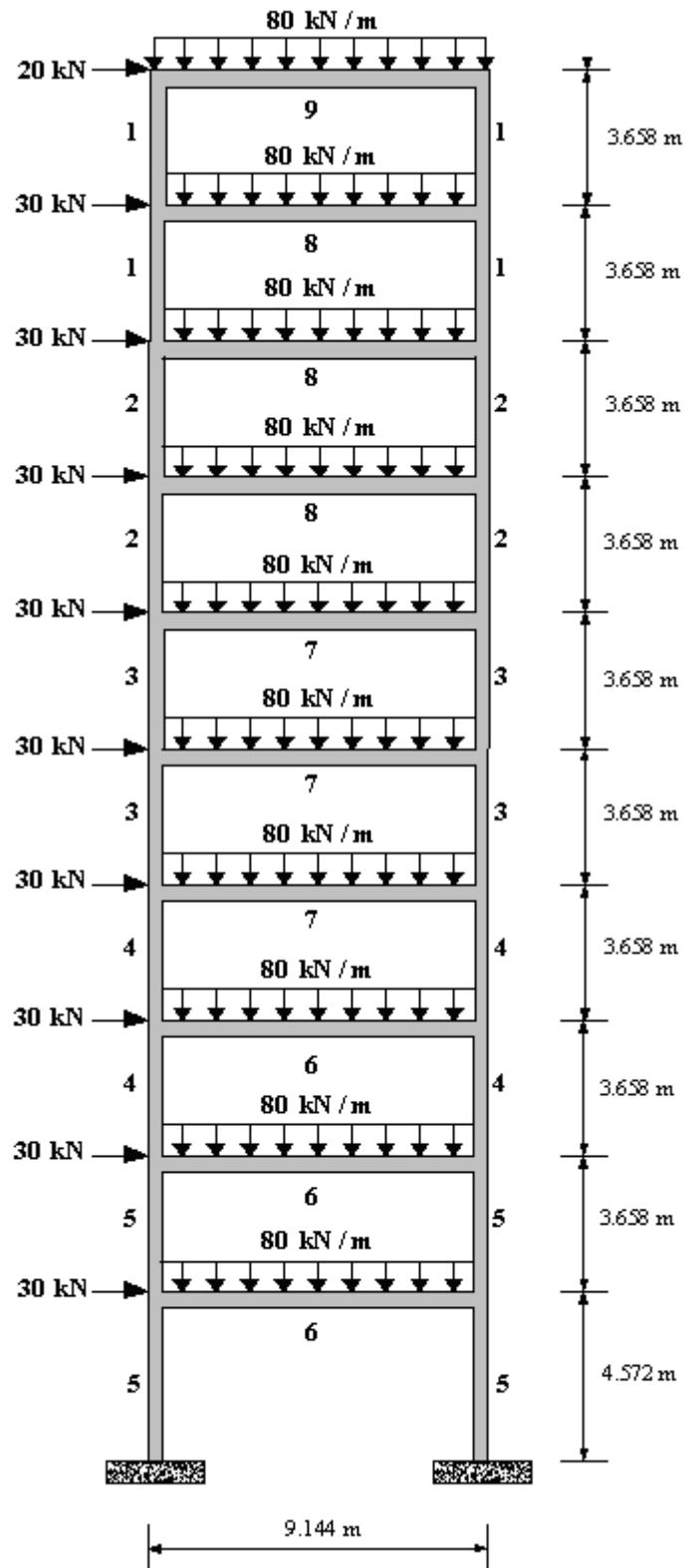
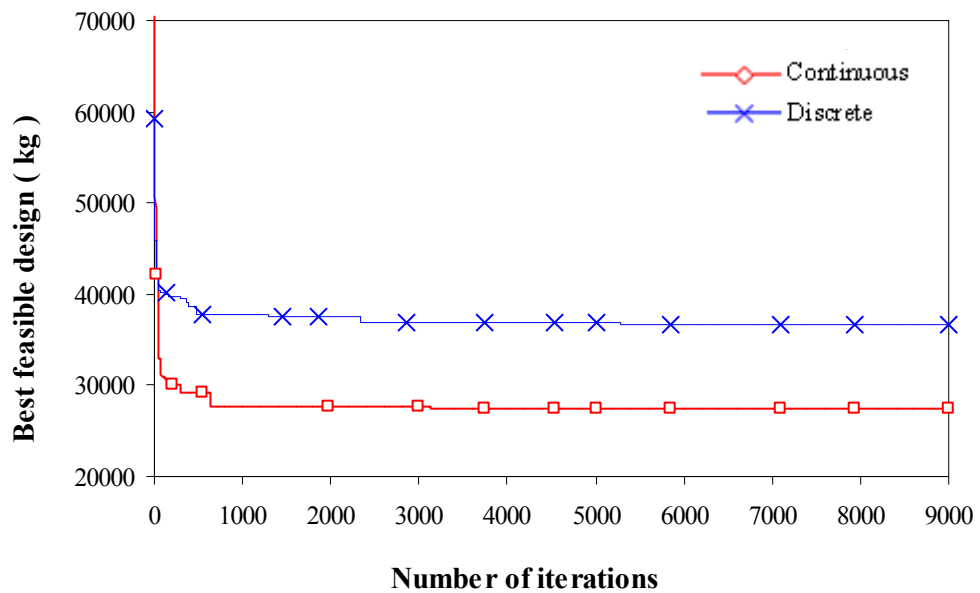


Figure 3.26 Ten storey-one bay steel frame.

The optimum W-sections designation and the cross sectional areas obtained by the particle swarm method are given in Table 3.5. The optimum continuous design is obtained only after 3200 iterations with the minimum weight of 27480.36kg while the minimum weight of discrete one is 36697.92kg which is attained after 5300 iterations. This means that continuous algorithm produces 34% lighter frame. The highest inter-storey drift ratio of discrete design is 0.38, while the maximum strength ratio is 1.00 which dominates this design. Continuous design, similarly, is dominated by the strength constraint. The maximum lateral displacement is recorded as 5.253cm and 3.602cm in the continuous and discrete design respectively. Design-history graphs of these designs are shown in Figure 3.27.

**Table 3.5** Optimum designs for ten-storey, one-bay rigid steel frame.

<b>Group No.</b>	<b>Member Type</b>	<b>Continuous variables Area (cm<sup>2</sup>)</b>	<b>Discrete variables W- sections- Area (cm<sup>2</sup>)</b>
1	Column	138.892	W530X150 (192)
2	Column	138.892	W530X150 (192)
3	Column	177.812	W1000X222 (283)
4	Column	223.616	W1000X314 (400)
5	Column	282.311	W1000X494 (630)
6	Beam	234.798	W840X176 (224)
7	Beam	223.563	W840X176 (224)
8	Beam	218.938	W760X185 (235)
9	Beam	215.985	W760X173 (221)
Max. Int. St. Drift Ratio		0.55	0.38
Maximum Strength Ratio		1.00	1.00
Top storey drift (cm)		5.253	3.602
Minimum Weight. kg (kN)		27480.360 (269.489)	36697.92 (359.882)



**Figure 3.27** Design history graph for ten-storey, one-bay steel frame.

### 3.4.5.6 Ten Storey, Three Bay Steel Frame

The three-bay, ten storey steel frame is considered as the sixth design example. The dimensions of the frame and the loadings are shown in the Figure 3.28. The frame consists of seventy members that are collected in nine groups as shown in the figure. The frame is subjected to gravity loading of 50kN/m on the beams of roof level and on the beams of each floor. The lateral load of 30kN is considered at each storey level. The lateral displacement of the top storey is limited to 11.83cm and the inter-storey drift is restricted to 1.17cm. The modulus of elasticity is assumed to be 200kN/mm<sup>2</sup>. Fixed supports are used for the connection of the columns to the foundation.

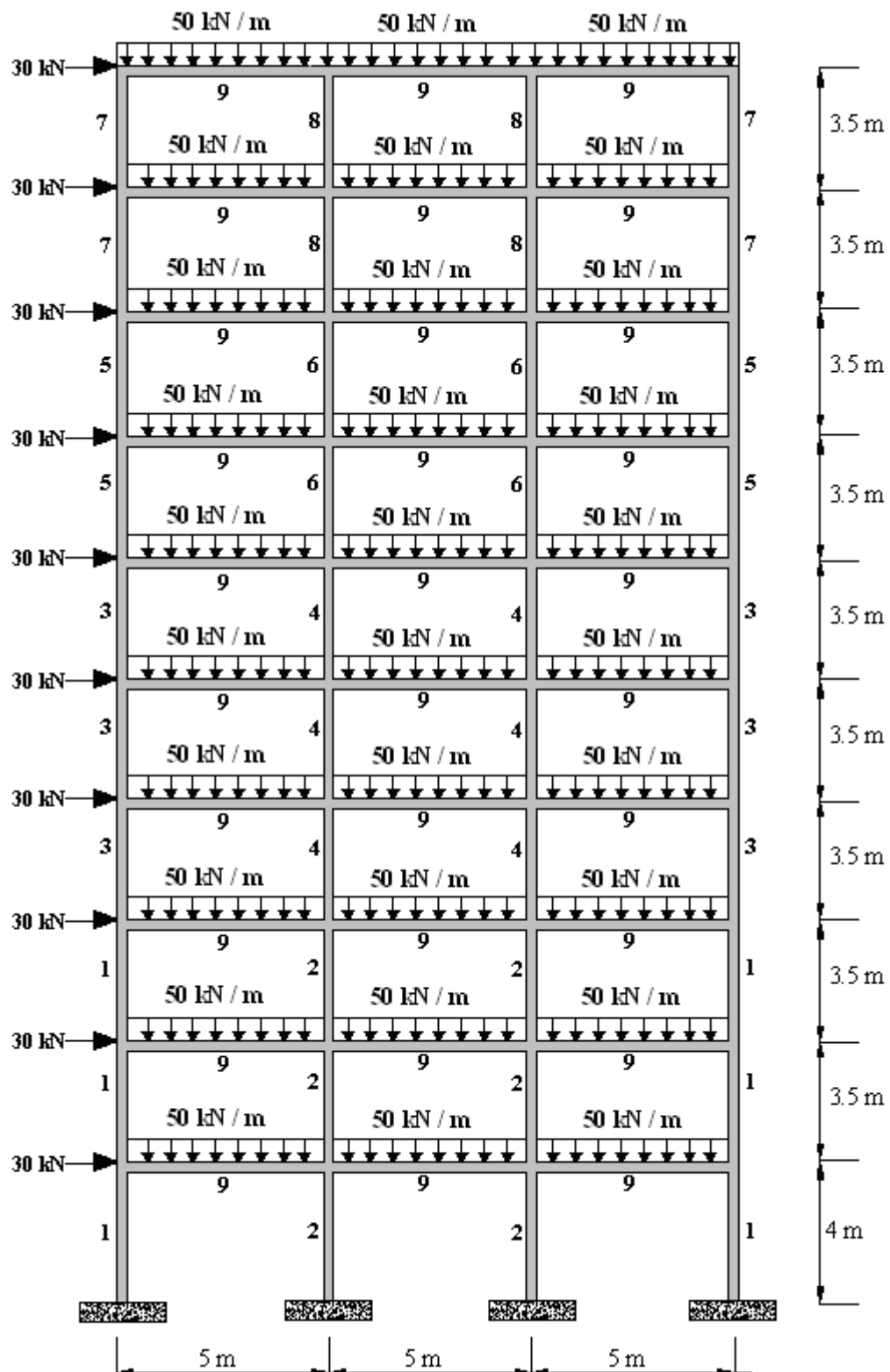


Figure 3.28 Ten storey- three bay steel frame.

Table 3.6 shows the optimum W-sections designation and the cross sectional areas obtained by the discrete and continuous particle swarm method respectively.

**Table 3.6** Optimum designs for ten-storey, three-bay rigid steel frame.

<b>Group No.</b>	<b>Member Type</b>	<b>Continuous variables Area (cm<sup>2</sup>)</b>	<b>Discrete variables W- sections- Area (cm<sup>2</sup>)</b>
1	Column	156.546	W610X153 (196)
2	Column	94.479	W610X113 (144)
3	Column	83.467	W530X92 (118)
4	Column	104.017	W460X82 (104)
5	Column	83.990	W310X60 (75.9)
6	Column	33.808	W410X53 (68.1)
7	Column	83.989	W310X60 (75.9)
8	Column	33.805	W410X53 (68.1)
9	Beam	83.744	W460X68 (87.3)
Max. Int. St. Drift Ratio		0.94	0.87
Maximum Strength Ratio		1.00	1.00
Top storey drift (cm)		8.76	7.86
Minimum Weight. kg		19720.07	22879.35
(kN)		(193.387)	(224.369)

The discrete optimum design is attained after 3370 iterations and the minimum weight of the frame is 22879.35kg while the continuous one is determined after 2600 cycles and the minimum weight is 19720.07kg. The convergence rate of the problem is shown in the design-history graphs given in Figure 3.29. It is clear from the results that continuous design algorithm produces 16% lighter frame. It is noticed that in the optimum frame obtained with discrete set the lateral displacement of top storey was 7.86 cm against its upper bound of 11.83cm. The highest ratio among the combined strength constraints was 1. The maximum inter-storey drift ratio is recorded as 0.87.

This clearly indicates that strength constraints dominate this design. Similarly, the maximum strength ratio which is attained as 1 dominates the continuous design.

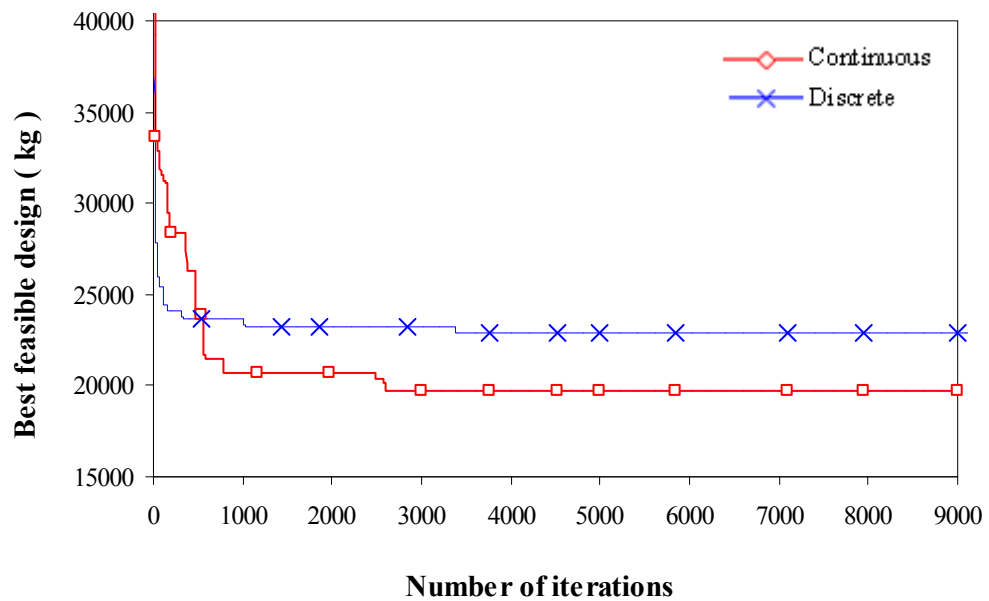


**Figure 3.29** Design history graph for ten-storey, three-bay steel frame

### 3.4.5.7 Fifteen Storey, Three Bay Steel Frame

The three-bay, fifteen-storey frame shown in Figure 3.30 is considered as the last design example. The dimensions and the loadings of the frame are shown in the figure. The frame is subjected to gravity loading of 12.4kN/m on the beams of roof level and 20kN/m on the beams of each floor. The modulus of elasticity is 200kN/mm<sup>2</sup>. Frame consists of 105 members that are collected in 12 groups. Inner columns and outer columns in every three story considered to be different groups.

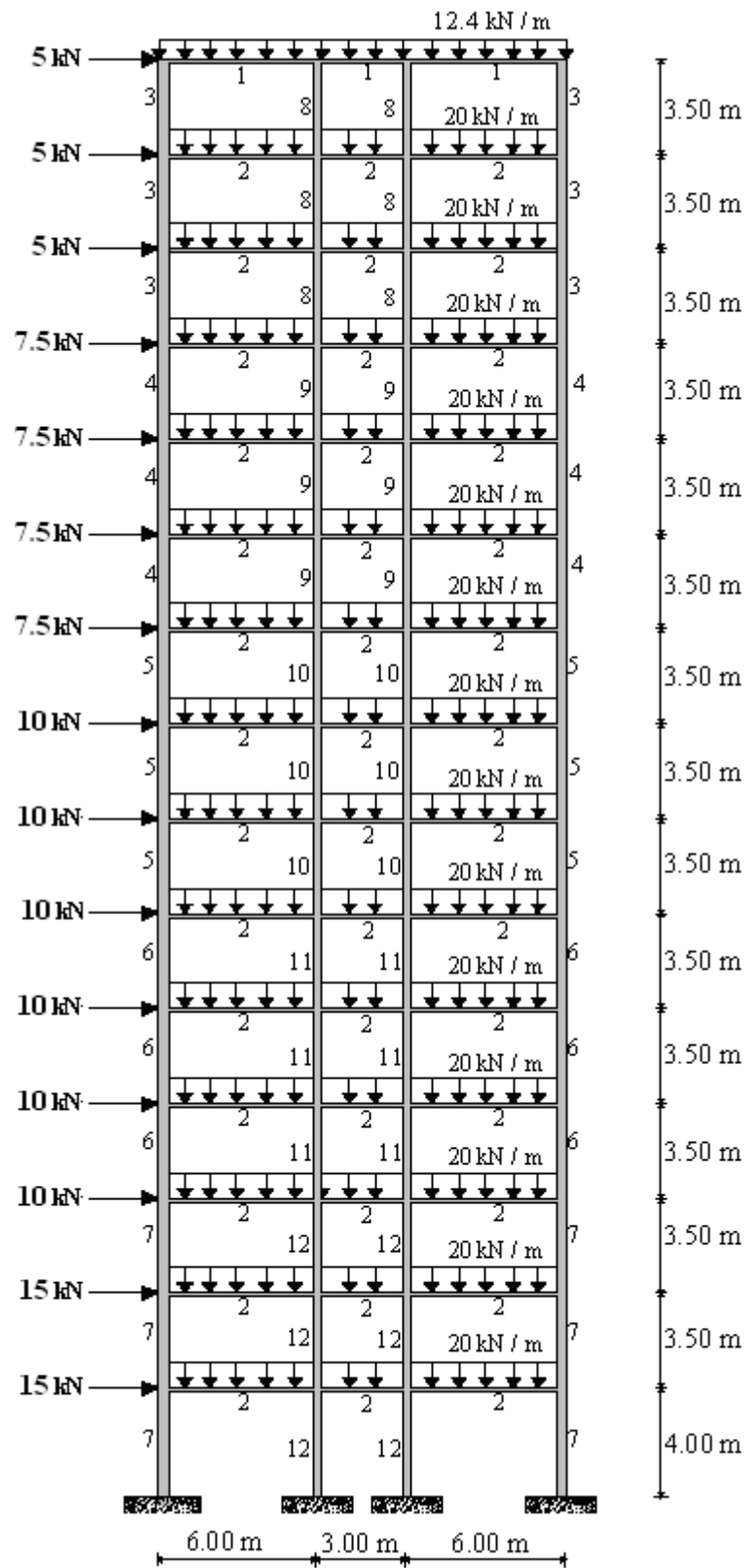


Figure 3.30 Fifteen-storey, three-bay steel frame.

The beams of roof and intermediate floors are considered to be two different groups as shown in the figure. The allowable inter-storey drift is 1.17cm while the lateral displacement of the top storey is limited to 17.67cm. Fixed supports are used for the connection of the columns to the foundation.

The optimum W-sections designation and the cross sectional areas obtained by the discrete and continuous algorithms are given in Table 3.7 and the design-history graph obtained for the problem is given in Figure 3.31. Discrete design is obtained after 3200 iterations and continuous solution is attained after 1570 cycles. The minimum weight of the discrete frame is 29092.81kg while the weight of continuous one is 18581.21kg. This means that the continuous design algorithm produces 57% lighter frame. It is noticed that in the discrete frame maximum inter storey drift ratio was 0.64 while the lateral displacement of top storey was 8.59cm against its upper bound of 17.67cm. The highest ratio among the combined strength constraints was 0.99 compare to 1 which was attained in member 81 which is the outer column of seventh storey. This clearly indicates that strength constraint dominates the design. In the continuous frame, similarly, the lateral displacement of top storey is 13.24cm and the highest ratios of inter storey drift and strength constraints are 0.99 and 1.00, respectively. This means that both the inter storey drift constraint and strength constraint is dominant.

**Table 3.7** Optimum designs for fifteen-storey, three-bay rigid steel frame.

Group No.	Member Type	Continuous variables Area (cm <sup>2</sup> )	Discrete variables W- sections- Area (cm <sup>2</sup> )
1	Column	41.679	W410X46.1 (58.9)
2	Column	65.899	W410X46.1 (58.9)
3	Column	36.112	W410X38.8 (49.9)
4	Column	36.114	W410X38.8 (49.9)
5	Column	50.655	W460X52 (66.3)
6	Column	64.263	W460X193 (246)
7	Column	73.879	W530X196 (250)
8	Beam	18.945	W250X32.7 (41.7)
9	Beam	30.454	W410X60 (75.8)
10	Beam	30.453	W410X60 (75.8)
11	Beam	41.966	W460X60 (75.9)
12	Beam	75.970	W690X170 (216)
Max. Int. St. Drift Ratio		0.99	0.64
Maximum Strength Ratio		1.00	0.99
Top storey drift (cm)		13.24	8.59
Minimum Weight. kg (kN)		18581.21 (182.218)	29092.81 (285.301)

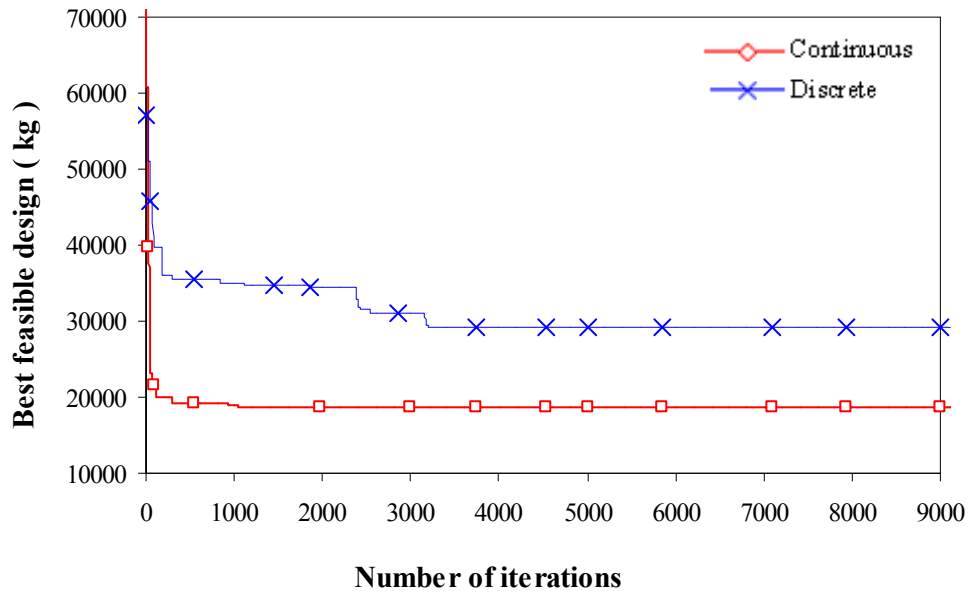


**Figure 3.31** Design history graph for fifteen-storey, three-bay steel frame.

## **CHAPTER 4**

### **OPTIMUM DESIGN OF SEMI-RIGID STEEL SWAY FRAMES TO LRFD**

#### **4.1 Semi-Rigid Connections**

The steel framework is one of the most common structural systems used in modern construction. In the analysis of such structural system, the modeling of structural elements requires some assumptions concerning the behavior of beam to column connections. The connections' behavior has an important effect on the frame performance, because they are the basic elements and integrated part of a steel frame.

The Load and Resistance Factor Design (LRFD) specification of the American Institute of Steel Construction (AISC) [49] divides the steel frame construction in two basic categories as in the following (Figure 4.1).

1. Fully restrained (FR) type construction, full continuity and sufficient rigidity of beam to column connections, which can retain the initial angles between intersection members.
2. Partially restrained (PR) type construction, which assumes that a connection possesses moment capacity in between complete fixity and the pin connection.

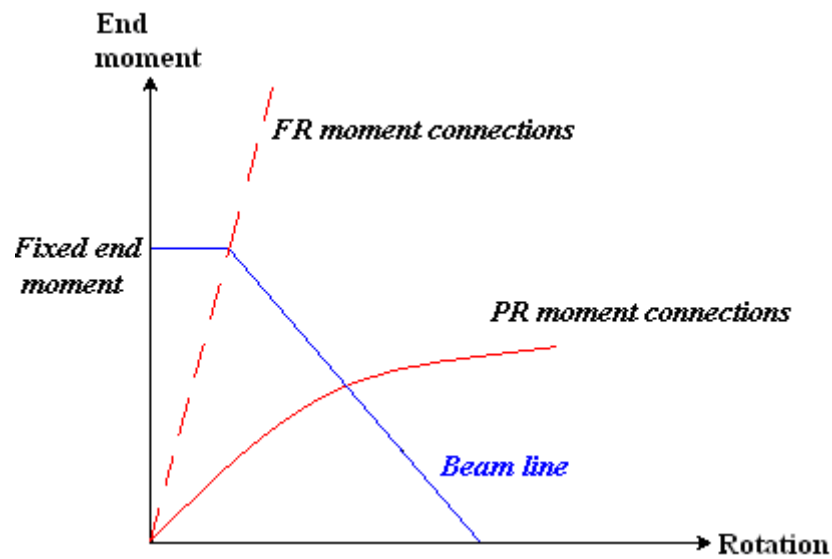


**Figure 4.1** Moment- rotation behavior of connections.

Steel frame designers use two idealized connection models in the conventional analysis methods. These models are called the rigid-joint model and the pinned-joint model. Former assumption implies that no relative rotation of the connection occurs and the beam transfers the whole end moment to the column. Contrary to this type, in the pinned-joint model, the connection moment is always zero and there is no restraint for rotation of the connection. Since the actual behavior of frame connections is between these extremes, in recent years, much attention has been focused towards more accurate modeling. As a result of these affords, advanced methods of structural analysis accounting for the actual behavior of beam to column joints are currently available. From the practical point of view, it is important to identify both the structural situations where the rotational behavior of joints needs to be accounted for and those allowing either the hinge or the fixed-end model to be assumed. Figure 4.2 shows the comparison between connection types.

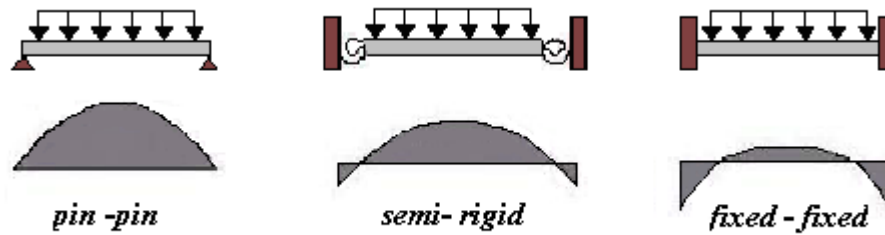


**Figure 4.2** Comparison of semi-rigid connections vs. pinned and fixed connections with respect to moment distribution.

In general, connections that fasten beam to column using plates, angles, welds, and bolts are deformable and perform a non-linear behavior between fully fixed and perfectly pinned conditions. Therefore, it is more reasonable to categorize all connections under the classification of semi-rigid, whereas rigid and pinned conditions being special cases.

One can neglect the effect of axial and shearing forces since their corresponding deformations are small compare to the rotational deformation of connections. Thus, it can be stated that the primary distortion of a steel beam to column connection is due to in-plane bending moment, which yields in a rotational deformation. When a moment  $M$  is applied to a beam-column connection, it rotates by an amount  $\theta_r$ , which is the angle between beam and column from their original position (Figure 4.3).

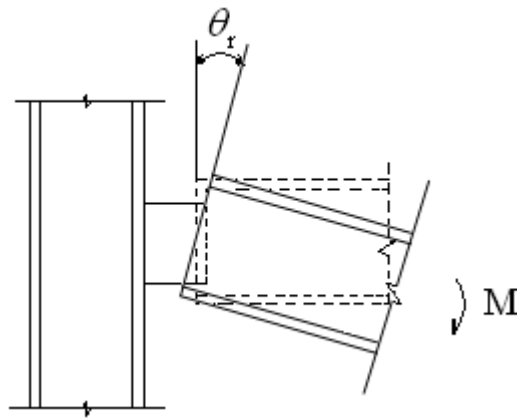


**Figure 4.3** Rotational deformation of a connection.

There also exists a destabilization effect on frame stability due to this end moment since additional drift will occur as a result of the decrease in effective stiffness of the members which the connections are attached to. Increased frame drift triggers the P- $\Delta$  effect and the overall stability of the frame will be affected. Figure 4.4 shows an unbraced frame subject to gravity and lateral forces.

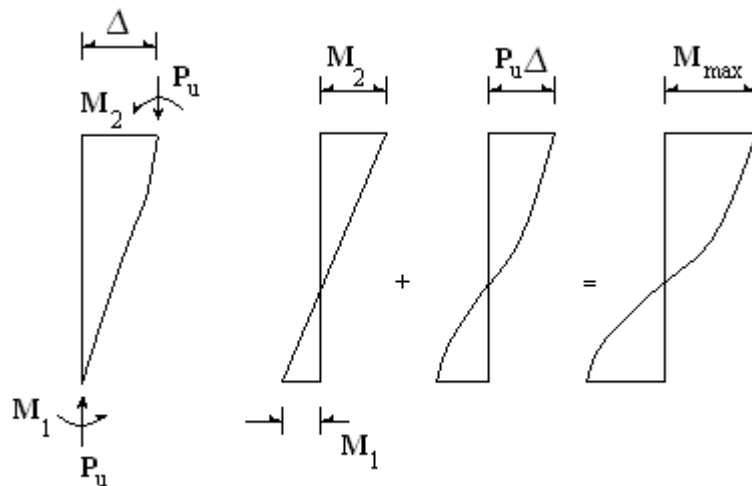


**Figure 4.4** P- $\Delta$  effect of unbraced frame.

In Figure 4.5, the moment rotation behavior of a variety of commonly used semi-rigid connections is illustrated. It is clear from this figure that the single web-angle connection is very flexible connection while the T-stub one is comparatively rigid. It can also be observed that a flexible connection has a smaller ultimate moment capacity and a larger rotation, and vice versa. The moment-rotation curves of all types of connections are nonlinear over entire range of loading.

The nonlinear behavior of the semi-rigid connections is due to a number of factors some of which are given as follows [80];

1. Material discontinuity of the connection assemblage: Since a connection is usually an arrangement of fasteners (such as welds or bolts) and structural shapes (such as angles and T-stubs), there exist irregular slips between components during loading.
2. Local yielding of parts of connection, which is the primary factor in the nonlinear behavior of connections.
3. Stress-strain concentrations resulted in by holes, fasteners and bearing contacts of elements in connection assemblage.
4. Local buckling of flanges and/or web of the beam and the column in the vicinity of a connection.
5. Overall geometric changes under the effect of applied loads.

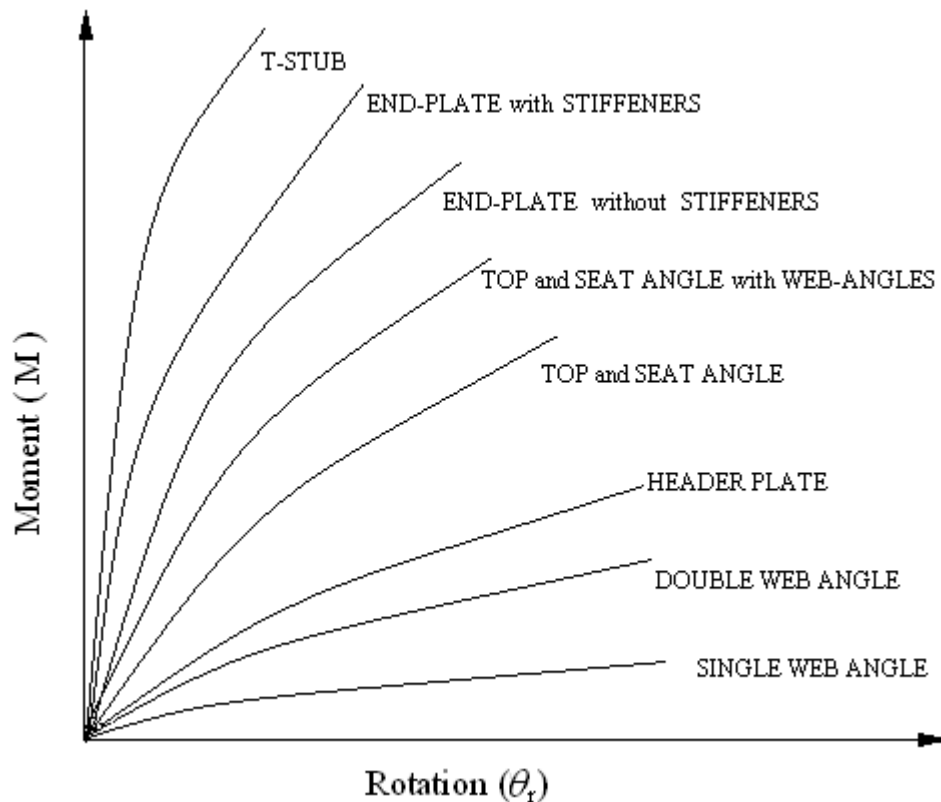


**Figure 4.5** Connection moment-rotation curves.

While fully restrained (FR) construction and partially restrained (PR) construction are defined, basic guidelines for the design of PR construction are not given, because, it is very difficult to evaluate the actual restraint of semi-rigid connections used in engineering practice. Moreover, for the majority of designers, design and analysis of frames with PR construction still seems impractical when compared to relative simplicity of traditional FR construction [81]. There are several interrelated obstacles that prevent today's designer of steel structures from embracing a semi rigid connection philosophy. A general listing of these concerns [82] are as follows;

- *Utilization Classification Concerns*: Traditional rules put frustrating constraints on the designer when semi rigid connections are contemplated.
- *Moment-Rotational Model*: The problem is that this information is scattered worldwide, and is normally in a mathematical formulation that is not comforting to the practicing engineer.
- *Serviceability and Stability Concerns*: Semi rigid connection parts depart from elastic strain limits and this inelasticity gives a soft connection effect, which will leave a residual deflection in the connected beam.

Besides all these obstacles, there are still advantages of semi rigid connections.

- First, the essential inelastic behavior of the connecting parts prevents high stress points in the connected members themselves, thus allowing more slender cross sections and the elimination of stiffeners, and reducing high stress concentration complications in ductility sensitive designs.
- Second, for inertia-oriented loads such as earthquakes, preliminary research indicates that the energy absorption of inelastic connections actually keeps excessive lateral drift within reason.
- Third, the use of plastic design in steel actually represents a higher order of optimization in its process of developing mechanism failure modes. Most semi rigid frameworks reach their useful limit at a serviceability limit rather than a strength limit. This implies a retrofit benefit in flexibly connected structures after an accident.

- Fourth, the extra technical nature of semi rigid analysis automatically draws the designer more intimately into the design process. This closer engagement is bound to create better designs as a result of this stimulation.
- Fifth, on a philosophical level it is apparent that neither pinned nor rigid connections are actually obtained in real structures. It would seem that as a profession we need to continually drive ourselves closer to reality. Even approximate estimates of frame flexibility are closer to truth than the assumed ideals of nil or full restraint in the connections.

## **4.2 Types of Semi-Rigid Connections**

The most common beam-to-column connections used in practice are divided into six categories as given in the following.

### **4.2.1 Single Web-angle Connections and Single Plate Connections**

Single web-angle connection involves an angle either bolted or welded to both the column and the beam web as shown in Figure 4.6. Single plate connections, on the other hand, use the plate instead of angle (Figure 4.7). Single plate connection requires less material than single-web angle connection. The rigidity of single plate connection is equal or greater than that of single web angle connection because one side of the plate in the single plate connection is fully welded to the column flange.

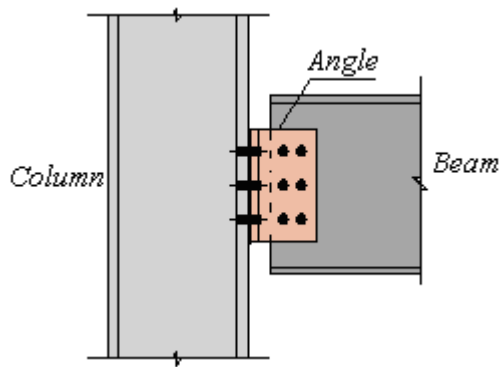


**Figure 4.6** Single web-angle connections.

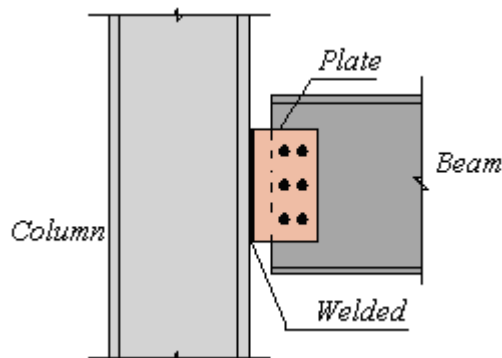


**Figure 4.7** Single plate connections.

### 4.2.2 Double Web-angle Connections

As shown in Figure 4.8, double web-angle connections involve two angles either bolted or riveted to both the column and the beam web. While in the earliest tests, rivets are used to fasten these types of connections, today, the double web-angle connections with high-strength bolts are more popular. The connection rigidity of this type is stiffer than that of the single web-angle and single plate connections.

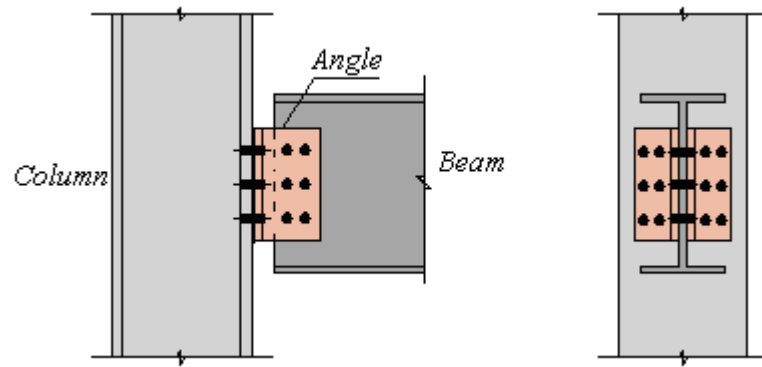


**Figure 4.8** Double web-angle connection.

### 4.2.3 Top and Seat Angle Connections

Figure 4.9 illustrates a typical top and seat angle connection. In this type of connection, top angle is used to provide lateral support of the compression flange of the beam instead of carrying any gravity loads. On the other hand, seat angle transfers only vertical reaction of the beam to the column. Experiments show that this type of connection can also resist some end moment of the beam.

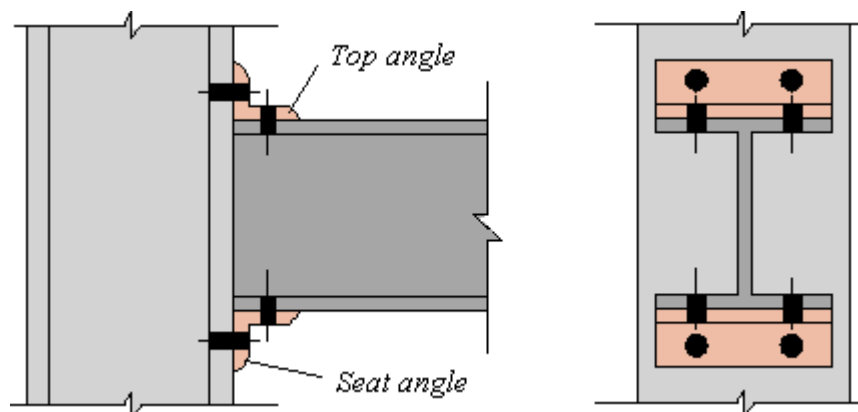


**Figure 4.9** Top and seat angle connection.

#### 4.2.4 Top and Seat Angle Connections with Double Web Angle

This type of connection can be expressed as a combination of top and seat angle connection and a double web angle connection. Geometry of this connection is given in Figure 4.10. Double web angle improves the connection restraint characteristics of top and seat angle connections.

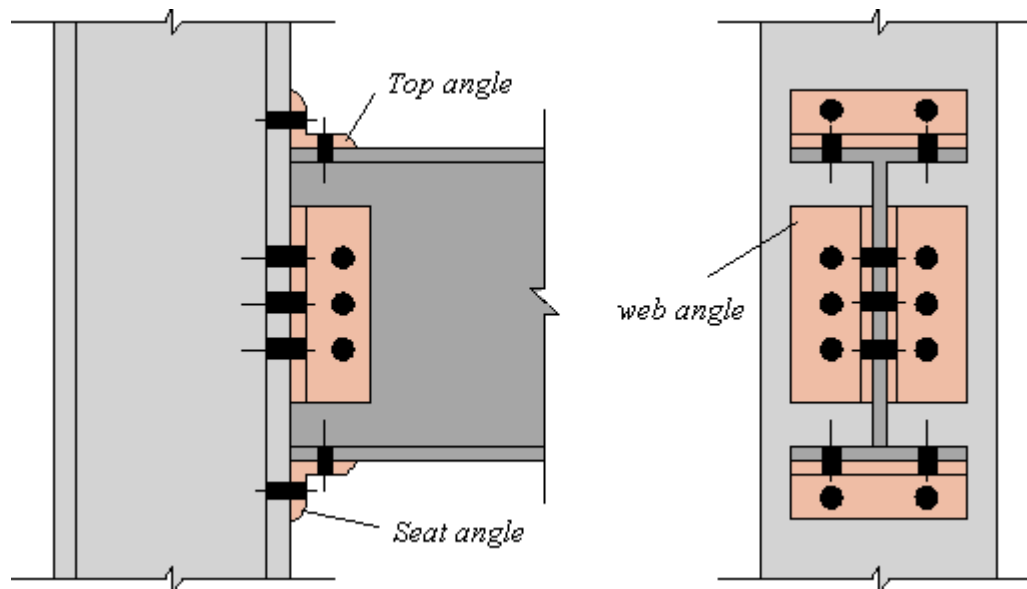


**Figure 4.10** Top and seat angle with double web angle connection.

#### 4.2.5 Extended End – Plate Connections and Flush End-Plate Connections

End plate is generally welded to the beam end along the flanges and web in the fabrication process and bolted to the column in the field. This type of

connection has been used extensively since the late 1960s. The extended end-plate connections are classified into two types – either on the tension side only or on both the tension and the compression sides. Figure 4.11 shows an extended end plate on the tension side only. However, the connection given in Figure 4.12 consists of an end plate on both the tension and compression sides.

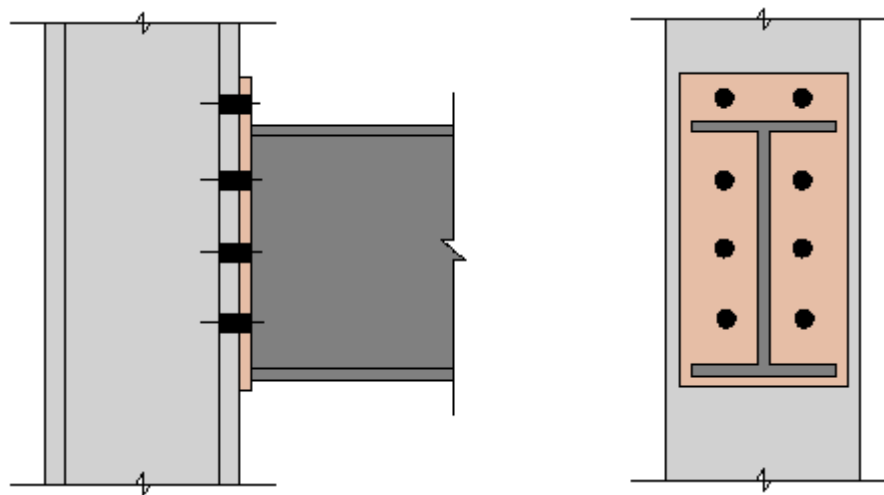
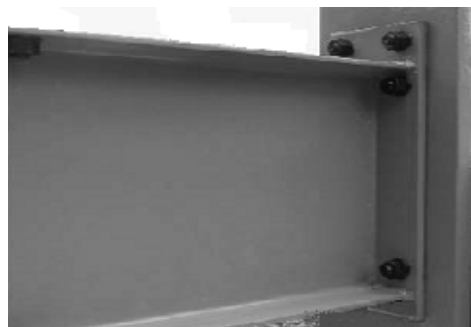


**Figure 4.11** Extended end – plate connections (Tension side only)

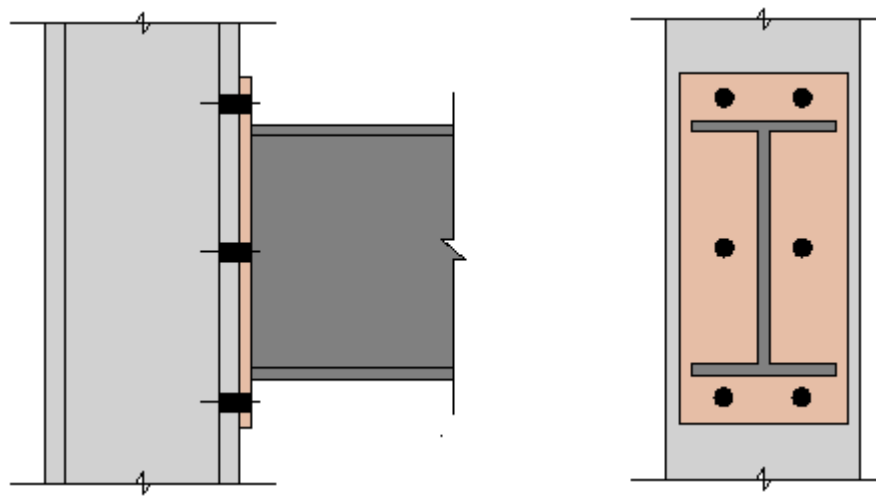
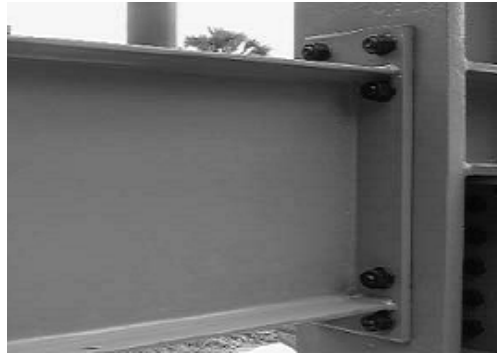


**Figure 4.12** Extended end-plate connections (Tension and compression sides)

A typical flush end-plate connection is shown in Figure 4.13. Since some extended end plate and flush end plate connections are assumed to be FR type construction rather than PR type connection, they have often been used as means of transferring beam end moment to the column. The extended end-plate connection on the tension side only is commonly used in practice. The extended end-plate connection on both sides is preferred when the frame structure is subjected to moment reversal, as during severe earthquake loading. Although the flush end-plate connection is weaker than the extended end-plate connection, the designers prefer to use this one in roof details. The behavior of

the end-plate connections is depended on whether the column flange near the connection is stiffened or not. The stiffeners of the column flanges prevent the flexural deformation of column flange, thereby influencing the behavior of the plate and fasteners.

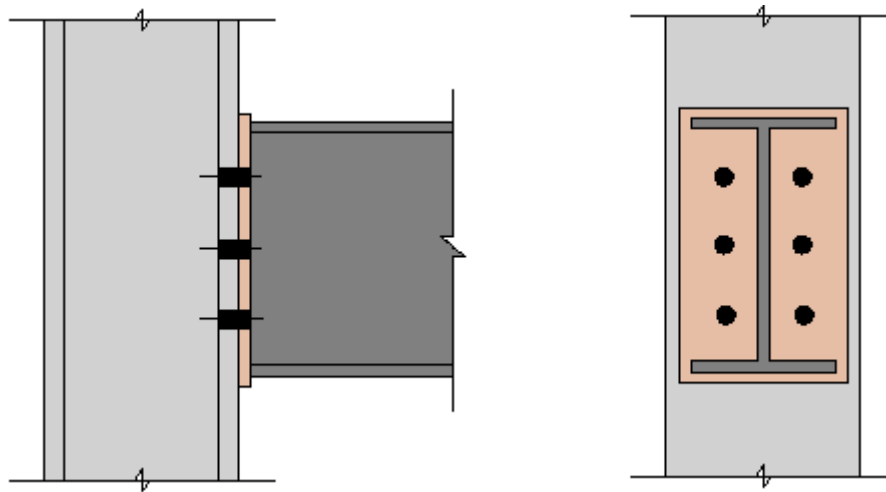


**Figure 4.13** Flush End-Plate Connections

#### **4.2.6 Header Plate Connections**

Similar to extended end plate connections, header plate connections consists of an end plate. However, unlike extended end plate connections, the length of this plate is less than the depth of the beam. It is welded to the beam and bolted to the column as shown in Figure 4.14. The moment- rotation characteristics of these connections are similar to those of double web-angle connections. Accordingly, a header plate connection is used mainly to transfer the reaction of the beam to the column.

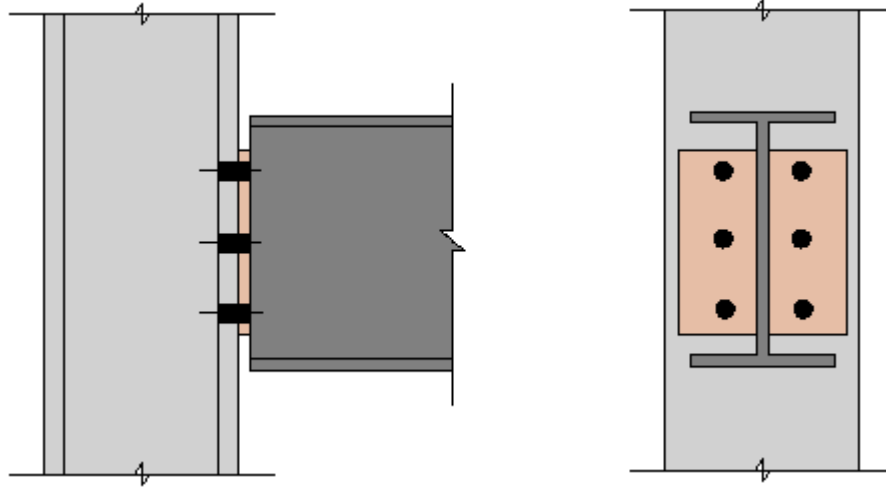


**Figure 4.14** Typical Header Plate Connections

Although the above most commonly used types of semi-rigid connections are introduced; extended end plate connections and top and seat angle connections with double angles will be examined in this study.

### **4.3 Modeling of Semi-Rigid Connections**

The necessary level of sophistication in the modeling of the beam-to-column connection behavior depends on the type of global structural analysis to be performed.

Experimental tests give the most accurate knowledge of the connection behavior; however, this method is too expensive for everyday design practice and is usually conducted for research purposes only.

The most important result obtained during the experimental tests is the moment-rotation curve that comes from experimental evidence. These moment-rotation curves for all the connection types mentioned in previous section have been developed since 1930s and are currently available in the literature.

There are several representative models proposed in the literature to represent the moment-rotation behavior [1]. Power model, linear model, exponential model, cubic B-spline model and polynomial model are the most popular ones. In this study, the semi-rigid connections are modeled by using polynomial model.

#### **4.3.1 Polynomial Model**

In practice, curve-fitting the experimental data with simple expressions is the most commonly used approach to describe the  $M-\theta_r$  curve of flexible connection. A polynomial model where  $M-\theta_r$  behavior is represented by an odd power polynomial, called Frye and Morris Model [1], is adopted in present study due to its easy implementation. The Frye and Morris model uses the method of least square to determine the constants of the polynomial and has the following form. (Equation 4.1)

$$\theta_r = C_1(KM)^1 + C_2(KM)^3 + C_3(KM)^5 \quad (4.1)$$

in which  $M$  is the moment acting on the connection,  $C_1$ ,  $C_2$ ,  $C_3$  are the curve-fitting constants and  $K$  symbolizes the standardization constant depended on

connection type and geometry. The values of these constants vary for each connection type and are given in Table 4.1 [83].

**Table 4.1** Standardized connection constants [1].

Connection types	Curve fitting constants	Standardization constants
<i>Single web-angle connection</i>	$c_1 = 4.28 \times 10^{-3}$ $c_2 = 1.45 \times 10^{-9}$ $c_3 = 1.51 \times 10^{-16}$	$\kappa = d_a^{-2.4} t_a^{-1.81} g^{0.15}$
<i>Double web-angle connection</i>	$c_1 = 3.66 \times 10^{-4}$ $c_2 = 1.15 \times 10^{-6}$ $c_3 = 4.57 \times 10^{-8}$	$\kappa = d_a^{-2.4} t_a^{-1.81} g^{0.15}$
<i>Top and seat angle with web-angles connection</i>	$c_1 = 2.23 \times 10^{-5}$ $c_2 = 1.85 \times 10^{-8}$ $c_3 = 3.19 \times 10^{-12}$	$\kappa = d^{-1.287} t^{-1.128} t_c^{-0.415} l_a^{-0.694} g^{1.35}$
<i>Top and seat angle without web-angles connection</i>	$c_1 = 8.46 \times 10^{-4}$ $c_2 = 1.01 \times 10^{-4}$ $c_3 = 1.24 \times 10^{-8}$	$\kappa = d^{-1.5} t^{-0.5} l_a^{-0.7} d_b^{-1.5}$
<i>End plate without column stiffeners connection</i>	$c_1 = 1.83 \times 10^{-3}$ $c_2 = 1.04 \times 10^{-4}$ $c_3 = 6.38 \times 10^{-6}$	$\kappa = d_g^{-2.4} t_p^{-0.4} d_b^{-1.5}$
<i>End plate with column stiffeners connection</i>	$c_1 = 1.79 \times 10^{-3}$ $c_2 = 1.76 \times 10^{-4}$ $c_3 = 2.04 \times 10^{-4}$	$\kappa = d_g^{-2.4} t_p^{-0.6}$
<i>T-stub connection</i>	$c_1 = 2.10 \times 10^{-4}$ $c_2 = 6.20 \times 10^{-6}$ $c_3 = -7.60 \times 10^{-9}$	$\kappa = d^{-1.5} t^{-0.5} l_t^{-0.7} d_b^{-1.1}$
<i>Header plate connection</i>	$c_1 = 5.10 \times 10^{-5}$ $c_2 = 6.20 \times 10^{-10}$ $c_3 = 2.40 \times 10^{-13}$	$\kappa = d_p^{-2.3} t_p^{-1.6} t_w^{-0.5} g^{1.6}$

#### 4.4 Analysis of Unbraced Steel Frames with Semi-Rigid Connections

In the analysis and design of semi-rigid steel frames connections can be represented by discrete, inelastic rotational springs. The effect of connection flexibility is modeled by attaching rotational springs with stiffness moduli  $K_A$  and  $K_B$  to the first and second ends of a member as shown in Figure 4.15.

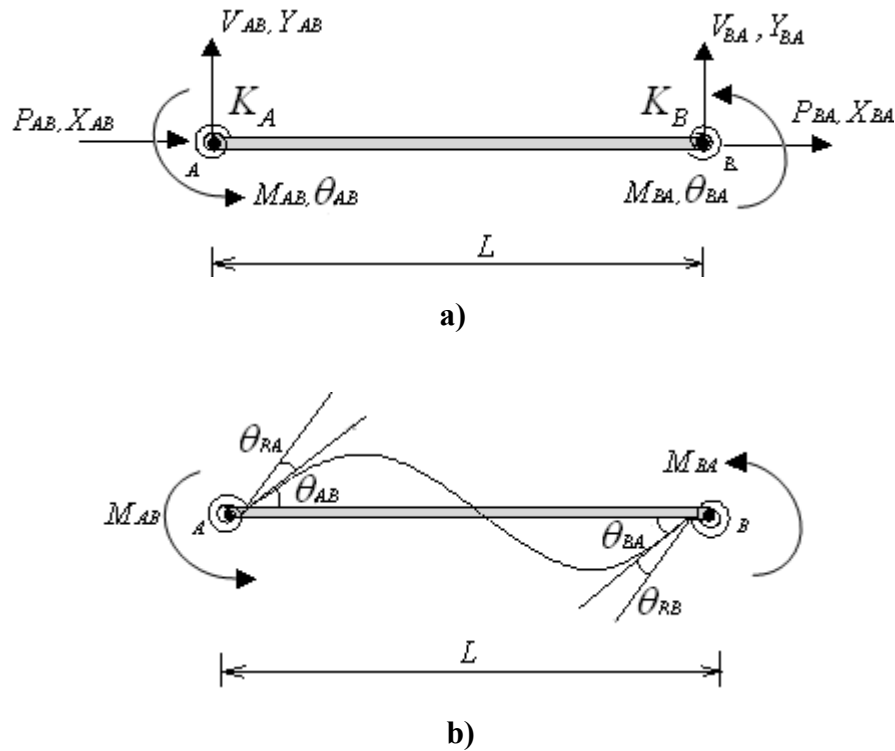


**Figure 4.15** Semi-rigid plane beam member with rotational springs. (a) End forces and end displacements (b) end rotations.

A beam member with semi-rigid end connections has the nonlinear stiffness matrix form shown in the following.

$$[ST] = \left[ \begin{array}{ccc|ccc} A & & & & & \\ B & D & & & & \\ C_1 & E_1 & F_1 & & & \\ \hline -A & -B & -C_1 & A & & \\ -B & -D & -E_1 & B & D & \\ C_2 & E_2 & F_2 & -C_2 & -E_2 & G \end{array} \right] \quad (4.2)$$

Where;

$$\begin{aligned} A &= \frac{EA}{L} + \frac{12EI}{L^3} f_{x1} \phi_5 \\ B &= \frac{EI}{L} - \frac{12EI}{L^3} f_{x1} \phi_5 \\ D &= \frac{EA}{L} - \frac{12EI}{L^3} f_{x1} \phi_5 \\ C_1 &= -\frac{6EI}{L^2} f_{x2} \phi_2 \\ C_2 &= -\frac{6EI}{L^2} f_{x3} \phi_2 \\ E_1 &= \frac{6EI}{L^2} f_{x2} \phi_2 \\ E_2 &= \frac{6EI}{L^2} f_{x3} \phi_2 \\ F_1 &= \frac{4EI}{L} f_{x6} \phi_3 \\ F_2 &= \frac{2EI}{L} f_{x5} \phi_3 \\ G &= \frac{4EI}{L} f_{x6} \phi_4 \end{aligned} \quad (4.3)$$

in which; E represents the modulus of elasticity,  $L, I, A$  are the length, moment of inertia and area of beam respectively. Above stiffness matrix includes the effect of the flexible connections. To be able to modify the stiffness matrix of rigid beam modification coefficients are used. These coefficients are calculated using following equations.

$$\begin{aligned}
KK &= K_A K_B + 4(K_A + K_B) + 12 \\
f_{x1} &= (K_A K_B + K_A + K_B) / KK \\
f_{x2} &= K_A(K_B + 2) / KK \\
f_{x3} &= K_B(K_A + 2) / KK \\
f_{x4} &= K_A(K_B + 3) / KK \\
f_{x5} &= K_A K_B / KK \\
f_{x6} &= K_B(K_A + 3) / KK
\end{aligned} \tag{4.4}$$

Stability functions are included in the stiffness matrix to consider the effect of axial forces on the deformed shape. To calculate the values of stability functions power series approximation is used. However, this method needs the trigonometric functions and one of which is  $\alpha \cot \alpha$  gives singular values at some  $\alpha$  values. For this reason Livesely's approximation [84] which is the sum of a power series in Euler critical load factor  $\rho$  and a rotational function Equation (4.5) is implemented. These stability functions are given as follows;

$$\phi_1 = \alpha \cot \alpha = \frac{64 - 60\rho + 5\rho^2}{(16 - \rho)(4 - \rho)} - \sum_{n=1}^7 \frac{a_n \rho^n}{2^{3n}} \tag{4.5}$$

in which; the constants take the values as;

$$\begin{aligned}
 a_1 &: 1.57973627 & a_4 &: 0.00547540 & a_7 &: 0.00005452 \\
 a_2 &: 0.15858587 & a_5 &: 0.00115281 & & \\
 a_3 &: 0.02748899 & a_6 &: 0.00024908 & & 
 \end{aligned}$$

$$\begin{aligned}
 \phi_2 &= \alpha^2 / (3 - 3\phi_1) \\
 \phi_3 &= (3\phi_2 + \phi_1) / 4 \\
 \phi_4 &= (3\phi_2 - \phi_1) / 2 \\
 \phi_5 &= \phi_2 \phi_1 \\
 \alpha &= 0.5\pi\sqrt{\rho}, \quad \rho = P / P_{cr} = Pl^2 / (\pi^2 EI)
 \end{aligned} \tag{4.6}$$

Where;  $P$  is the axial force in beam member,  $P_{cr}$  is the Euler critical load of beam member.

In addition to stiffness matrix, relative stiffness ratios  $\gamma_1$  and  $\gamma_2$ , thereby effective length factor, introduced in previous chapter, require some modifications. Hence, these parameters take the following form.

$$\gamma_1 = \frac{\sum I_{c1} / \ell_{c1}}{\sum \alpha_{uf} (I_{b1} / \ell_{b1})} \quad \text{and} \quad \gamma_2 = \frac{\sum I_{c2} / \ell_{c2}}{\sum \alpha_{uf} (I_{b2} / \ell_{b2})} \tag{4.7}$$

where;  $\alpha_{uf}$  is a coefficient which represents the connection condition. It is equal to 1 for rigid connections and computed for semi-rigid connections from the equation given in the following.

$$\alpha_{uf} = \left(1 + \frac{2EI_b}{L_b K^*}\right) \frac{1}{R^*} \quad (4.8)$$

Where;

$$R^* = \left(1 + \frac{4EI_b}{L_b K_A}\right) \left(1 + \frac{4EI_b}{L_b K_B}\right) - \left(\frac{EI_b}{L_b}\right)^2 \frac{4}{K_A K_B} \quad (4.9)$$

in which  $K_A$  and  $K_B$  symbolize the rotational stiffness of the semi-rigid connections at the first and the second ends of the beam.  $I_b$  and  $L_b$  are the moment of inertia and the length of the beam respectively. The smaller of  $K_A$  and  $K_B$  is symbolized as  $K^*$  in the equation.

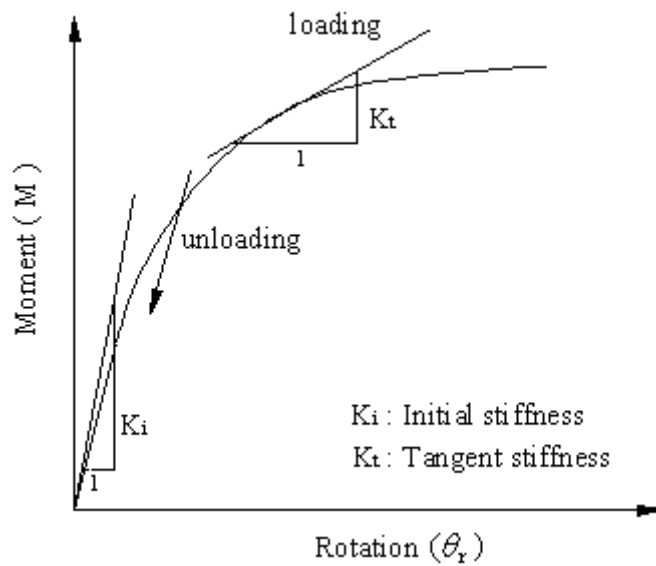


**Figure 4.16** Moment rotation behavior of semi-rigid connection

$K_A$  and  $K_B$ , called the rotational stiffness of the springs at each end of the flexible frame member, are calculated as a tangent stiffness using above given nonlinear standardized function (Equation 4.1). To achieve this, first flexibility of connection is determined as  $d\theta_r / dM$ . Then, the stiffness of the connection which is to be used in the modification of general stiffness matrix is obtained as a reciprocal of the connection flexibility calculated for a certain value of a moment, when connection is loaded [83]. If the state is unloading, the stiffness of the connection is assumed as its initial stiffness. These two states are shown in Figure 4.16.

#### 4.4.1 End-plate without Column Stiffeners Model

The design of end-plate without column stiffeners model necessitates the determination of required length and thickness of end plates as well as the placement and size of the bolts. These parameters are determined through the consideration of connection design specifications given in LRFD-AISC [49].

As shown in Figure 4.17, due to bending moment and vertical force acting on the connection, the bolts are subjected to tensile force ( $T$ ) and shear ( $P$ ). Equations (4.10) and 4.11) are used to perform tension and shear check for the connection bolts.

$$P_t = 0.75.F_t \cdot 0.85A_g \quad \text{Strength capacity of bolts under tension} \tag{4.10}$$

$$P_s = 0.75.F_s \cdot 0.85A_g \quad \text{Strength capacity of bolts under shear}$$

$$\frac{P}{mP_s} + \frac{T}{nP_t} \leq 1 \quad (4.11)$$

Where; the nominal strength of a bolt in shear and nominal strength of a bolt in tension are defined by  $F_s$  and  $F_t$ , which are given in LRFD-AISC [49] as 33 kN/cm<sup>2</sup> and 62 kN/cm<sup>2</sup>, respectively.  $A_g$ ,  $m$  and  $n$  are referred to as the cross-sectional area of a bolt, number of bolts in shear and number of bolts in tension, respectively.

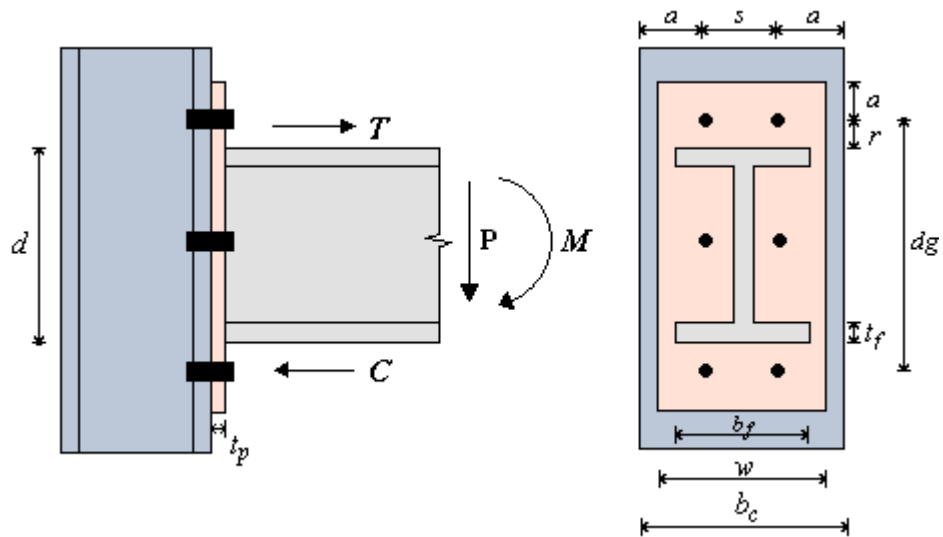


**Figure 4.17** End-plate without column stiffeners

Bolts are placed according to the provisions given in LRFD-AISC [49] as follows;

$$r \geq 2d_b \quad (4.12)$$

$$a \geq 3d_b$$

$$3d_b \leq s \leq 14t \leq 17.78 \text{ cm}$$

Where;  $a$ ,  $s$  and  $r$  are shown in Figure. 4.17 and  $d_b$  is the diameter of the bolt selected.

Once the bolts are placed, required thickness  $t_p$  and the width  $w$  of end plates can be determined from Equations (4.13) and (4.14). The distance ( $d_g$ ) between two bolts at the top and bottom of end plate is calculated according to Equation (4.15).

$$t_p \geq \sqrt{\frac{4.44 T b'}{w F_y}} \quad (4.13)$$

$$b' = r - \frac{1}{2} d_b$$

$$w \geq s + 6d_b \quad (4.14)$$

$$b_c \geq w \geq b_f$$

$$d_g \geq d + 4d_b \quad (4.15)$$

Where;  $T$  and  $F_y$  represent the tensile force and the yield stress, respectively.  $b_c$  and  $b_f$  are the flange width of column and beam, respectively.  $d$  defines the depth of the beam.

Design steps of end plate without column stiffeners model can be stated as follows;

- 1) Resulting end forces ( $P$  and  $M$ ), acting on the connection are taken from the analysis.

- 2) Bolt diameter is selected from the available bolt list given in [49].
- 3) Nominal shear and tension strengths of bolt are determined through the use of Equation (4.10) and it is checked if the strength requirement given in Equation (4.11) is satisfied. If not, another one is selected and the strength check is performed again. This procedure is repeated until an appropriate one is reached.
- 4) Required thickness, length and width of end plates are attained using Equation (4.13) through Equation (4.15).

Curve-fitting and standardization constants of end plate without column stiffeners connection shown in Figure 4.17 are given as in the following.

$$\begin{aligned}
 C_1 &= 1.83 \times 10^{-3} \\
 C_2 &= 1.04 \times 10^{-4} \quad \text{and} \quad K = d_g^{-2.4} t_p^{-0.4} d_b^{-1.5} \\
 C_3 &= 6.38 \times 10^{-6}
 \end{aligned}
 \tag{4.16}$$

#### 4.4.2 Top and Seat Angle with Web Cleats Model

The design of top and seat angle with web cleats model necessitates the determination of required width and thickness of angle as well as the placement and size of the bolts.

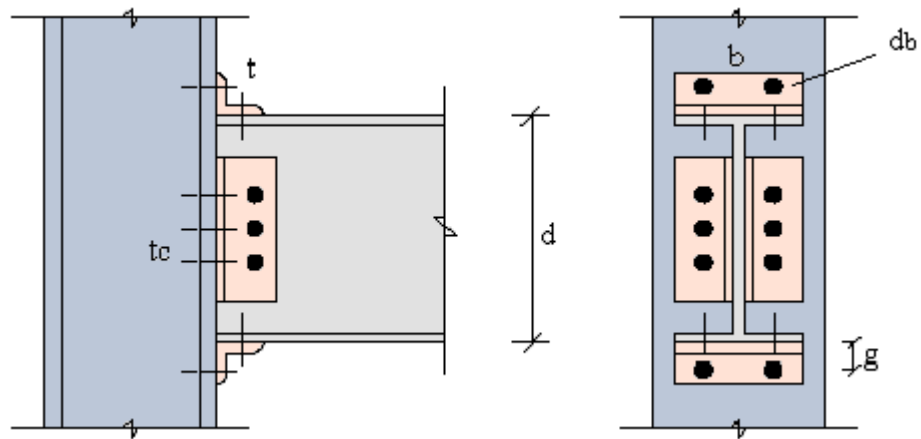


**Figure 4.18** Top and seat angle with web cleats connection

Required seat width is calculated from the bearing length  $N$ , which is based on the local web yielding limit state and web crippling limit state as given in LRFD-AISC [49]. Local web yielding usually controls the bearing length, which is obtained from Equation (4.17).

$$N = \frac{P_u}{\phi F_{yw} t_w} \geq 3.5k \quad (4.17)$$

Where;  $P_u$  represents the factored load reaction,  $\phi$  defines the resistance factor (1),  $t_w$  and  $F_{yw}$  and  $k$  are web thickness and yield stress of supported beam and distance from outer face of flange to web toe of fillet, respectively.

Web crippling, on the other hand, is carried out through the use of following equation.

$$P \leq P_n = 68t_w^2 \left[ 1 + 3 \left( \frac{N}{d} \right) \left( \frac{t_w}{t_f} \right)^{1.5} \right] \sqrt{\frac{F_{yw}t_f}{t_w}} \quad \text{for } N/d \leq 0.2 \quad (4.18)$$

$$P \leq P_n = 68t_w^2 \left[ 1 + \left( \frac{4N}{d} - 0.2 \right) \left( \frac{t_w}{t_f} \right)^{1.5} \right] \sqrt{\frac{F_{yw}t_f}{t_w}} \quad \text{for } N/d > 0.2$$

Bending moment on the critical section of the angle is calculated as in the following;

$$M_u = P_u e \quad (4.19)$$

$$e_f = \text{clearance} + \frac{N}{2} \quad (4.20)$$

$$e = e_f - t - \frac{3}{8}$$

Where,  $P_u$  is referred to as the factored reaction to be carried.  $e$  and  $e_f$  are the moment arms and  $P$  is the shear force acting on the connection.

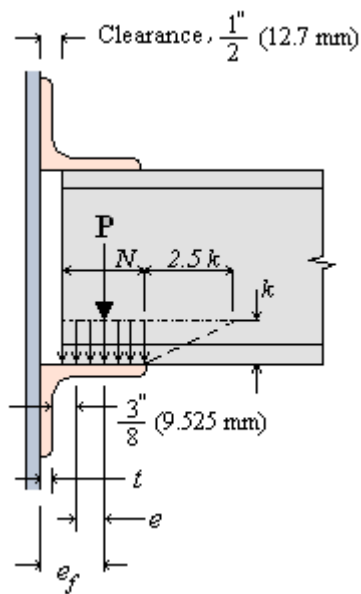


**Figure 4.19** Bearing stress assumptions for seated connections

Equation (4.21) is used for the determination of required thickness of top and seat angles.

$$t^2 = \frac{4P_u e}{\Phi_b F_y L} \quad (4.21)$$

Shear capacity of outstand leg of cleats are determined from the following equation.

$$V = 0.6 P_y 0.9 B_f t > P_u \quad (4.22)$$

In which,  $\phi_b$  symbolizes the resistance factor (0.9) and  $L$ ,  $B_f$  and  $F_y$  are referred to as length, width and the yield stress of top and seat angles, respectively.

As shown in Figure 4.20, due to moment acting on the connection, the bolts used to connect the top angles to the columns are subjected to tensile force ( $T$ ) and the ones used to connect the top angles to the beams are subjected to shear. On the other hand, the bolts used in the web side of the beams are subjected to shear. Equation (4.10) and Equation (4.11) are used to perform tension and shear check for the connection bolts.

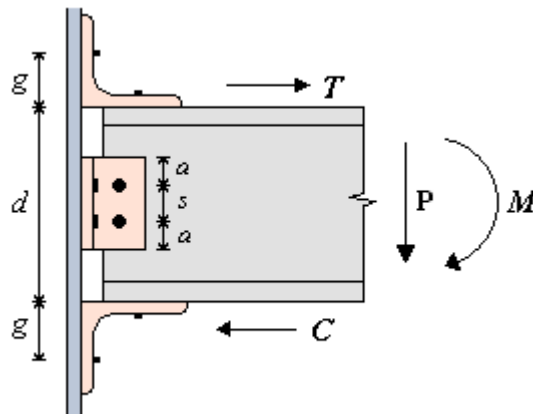


**Figure 4.20** Top and seat angle with web cleats connection detail

Bolts are placed according to the provisions given in LRFD-AISC [49] as in the following.

$$3d_b \leq s \leq 14t \leq 17.78 \text{ cm} \quad (4.23)$$

$$a \geq 3d_b$$

Hence, the length of web cleats is determined from the following equation.

$$6d_b + s(N - 1) = L \leq d_b - 2k \quad (4.24)$$

Where;  $s$  represents the distance between bolts and  $t$  symbolizes the smaller of angle thickness and column flange thickness.  $d_b$ ,  $N$  and  $L$  are the diameter of bolts, number of bolts and length of web angles.

Design steps of top and seat angles with web cleats model can be stated as follows;

- 1) Resulting end forces ( $P$  and  $M$ ), acting on the connection are taken from the analysis.
- 2) Angle sections are selected from ready angle section tables given in LRFD-AISC [49].
- 3) Web yielding and web crippling are carried out using Equations (4.17) through (4.20). Required thickness of top and seat angles are determined (Equation 4.21). If the thickness of selected angle is less than the required one, another angle section is selected. This procedure is repeated until an appropriate one is reached.
- 4) Shear capacity check of outstand leg of cleats is performed by use of Equation (4.22).

- 5) Bolt diameter is selected from the available bolt list given in [49].
- 6) Nominal shear and tension strengths of bolt are determined through the use of Equation (4.10) and it is checked if the strength requirement given in Equation (4.11) is satisfied. If not, another one is selected and the strength check is performed again. This procedure is repeated until an appropriate one is reached.

Size parameters given in Figure 4.18 are used to calculate the standardization constant through the consideration of parameter tables given in [1]. For the top and seat angle with web cleats connection model, curve-fitting and standardization constants are given as in the following. (Equation 4.25)

$$\begin{aligned}
 C_1 &= 2.23 \times 10^{-5} \\
 C_2 &= 1.85 \times 10^{-8} \\
 C_3 &= 3.19 \times 10^{-12}
 \end{aligned}
 \tag{4.25}$$

and

$$K = d^{-1.287} t^{-1.128} tc^{-0.415} b^{-0.694} (g - d_b / 2)^{1.350}$$

where  $d_b$ ,  $t$ ,  $b$ ,  $d$ ,  $tc$ ,  $g$  are; the diameter of bolts, the thickness of angles, flange width of beam, depth of beam web, flange thickness of column and gauge distance respectively.

An increase in lateral displacements occurs in the analysis of steel frames with semi-rigid connections. Hence, consideration of the effect of axial forces in the

response of semi-rigid frame becomes a necessity. The following steps give details about the algorithm which accounts for  $P-\Delta$  effect in the analysis of frame.

1. In the beginning of the procedure, axial forces in members are assumed to be zero.
2. Overall stiffness matrix is constructed then the frame is analyzed under the external loads and joint displacements and member forces are calculated.
3. Corresponding stability functions are determined using the axial forces obtained for the members.
4. The steps from 2 are repeated until the difference between two successive sets of axial forces is smaller than a specific tolerance.

The determinant of the overall stiffness matrix is calculated and loss of stability is checked during these iterations. If no loss of stability occurs and the convergence in the axial forces is obtained, the joint displacements and member forces determined in this nonlinear response are used in the computation of fitness values for this particle. During the analysis the design load is applied immediately and the iterations are carried out at this load. It should be pointed out that fixed end moments change from one iteration to another due to rotational springs. The modified fixed end moments are determined by considering the flexible end connection.

#### **4.5 Particle Swarm Optimization Design of Unbraced Steel Frames with Semi-Rigid Connections**

In this section the optimum design procedure developed for semi-rigid steel frames is introduced. The algorithm is based on the particle swarm optimization method explained in the previous chapter. Design algorithm is similar to the one developed for rigid steel frames which is given in Chapter 3. However, there are additional routines required for the design of partially restrained end connections. This routine is written for two types of connections; “Top and Seat Angle with Web Cleats (TSWC)” and “End Plate without Column Stiffeners”. Computer program is coded in such a way that user has the option of selecting the connection type through only one command. Steps of this optimization procedure can be summarized as follows;

1. The geometry and applied loading of the frame are defined. The beam-to-column connection type is selected. Beams and columns of the structure are grouped together.
2. Particle swarm design algorithm is started by generating initial values (positions of particles) randomly for the design variables i.e. sequence numbers of steel section tables. Once the steel sections for the member groups are selected then all the other cross sectional properties such as moment of inertia, sectional modulus and radius of gyration belonging to each group becomes available.
3. Frame is analyzed with the use of analysis subroutine which is based on matrix stiffness method. Member forces and displacements are

computed. Beam-to-column connections are designed and required size of connection elements such as angles, bolts and plates are determined.

4. Fly-back mechanism is used to handle the design constraints. It is checked if the strength and displacement requirements given in design code are satisfied. If one or a number of constraints are not satisfied, this design is discarded and new one is generated randomly.
5. After feasible designs are obtained, particle swarm iterations is initialized. Objective function values, weights of frames belonging to each design, are calculated. The particle which has the minimum weight is accepted as current optimum design. After, values of design variables are updated using velocity and position update equations of particle swarm algorithm and new designs are generated.
6. Analysis routine is repeated for these new designs and constraints are checked. If all the constraints are satisfied, weights of these designs are computed. If the lightest among them is also lighter than the current optimum design, it is accepted as the new optimum.
7. This iteration procedure is repeated until the predefined number of iteration is completed. The design from which the minimum weight obtained at the end of this iteration process is taken as optimum design.

#### **4.6 Design Examples**

In this section, six unbraced steel frames with semi-rigid connections are designed. Two beam-to-column connection models namely top and seat angle

with web cleats and end plates without column stiffeners are selected for the representation of partially restrained connections. Each of these examples is analyzed by taking into account the nonlinear  $M-\theta$  curve of the connection and  $P-\Delta$  effect that considers the increase in the lateral displacements. In the design of top and seat angles with web cleats models, angles are chosen from the available angle list given in [49]. In addition to the restrictions for the feasible design of frame members, given in the previous chapter, design limitations of both connection types are also included in the optimum design algorithm. Example frames are also designed by assuming the end connections to be rigid with the use of discrete variables. Results are tabulated in the same table to compare the overall weight of the structure obtained with each approach. Furthermore, the convergence rate of each example is illustrated with design-history graphs.

#### **4.6.1 Three Storey, Two Bay Steel Frame**

Figure 4.21 designates the two bay-three storey steel frame, which is the first example of this section. The dimensions, member grouping and the external loading of the system are also shown in this figure. The upper bound imposed on lateral deflections of the top storey joints is limited to 1/300 of the frame height, which corresponds to 30.48 mm. The system is designed by collecting the frame members in two different groups. Columns are considered as group 1 while beams are taken as group 2 as shown in figure. Hence there are only two design variables in the design problem. A single distributed load of 40 kN/m and lateral loading of 20kN is applied to each horizontal member of the frame. Fixed supports are used for the connection of the columns to the foundation.

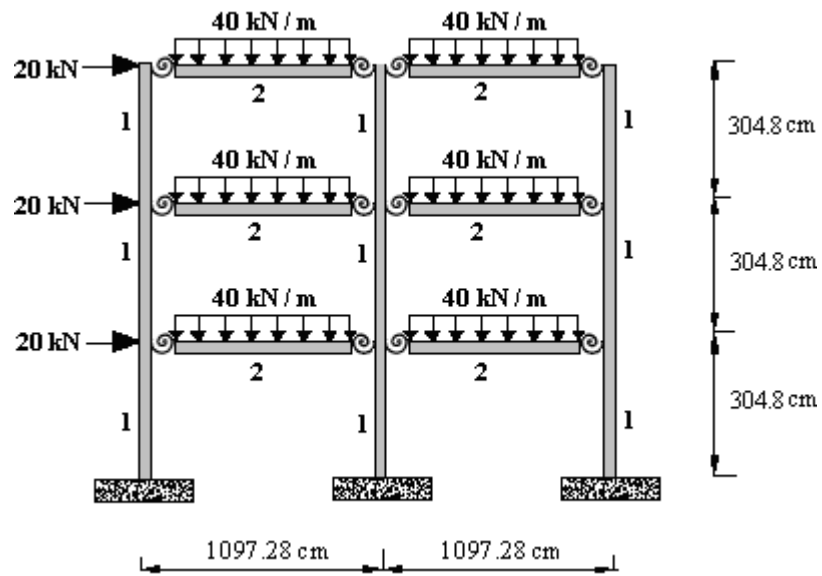


**Figure 4.21** Three storey-two bay steel frame.

The frame is designed by using both semi-rigid and rigid optimum design algorithms. The design history of these runs is shown in Figure 4.22. Best designs obtained by the optimum design algorithms are tabulated in Table 4.2 with section designations attained for each member group. In this example, semi-rigid algorithms produce heavier designs, as indicated in Figure 4.22. The one with TSWC is 5%, the one with end plate without column stiffeners is 3% heavier than rigid frame. The strength ratios obtained are 0.97, 0.93 and 0.98 and top storey drifts are 1.650cm, 1.100cm and 0.80cm for semi-rigid frame with top and seat angle with web cleats, the one with end plate without column stiffeners and rigid discrete frame respectively. This indicates that strength constraints dominate the designs.

**Table 4.2** Optimum designs for three-storey, two-bay rigid steel frame.

Group No.	Member Type	Semi-rigid frame		Rigid frame Wsections- Area(cm <sup>2</sup> )
		T.S.W.C Connect. Wsections- Area(cm <sup>2</sup> )	End plate Connect. Wsections- Area(cm <sup>2</sup> )	
1	Column	W690X125 (160)	W250X115 (146)	W250X73 (92.8)
2	Beam	W610X140 (179)	W610X140 (179)	W690X152 (194)
Max. Int. St. Drift Ratio		0.75	0.42	0.30
Max. Strength Ratio		0.97	0.93	0.98
Top storey drift (cm)		1.650	1.100	0.80
Minimum Weight.kg (kN)		12638.18 (123.937)	12358.45 (121.194)	12005.990 (117.738)

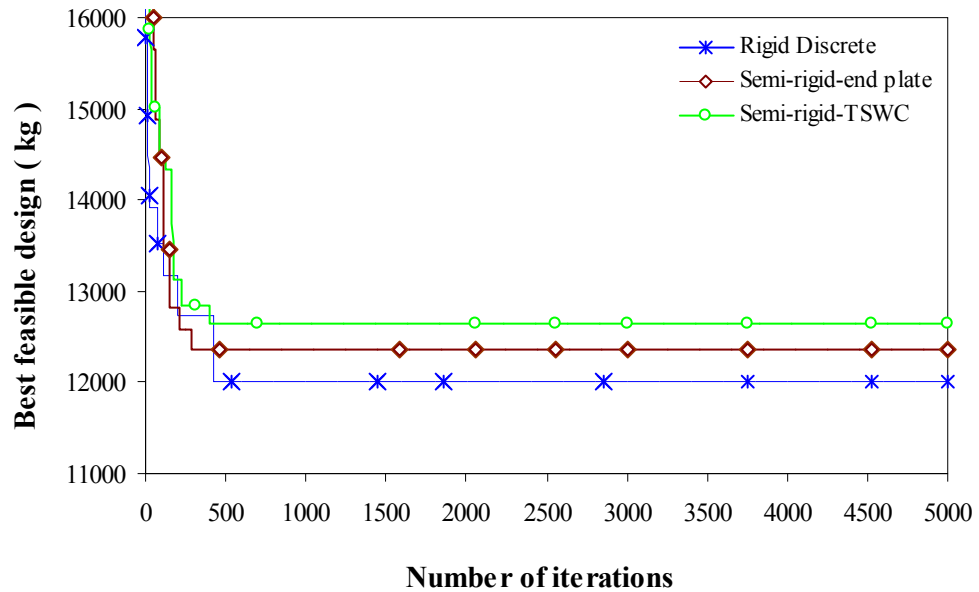


**Figure 4.22** Design history graph for three-storey, two-bay steel frame.

#### 4.6.2 Four storey, four bay steel frame

The four-bay, four storey steel frame shown in Figure 4.23 is considered as the second design example. The frame consists of thirty-six members that are collected in two groups as shown in the figure. Columns are considered to be group 1 while beams are taken as group 2. The lateral displacement of the top storey is limited to 4cm and maximum inter-storey drift is restricted to 1cm. The modulus of elasticity is  $200\text{kN/mm}^2$ . A distributed load of  $35\text{ kN/m}$  is applied to all beams and lateral loads are considered at each storey level as shown in Figure 4.23. Columns are assumed to be rigidly connected to the foundations.

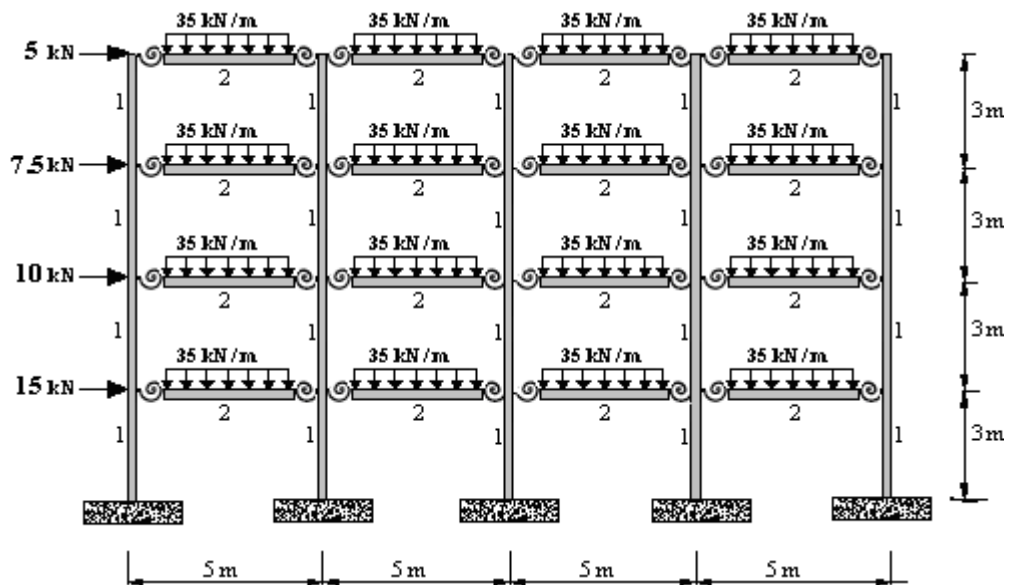
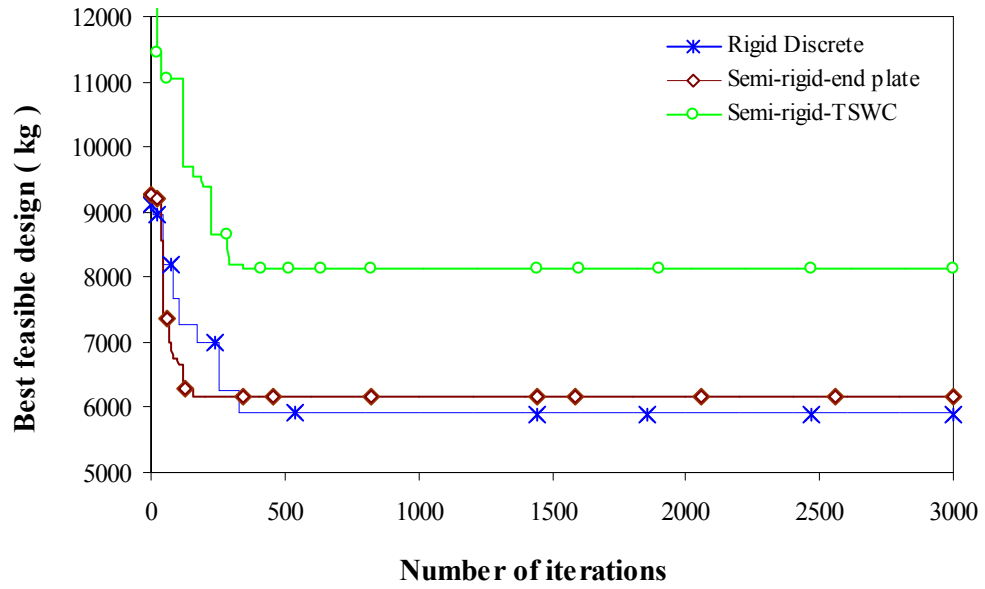


Figure 4.23 Four storey- four bay steel frame.

Table 4.3 tabulates the optimum designs of semi-rigid steel frames together with the results obtained with rigid connection assumption. The design histories of both minimum weight designs of frames are shown in Figure 4.24. It is apparent from the figure that the algorithm assuming the connections to be rigid with discrete variables produces the lightest frame. Moreover, it is noticed that the design with top and seat angle with web cleats is heavier than the one with end plate connections. This design is attained after 346 iterations and the minimum weight is 8123.09kg while the one with end plate without column stiffeners has the minimum weight of 6167.268kg obtained after 160 iterations. This means that the design with TSWC is 37%, the one with end plate without column stiffeners is %4.2 heavier than rigid frame. It is noticed that the dominant constraint of the former type semi-rigid connection design is inter-storey drift with the ratio of 0.95; while the frame design with end plate connection is dominated by strength constraint with the ratio of 0.95.

**Table 4.3** Optimum designs for four-storey, four-bay steel frame.

Group No.	Member Type	Semi-rigid frame		Rigid frame Wsections-Area(cm <sup>2</sup> )
		T.S.W.C Connect. Wsections- Area(cm <sup>2</sup> )	End plate Connect. Wsections-Area(cm <sup>2</sup> )	
1	Column	W250X58 (74.2)	W360X44 (57.3)	W150X37.1 (47.3)
2	Beam	W250X58 (74.2)	W360X44 (57.3)	W410X46.1 (58.9)
Max. Int. St. Drift Ratio		0.95	0.57	0.47
Max. Strength Ratio		0.91	0.95	0.99
Top storey drift (cm)		3.277	1.96	1.59
Minimum Weight.kg (kN)		8123.09 (79.66)	6167.268 (60.480)	5914.37 (58.00)



**Figure 4.24** Design history graph for four-storey, four-bay steel frame.

### 4.6.3 Five storey, three bay steel frame

Third example is the three -bay, five storey steel frame as shown in Figure 4.25. The frame shown is designed by using the algorithms developed as a rigid frame as well as semi-rigid frame.

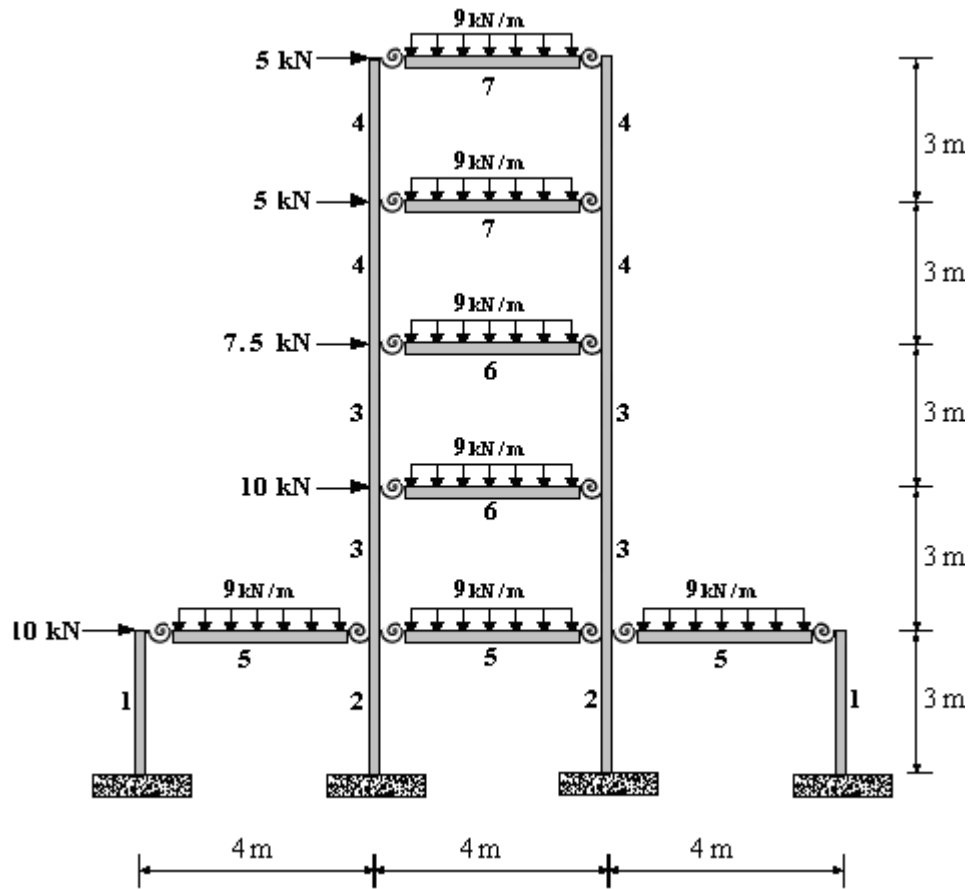


**Figure 4.25** Five storey- three bay steel frame.

The frame consists of nineteen members that are collected in seven groups as shown in the figure. First four groups are assigned to columns and the rest three groups are assigned to beams of the frame. The allowable inter-storey drift is 10mm while the lateral displacement of the top storey is limited to 50mm. The modulus of elasticity is  $200\text{kN/mm}^2$ . Fixed supports are used for the connection of the columns to the foundation.

The optimum W-section designations of semi-rigid and rigid frames obtained by the particle swarm method are given in Table 4.4.

**Table 4.4** Optimum designs for five-storey, three-bay steel frame.

Group No.	Member Type	Semi-rigid frame		Rigid frame Wsections- Area(cm <sup>2</sup> )
		T.S.W.C Connect. Wsections- Area(cm <sup>2</sup> )	End plate Connect. Wsections- Area(cm <sup>2</sup> )	
1	Column	W530X74 (95.2)	W410X67 (86)	W360X32.9 (41.7)
2	Column	W360X44 (57.3)	W200X22.5 (28.6)	W250X22.3 (28.5)
3	Column	W360X72 (91.1)	W360X32.9 (41.7)	W250X32.7 (41.7)
4	Column	W200X35.9 (45.8)	W310X21 (26.9)	W150X29.8 (37.9)
5	Beam	W250X17.9 (22.7)	W310X21 (26.9)	W310X21 (26.9)
6	Beam	W250X28.4 (36.3)	W360X32.9 (41.7)	W360X32.9 (41.7)
7	Beam	W250X17.9 (22.7)	W200X15 (19.1)	W310X21 (26.9)
Max. Int. St. Drift Ratio		0.99	0.99	1.00
Max. Strength Ratio		0.94	0.97	0.98
Top storey drift (cm)		3.700	4.057	4.19
Minimum Weight.kg (kN)		2589.68 (25.396)	1819.996 (17.848)	1375.194 (13.486)

The design of semi-rigid frame with end plates is attained after 415 iterations and the minimum weight is 1819.996kg while the one with top and seat angle with web cleats has the minimum weight of 2589.68kg obtained after 1800 iterations. Rigid frame with discrete variables, which is designed in chapter 3, has the weight of 1375.194kg. It is noticed that the dominant constraint of the former design is inter-storey drift ratio with the value of 0.99; similarly the design of the frame with top and seat angle with web cleats is dominated by inter-storey drift ratio with the value of 0.99. The strength constraints are computed as 0.97 and 0.94 respectively. Design history graph of this frame is shown in Figure 4.26.

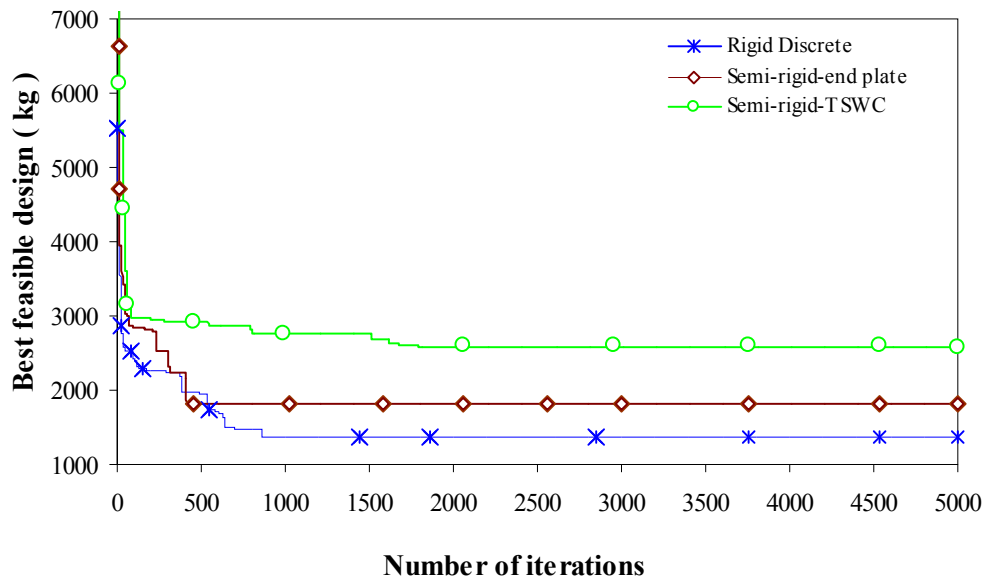


**Figure 4.26** Design history graph for five-storey, three-bay steel frame.

#### 4.6.4 Six Storey, Two Bay Steel Frame

Fourth design example is two-bay, six storey steel frame shown in Figure 4.27, which is also carried out in Chapter 3. Geometry and grouping of the frame is illustrated in this Figure.

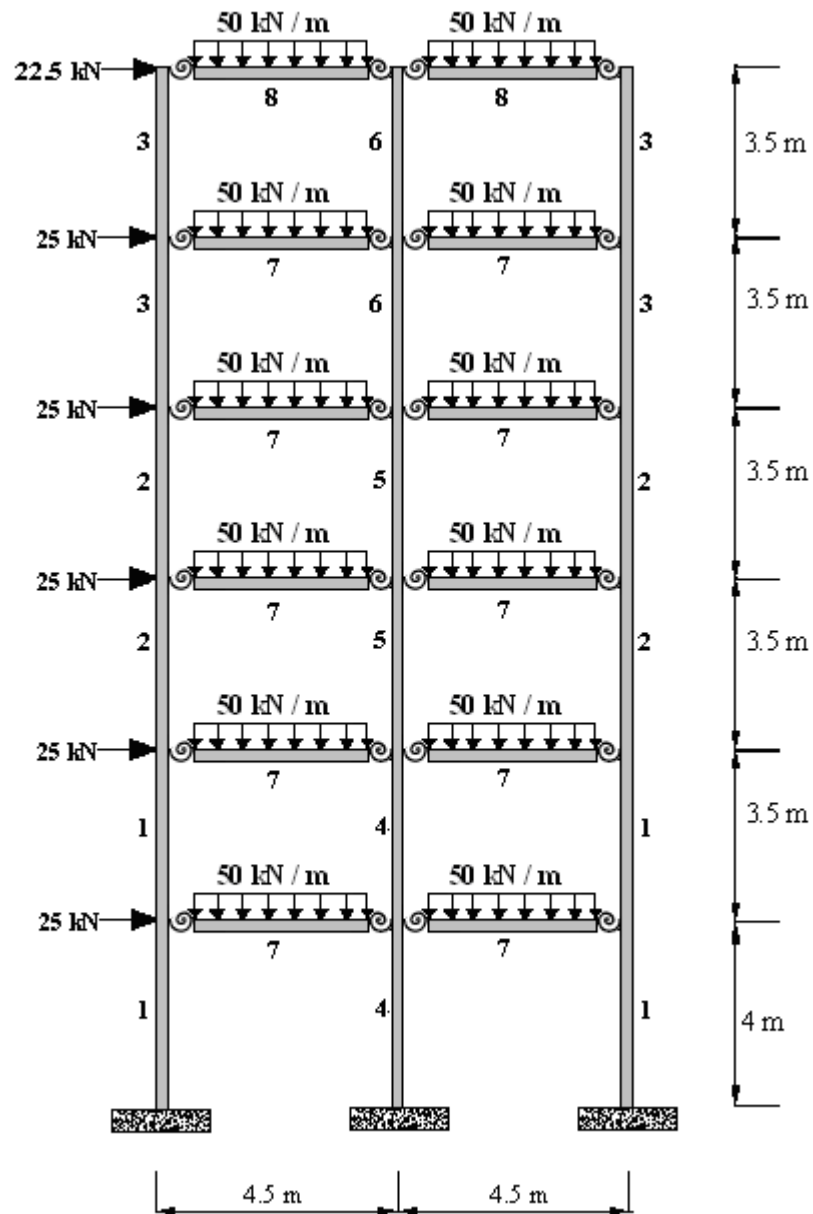


**Figure 4.27** Six storey- two bay steel frame.

Frame consists of thirty members that are collected in eight groups as shown in the figure. Outer columns and inner columns of each two storeys are considered to be a different group separately. Beams of first seven storeys are

taken as group 7 and those of top storey are grouped as group 8. The lateral displacement of the top storey is limited to 4cm. The modulus of elasticity is  $200\text{kN/mm}^2$ . A distributed load of  $50\text{kN/m}$  and a single lateral load is applied to each horizontal member of the frame. Fixed supports are used for the connection of the columns to the foundation.

In the modeling of end connections of this frame, both end plate without column stiffeners and top and seat angles with web cleats are used. The optimum W-section designations of semi-rigid and rigid frames obtained by the particle swarm method are given in Table 4.5.

**Table 4.5** Optimum designs for six-storey, two-bay steel frame.

Group No.	Member Type	Semi-rigid frame		Rigid frame Wsections- Area( $\text{cm}^2$ )
		T.S.W.C Connect. Wsections- Area( $\text{cm}^2$ )	End plate Connect. Wsections- Area( $\text{cm}^2$ )	
1	Column	W690X125 (160)	W530X74 (95.2)	W530X74 (95.2)
2	Column	W610X101 (130)	W360X51 (64.5)	W310X52 (66.7)
3	Column	W250X73 (92.8)	W310X38.7 (49.4)	W200X41.7 (53.1)
4	Column	W1100X343 (436)	W610X140 (179)	W460X89 (114)
5	Column	W610X101 (130)	W530X66 (83.7)	W460X89 (114)
6	Column	W360X91 (116)	W200X35.9 (45.8)	W360X72 (91.1)
7	Beam	W310X74 (94.9)	W530X66 (83.7)	W460X60 (75.9)
8	Beam	W250X67 (85.5)	W460X60 (75.9)	W460X68 (87.3)
Max. Int. St. Drift Ratio		1.00	1.00	0.78
Max. Strength Ratio		0.95	0.99	0.99
Top storey drift (cm)		5.206	5.531	4.5325
Minimum Weight.kg (kN)		12167.20 (119.319)	7637.091 (74.894)	7532.11 (73.865)

The minimum weights obtained are 12167.20kg, 7637.091kg and 7532.11kg for semi-rigid frame with top and seat angle with web cleats, the one with end plate without column stiffeners and rigid discrete frame respectively. This indicates that rigid frame is 1.4% and 61% lighter than the frame with end plate connection and TSWC, respectively. It is noticed that the dominant constraint of the semi-rigid design is maximum inter-storey drift ratio with the value of 1.00; while maximum strength ratio, which is 0.99, dominates the rigid frame design. Top storey drift of semi-rigid frames and rigid discrete frames are 5.206cm, 5.531cm and 4.533cm, respectively. Convergence rate of this frame is shown in Figure 4.28.

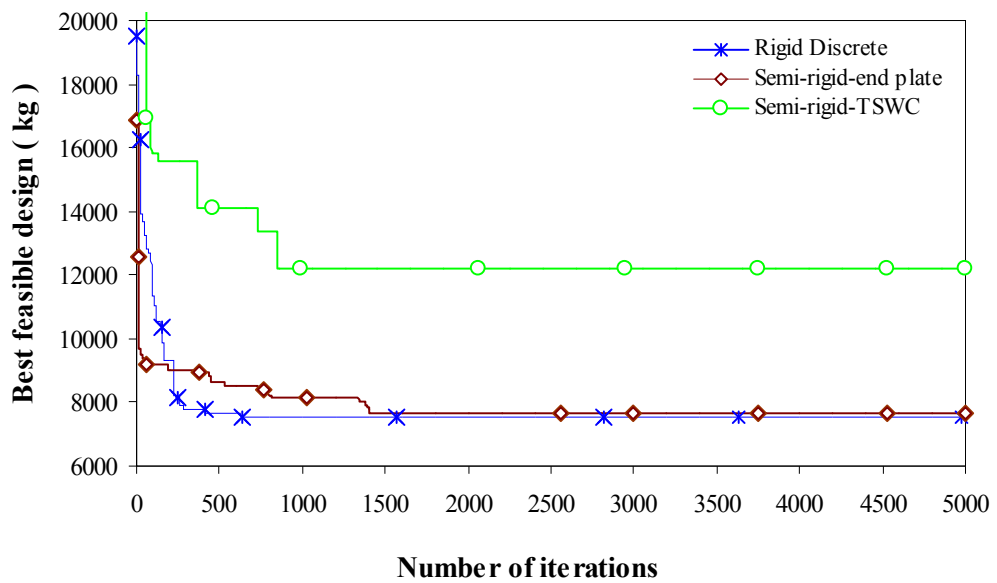


**Figure 4.28** Design history graph for six-storey, two-bay steel frame.

#### **4.6.5 Ten Storey, Three Bay Steel Frame**

The three-bay, ten storey steel frame is considered as fifth design example. The dimensions of the frame and the loading are shown in the Figure 4.29. The frame consists of seventy members that are collected in nine groups as shown in the figure. First eight of these groups are assigned to the columns and the last is assigned to the beams. The frame is subjected to gravity loading of 12.4kN/m on the beams of roof level and 25kN/m on the beams of each floor. The lateral loading is the single load varying between 15kN and 5kN acting on the beams of each floor. The lateral displacement of the top storey is limited to 11.83cm and the maximum inter-storey drift is restricted to 1.17cm. The modulus of elasticity is assumed to be 200kN/mm<sup>2</sup>. Maximum number of iterations is selected as 12000. Columns are assumed to be rigidly connected to the foundations.

Table 4.6 reveals the optimum W-sections designation obtained by rigid and semi-rigid optimum design algorithms. The discrete optimum design for rigid frame is attained after 3370 iterations and the minimum weight of the frame is 22879.35kg. Optimum design for semi-rigid frame with end plate without column stiffeners is attained after 2500 cycles with the weight of 25297.30kg. It is clear from the results that rigid discrete optimum design algorithm produces 11% lighter frame. The convergence rate of the problem is illustrated in the design-history graph given in Figure 4.30.

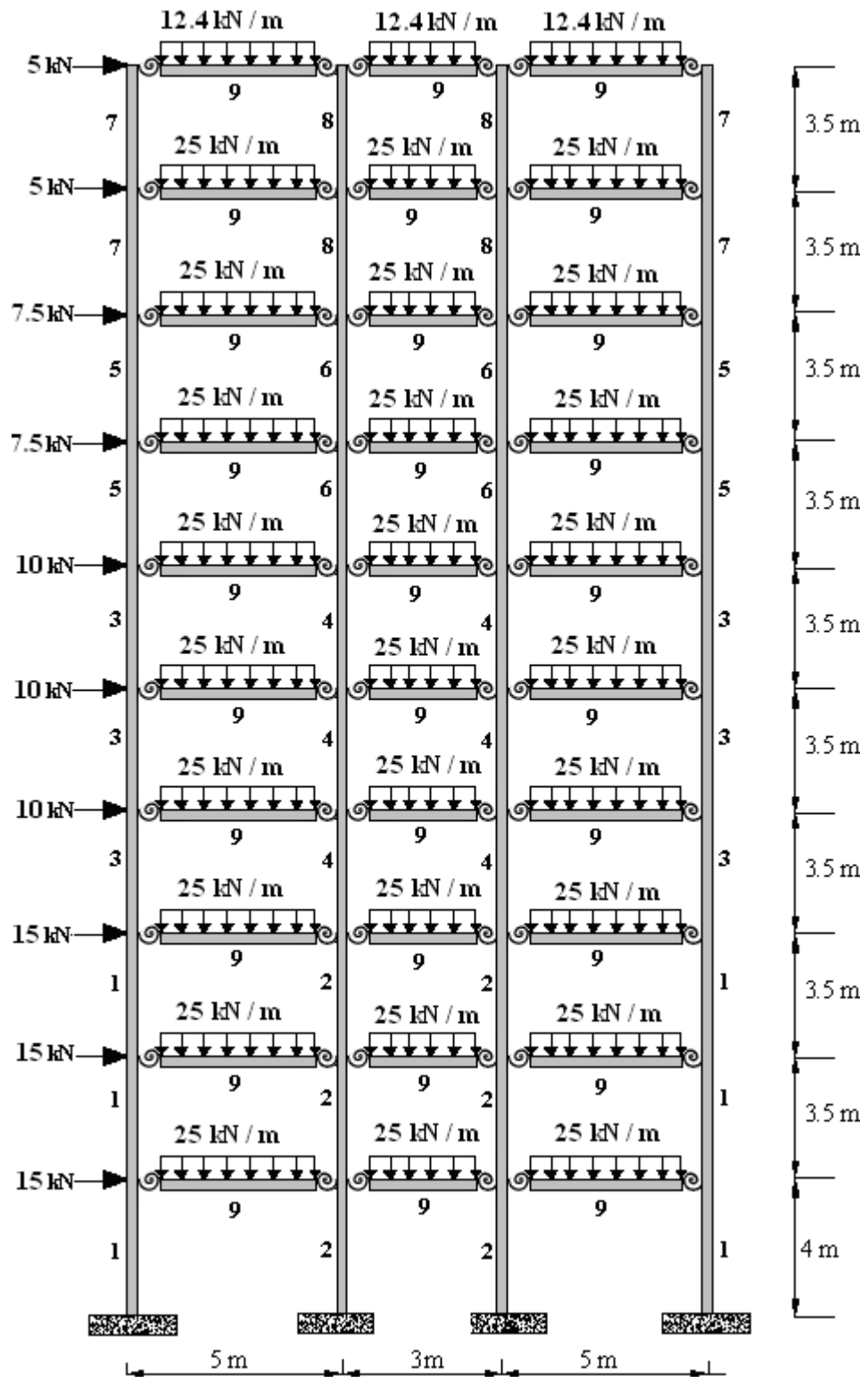
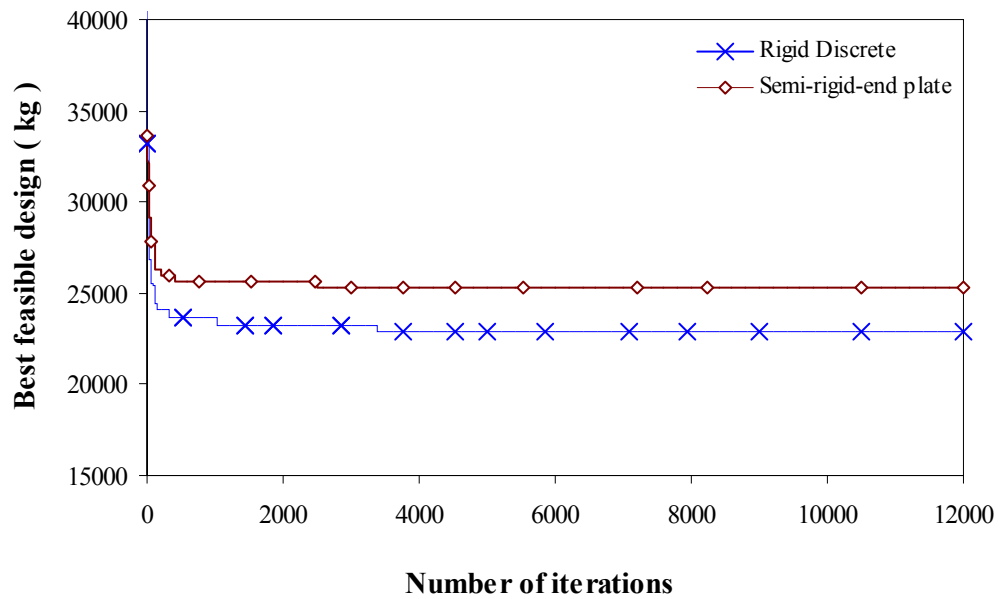


Figure 4.29 Ten storey- three bay steel frame.

**Table 4.6** Optimum designs for ten-storey, three-bay steel frame.

<b>Group No.</b>	<b>Member Type</b>	<b>Semi-rigid frame</b> (End plate Connect.) W sections-Area(cm <sup>2</sup> )	<b>Rigid frame</b> W sections-Area(cm <sup>2</sup> )
1	Column	W530X150 (192)	W610X153 (196)
2	Column	W610X125 (159)	W610X113 (144)
3	Column	W460X89 (114)	W530X92 (118)
4	Column	W610X82 (104)	W460X82 (104)
5	Column	W250X58 (74.2)	W310X60 (75.9)
6	Column	W410X60 (75.8)	W410X53 (68.1)
7	Column	W250X58 (74.2)	W310X60 (75.9)
8	Column	W410X60 (75.8)	W410X53 68.1)
9	Beam	W610X82 (104)	W460X68 (87.3)
Max. Int. St. Drift Ratio		0.98	0.87
Max. Strength Ratio		0.99	1.00
Top storey drift (cm)		8.826	7.86
Minimum Weight.kg (kN)		25297.30 (248.080)	22879.35 (224.369)

It is noticed that in the optimum frame with semi-rigid connections, the lateral displacement of top storey was 8.826cm against its upper bound of 11.83cm. The highest ratio among the combined strength constraints was 0.99 compare to 1, which was attained. Moreover, the maximum inter-storey drift ratio is recorded as 0.98. This clearly indicates that strength constraints dominate this design. On the other hand, the maximum strength ratio of rigid discrete design is attained as 1.00.



**Figure 4.30** Design history graph for ten-storey, three-bay steel frame

#### 4.6.6 Fifteen Storey, Three Bay Steel Frame

The three-bay, fifteen-storey frame shown in Figure 4.31 is considered as the last design example. The dimensions of the frame and the loading are shown in the figure. The frame is subjected to gravity loading of 12.4kN/m on the beams of roof level and 20kN/m on the beams of each floor. The lateral loading is the wind loading. The modulus of elasticity is 200kN/mm<sup>2</sup>. Frame consists of 105 members that are collected in 12 groups.

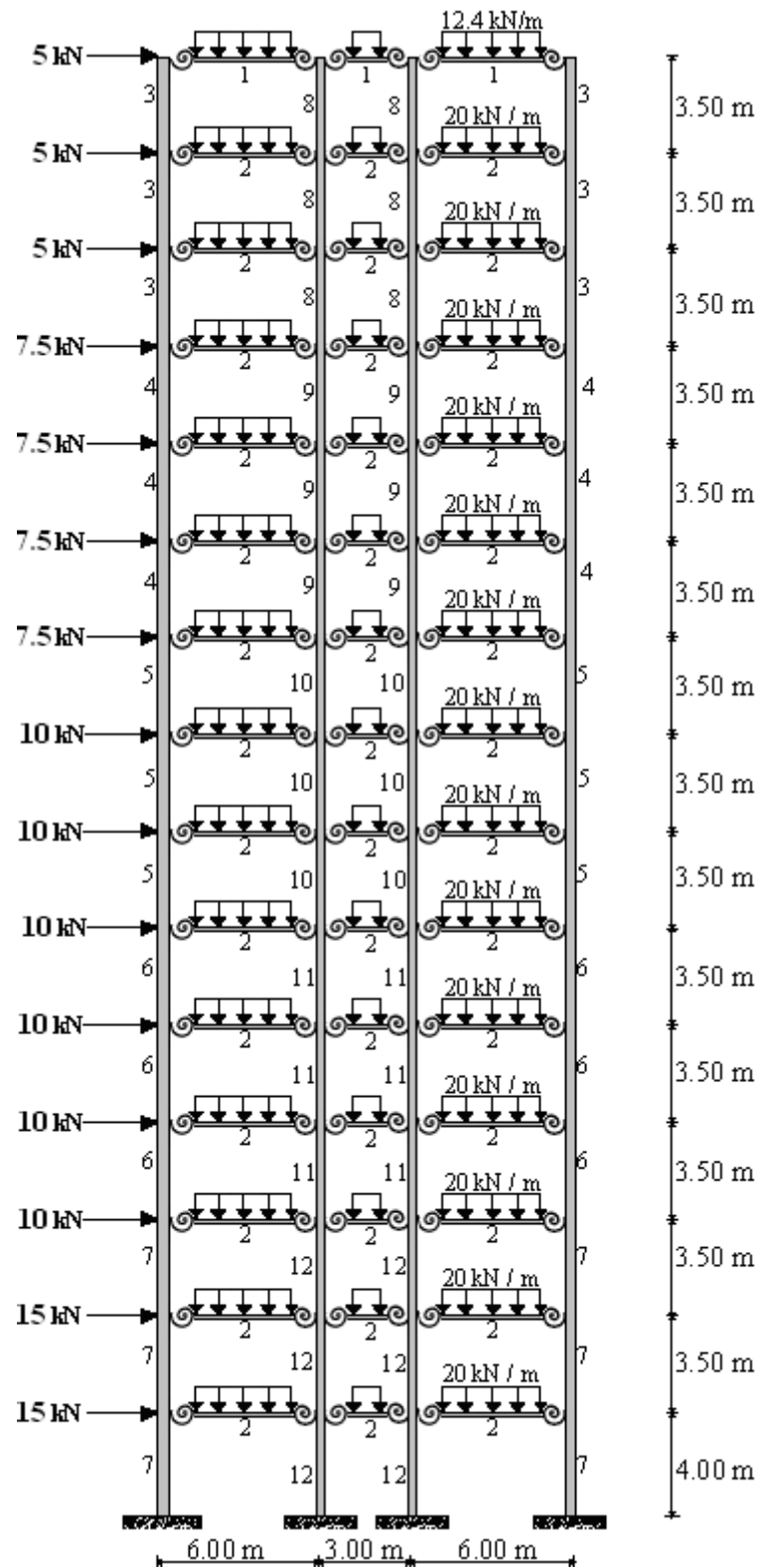


Figure 4.31 Fifteen-storey, three-bay steel frame.

Inner columns and outer columns in every three storey considered to be different groups. The beams of roof and intermediate floors are considered to be two different groups as shown in the figure. The allowable inter-storey drift is 1.17cm while the lateral displacement of the top storey is limited to 17.67cm. The strength capacities of steel members are computed according to LRFD-AISC. Fixed supports are used for the connection of the columns to the foundation.

Optimum W-sections designation obtained by rigid and semi-rigid optimum design algorithms are revealed in Table 4.7. The discrete optimum design for rigid frame is attained after 3200 iterations and the minimum weight of the frame is 29092.81kg. Optimum design for semi-rigid frame with end plate without column stiffeners is attained after 330 cycles with the weight of 30322.06kg. It is clear from the results that rigid discrete optimum design algorithm produces the lighter frame. It is noticed that in the optimum frame with semi-rigid connections, the lateral displacement of top storey was 12.06cm against its upper bound of 17.67cm. The highest ratio among the combined strength constraints was 0.94 compare to 1. However, the maximum inter-storey drift ratio is recorded as 0.96. This clearly indicates that once again the drift constraints dominate the design. On the other hand, the maximum strength ratio of rigid discrete design is attained as 0.99. The convergence rate of the problem is illustrated in the design-history graph given in Figure 4.32. Results indicate that semi-rigid frame is 4.2% heavier than the rigid one.

**Table 4.7** Optimum designs for fifteen-storey, three-bay steel frame.

Group No.	Member Type	Semi-rigid frame (End plate Connect.) Wsections-Area(cm <sup>2</sup> )	Rigid frame Wsections-Area(cm <sup>2</sup> )
1	Beam	W460X60 (83.7)	W410X46.1 (58.9)
2	Beam	W460X52 (66.3)	W410X46.1 (58.9)
3	Column	W360X72 (74.2)	W410X38.8 (49.9)
4	Column	W360X72 (74.2)	W410X38.8 (49.9)
5	Column	W250X115 (85.5)	W460X52 (66.3)
6	Column	W310X143 (101)	W460X193 (246)
7	Column	W690X125 (289)	W530X196 (250)
8	Column	W460X60 (74.2)	W250X32.7 (41.7)
9	Column	W360X57.8 (74.2)	W410X60 (75.8)
10	Column	W360X57.8 (114)	W410X60 (75.8)
11	Column	W530X92 (216)	W460X60 (75.9)
12	Column	W460X74 (224)	W690X170 (216)
Max. Int. St. Drift Ratio		0.96	0.64
Max. Strength Ratio		0.94	0.99
Top storey drift (cm)		12.06	8.59
Minimum Weight.kg (kN)		30322.06 (297.356)	29092.81 (285.301)

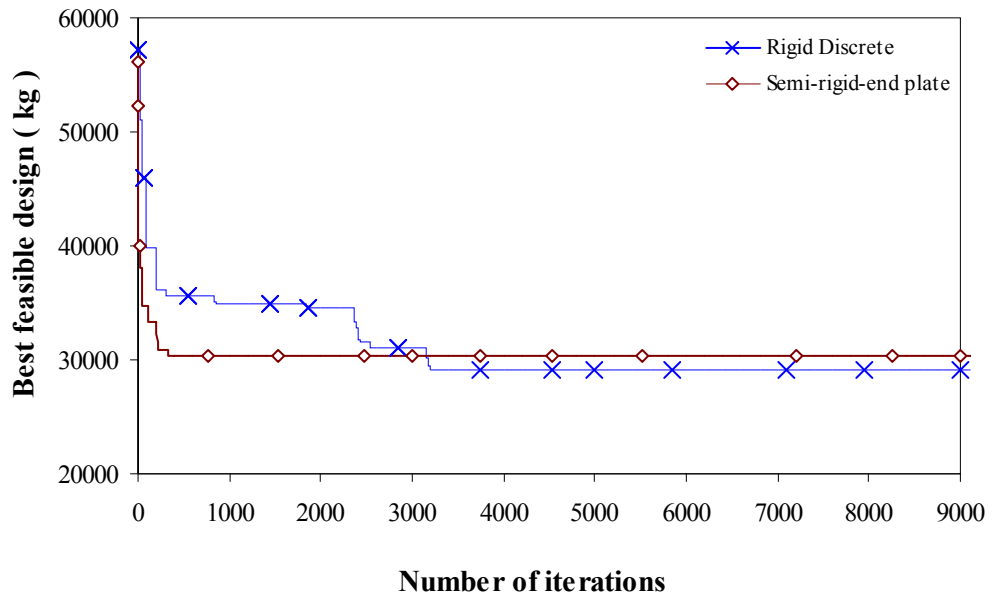


**Figure 4.32** Design history graph for fifteen-storey, three-bay steel frame

## **CHAPTER 5**

### **OPTIMUM DESIGN OF RIGID AND SEMI-RIGID STEEL SWAY FRAMES INCLUDING SOIL-STRUCTURE INTERACTION**

#### **5.1 Characteristics of Soils**

Soil can be considered as a geometrical material formed from the physical and chemical weathering of rocks. Physical weathering is the process by which rocks are broken down into smaller pieces by physical forces such as running water, wind, ocean waves. In chemical process, on the other hand, mineral form of the rock changes due to the action of water, oxygen and carbon dioxide.

Soil usually has three phases, namely, solid, liquid and gas as shown in Figure 5.1. Mechanical properties of soils are directly dependent on the interactions of these phases with each other. Interactions with applied potentials such as temperature difference and stress are also important factors affecting the properties of soil.

The gas phase, in partially saturated soils, is generally air, although there may exist some organic gases in zones of high biological activity or in chemically contaminated soils.

Second part of soils, called liquid phase, commonly involves water containing various types and amounts of dissolved electrolytes. Due to chemical spills, leaking wastes, and contaminated groundwater, both soluble and immiscible are present in soils.

Solid part of soils involves various amounts of organic matter, precipitated salts and crystalline or non-crystalline clay materials. In spite of the fact that the amount of non-clay material is greater than that of organic material and clay, the latter have a greater effect in the behavior of soils. Solid particles of soil are classified by size as clay, silt, sand, gravel, cobbles, or boulders.

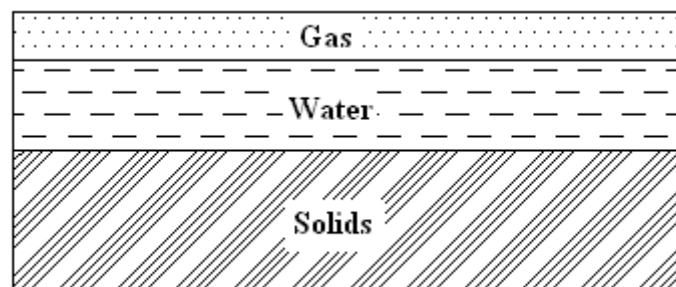


**Figure 5.1** Diagrammatic representation of soil as a three-phase system.

Mechanical behavior of soils, that is the response of soils to loads, depends on the type of minerals present. Thus, load-carrying ability and compressibility of soils is controlled by soil mineralogy.

Like any other engineering material, soil distorts when placed under a load. This distortion may be of two kinds as shearing and compression. Soils, generally, cannot withstand tension. However, in some situations the particles can be cemented together and withstand a small amount of tension but not for long periods. Due to these complexities in the structure of soil, its actual

behavior is nonlinear and this behavior must be considered in the analysis of structural systems.

## **5.2 Nonlinear Behavior of Soils**

Soil, as an elastic material, behaves nonlinearly after the initial loading. This behavior is so complex that its mathematical simulation has always been a challenging task to the engineers. This behavior is also time-dependent. This nonlinearity is the main factor of the uncertainties of static behavior of soil-foundation-superstructure system after construction.

From the physical point of view, it is clear that when an external load is applied on the soil mass, the soil particles show a tendency to attain such a structural configuration that their potential energy will be a minimum and hence stability is achieved. Until a certain stress level is reached, strain passed on to the soil mass in this process is elastic. After a while, depending on the magnitude of applied load, it may enter the plastic range. This is followed by a visco-plastic deformation due to viscous inter-granular behavior, by which strain with passage of time is implied.

Some of the factors that affect the behavior of soil are as follows;

- a) Heterogeneous distribution
- b) Anisotropy
- c) Geometric differences ( large displacements )
- d) The nonlinear behavior between the interfaces
- e) Cracks
- f) Underground water consolidation

### 5.3 Soil-structure interaction

Soil-structure interaction, basically, can be defined as a collection of phenomena in the response of structures resulted from the flexibility of soil under the foundation, as well as in the response of soils caused by the presence of structures.

A complete soil-foundation-structure system is composed of a frame in superstructure, its foundation and the soil on which it rests as illustrated in Figure 5.2. Both the axial forces and the moments in the structural members may change with the differential settlement among various parts of the structure.

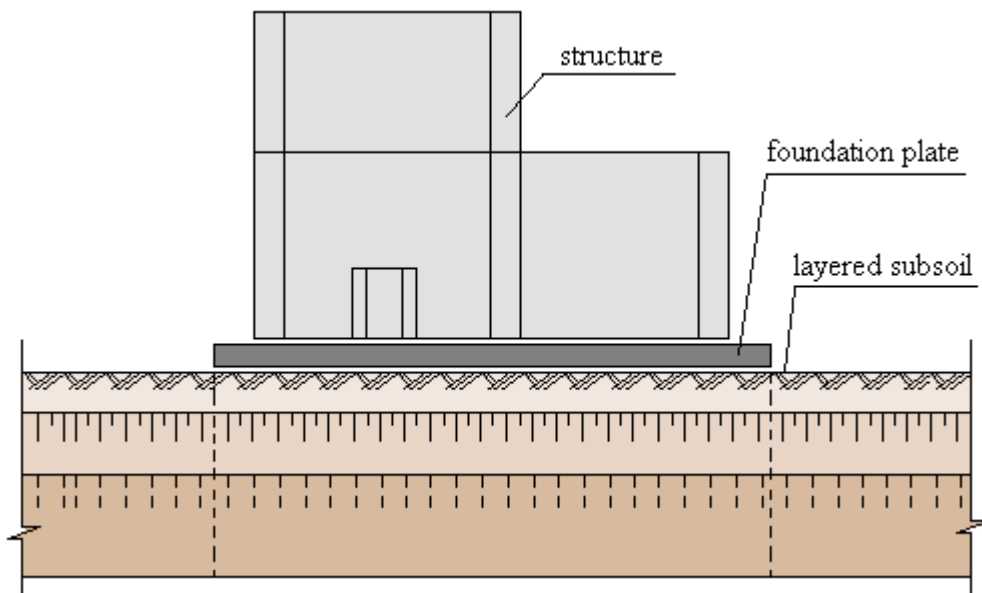


**Figure 5.2** Interaction between structure, foundation plate and soil

Rigidity of the structure and the load-settlement characteristics of soil affect the amount of redistribution of loads acting on the constructional members of the structure. Subsequently, there exist several studies in the literature conducted to estimate the effect of this factor, a critical review of which is given in [85].

It is a common belief that the response of any system including more than one component is always interdependent. For instance, consider a beam which is supported by three columns with isolated footing (Figure 5.3) [57]. Soil below the footing tends to settle more due to the existence of higher concentration of the load over the central support. On the other hand, as soon as the central column tends to settle more, the framing action induced by the beam will cause a load transfer to the end column. Therefore, interactive analysis of the soil–structure–foundation system is required to obtain the force quantities and the settlement at the finally adjusted condition. That is why the consideration of soil–structure interaction is so important in the accurate analysis of structural systems.

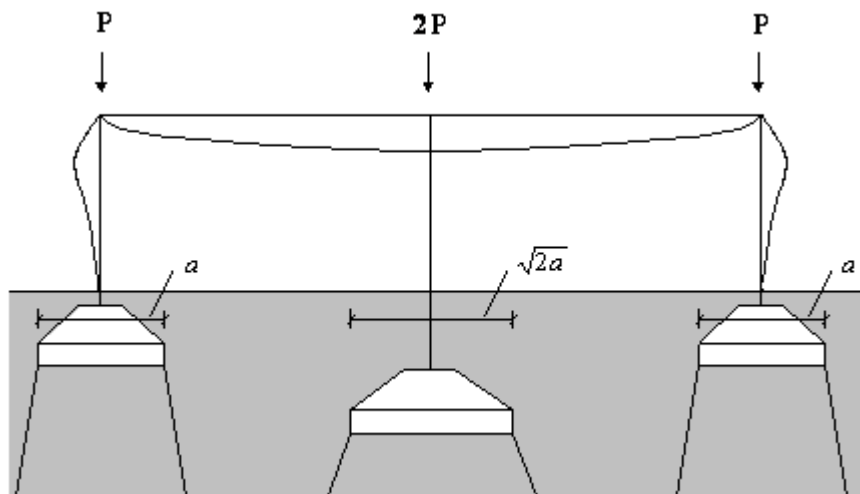


**Figure 5.3** Redistribution of loads in a frame due to soil–structure interaction

### **5.3.1 Modeling the Soil-Structure Interaction**

Successful applications of the principles of structural engineering are directly in connection with the ability of the engineer to simulate the structure and its support conditions to conduct an accurate analysis and thereby to perform a subsequently realistic design. It is complicated for the designers to arrive a realistic model in foundation analysis by the extreme difficulty of modeling the soil-structure interaction.

Ultimately, the overall loads of the structure must be transferred to the soil continuum, and both the structure and soil act together to resist and support the loads. As mentioned previously, soil is truly a non-homogeneous and an anisotropic medium that behaves in a nonlinear manner, while steel and concrete structures can be adequately modeled and analyzed, assuming isotropic and linear behavior. Besides, the properties of structural building materials are well known so that the stiffness of the structure may be readily determined, given member sizing and structure geometry.

On the other hand, taking into account the fact that the most important phase of interaction between soil and structure is the estimation of ground response at the site of a structure, one can say that laboratory testing of soil medium samples is required to determine the mechanical properties of soil. However, in addition to the characteristics discussed in previous sections, soil is a soft material, which makes it very difficult to obtain testing samples and thus, to estimate actual “in-ground” behavior.

The simplest soil-structure interaction models proposed in the literature are the ones in which the structure is supported by a rigid foundation. These models necessitate six degrees of freedom, three of which are translations and the rest

of which are rotations; however, they would be too simple for the practical applications. Because they do not take into account the characteristics of soil, thereby the nonlinear stress-strain relationship of the same.

### **5.3.1.1 Idealized Soil Behavior Models**

The factors expressed in previous section make it impossible to determine the time properties and constitutive relations of the soil continuum. Therefore, it is required to make a number of simplifying assumptions to analyze the soil-structure interaction. In view of these assumptions, researchers have proposed a number of models representing the soil media in the soil-structure interaction. These models are based on the classical theories of elasticity and plasticity for the analysis of soil-foundation interaction problems. Some important idealized models of soil-foundation interaction are briefly presented in the followings. Each model is characterized by the surface deflection it experiences under the action of a system of forces.

#### **5.3.1.1.1 Elastic Models**

The simplest type of idealized soil response is to assume the behavior of supporting soil medium as a linear elastic continuum. Therefore, the deformations are assumed as linear and reversible. Applications of these models to soil-foundation interaction have been subject of extensive research and significant developments have been made in obtaining exact and approximate solutions.

### 5.3.1.1.1 Winklerian Spring Model

Assuming that the surface displacement of the soil medium at every point is directly proportional to the stress applied to it at that point, Winkler's approach represents the soil medium as a system of identical but mutually independent, closely spaced, discrete, linearly elastic springs [57]. Figure 5.4 shows physical representation of winklerian spring models under different loadings. This idealization states that deformation of foundation due to applied load is confined to loaded regions only.

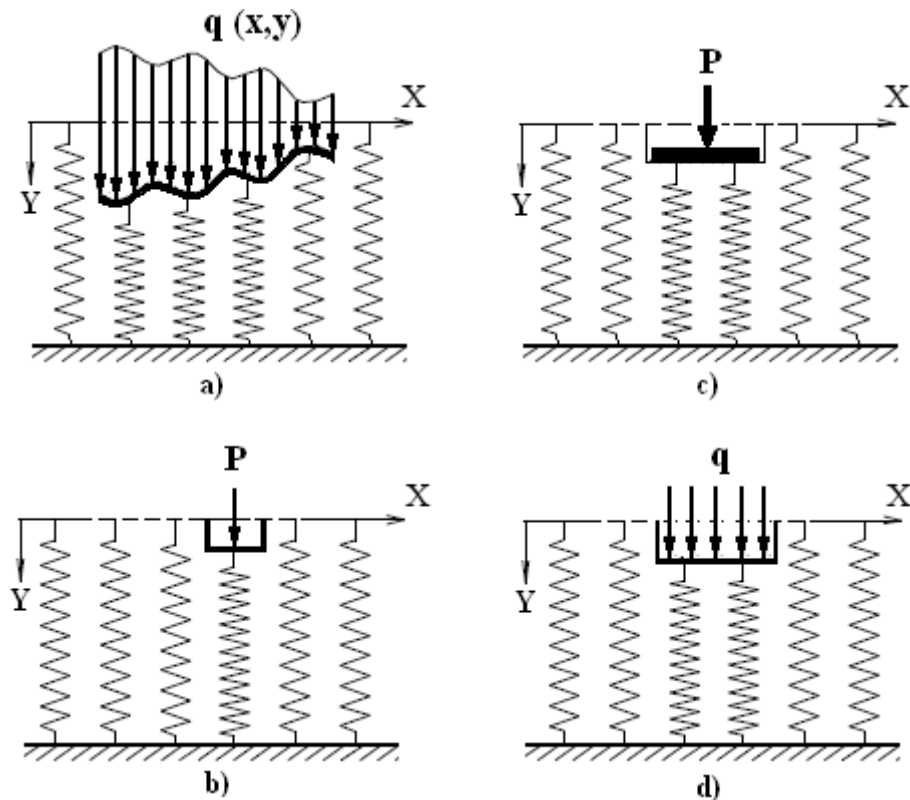


**Figure 5.4** Surface displacements of the Winkler approach due to (a) Non-uniform load, (b) A concentrated load, (c) A rigid load, (d) A uniform flexible load.

According to Winkler approach, force-deformation relationship of elastic springs at any point is given by;

$$P = ky \tag{5.1}$$

Where;

$P$  is the pressure,  $k$  is the coefficient of sub-grade reaction or sub-grade modulus, and  $y$  is the deflection.

There have been a number of soil–structure interaction studies [86–90], based on the Winkler hypothesis for its simplicity. The main problem with the use of this model is the determination of the stiffness of elastic springs used to replace the soil below foundation. Since the Winkler model has only one parameter, what is called the sub-grade stiffness, to idealize the physical behavior of the sub-grade, care must be taken to determine it numerically to use in a practical problem.

Therefore, several methods such as Plate load test, Consolidation test, tri-axial test, CBR test, proposed in the literature to estimate the modulus of sub-grade reaction.

Plate load test are generally used to determine bearing capacity and settlement of shallow footings. This test is conducted by pressing a steel bearing plate into the surface to be measured with a hydraulic jack. Using dial micrometers near the plate edge, the resulting surface deflection is read and the modulus of sub-grade reaction is determined by the following equation

$$k = \frac{P}{\Delta} \tag{5.2}$$

Where;

$k$  represents the modulus of sub-grade reaction (spring constant),  $P$  and  $\Delta$  are applied pressure and measured deflection respectively.

Consolidation can be defined as the decrease in the volume of a soil due to the expulsion of water. An undisturbed sample of cohesive soil is used in the laboratory consolidation test to determine its compressibility characteristics. To obtain these, under different loadings, the change in the height of the soil sample, resulting from a sequence of vertical stress, is monitored. By plotting the graphs of the volumetric strain versus applied vertical stress at the end of each load increment, desired settlement parameters can be achieved.

Tri-axial tests are reliable and widely used methods to determine the mechanical behavior of soils. In this test, first a cylindrical sample of soil is prepared and put into a tri-axial testing apparatus. Then, it is laterally confined by a membrane and radial stress is applied by pressurizing water in a chamber. Afterwards, axial deformations, volume changes, stress distributions and thus sub-grade stiffness are determined.

The California bearing ratio (CBR) can be pointed out as a penetration test for the evaluation of mechanical strength of sub-grades. It was developed by the California Department of Transportation. The test is conducted by measuring the pressure necessary for the penetration of a soil sample with a plunger of standard area. After, this value is divided by the pressure required to obtain an equal penetration on a standard crushed rock material. Sub-grade stiffness is then obtained by using this value.

### 5.3.1.1.2 Elastic Continuum Models

Elastic continuum model is a conceptual approach of physical representation of the infinite soil media (Figure 5.5). Soil mass is basically composed of discrete particles compacted by some inter-granular forces. Boundary distances and loaded areas, very large compared to the size of the individual soil grains, are the common features of the problems dealt in soil mechanics. Therefore, in effect, the body involving discrete molecules gets transformed into a macroscopic equivalent prone to mathematical analysis. So, it seems to be very reasonable to invoke to the theory of continuum mechanics for idealizing the soil media [91].

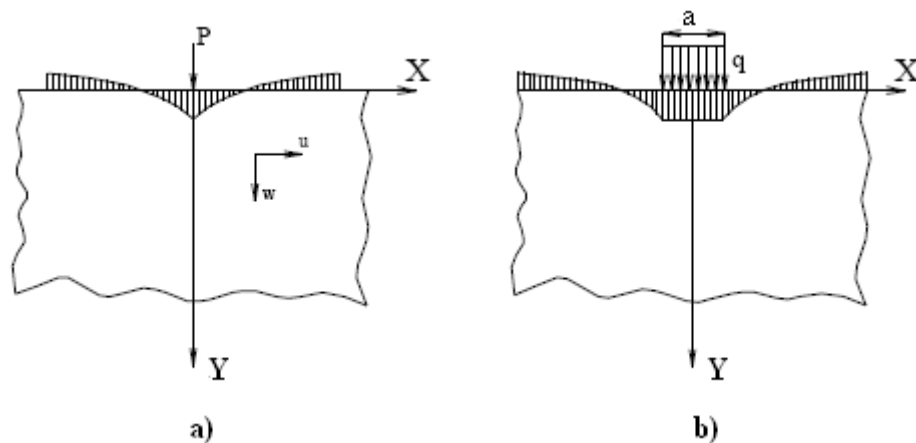


**Figure 5.5** Typical surface displacement profiles of an elastic continuum subjected to, **a)** A line load  $P$ , **b)** A uniform load  $q$  of width  $a$ .

The analysis of elastic continuum model is similar to the one of a semi-infinite, homogeneous, isotropic, linear elastic solid subjected to a

concentrated force acting normal to the plane boundary, where the theory of elasticity is used. In this case, the behavior of soil medium is represented by some continuous functions. Hence, this application of continuum theory of elasticity to soil-foundation interaction presents a complex boundary value problem. During the analysis, it is assumed that the distribution of displacements and stresses in soil medium remain continuous under the action of external force systems.

The simplicity of the input parameters such as modulus of elasticity and Poisson's ratio can be pointed out as an important advantage of this approach. Besides, this approach provides much information on the stress and deformations within soil mass. However, it is observed that for soil in reality, the surface displacements away from the loaded region decreased more rapidly than what is predicted by this approach [57]. Moreover, there exists inaccuracy in reactions calculated at the outer borders of the foundation. These drawbacks conclude that this idealization is not only difficult to compute but often fails to represent the physical behavior of soil very closely, too.

#### **5.3.1.1.1.3 Two Parameter Elastic Models**

Two parameter models possess some of the characteristic features of continuous elastic continuum models. The term "Two Parameter" means that the model is defined by two independent elastic constants. Various two parameter models have been developed along following different lines.

- a) The first type is originated from the discontinuous Winkler's model and removes this discontinuity by providing mechanical interaction between the individual spring elements by use of either elastic membranes and

elastic beams or elastic layers capable of purely shearing deformations [92].

- b) The models included in the class of second approach are related to the elastic continuum model and introduce constraints or simplifying assumptions with respect to the distribution of displacements and stresses [92].

#### **5.3.1.1.4 Finite Element Models**

Because of the fact that the scope of numerical methods is wider than that of analytical methods, the use of general-purpose finite element method has gained a great increase to study the complex interactive behavior. The method is so general that it is possible to model many complex conditions with a high degree of accuracy, including nonlinear stress–strain behavior, non-homogeneous material conditions, and changes in geometry and so on.

The method is a special extended form of matrix analysis based on variational approach, in which the whole system, that is the frame, soil and foundation in this study, is discretized into a finite number of elements connected at different nodal points as shown in Figure 5.6. Displacements functions, i.e., the displacement within the element is unknown and therefore to be assumed in a sensible manner. Hence, knowing the stiffness matrix for each element, overall stiffness matrix may be obtained. Then, from the boundary conditions and global loading conditions nodal unknowns may be generated.

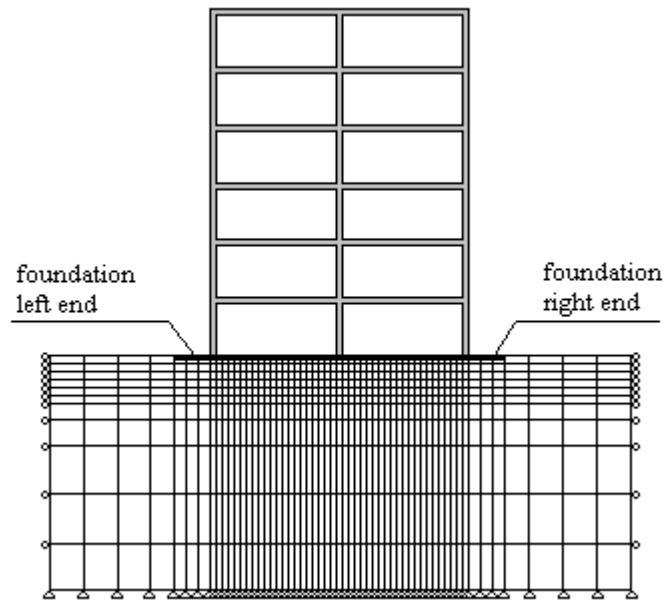


**Figure 5.6** Representation of soil-structure interaction with finite element approach

### 5.3.1.1.2 Elastic-Plastic, Perfectly Plastic Models

Elastic-plastic or irreversible behavior of the soil medium is not considered in the elastic soil models. The basic difference between the purely elastic and elastic-plastic models is that, in the latter case, the stresses that can be induced in the soil medium are restricted owing to the introduction of a yield or failure criterion. Foundation model, presented in [92], can be pointed out as an example of a purely mechanical type. This model assumes that the shear layer used to interconnect the spring elements of the Pasternak foundation model [92] has the ability of sustaining finite shearing stresses. The shear stress-shear strain relationship for the elastic layer is of an elastic-rigid plastic type. By use of this particular model, the distribution of contact stresses beneath a rigid

foundation, which is subjected to a symmetric load, is investigated. The results show that the consideration of such yielding characteristics can change both the magnitude and distribution of contact stresses that are developed at soil-foundation interface.

### **5.3.1.2 Winklerian Modeling of Planar Steel Frame-Soil Interaction System**

In some cases, a structural support may not fully prevent motion, which may result in undesired effects in the response of structural system as a whole. The designers, thus, want to investigate the response of a structure resting on a soil mass that deforms with load. Provided that the properties of the soil are known, it may be possible to represent the supporting material by a set of springs. Winkler model, known as Winklerian springs, is the most popular modeling used to solve the soil-structure interaction problems.

Figure 5.7 illustrates the representation of a simple beam, displacements of which are controlled by one rigid and one semi-rigid support. At joint 1, beam has two degrees of freedom of rotation and horizontal displacement, which means that it is restrained only along vertical direction. Thus, only one spring is required to represent the supporting soil under the beam.

In Figure 5.7a, the original form of a beam member is shown. As stated in Figure 5.7b, Winkler spring may be used to represent the support. Rigidity of this physical element is included in the overall stiffness matrix by assuming it as an additional structural element as shown in Figure 5.7c.

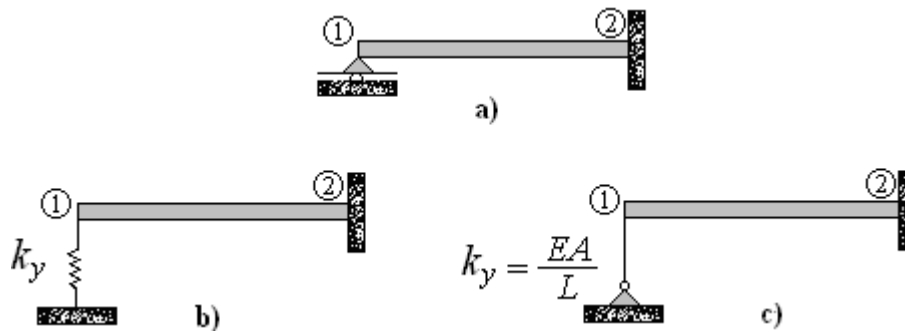


**Figure 5.7** A simple beam element with one rigid and one semi-rigid supports.

In the case where the supported joints are fully restrained as shown in Figure 5.8, soil is represented by three spring elements, horizontal, vertical and rotational stiffness of which are symbolized by  $k_x$ ,  $k_y$ ,  $k_\theta$  respectively. In the matrix formulation these values are added to the main diagonal term of the degree of freedom in the direction of the spring. Numerical values of these coefficients are determined from the experimental soil tests described in previous sections.

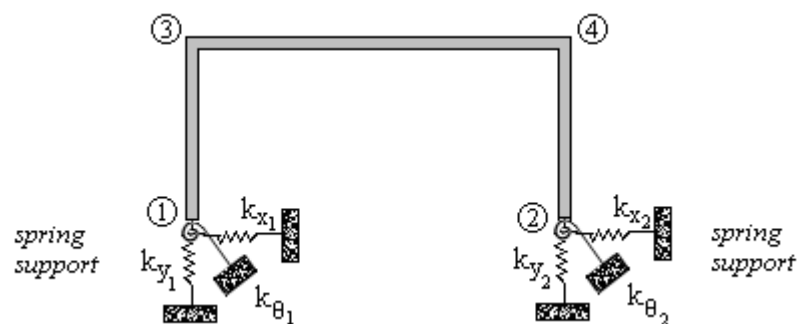


**Figure 5.8** Representation of a simple planar frame-soil interaction

A more realistic representation of soil-structure interaction system can be achieved by including foundation slab in the analysis (Figure 5.9). In this study, the steel frame is assumed to be supported by rigid strip foundations made up of reinforced concrete and soil, on which these foundation slabs rest, is simulated by elastic springs as described previously.

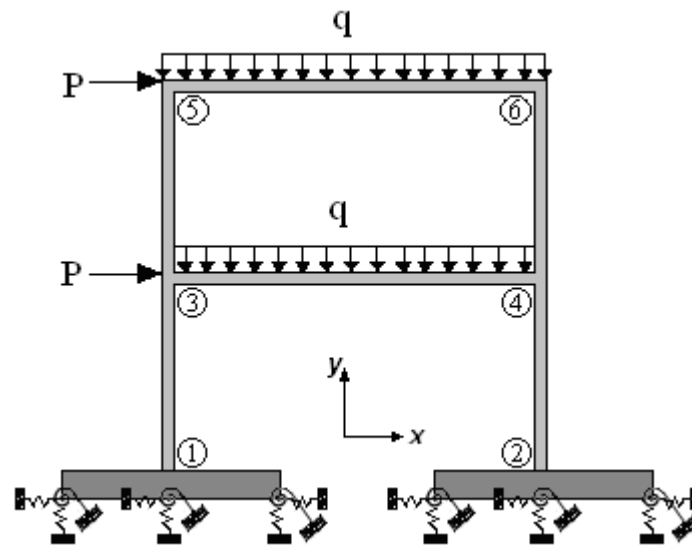


**Figure 5.9** Soil-foundation-structure interaction systems

To do this, a set of closely spaced independent fictitious vertical springs are inserted underneath the rigid footings along their lengths [93]. Stiffness of rotational springs is assumed to be zero and only one horizontal spring is used to support the system along  $x$ -direction. Each of these vertical springs, thereby, of the axial elements which can be used instead, has the same experimental stress-strain relationship as that of granular soil, which is obtained by carrying out standard drained tri-axial compression test conducted

in [94] (Figure 5.10a). Using this relationship, a load-settlement diagram can be produced (Figure 5.10b). Through the use of this diagram, the nonlinear behavior of soil is taken into account in the analysis, by performing an iterative nonlinear analysis method.

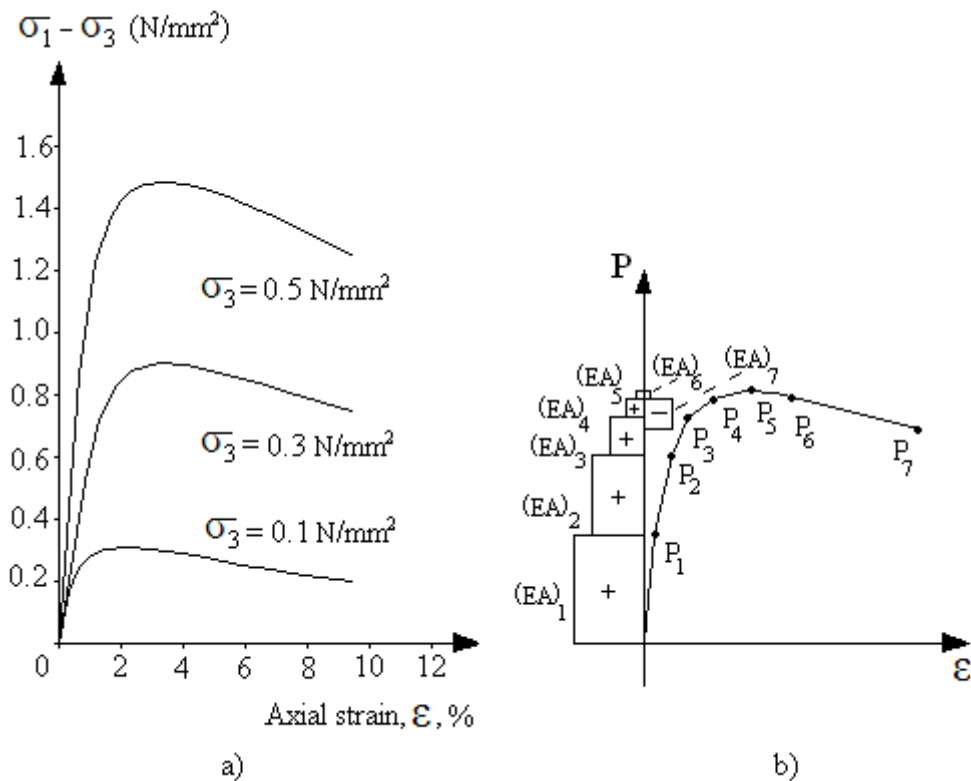


**Figure 5.10** a) Stress-strain curves for drained triaxial test on dense silica sand, b) Linearized load-deformation diagram for  $\sigma_3 = 0.3$  N/mm<sup>2</sup>

The method conducted, first approximates this nonlinear load-settlement diagram by a number of straight lines (Figure 5.10b). The intersection points of these lines indicate that as the load increases the slope of the linear segments changes implying the variations in the axial stiffness ( $EA$ ) of the

member. In other words, the modulus of elasticity becomes a variable which describes soil behavior at a particular stress condition. The effect of sign changes from positive to negative in the slope of load-deformation diagram is also considered by substituting  $(-EA)$  for the axial stiffness of the member. These stress  $(\sigma_1-\sigma_7)$  and corresponding modulus of elasticity  $(E_1-E_7)$  values are tabulated in Table 5.1. Axial stiffness of horizontal member is taken from [95] as  $Sk = 0.04714$  kN/cm and the dimensions of foundation slab is considered as  $200 \times 50 \times 70$  cm.

**Table 5.1** Stress-strain and corresponding modulus of elasticity values of each linear segment obtained from nonlinear stress-stress curve.

	<b>Linear segment number</b>						
	<b>1</b>	<b>2</b>	<b>3</b>	<b>4</b>	<b>5</b>	<b>6</b>	<b>7</b>
<b><math>\sigma</math>(kN/cm<sup>2</sup>)</b>	0.05	0.07	0.082	0.088	0.09	0.089	0.079
<b><math>\epsilon</math>(%)</b>	0.4	0.7	1.3	2.2	3.4	4.5	9.2
<b><math>E</math>(kN/cm<sup>2</sup>)</b>	12.5	6.667	2	0.667	0.167	-0.111	-0.212

Once the axial stiffness of all the members are specified up to failure, the nonlinear analysis is easily carried out by allowing these changes in the stiffness of the members during the increase of external loads. This is performed as follows;

- 1) Foundation is analyzed under the external loads and member forces and joint displacements are determined.

- 2) As the load is increased, the initial stiffness of the structure does not change until one of the axial elements reaches its critical point. This change is controlled by load factor which is obtained by first computing the lowest incremental load factor.

$$\Delta\lambda_i = (CF_i - |P_{ai}^m|) / P_i^m \quad i = 1, \dots, nm \quad (5.3)$$

Where;

$\Delta\lambda_i$  is the incremental load factor,  $CF_i$  is critical force for member  $i$ ,  $P_{ai}^m$  and  $P_i^m$  represent the actual force and the force due to external loads in member  $i$  at step  $m$ . It is clear that initially actual member forces are equal to zero. If the minimum in the equation (5.3) is  $\Delta\lambda^m$  then the next critical load factor is obtained as;

$$\lambda^m = \lambda^{m-1} + \Delta\lambda^m \quad (5.4)$$

- 3)  $P_a$  and  $x_a$ , representing the actual member forces and joint displacements, are updated in every cycle as;

$$P_a^m = P_a^{m-1} + (\lambda^m - \lambda^{m-1}) P^{m-1} \quad (5.5)$$

$$x_a^m = x_a^{m-1} + (\lambda^m - \lambda^{m-1}) x^{m-1} \quad (5.6)$$

Where;

$\lambda^m$  and  $\lambda^{m-1}$  are the load factors at the current and previous steps respectively while  $P$  and  $x$  represent the member forces and joint displacements obtained by linear analysis in step number  $m$ .

- 4) After the critical point is reached,  $(EA)_j$ , which is the axial rigidity of member  $i$ , is required to be replaced with  $(EA)_{j+1}$  which is specified by the next portion of the load-deformation diagram. This requires the reanalysis of the structure with axial member  $i$  having stiffness  $(EA)_{j+1}$  resulting new set of member forces and joint displacements.
- 5) Steps 2, 3, 4 are repeated until the load factor reaches to a predetermined value  $\lambda_u$ , or settlements become excessive.

It is apparent from the Figure 5.10 that when the procedure moves from one critical point to another, stiffness coefficient  $EA/L$  of each axial element changes each time. As a result, at each critical point the contribution matrix of that element is adjusted and stiffness equations are solved to obtain the new set of member forces and joint displacements.

In order to clarify the working steps of the algorithm the following simple soil-structure interaction problem where a strip foundation is supported by a number of axial elements is considered.

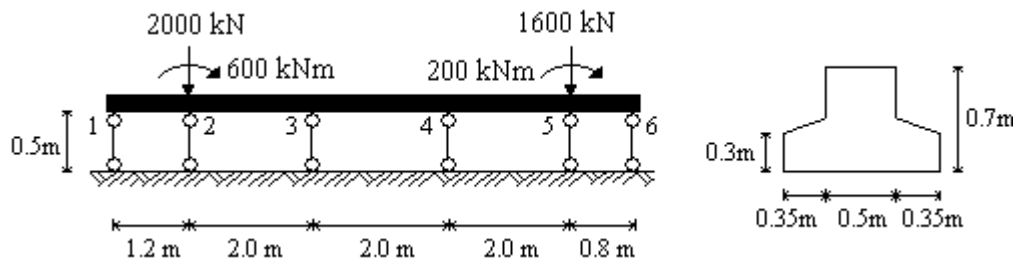


**Figure 5.11** A simple strip foundation-soil interaction problem.

The strip foundation is assumed to be resting on dense silica sand and it is subjected to external loading, which is also illustrated in Figure (5.11). The length of the axial elements and the height of the foundation are assumed to be 0.5m and 0.7m, respectively. Cross-sectional area of each axial element is assumed to be  $20\text{cm}^2$ . The geometry of the foundation is shown in the figure in detail. Linearized load-deformation diagram given in Figure 5.10 is used for the representation of nonlinear soil.

The foundation is analyzed twice, employing linear and nonlinear analysis procedures. The settlements obtained in both cases are shown in Figure 5.12. It is observed that due to the direction of external moments the maximum settlement occurs at point 6 in linear elastic analysis. However, when nonlinear analysis procedure is employed, the location of maximum settlement changes from point 6 to point 2. This is apparent from the fact that the axial element under external loading reaches to its critical load value before the others. The soil under this point becomes weaker, leading to greater settlement. It is also noticed that the difference between the settlements obtained with linear and nonlinear analysis is 75%.

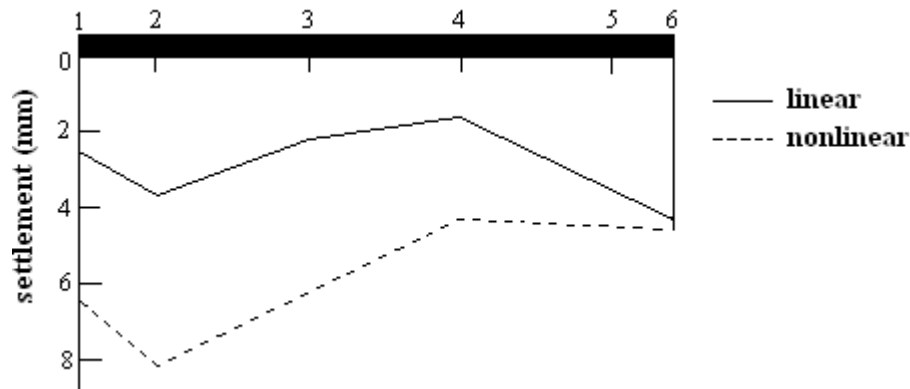


**Figure 5.12** Settlements of strip foundation resting on dense silica sand

#### **5.4 Particle Swarm Optimization Design of Rigid and Semi-Rigid Steel Frames Including Soil-Structure Interaction**

In this section, optimum design algorithms for rigid and semi-rigid steel frames where the soil-structure interaction is included are introduced. The previous optimum design algorithm is extended the design algorithm to contain the nonlinear soil analysis in the frame analysis routine. The procedure can be summarized as follows;

1. The geometry and loadings of the frame including the fictitious elements that represent the soil are defined. The load-deformation diagram of nonlinear soil is given. If the beam-to-column connections are semi-rigid then the connection type is selected. The beams and columns of the frame are grouped together.
2. Particle swarm design optimization algorithm is started by generating initial values (positions of particles) for the design variables i.e.

sequence numbers of steel profiles in steel section tables for discrete design. Once the steel sections are specified for the member groups, all the cross sectional properties such as moment of inertia, sectional modulus and radius of gyration become available. If the end connections are partially restrained, connection design process is conducted, i.e. the connection parameters such as angles, plates, bolts etc. are selected depending on the connection type decided initially.

3. The frame is analyzed with the steel sections adopted for its members using analysis subroutine which is based on matrix stiffness method. Nonlinear analysis of soil elements is also performed. Member end forces and displacements are computed.
4. Design constraints are then checked by using fly-back mechanism. If the strength and displacement requirements given in LRFD-AISC [49] are satisfied then this design is accepted, otherwise, it is discarded and new one is generated.
5. After feasible designs are obtained, particle swarm iteration process is initialized. Objective function values, weights of frames belonging to each design, are calculated. The particle which has the minimum weight is accepted as the current optimum design. After, values of design variables are updated using velocity and position update equations of particle swarm algorithm and new designs are generated.
6. These new design candidates are all analyzed under the external loading and the design constraints are checked. If all the constraints are satisfied, weights of these new designs are computed and the lightest among them is taken as the new optimum design, if it is lighter than the current optimum.

7. This iteration procedure is repeated until the predefined number of iteration is completed. The design from which has the minimum weight at the last iteration process is taken as the optimum design.

### **5.4.1 Design Examples**

Two unbraced steel frames are designed using the optimum design algorithm presented. Frames are assumed to be resting on nonlinear soil. The nonlinear behavior of the soil is represented by using fictitious axial elements. Distance between each vertical axial element is assumed to be 50 cm. Differential settlement of the frames is restricted to 5cm. Besides, when the analysis procedure is performed, beam-to-column connections are assumed as fully restrained or partially restrained. Latter approach is implemented in such a way that the end connections are designed with end plate without column stiffener model. Overall weights of fully supported and partially supported versions of each frame are compared to have an idea about how much the consideration of soil affects the behavior of complete structure. In the design process the discrete set from which the design algorithm selects the sectional designations for frame members is considered to be the complete set of 272 W-sections starting from W100x19.3 to W1100x499mm as given in LRFD-AISC [49].

#### **5.4.1.1 Three Storey-Two Bay Steel Frame**

The two bay, three storey frame shown in Figure 5.13 is selected as first design example, to demonstrate the application of the optimum design

algorithm developed. The dimensions, member grouping and the external loading of the system are also shown in the figure. The upper bound imposed on lateral deflections of the top storey joints is limited to  $1/300$  of the frame height, which corresponds to 30.48 mm. The frame members are collected in two different groups. Columns are considered to be group 1 while beams are taken as group 2 as shown in the figure. Hence there are only two design variables in the design problem. A single distributed load of 40kN/m is applied on each beam of the frame and lateral load of 20kN is applied to each storey level. The strength capacities of steel members are computed according to LRFD-AISC [49]. Beam-to-column connections are designed as end plate without column stiffeners model. Each foundation slab has five vertical axial elements and one horizontal axial element to support the structure along horizontal direction as shown in Figure 5.13.

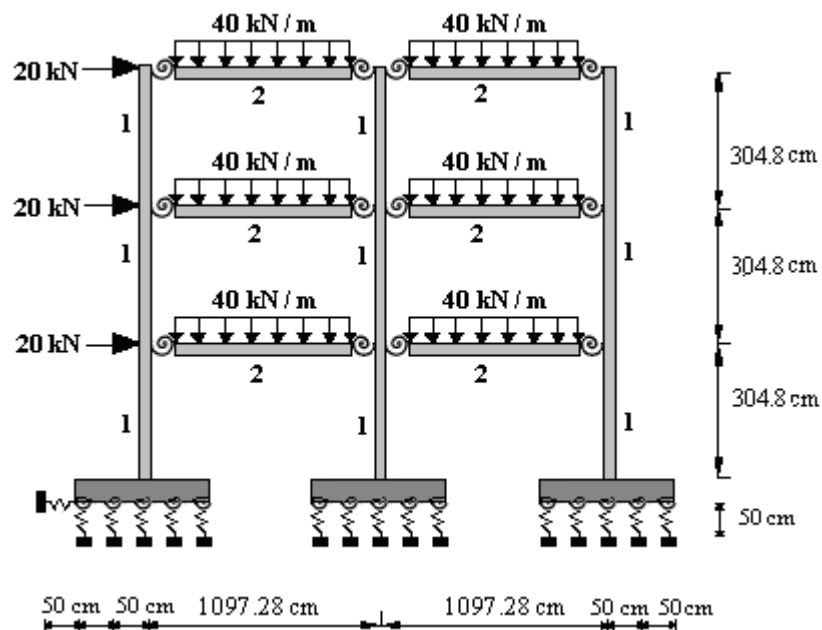


**Figure 5.13** Three storey-two bay steel frame

The frame is designed twice considering both semi-rigid and rigid beam-to-column connections. The design history of these runs is shown in Figure 5.14. Best designs are tabulated in Table 5.2 with section designations attained for each member group. As indicated in this table, when the nonlinear behavior of soil is neglected, particle swarm method based optimum design algorithm produces a rigidly connected frame which has the minimum weight of which is 12005.990kg. On the other hand, the one obtained under the consideration of nonlinear soil has the weight of 12459.16kg. This means that the inclusion of soil-structure interaction in the design algorithm leads to an increase in the overall weight of the frame. In the former and latter design, the governing design constraint is the maximum strength ratio, with the same value of 0.98. On the other hand, partially restrained frames, designed by use of design algorithms where the soil-structure interaction is excluded and included, have the weights of 12358.45kg and 13192.05kg respectively. Dominant constraint of both designs is the maximum strength ratio with the values of 0.93 and 1.00, respectively. It is clear from the results that when the nonlinear behavior of soil is taken into account, the algorithm produces 4% heavier frame in the case of rigid connections and 7% heavier frame in the case of semi-rigid connections.

**Table 5.2** Optimum designs for three-storey, two-bay steel frame.

Group No.	Member Type	Fixed support		Soil-structure interaction	
		Fully rigid connect. Wsections-Area(cm <sup>2</sup> )	Semi-rigid connect. (End plate) Wsections-Area(cm <sup>2</sup> )	Fully rigid connect. Wsections-Area(cm <sup>2</sup> )	Semi-rigid connect. (End plate) Wsections-Area(cm <sup>2</sup> )
1	Column	W250X73 (92.8)	W250X115 (146)	W760X134(170)	W310X454(578)
2	Beam	W690X152 (194)	W610X140 (179)	W760X134(170)	W690X192(244)
	Max. Int. St. Drift Ratio	0.30	0.42	0.93	0.60
	Max. Strength Ratio	0.98	0.93	0.98	1.00
	Top storey drift (cm)	0.80	1.100	2.329	1.521
	Minimum Weight. kg(kN)	12005.990 (117.738)	12358.45 (121.194)	12459.16 (122.182)	13192.05 (129.369)

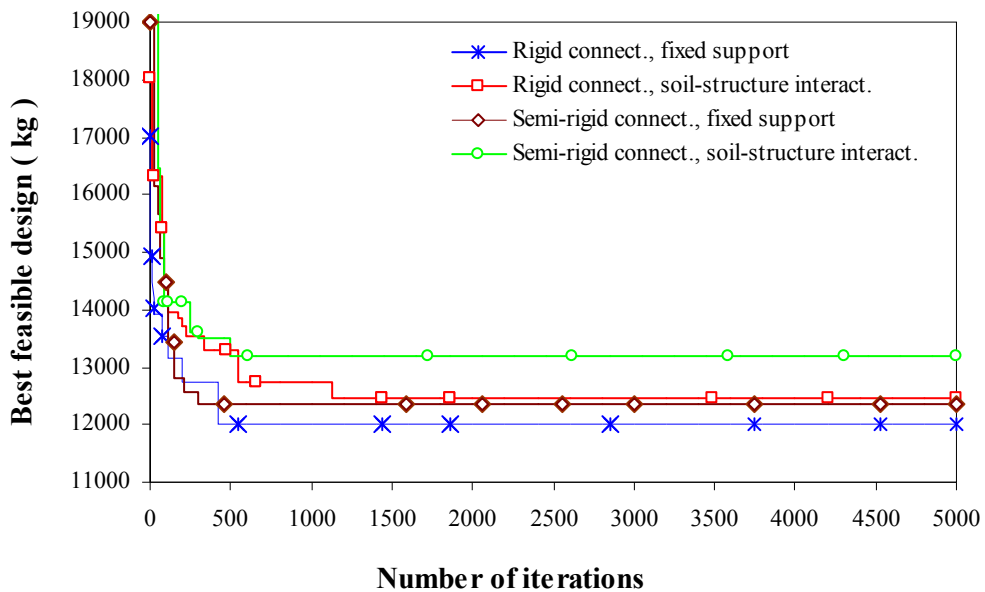


**Figure 5.14** Design history graph for three-storey, two-bay steel frame.

### 5.4.1.2 Four Storey-Four Bay Steel Frame

Four storey-four bay steel frame is considered as the second example. Loadings and dimensions of the frame are shown in Figure 5.15. The frame consists of thirty-six members that are collected in two groups as shown in the figure. Columns are taken as group 1 and beams are considered as group 2. The lateral displacement of the top storey is limited to 4cm and maximum inter-storey drift is restricted to 1cm. The modulus of elasticity is  $200\text{kN/mm}^2$ . A single distributed load of  $35\text{ kN/m}$  and a single lateral load is applied to each horizontal member of the frame.

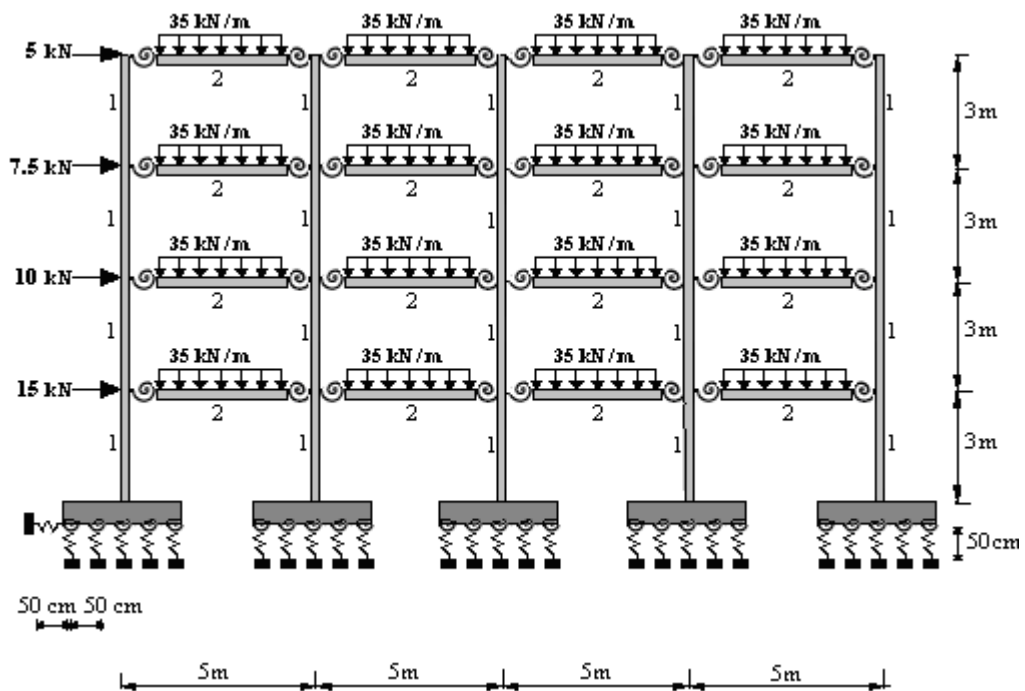


Figure 5.15 Four storey-four bay steel frame

The optimum W-section designations of semi-rigid and rigid frames obtained by the particle swarm method are given in Table 5.3. The design of semi-rigid frame resting on nonlinear soil is attained after 760 iterations and the minimum weight is 7290.995kg while the one, produced under the consideration of supports as fully rigid, has the minimum weight of 6167.268kg which is obtained after 160 iterations. In the case of rigid beam-column connection resting on rigid supports, the minimum weights are obtained as 7219.616kg and 5914.37kg respectively. It is noticed that the maximum strength ratio governs the designs. Design history graphs of this frame are shown in Figure 5.16. It is noticed that the rigid frame produced by the algorithm which includes the soil-structure-interaction is 22% heavier than the one having fixed supports. Similarly, the same approach leads to the production of 18% heavier frame in the case of semi-rigid beam-to-column connections.

**Table 5.3** Optimum designs for four-storey, four-bay steel frame.

Group No.	Member Type	Fixed support		Soil-structure interaction	
		Fully rigid connect. Wsections-Area(cm <sup>2</sup> )	Semi-rigid connect. (End plate) Wsections-Area(cm <sup>2</sup> )	Fully rigid connect. Wsections-Area(cm <sup>2</sup> )	Semi-rigid connect. (End plate) Wsections-Area(cm <sup>2</sup> )
1	Column	W150X37.1 (47.3)	W360X44 (57.3)	W360X51(64.5)	W410X60 (75.8)
2	Beam	W410X46.1 (58.9)	W360X44 (57.3)	W460X52(66.3)	W410X46.1 (58.9)
	Max. Int. St. Drift Ratio	0.47	0.57	0.58	0.50
	Max. Strength Ratio	0.99	0.95	0.92	0.95
	Top storey drift (cm)	1.59	1.96	1.92	1.699
	Minimum Weight. kg(kN)	5914.37 (58.00)	6167.268 (60.480)	7219.616 (70.80)	7290.995 (71.50)

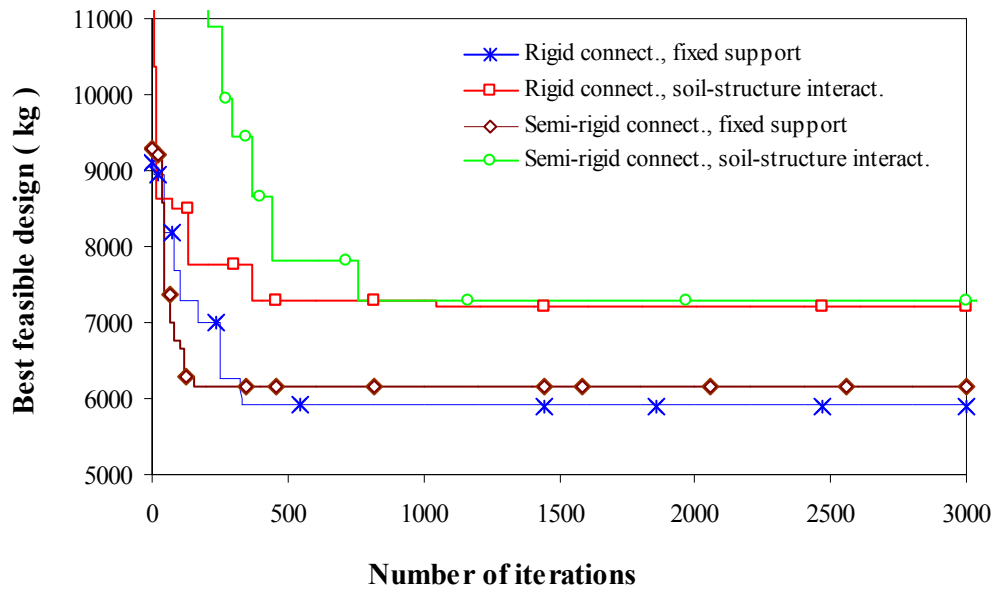


Figure 5.16 Design history graph for four-storey, four-bay steel frame.

## **CHAPTER 6**

### **SUMMARY AND CONCLUSIONS**

#### **6.1 Overview and summary of the thesis**

In this study, new approaches are developed for the optimum design of rigid and semi-rigid unbraced plane steel frames including soil-structure interaction. This study can be divided into four parts, the results obtained in each of which are discussed in the following.

In the first part of the study particle swarm optimization (PSO) algorithm is introduced. It is intended in this section to investigate the performance of this technique in the solution of benchmark problems. First benchmark problem solved with this algorithm is called the Himmelblau's function [62] which has five design variables and three constraints. PSO result of this problem is -30665.40, which is the second best objective function value among the ones obtained with four different optimization methods. Second example is the welded beam design in which the PSO algorithm shows great performance. The minimum objective function value obtained with PSO algorithm is 25% lighter than the best of the rest. Similarly, in the pressure vessel design and spring design problems, PSO obtained the best results. During these tests, PSO parameters are also analyzed so that the most appropriate ones are determined. These observations indicate that the variations in the parameter set have great effect on the performance of the algorithm. It is noticed that even only change

of one parameter in the set can lead to a huge disorder in the convergence and thereby the final result of the problem. This fact comes from the stochastic nature of combinatorial optimization algorithms. On the other hand, it is also noticed that the PSO algorithm has a better convergence rate in the solution of benchmark problems. It does not require much computation time. Besides, the results obtained at the end of the iteration process do imply that the technique is robust and can be applied to the structural design problems. One of the previous studies, carried out by He et al. [22] has stated the same conclusion.

In the second part of the study, the minimum weight design of seven unbraced steel frames is presented. Each numerical example is solved with both continuous and discrete design algorithms. It is observed that the assumption of continuous set of sections produces 9.5%, 9.6%, 10%, 24%, 34%, 16%, 57% lighter frames. These values imply that the relative difference between the weights of best designs obtained with each approach is problem dependent. Additionally, the ascending trend in the values with increasing number of stories, with the exception of the ten-story-three-bay frame, demonstrate the advantages of continuous over discrete design with increasing number of stories. Therefore, approaching the design from discrete to continuous through the use of built-up sections for a selected number of members might prove to be economically advantageous in the case of high-rise building frames.

The third part of the study is dedicated to the optimum design of unbraced steel frames with partially restrained connections. Two types of end connections are considered in this section. Namely, end plate without column stiffeners and top and seat angle with web cleats (TSWC). First six examples are designed with both connection types separately and only the former connection type is used for the rest. The results indicate that the consideration of connection flexibility in the design leads to an increase in the overall weight. Additionally, it is observed that the design algorithm finds much

heavier frames when the connections are modeled as TSWC. For example, if the three storey-three bay steel frame is taken into consideration, it can be clearly seen that the optimum frame with TSWC is 2.3% heavier than the one with end plates without column stiffeners. This is due to the high amount of dependent connection parameters in the design and the insufficient variety of angle sections given in the ready angle list.

In the last part, the effect of soil-structure interaction is considered in the optimum design of steel frames. Both types of end connections are taken into account in the design. As expected, the inclusion of soil-structure interaction in the design leads to a considerable increase in the overall weight. It is apparent from the results that this is valid for all examples. For example, in the problem of four-storey, four bay steel frame, the algorithm produces 22% heavier rigid frame and 18% heavier semi-rigid frame, when the soil nonlinearity is included. It is also clear from the results that as the number of story increases, the effect of soil nonlinearity on the overall weight also increases.

## **6.2 Conclusions**

In this study, the particle swarm optimizer is used to develop an optimum design algorithm for moment resisting steel frames. Additionally, the flexibility of beam-to-column connections is also taken into account in the structural analysis of the frame. End connection models of top and seat angle with web cleats and end plate without column stiffeners are used to represent the beam-to-column connections. Due to the fact that the connection flexibility affects the distribution of forces in the frame and leads to an increase in the drift of whole structure,  $P-\Delta$  effect is required to be considered in the frame

analysis. Further, the soil-structure interaction is included in the design algorithm. Contrary to the practical implementations in which the columns are connected to the soil with fixed support, the frames in the present study are modeled as it is supported with the foundations resting on nonlinear elastic soil. This is achieved through the use of Winkler springs. The nonlinear behavior of soil is taken into account in the analysis, by performing an iterative nonlinear analysis method.

The particle swarm optimization based design algorithm is mathematically quite simple but effective in finding the solutions of combinatorial optimization problems. The optimum design algorithm presented selects optimum W-sections from American steel sections table for beams and columns of unbraced rigid and semi-rigid steel frames such that design constraints described in LRFD-AISC are satisfied and the frame has the minimum weight. Continuous numbers generated in the algorithm are converted to integer ones with rounding off method and these discrete variables are used to obtain sequence numbers of ready steel section list. Constraints are handled with fly-back mechanism and feasible ones being candidate solutions to give the minimum frame weight are determined. Numerical examples show that rounding-off and fly-back mechanisms are effective in particle swarm optimization technique.

In view of the results obtained, it can be concluded that the inclusion of joint flexibility and soil-structure interaction in the analysis leads to a change in the response of the structural members and therefore an increase in the overall weight of the frame. It is noticed that when the partially restrained behavior of connections is considered, the algorithm produces heavier frames. Besides, the effect of soil-structure interaction results in a further increase in the overall weight. Therefore, to achieve a more realistic design one should perform the structural analysis through the consideration of these behaviors.

## REFERENCES

- [1] W.F. Chen, “Practical Analysis for Semi-rigid Frame Design”, World Scientific, Singapore (1999) 268-275.
- [2] E.S. Kameshki, M.P. Saka, “Optimum design of nonlinear steel frames with semi-rigid connections using a genetic algorithm”, Computers and Structures 79 (2001) 1593-1604.
- [3] M. Dorigo, G.D. Caro, L.M. Gambardella, “An algorithm for discrete optimization”, Artificial Life 5 (1999) 137-172.
- [4] R.H. Gallagher, O.C. Zienkiewicz, “Optimum Structural Design; Theory and Applications”, John Wiley and Sons, NY, USA (1973) 150-175.
- [5] J.S. Arora, “Optimization of Structural and Mechanical Systems”, World Scientific, Singapore (2007) 59-195.
- [6] P.W. Christensen, “An Introduction to Structural Optimization”, Springer, Linköping, Sweden (2008) 179-200.
- [7] H.A. Eschenauer, C. Mattheck, N. Ohloff, “Engineering optimization in design processes”, Proceedings of the International Conference, Karlsruhe Research Center, Karlsruhe, Germany (1990).
- [8] R.T. Haftka, “Elements of Structural Optimization”, Springer, Dordrecht, Netherlands (1992) 347-387.
- [9] M. Kurt, “Stochastic Optimization Methods”, Springer, Munich, Germany (2005) 3-43.
- [10] J. Holland, “Genetic algorithms and the optimal allocation of trials”, Society for Industrial and Applied Mathematics Journal of Computing 2 (1973) 88-105.
- [11] F. Glover, “Tabu Search”, Kluwer Academic Publications, MA, USA (1997) 1-54.

- [12] Y.L. Kwang, M.A. El-Sharkawi, "Modern Heuristic Optimization Techniques: Theory and Applications to Power Systems", Institute of Electrical and Electronics Engineers Press, NJ, USA (2008) 43-147.
- [13] B.V. Babu, G.C. Onwubolu, "New Optimization Techniques in Engineering", Springer, Berlin, Germany (2008) 101-123.
- [14] Z.W. Geem, J.H. Kim, "A new heuristic optimization algorithm: Harmony search", *Simulation* 76 (2001) 60-68.
- [15] Z.W. Geem, K.S. Lee, Y. Park, "Application of harmony search to vehicle routing", *American Journal of Applied Sciences* 12 (2005) 1552-1557.
- [16] O.K. Erol, I. Eksin, "A new optimization method: Big bang-big crunch", *Advances in Engineering Software* 37 (2006) 106-111.
- [17] J. Kennedy, R. Eberhart, "Particle swarm optimization", Institute of Electrical and Electronics Engineers Press 4 (1995) 1942-1948.
- [18] J. Kennedy, R.C. Eberhart, "A discrete binary version of the particle swarm algorithm", *Proceedings of the World Multi-Conference on Systemic, Cybernetics and Informatics*, NJ, USA (1997).
- [19] K.E. Parsopoulos, M.N. Vrahatis, "Particle swarm optimization method for constrained optimization problems", *Intelligent Technologies Theory and Applications: New Trends in Intelligent Technologies* 76 (2002) 214-220.
- [20] P. Fourie, A. Groenwold, "The particle swarm optimization algorithm in size and shape optimization", *Structural and Multidisciplinary Optimization* 23 (2002) 259-267.
- [21] S. He, Q.H. Wu, J.Y. Wen, J.R. Saunders, R.C. Paton, "A particle swarm optimizer with passive congregation" *Biosystem* 78 (2004) 135-147.
- [22] S. He, E. Prempain, Q.H. Wu, "An improved particle swarm optimizer for mechanical design optimization problems", *Engineering Optimization* 36 (2004) 585-605.

- [23] M.F. Tasgetiren, Y.C. Liang, M. Sevkli, G. Gencyilmaz, “Particle swarm optimization algorithm for makespan and maximum lateness minimization in permutation flowshop sequencing problem”, Proceedings of the Fourth International Symposium on Intelligent Manufacturing Systems, Sakarya, Turkey (2004).
- [24] H. Liu, S. Shichang, A. Ajith, “Particle swarm approach to scheduling work-flow applications in distributed data-intensive computing environments”, Proceedings of the Sixth International Conference on Intelligent Systems Design and Applications, Jinan, China (2006).
- [25] M.S. Arumugam, M.V.C. Rao, A. Chandramohan, “A new and improved version of particle swarm optimization algorithm with global–local best parameters”, Knowledge and Information Systems 16 (2008) 331-357.
- [26] L. Li, Z. Huang, F. Liu, “An improved particle swarm optimizer for truss structure optimization”, Lecture Notes in Computer Science, Springer 4456 (2007) 1-10.
- [27] A. Kaveh, S. Talatahari, “A hybrid particle swarm and ant colony optimization for design of truss structures”, Asian Journal of Civil Engineering 9 (2008) 329-348.
- [28] A. Carlos, C. Coello, “Theoretical and numerical constraint handling techniques used with evolutionary algorithms: A survey of the state of the art”, Computer Methods in Applied Mechanics and Engineering 191 (2002) 1245–1287.
- [29] M.R. Khan, “Optimality criterion techniques applied to frames having general cross-sectional relationships”, American Institute of Aeronautics and Astronautics Journal 22 (1984) 669-676.
- [30] “Manual of Steel Construction: Allowable Stress Design”, American Institute of Steel Construction, CA, USA (1989) 85-256.
- [31] C.V. Camp, S. Pezeshk, G. Cao, “Design of framed structures using a genetic algorithm”, Proceedings of Advances in Structural Optimization, NY, USA (1997).
- [32] M.W. Huang, J.S. Arora, “Optimal design steel structures using standard sections”, Structural Optimization 14 (1997) 24-35.

- [33] M.P. Saka, E.S. Kameshki, "Optimum design of unbraced rigid frames", *Computers and Structures* 69 (1998) 433-442.
- [34] M.P. Saka, E.S. Kameshki, "Optimum design of multistory sway steel frames to BS 5950 using a genetic algorithm", *Journal of Constructional Steel Research* 65 (2009) 36-43.
- [35] H.S. Park, C.W. Sung, "Optimization of steel structures using distributed simulated annealing algorithm on a cluster of personal computers", *Computers and Structures* 80 (2002) 1305-1316.
- [36] C.V. Camp, J.B. Barron, P.S. Scott, "Design of steel frames using ant colony optimization", *Journal of Structural Engineering* 131 (2005) 369-379.
- [37] S.O. Degertekin, "A comparison of simulated annealing and genetic algorithm for optimum design of non-linear steel space frames", *Structural and Multidisciplinary Optimization* 34 (2007) 347-359.
- [38] M.P. Saka, "Optimum design of steel frames using stochastic search techniques based on natural phenomena", *Saxe-Coburgh Publications, Stirlingshire, UK* 6 (2007) 105-147.
- [39] E. Dogan, M.P. Saka, "Optimum design of unbraced steel frames to the LRFD-AISC code using particle swarm optimization", *Proceedings of the Ninth International Conference on Computational Structures Technology, Athens, Greece* (2008).
- [40] W.F. Chen, N. Kishi, "Semi-rigid steel beam-to-column connections: data base and modeling", *Journal of Structural Engineering* 115 (1989) 105-119.
- [41] S.H. Hsieh, G.G. Deierlein, "Nonlinear analysis of three-dimensional steel frames with semi-rigid connection", *Computers and Structures* 41 (1990) 995-1009.
- [42] L. Xu, "Practical Computer-based Analysis of Semi-rigid Steel Frames", *Practical Analysis for Semi-Rigid Frame Design* (2000) 176-199.
- [43] M.A. Hadianfard, R. Razani, "Effects of semi-rigid behaviour of connections in the reliability of steel frames", *Structural Safety* 25 (2003) 123-138.

- [44] L. Xu, A.N. Sherbourne, D.E. Grierson, “Optimal cost design of semi-rigid, low-rise industrial frames”, *Engineering Journal* 32 (1995) 87-97.
- [45] L. Xu, “Design and optimization of semi-rigid framed structures”, *Recent Advances in Optimal Structural Design* 147 (2002) 134-150.
- [46] M.S. Hayalioglu, S.O. Degertekin, “Minimum cost design of steel frames with semi-rigid connections and column bases via genetic optimization”, *Computers and Structures* 83 (2005) 1849-1863.
- [47] E.S. Kameshki, M.P. Saka, “Genetic algorithm based optimum design of nonlinear planar steel frames with various semi-rigid connections”, *Journal of Constructional Steel Research* 59 (2003) 109-134.
- [48] E. Doğan, M.P. Saka, “Particle swarm optimization design of moment resisting steel frames with semi-rigid connections to LRFD-AISC”, *Proceedings of the Eight World congress on Structural and Multidisciplinary Optimization* (2009).
- [49] LRFD-AISC, “Load and Resistance Factor Design”, American Institute of Steel Construction, IL, USA (1999) 62-564.
- [50] D. Morris, “Interaction of continuous frames and soil media”, *Journal of Structural Engineering* 5 (1966) 13-43.
- [51] I.K. Lee, P.T. Brown, “Structures–foundation interaction analysis”, *Journal of Structural Engineering* 11 (1972) 2413-2431.
- [52] K.S. Subbaa, H. Rao, B.V. Sharaadaa, “Interaction analysis of frames with beam footing”, *Indian Geotechnical Conference Roorkee I* (1985) 389-395.
- [53] J. Lysmer, R.L. Kuhlemeyer, “Finite dynamic model for infinite media”, *Journal of Engineering Mechanics* 95 (1969) 859–877.
- [54] P.N. Godbole, M.N. Viladkar, J. Noorzaei, “Nonlinear soil-structure interaction analysis using coupled finite-infinite elements”, *Computers and Structures* 36 (1990) 1089-1096.
- [55] D.C. Rizos, “Development of a BEM-FEM coupled algorithm for dynamic soil-structure interaction analysis”, *Proceedings of the United States Association for Computational Mechanics Congress, CO, USA* (1999).

- [56] J.H. Park, J. Park, K. Park, S. Ok, "Analysis of soil-structure interaction considering complicated soil profile", Proceedings of the International Conference on Numerical Methods and Applications, Borovets, Bulgaria (2007).
- [57] S.C. Dutta, R. Roy, "A critical review on idealization and modeling for interaction among soil–foundation–structure system", Computers and Structures 80 (2002) 1579-1594.
- [58] A.B. Vesic, "Beams on elastic subgrade and Winkler's hypothesis", Proceedings of the International Conference on Soil Mechanics and Foundation Engineering, Paris, France (1961).
- [59] M.M. Allam, K.S. Subba Rao, "Frame soil interaction and Winkler model", Institution of Civil Engineers Journal 2 (1991) 477-494.
- [60] S. Hackwood, J. Wang, "The engineering of cellular robotic systems", Proceedings of Institute of Electrical and Electronics Engineers Internatioal Symposium, Arlington, Virginia, USA (1988).
- [61] M.M. Millonas, "Swarms, phase transitions, and collective intelligence", Artificial Life 3 (1994) 417-445.
- [62] D.M. Himmelblau, "Applied Nonlinear Programming", Mc-Graw Hill, Daryaganj, New Delhi, India (1972) 35-152.
- [63] M. Gen, R. Cheng, "Genetic Algorithms and Engineering Design", John Wiley and Sons, NY, USA (1997) 42-96.
- [64] T.P. Runarsson, X. Yao, "Stochastic ranking for constrained evolutionary optimization", Institute of Electrical and Electronics Engineers International Transactions on Evolutionary Computation 4 (2000) 284-294.
- [65] K.M. Ragsdell, D.T. Phillips, "Optimal design of a class of welded structures using geometric programming", American Society of Mechanical Engineering Journal of Engineering for Industries 98 (1976) 1021-1025.
- [66] K. Deb, "Optimal design of a welded beam via genetic algorithms", American Institute of Aeronautics and Astronautics Journal 29 (1991) 2013-2015.

- [67] T. Ray, K.M. Liew, "Society and civilization: An optimization algorithm based on the simulation of social behavior", Institute of Electrical and Electronics Engineers International Transactions on Evolutionary Computation 7 (2003) 386-396.
- [68] E. Sandgren, "Nonlinear integer and discrete programming in mechanical design optimization", Journal of Mechanical Design 112 (1990) 223-229.
- [69] K. Deb, "Geneas: A robust optimal design technique for mechanical component design", Evolutionary Algorithms in Engineering Applications 185 (1997) 497-514.
- [70] Y.J. Cao, Q.H. Wu, "A mixed variable evolutionary programming for optimization of mechanical design", International Journal of Engineering Intelligent Systems for Electrical Engineering and Communications 7 (1999) 77-82.
- [71] A.D. Belegundu, "A study of mathematical programming methods for structural optimization", International Journal for Numerical Methods in Engineering 21 (1985) 1583-1599.
- [72] J.S. Arora, "Introduction to Optimum Design", McGraw-Hill, NY, USA (1989) 105-165.
- [73] C. Coello, A. Carlos, "Use of a self-adaptive penalty approach for engineering optimization problems", Computers in Industry 41 (2000) 113-127.
- [74] W.M. Jenkins, "Plane frame optimum design environment based on genetic algorithm", Journal of Structural Engineering 118 (1992) 3103-3112.
- [75] L. Shi, H. Fu, "A delimitative and combinatorial algorithm for discrete optimum design with different discrete sets", Computational and Information Science 3314 (2004) 443-448.
- [76] D. Schodek, "Structures", Prentice Hall, NJ, USA (2008) 152-365.
- [77] A. Kassimali, "Structural Analysis", Thomson, Ontario, Canada (2005) 89-160.

- [78] W. McGuire, "Steel Structures", Prentice Hall, NJ, USA (1968) 236-283.
- [79] E. Dogan, M.P. Saka, "Optimum design of steel frames to LRFD-AISC using particle swarm optimization", Advances in Engineering Software (under review).
- [80] W.F. Chen, "LRFD Steel Design Using Advanced Analysis", Chemical Rubber Company Press, NJ, USA (1997) 122-146.
- [81] M.A. Bhatti, J.D. Hingtgen, "Effects of connection stiffness and plasticity on the service load behaviour of unbraced steel frames", Engineering Journal 32 (1995) 21-33.
- [82] F.H. Wu, "Semi-Rigid Connections in Steel Frames", Dissertation Abstracts International 50 (1989) 228.
- [83] W.F. Chen, E.M. Lui, "Stability Design of Steel Frames", Chemical Rubber Company Press, FL, USA (1997) 205-350.
- [84] K.I. Majid, "Nonlinear Structures", London Butterworth, London, England (1972) 100-115.
- [85] R. Roy, S.C. Dutta, D. Moitra, "Soil-structure interaction in buildings with isolated and grid foundations: A critical study on the state of the art with recommendations", The Bridge and Structural Engineers 31 (2002) 15-36.
- [86] M. Hetenyi, "Beams on Elastic Foundations", University of Michigan Press, MI, USA (1946) 179-214.
- [87] E.P. Popov, "Successive approximation for beams on elastic foundations", Transactions American Society of Civil Engineers 116 (1951) 1083-1108.
- [88] A.B. Vesic, "Bending on beams resting on isotropic elastic solid", Journal of Engineering Mechanics 2 (1961) 35-53.
- [89] F. Kramrisch, P. Rogers, "Simplified design of combined footings", Journal of Soil Mechanics 87 (1961) 19-44.
- [90] C.B. Brown, J.M. Laurent, J.R. Tilton, "Beam-plate system on Winkler foundation", Journal of Engineering Mechanics 103 (1977) 589-600.

- [91] ME. Harr, "Foundation of Theoretical Soil Mechanics", McGraw-Hill, London, England (1966) 150-215.
- [92] Y.H. Wang, L.G. Tham, Y.K. Cheung, "Beams and plates on elastic foundations", *Structural Engineering Materials* 7 (2005) 174-182.
- [93] M.P. Saka, A.R. Buzdar, "Nonlinear analysis of strip foundations through microcomputers", *Proceedings of the International Conference on Foundation and Tunnels*, Edinburgh, England (1989).
- [94] J.M. Duncan, C.Y. Chang, "Nonlinear analysis of stress and strain in soils", *Journal of Soil Mechanics and Foundations* 96 (1970) 1629-1653.
- [95] J.A. Langer, E.T. Mosley, C.D. Thompson, "Laterally Loaded Deep Foundations", *American Society for Testing and Materials*, PA, USA (1983) 1-30.

# CURRICULUM VITAE

## PERSONAL INFORMATION

Surname, Name : Doğan, Erkan  
Nationality : Turkish (TC)  
Date of Place and Birth : 18.03.1981, Erzurum  
Marital Status : Single  
Email : [derkan@metu.edu.tr](mailto:derkan@metu.edu.tr)

## EDUCATION

Degree	Institution	Year of Graduation
BS	Atatürk University Civil Eng.	2002

## WORK EXPERIENCE

Year	Place	Enrollment
2004-Present	METU Engineering Sciences Dept.	Research Assistant

## PUBLICATIONS

- 1) E. Doğan, M.P. Saka, “Optimum design of steel frames to LRFD-AISC using particle swarm optimization”, Computers and Structures (under review).
- 2) E. Doğan, O. Hasançebi, M.P. Saka, “A refinement of discrete particle swarm optimization for large-scale truss structures”, Asian Journal of Civil Engineering 10(3) (2009).

## INTERNATIONAL CONFERENCE PROCEEDINGS

- 1) E. Doğan, M.P. Saka, "Particle swarm optimization design of moment resisting steel frames with semi-rigid connections to LRFD- AISC ", Proceedings of Eighth World Congress on Structural and Multidisciplinary Optimization (2009).

- 2) E. Dođan, M.P. Saka, “Optimum design of steel frames to LRFD-AISC using particle swarm optimization”, Proceedings of The Ninth International Conference on Computational Structures Technology (2008).
- 3) E. Dođan, F. Erdal, M.P. Saka, “Optimum design of grillage systems under code provisions using particle swarm optimization”, Proceedings of Genetic and Evolutionary Computation Conference (2010).

#### **NATIONAL CONFERENCE PROCEEDINGS**

- 1) E. Dođan, M.P. Saka, "Çelik çerçeveselerin LRFD-AISC şartnamesine göre parçacık küme optimizasyon yöntemi kullanılarak optimum boyutlandırılması", XVI. Ulusal Mekanik Kongresi Türkiye (2010).

#### **INTERNATIONAL COURSES AND SEMINARS ATTENDED**

- 1) "High performance computations for engineering" course, 17- 22 May 2009 Pecs Hungary.
- 2) L.E. Garcia, “Rc structures under extreme loading”, 19-20 February, 2009, Ankara, Turkey.

#### **RESEARCH PROJECTS UNDERTAKEN**

- 1) O.Hasançebi, M. P. Saka, Ö. Kurç, S. Çarbaş, E. Dođan, F. Erdal and T. Bahçeliođlu, “Optimum Design of Three Dimensional Steel Skeleton Structures Using Stochastic Search Techniques and its National Structural Engineering Applications”, Turkish Scientific and Technical Research Council (TUBITAK), Ankara, Turkey, Project No:108M070, (75000 US\$), started on 1st June 2008, To be Completed on:1st December 2010.
- 2) Middle East Technical University Research 1465 Funding (BAP-2008-03- 03-02).